



# DISSERTATION

Titel der Dissertation

The cell envelope of environmental chlamydiae

verfasst von

Mag<sup>a</sup>. Karin Aistleitner

angestrebter akademischer Grad

Doktorin der Naturwissenschaften (Dr. rer. nat)

Wien, 2014

Studienkennzahl lt. Studienblatt: A 091 444

Dissertationsgebiet lt.  
Studienblatt: Ökologie

Betreuerin / Betreuer: Univ.-Prof. Dr. Matthias Horn



<b>Chapter I</b>	Introduction	5
<b>Chapter II</b>	Synopsis	15
<b>Chapter III</b>	Architecture and host interface of environmental chlamydiae revealed by electron cyrotomography	21
<b>Chapter IV</b>	Discovery of chlamydial peptidoglycan reveals bacteria with murein sacculi but without FtsZ	47
<b>Chapter V</b>	Conserved features and major differences in the outer membrane protein composition of chlamydiae	71
<b>Chapter VI</b>	Identification and characterization of a novel porin family highlights a major difference in the outer membrane of chlamydial symbionts and pathogens	151
<b>Chapter VII</b>	Conclusions and future perspectives	179
<b>Chapter VIII</b>	Abstract & Zusammenfassung	187
<b>Appendix</b>		193



# **Chapter I**

## **Introduction**

## Introduction

The phylum *Chlamydiae* comprises a highly successful group of obligate intracellular bacteria that have been associated with eukaryotes for more than 700 million years [7,8], and that are even suggested to have contributed to the evolution of algae and plants [9-11]. The best-studied members belong to the family *Chlamydiaceae*, which includes important human and animal pathogens like *Chlamydia trachomatis* and *Chlamydia pneumoniae*. However, the known chlamydial diversity has expanded enormously in the last two decades. Members of the recently designated chlamydial families *Parachlamydiaceae*, *Criblamydiaceae*, *Rhabdochlamydiaceae*, *Piscichlamydiaceae*, *Waddliaceae* and *Simkaniaceae* (collectively also termed “environmental chlamydiae”) were identified as symbionts of amoebae and arthropods [12-15] (Fig. 1), in fish gills [16,17], as a cell culture contaminant [18] and in an aborted bovine fetus [19], and the actual diversity of chlamydiae is expected to be even much larger [20]. The obligate intracellular life style of chlamydiae combined with the lack of routine genetic tools makes their study challenging. Many of the initial observations in chlamydial cell biology were obtained by electron microscopy, including the existence of two developmental stages, which can be distinguished based on their ultrastructure [21-23]: the elementary body (EB) which is characterized by its condensed DNA and represents the stable, extracellular and infectious life stage, and the reticulate body (RB) which represents the more fragile, intracellular and replicating life stage (Fig. 1). These two forms alternate during the chlamydial developmental cycle: EBs are taken up by host cells, convert into RBs and divide several times before they re-differentiate to EBs and leave the host cell to start a new round of infection [24]. An additional infectious developmental stage, the sickle shaped crescent body, was first described for the amoeba symbiont *Parachlamydia acanthamoebae* [25], and was later also found for other environmental chlamydiae [26,27].

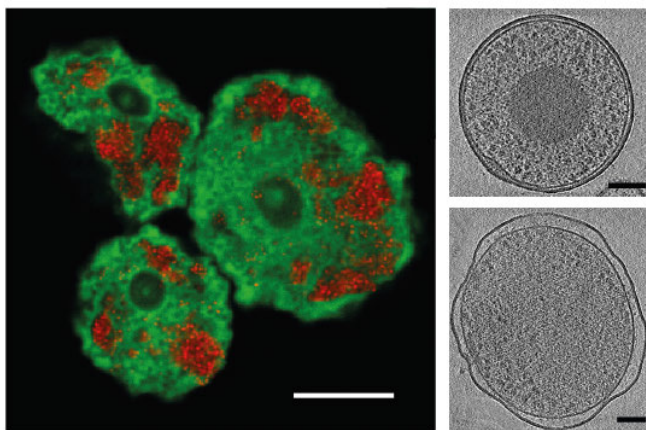


**Figure 1: Chlamydiae are obligate intracellular bacteria that switch between two developmental stages.** Left: The chlamydial amoeba symbiont *Simkania negevensis* (red) inside its host *Acanthamoeba castellanii* (green) detected by fluorescence *in situ* hybridization and staining with 4',6-Diamidino-2-phenylindol. Bar 10  $\mu\text{m}$ ; Right: Elementary body (upper panel) and reticulate body (lower panel) of *S. negevensis*. Shown are slices through cryotomograms. Bars 100 nm;

## The chlamydial cell envelope

The cell envelope of bacteria functions as a protective boundary from the environment. Chlamydiae deviate from the canonical structure of the Gram-negative cell wall in that they do not contain detectable amounts of peptidoglycan [28-31]. This stabilizing mesh-like layer is built of linear chains of alternating N-acetylmuramic acid and N-acetylglucosamine units, which are connected by short peptide chains. Peptidoglycan is found in the periplasm of nearly all Gram-negative bacteria and is responsible for defining and maintaining the bacterial shape against the internal osmotic pressure. The absence of peptidoglycan in chlamydiae has been controversially discussed for decades [28,30,32]. Despite their highly reduced genomes, chlamydiae encode a nearly complete pathway required for the synthesis of peptidoglycan (Fig. 2), the respective genes are transcribed [33,34] and the corresponding proteins are functional when heterologously expressed [1-6]. Only few genes of the pathway are missing: a glycosyltransferase catalyzing the polymerization of glycan chains is absent from all chlamydial genomes, while racemases that convert L- alanine and L- glutamate into their D- enantiomers are missing only in genomes of members of the *Chlamydiaceae* and in *Simkania*

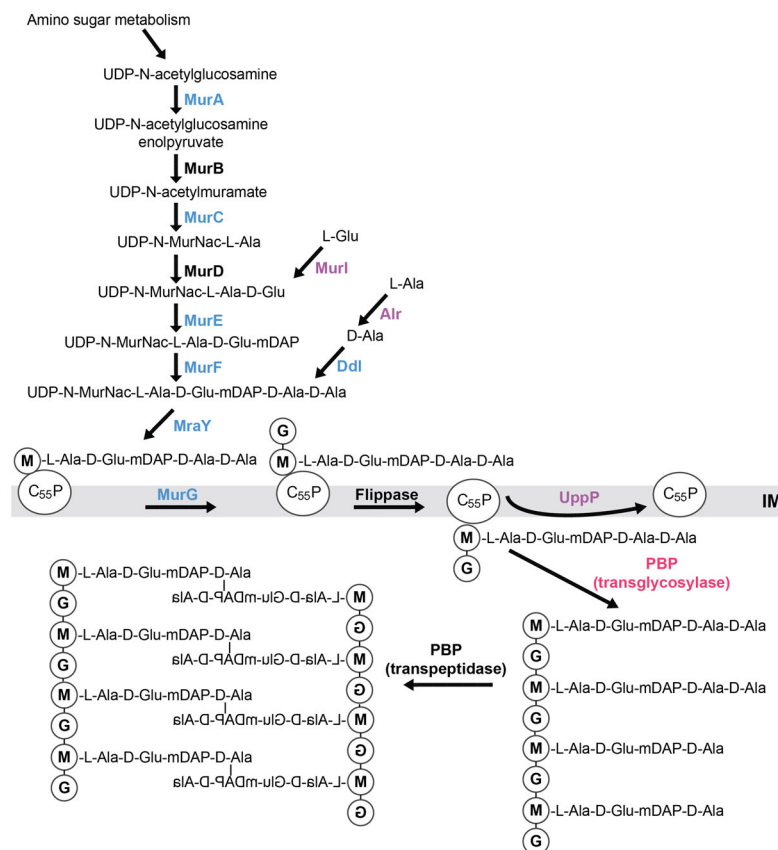


**Figure 2: The chlamydial peptidoglycan biosynthesis pathway.** Chlamydiae do not contain detectable amounts of peptidoglycan, but encode a nearly complete pathway for its synthesis. Enzymes that are absent in the genomes of all chlamydiae are colored in pink, enzymes that are only absent in the genomes of *Chlamydiaceae* and *Simkania negevensis* are colored in purple; enzymes that have been shown to be functional when heterologously expressed [1-6] are colored in blue. M or MurNac, N-acetylmuramic acid; G, N-acetylglucosamine; PBP, penicillin-binding protein; IM, inner membrane;

*negevensis*. In addition, members of the *Chlamydiaceae* are sensitive to cell wall synthesis inhibitors like beta-lactam antibiotics. The probable existence of peptidoglycan in chlamydiae is further supported by the detection of chlamydial infections by the intracellular pattern recognition receptor Nod1 [35,36], which specifically detects peptidoglycan fragments containing meso-diaminopimelic acid (mDAP). Interestingly, chlamydiae lack *dapC*, *dapD* and *dapE* that are involved in the synthesis of mDAP in other bacteria. Instead, they share the use of the aminotransferase pathway for the synthesis of mDAP [37] with plants and cyanobacteria [38], further supporting an evolutionary relationship between chlamydiae and chloroplasts/cyanobacteria [39]. Despite the evidence for the presence of peptidoglycan, all attempts to detect it in or to purify it from chlamydiae have been unsuccessful, and while electron microscopy of the chlamydial developmental stages clearly identified inner and outer membrane, no additional periplasmic layers indicative of peptidoglycan were observed [40,41]. The susceptibility of members of the *Chlamydiaceae* to beta-lactam antibiotics in the absence of detectable peptidoglycan has coined the term “chlamydial anomaly” [30].

In the absence of peptidoglycan, the two cysteine-rich proteins outer membrane proteins OmcA and OmcB were proposed to substitute for its stabilizing role by the formation of a disulfide-linked supramolecular complex in the periplasm of chlamydiae [42] (Fig. 3). In addition to providing stability, these proteins also contribute to the differences observed between the two life stages by changes in the redox-state of their cysteine-residues in the course of the developmental cycle [43-46]. Outside the host cell, the sulfhydryl-groups of the cysteine-residues of OmcA and OmcB are oxidized and extensively linked via disulfide-bridges, resulting in the extremely stable extracellular EB. Upon entering the host cell, disulfide-bridges are reduced accompanied by a decrease in the amount of OmcA and OmcB in the cell envelope, resulting in the more fragile and flexible RB [44].

Besides its role in stabilization, the cell envelope also acts as a barrier impermeable for larger molecules and thereby as protection against the environment. The passive uptake of molecules through this barrier is facilitated and regulated by porins, beta-barrel proteins that form water-filled pores in the outer membrane [47]. The most abundant protein in the outer membrane of the *Chlamydiaceae* is the major outer membrane protein (MOMP) [48], which functions as porin [49] (Fig. 3). MOMP makes up approximately 60% of the protein content of the outer membrane [50] and forms together with OmcA and OmcB the chlamydial outer membrane complex.



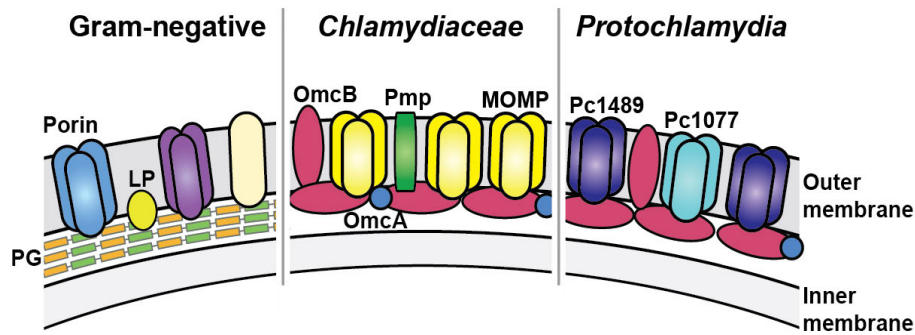


**Figure 3: Main components of the cell envelope of Gram-negative bacteria, *Chlamydiaceae* and *Protochlamydia amoebophila*.** While the most abundant proteins of the outer membrane are conserved in all *Chlamydiaceae*, variations can be seen compared to *P. amoebophila*, a member of the *Parachlamydiaceae*: MOMP is the most abundant protein in the outer membrane of all *Chlamydiaceae*, whereas Pc1489 and Pc1077, belonging to a family of hypothetical proteins, dominate the outer membrane of *P. amoebophila*. The two cysteine-rich proteins OmcA and OmcB are considered to substitute for the absence of peptidoglycan in chlamydiae compared to Gram-negative bacteria. LP, lipoprotein; PG, peptidoglycan

Opening and closing of the pore is regulated by intramolecular disulfide-bridges [49]. Similar to OmcA and OmcB, these bridges are reduced after entry into the host cell, which results in a strongly enhanced permeability that allows fuelling the needs of the metabolically highly active RB [49].

In order to successfully acquire nutrients from their host, chlamydiae manipulate the organelle distribution of their host cell. This includes the fragmentation of the Golgi-apparatus into mini-stacks to facilitate the uptake of lipids [51] and the recruitment of the endoplasmic reticulum for the uptake of ceramide by *C. trachomatis* [52,53]. To initiate these processes, chlamydiae need to export effector proteins across the barrier of the cell envelope into the host cell cytoplasm. Structures resembling secretion systems were observed on the surface of chlamydiae by electron microscopy early on [54,55], and genome sequencing showed the presence of type III secretion systems in all chlamydial genomes [56]. The arsenal of effector proteins translocated by the type III secretion system [57] plays an essential role in the initiation of infection [58,59], and the detachment of the type III secretion system from the vacuole membrane was suggested as the signal for re-differentiation of RBs to EBs at later stages of the developmental cycle [56]. Some members of the environmental chlamydiae additionally encode type IV secretion systems [7,60].

In the obligate intracellular chlamydiae, proteins in the outer membrane also play an important role for the attachment to and uptake by the host cell. Members of the polymorphic outer membrane protein family, a group of autotransporters, which are present in 9 (*C. trachomatis*) to 21 (*C. pneumoniae*) copies in the genomes of members of the *Chlamydiaceae*, were suggested to be involved in these processes [61] and to confer tissue specificity [62].

## Variations and conserved themes in the cell envelope of chlamydiae

Due to their importance as human and animal pathogens and the elaborate search for vaccine candidates, the cell envelope of the *Chlamydiaceae* has been thoroughly investigated and its main components were found to be conserved in all members of this family. However, genome analyses of members of the environmental chlamydiae suggested not only a higher diversity in the protein composition of their outer membrane, but also showed a more complete pathway for the synthesis of peptidoglycan in these organisms (Fig. 2) [7,60,63]. So far, only the outer membrane protein composition of the first sequenced member of the environmental chlamydiae, the amoeba symbiont *Protochlamydia amoebophila*, has been studied in detail [64,65]. Mass spectrometry analysis detected homologues of the cysteine-rich proteins OmcA and OmcB, but no homologue of MOMP in outer membrane protein fractions of this organism [64]. Instead, a family of four hypothetical proteins was suggested to functionally replace MOMP [64] (Fig. 3), indicating that main aspects of the outer membrane protein composition might vary between different chlamydial families.

In this thesis, I investigated selected aspects of the cell envelope of environmental chlamydiae in order to identify conserved themes and differences between chlamydial families. These findings provide novel insights into chlamydial evolution, but also challenge the current view of the presence and role of peptidoglycan in the chlamydial cell envelope.

## References

1. Hesse L, Bostock J, Dementin S, Blanot D, Mengin-Lecreux D, et al. (2003) Functional and Biochemical Analysis of *Chlamydia trachomatis* MurC, an Enzyme Displaying UDP-N-Acetylmuramate:Amino Acid Ligase Activity. *J Bacteriol* 185: 6507-6512.
2. McCoy AJ, Sandlin RC, Maurelli AT (2003) In vitro and in vivo functional activity of *Chlamydia* MurA, a UDP-N-acetylglucosamine enolpyruvyl transferase involved in peptidoglycan synthesis and fosfomicin resistance. *J Bacteriol* 185: 1218-1228.
3. Patin D, Bostock J, Blanot D, Mengin-Lecreux D, Chopra I (2009) Functional and biochemical analysis of the *Chlamydia trachomatis* ligase MurE. *J Bacteriol* 191: 7430-7435.
4. Patin D, Bostock J, Chopra I, Mengin-Lecreux D, Blanot D (2012) Biochemical characterisation of the chlamydial MurF ligase, and possible sequence of the chlamydial peptidoglycan pentapeptide stem. *Archives of Microbiology* 194: 505-512.
5. Henrichfreise B, Schiefer A, Schneider T, Nzukou E, Poellinger C, et al. (2009) Functional conservation of the lipid II biosynthesis pathway in the cell wall-less bacteria *Chlamydia* and *Wolbachia*: why is lipid II needed? *Mol Microbiol* 73: 913-923.

6. McCoy AJ, Maurelli AT (2005) Characterization of *Chlamydia* MurC-Ddl, a fusion protein exhibiting D-alanyl-D-alanine ligase activity involved in peptidoglycan synthesis and D-cycloserine sensitivity. *Mol Microbiol* 57: 41-52.
7. Horn M, Collingro A, Schmitz-Esser S, Beier CL, Purkhold U, et al. (2004) Illuminating the evolutionary history of chlamydiae. *Science* 304: 728-730.
8. Kamneva OK, Knight SJ, Liberles DA, Ward NL (2012) Analysis of genome content evolution in pvc bacterial super-phylum: assessment of candidate genes associated with cellular organization and lifestyle. *Genome Biology and Evolution* 4: 1375-1390.
9. Subtil A, Collingro A, Horn M (2013) Tracing back to primordial chlamydiae, extinct parasites of plants? . *Trends Plant Science* in press.
10. Huang J, Gogarten J (2007) Did an ancient chlamydial endosymbiosis facilitate the establishment of primary plastids? *Genome Biology* 8: R99.
11. Facchinelli F, Colleoni C, Ball SG, Weber APM Chlamydia, cyanobiont, or host: who was on top in the ménage à trois? *Trends in Plant Science* 18: 673-679.
12. Amann R, Springer N, Schonhuber W, Ludwig W, Schmid EN, et al. (1997) Obligate intracellular bacterial parasites of acanthamoebae related to *Chlamydia* spp. *Appl Environ Microbiol* 63: 115-121.
13. Kostanjsek R, Strus J, Drobne D, Avgustin G (2004) '*Candidatus* Rhabdochlamydia porcellionis', an intracellular bacterium from the hepatopancreas of the terrestrial isopod *Porcellio scaber* (Crustacea: Isopoda). *Int J Syst Evol Microbiol* 54: 543-549.
14. Thomas V, Casson N, Greub G (2006) *Criblamydia sequanensis*, a new intracellular *Chlamydiales* isolated from Seine river water using amoebal co-culture. *Environ Microbiol* 8: 2125-2135.
15. Horn M, Wagner M, Muller KD, Schmid EN, Fritsche TR, et al. (2000) *Neochlamydia hartmannellae* gen. nov., sp. nov. (*Parachlamydiaceae*), an endoparasite of the amoeba *Hartmannella vermiformis*. *Microbiology* 146: 1231-1239.
16. Draghi A, 2nd, Popov VL, Kahl MM, Stanton JB, Brown CC, et al. (2004) Characterization of "*Candidatus* Piscichlamydia salmonis" (order *Chlamydiales*), a chlamydia-like bacterium associated with epitheliocystis in farmed Atlantic salmon (*Salmo salar*). *J Clin Microbiol* 42: 5286-5297.
17. Karlsen M, Nylund A, Watanabe K, Helvik JV, Nylund S, et al. (2008) Characterization of '*Candidatus* Clavochlamydia salmonicola': an intracellular bacterium infecting salmonid fish. *Environ Microbiol* 10: 208-218.
18. Kahane SEM, Friedman MG (1995) Evidence that the novel microorganism 'Z' may belong to a new genus in the family *Chlamydiaceae*. *FEMS Microbiol Lett* 126: 203-208.
19. Rurangirwa FR, Dilbeck PM, Crawford TB, McGuire TC, McElwain TF (1999) Analysis of the 16S rRNA gene of microorganism WSU 86-1044 from an aborted bovine foetus reveals that it is a member of the order *Chlamydiales*: proposal of *Waddliaceae* fam. nov., *Waddlia chondrophila* gen. nov., sp. nov. *Int J Syst Bacteriol* 49: 577-581.
20. Lagkouvardos I, Weinmaier T, Lauro FM, Cavicchioli R, Rattei T, et al. (2014) Integrating metagenomic and amplicon databases to resolve the phylogenetic and ecological diversity of the *Chlamydiae*. *ISME J* 8: 115-125.

21. Bedson SP, Bland JOW (1932) A Morphological Study of Psittacosis Virus, with the Description of a Developmental Cycle. *Br J Exp Pathol* 13: 461-466.
22. Armstrong JA, Reed SE (1964) Nature and origin of initial bodies in lymphogranuloma venereum. *Nature* 201: 371-373.
23. Bernkopf H, Mashiah P, Becker Y (1962) Correlation between morphological and biochemical changes and the appearance of infectivity in FL cell cultures infected with trachoma agent. *Ann N Y Acad Sci* 98: 62-81.
24. Abdelrahman YM, Belland RJ (2005) The chlamydial developmental cycle. *FEMS Microbiol Rev* 29: 949-959.
25. Greub G, Raoult D (2002) Crescent bodies of *Parachlamydia acanthamoebae* and its life cycle within *Acanthamoeba polyphaga*: an electron micrograph study. *Appl Environ Microbiol* 68: 3076-3084.
26. Lamoth F, Greub G (2010) Amoebal pathogens as emerging causal agents of pneumonia. *FEMS Microbiology Reviews* 34: 260-280.
27. Nakamura S, Matsuo J, Hayashi Y, Kawaguchi K, Yoshida M, et al. (2010) Endosymbiotic bacterium *Protochlamydia* can survive in acanthamoebae following encystation. *Environ Microbiol Rep* 2: 611-618.
28. McCoy AJ, Maurelli AT (2006) Building the invisible wall: updating the chlamydial peptidoglycan anomaly. *Trends Microbiol* 14: 70-77.
29. Barbour AG, Amano K, Hackstadt T, Perry L, Caldwell HD (1982) *Chlamydia trachomatis* has penicillin-binding proteins but not detectable muramic acid. *Journal of Bacteriology* 151: 420-428.
30. Moulder JW (1993) Why is *Chlamydia* sensitive to penicillin in the absence of peptidoglycan? *Infect Agents Dis* 2: 87-99.
31. Fox A, Rogers JC, Gilbert J, Morgan S, Davis CH, et al. (1990) Muramic acid is not detectable in *Chlamydia psittaci* or *Chlamydia trachomatis* by gas chromatography-mass spectrometry. *Infect Immun* 58: 835-837.
32. Ghuyesen JM, Goffin C (1999) Lack of cell wall peptidoglycan versus penicillin sensitivity: new insights into the chlamydial anomaly. *Antimicrob Agents Chemother* 43: 2339-2344.
33. Belland RJ, Zhong G, Crane DD, Hogan D, Sturdevant D, et al. (2003) Genomic transcriptional profiling of the developmental cycle of *Chlamydia trachomatis*. *Proc Natl Acad Sci U S A* 100: 8478-8483.
34. Albrecht M, Sharma CM, Reinhardt R, Vogel J, Rudel T (2010) Deep sequencing-based discovery of the *Chlamydia trachomatis* transcriptome. *Nucleic Acids Research* 38: 868-877.
35. Opitz B, Förster S, Hocke AC, Maass M, Schmeck B, et al. (2005) Nod1-Mediated Endothelial Cell Activation by *Chlamydophila pneumoniae*. *Circulation Research* 96: 319-326.
36. Welter-Stahl L, Ojcius DM, Viala J, Girardin S, Liu W, et al. (2006) Stimulation of the cytosolic receptor for peptidoglycan, Nod1, by infection with *Chlamydia trachomatis* or *Chlamydia muridarum*. *Cellular Microbiology* 8: 1047-1057.
37. Hudson AO, Singh BK, Leustek T, C. G (2006) An LL-diaminopimelate aminotransferase defines a novel variant of the lysine biosynthesis pathway in plants. *Plant Physiol* 140: 292-301.

38. McCoy AJ, Adams NE, Hudson AO, Gilvarg C, Leustek T, et al. (2006) l,l-diaminopimelate aminotransferase, a trans-kingdom enzyme shared by *Chlamydia* and plants for synthesis of diaminopimelate/lysine. *Proceedings of the National Academy of Sciences* 103: 17909-17914.
39. Brinkman FSL, Blanchard JL, Cherkasov A, Av-Gay Y, Brunham RC, et al. (2002) Evidence That Plant-Like Genes in *Chlamydia* Species Reflect an Ancestral Relationship between *Chlamydiaceae*, Cyanobacteria, and the Chloroplast. *Genome Research* 12: 1159-1167.
40. Huang Z, Chen M, Li K, Dong X, Han J, et al. (2010) Cryo-electron tomography of *Chlamydia trachomatis* gives a clue to the mechanism of outer membrane changes. *Journal of Electron Microscopy* 59: 237-241.
41. Tamura A, Matsumoto A, Manire GP, Higashi N (1971) Electron Microscopic Observations on the Structure of the Envelopes of Mature Elementary Bodies and Developmental Reticulate Forms of *Chlamydia psittaci*. *J Bacteriol* 105: 355-360.
42. Hatch T (1996) Disulfide cross-linked envelope proteins: the functional equivalent of peptidoglycan in chlamydiae? *J Bacteriol* 178: 1-5.
43. Hatch TP, Allan I, Pearce JH (1984) Structural and polypeptide differences between envelopes of infective and reproductive life cycle forms of *Chlamydia* spp. *Journal of Bacteriology* 157: 13-20.
44. Hatch TP, Miceli M, Sublett JE (1986) Synthesis of disulfide-bonded outer membrane proteins during the developmental cycle of *Chlamydia psittaci* and *Chlamydia trachomatis*. *J Bacteriol* 165: 379-385.
45. Hackstadt T, Todd WJ, Caldwell HD (1985) Disulfide-mediated interactions of the chlamydial major outer membrane protein: role in the differentiation of chlamydiae? *Journal of Bacteriology* 161: 25-31.
46. Newhall WJ, 5th (1987) Biosynthesis and disulfide cross-linking of outer membrane components during the growth cycle of *Chlamydia trachomatis*. *Infect Immun* 55: 162-168.
47. Nikaido H (2003) Molecular basis of bacterial outer membrane permeability revisited. *Microbiol Mol Biol Rev* 67: 593-656.
48. Hatch TP, Vance DW, Jr., Al-Hossainy E (1981) Identification of a major envelope protein in *Chlamydia* spp. *J Bacteriol* 146: 426-429.
49. Bavoil P, Ohlin A, Schachter J (1984) Role of disulfide bonding in outer membrane structure and permeability in *Chlamydia trachomatis*. *Infection and Immunity* 44: 479-485.
50. Caldwell HD, Kromhout J, Schachter J (1981) Purification and partial characterization of the major outer membrane protein of *Chlamydia trachomatis*. *Infect Immun* 31: 1161-1176.
51. Heuer D, Lipinski AR, Machuy N, Karlas A, Wehrens A, et al. (2009) *Chlamydia* causes fragmentation of the Golgi compartment to ensure reproduction. *Nature* 457: 731-735.
52. Dumoux M, Clare DK, Saibil HR, Hayward RD (2012) Chlamydiae Assemble a Pathogen Synapse to Hijack the Host Endoplasmic Reticulum. *Traffic* 13: 1612-1627.
53. Derré I, Swiss R, Agaisse H (2011) The Lipid Transfer Protein CERT Interacts with the *Chlamydia* Inclusion Protein IncD and Participates to ER-*Chlamydia* Inclusion Membrane Contact Sites. *PLoS Pathog* 7: e1002092.
54. Matsumoto A (1982) Electron microscopic observations of surface projections on *Chlamydia psittaci* reticulate bodies. *J Bacteriol* 150: 358-364.

55. Nichols BA, Setzer PY, Pang F, Dawson CR (1985) New view of the surface projections of *Chlamydia trachomatis*. J Bacteriol 164: 344-349.
56. Peters J, Wilson DP, Myers G, Timms P, Bavoil PM (2007) Type III secretion a la *Chlamydia*. Trends Microbiol 15: 241-251.
57. Saka HA, Thompson JW, Chen Y-S, Kumar Y, Dubois LG, et al. (2011) Quantitative proteomics reveals metabolic and pathogenic properties of *Chlamydia trachomatis* developmental forms. Molecular Microbiology 82: 1185-1203.
58. Clifton DR, Fields KA, Grieshaber SS, Dooley CA, Fischer ER, et al. (2004) A chlamydial type III translocated protein is tyrosine-phosphorylated at the site of entry and associated with recruitment of actin. Proc Natl Acad Sci U S A 101: 10166-10171.
59. Betts HJ, Wolf K, Fields KA (2009) Effector protein modulation of host cells: examples in the *Chlamydia* spp. arsenal. Current Opinion in Microbiology 12: 81-87.
60. Collingro A, Tischler P, Weinmaier T, Penz T, Heinz E, et al. (2011) Unity in Variety—The Pan-Genome of the *Chlamydiae*. Molecular Biology and Evolution 28: 3253-3270.
61. Crane DD, Carlson JH, Fischer ER, Bavoil P, Hsia R-c, et al. (2006) *Chlamydia trachomatis* polymorphic membrane protein D is a species-common pan-neutralizing antigen. Proc Natl Acad Sci U S A 103: 1894-1899.
62. Gomes JP, Hsia RC, Mead S, Borrego MJ, Dean D (2005) Immunoreactivity and differential developmental expression of known and putative *Chlamydia trachomatis* membrane proteins for biologically variant serovars representing distinct disease groups. Microbes Infect 7: 410-420.
63. Bertelli C, Collyn F, Croxatto A, Ruckert C, Polkinghorne A, et al. (2010) The Waddlia genome: a window into chlamydial biology. PLoS ONE 5: e10890.
64. Heinz E, Pichler P, Heinz C, op den Camp HJM, Toenshoff ER, et al. (2010) Proteomic analysis of the outer membrane of *Protochlamydia amoebophila* elementary bodies. PROTEOMICS 10: 4363-4376.
65. Heinz E, Tischler P, Rattei T, Myers G, Wagner M, et al. (2009) Comprehensive in silico prediction and analysis of chlamydial outer membrane proteins reflects evolution and life style of the *Chlamydiae*. BMC Genomics 10: 634.

# **Chapter II**

## **Synopsis of the Publications/Manuscripts**

**Chapter III** provides a detailed description of the ultrastructure of the three environmental chlamydiae *Parachlamydia acanthamoebae*, *Protochlamydia amoebophila* and *Simkania negevensis*, and of their surroundings inside their amoeba host. Samples were prepared by plunge freezing of purified chlamydiae or by high-pressure freezing and cryo-sectioning of *Acanthamoeba castellanii* infected with chlamydiae. Cryo-electron tomography of these samples allowed the visualization of the different developmental stages and the architecture of chlamydial inclusions inside the host in a near-native state at macromolecular resolution in three dimensions as well as the first description of type III secretion systems of environmental chlamydiae. We showed that *S. negevensis* influences the organization of host cell organelles by recruiting the endoplasmic reticulum to the inclusion at an early stage and stays associated with it during the developmental cycle similar to *Chlamydia trachomatis*. In addition, the comparison of chemically and cryo-fixed samples revealed the crescent body, a morphotype described as an additional developmental stage for environmental chlamydiae, as an artifact of fixation and dehydration during sample processing for conventional electron microscopy.

Authors names: Martin Pilhofer\*, **Karin Aistleitner\***, Mark S. Ladinsky, Lena König, Matthias Horn, Grant J. Jensen

\*contributed equally

Manuscript Title: **Architecture and host interface of environmental chlamydiae revealed by electron cryotomography**

Reference: Environmental Microbiology 2014; 16(2):417-29

**Contributions:** Experiments were designed and performed by KA and MP except for scanning electron microscopy, high-pressure freezing and cryo-sectioning of samples which were done by LK and MSL. KA and MP analyzed the data and prepared the draft manuscript, which was edited by MH and GJJ.



**Chapter IV** reports on the identification of peptidoglycan in a member of the *Chlamydiae* for the first time. In contrast to previous studies that focused exclusively on members of the *Chlamydiaceae*, an additional layer reminiscent of peptidoglycan of Gram-negative bacteria was visualized in the periplasm of *Protochlamydia amoebophila* by cryo-electron tomography. Preparation of sacculi from *P. amoebophila* allowed the biochemical characterization of the structure as peptidoglycan that features unusual modifications. Furthermore, treatment of amoeba cultures infected with *P. amoebophila* with fosfomycin, an antibiotic that targets the first step of peptidoglycan synthesis, resulted in lower infection rates and the formation of huge aberrant bodies. By using fluorescently labeled D-amino acids, we could show that *P. amoebophila* incorporates D-alanine *in vivo*. In contrast, no sacculi could be purified from *Simkania negevensis*, which shares a less complete peptidoglycan synthesis pathway with the *Chlamydiaceae*, and incorporation of fluorescently labeled D-alanine was not detected.

Authors names: Martin Pilhofer\*, **Karin Aistleitner\***, Jacob Bilboy, Joe Gray, Erkin Kuru, Edward Hall, Yves V. Brun, Michael S. VanNieuwenzhe, Waldemar Vollmer, Matthias Horn, Grant J. Jensen

\* contributed equally

Manuscript title: **Discovery of chlamydial peptidoglycan reveals bacteria with murein sacculi but without FtsZ**

Reference: Nature Communications 2013; 4:2856

**Contributions:** KA and MP performed all experiments except HPLC/MS, analyzed the data and drafted the manuscript. The manuscript was edited by MH and GJJ. HPLC/MS was done by JB, JG and WV. Fluorescently labeled D-amino acids were provided by EK, EH, YVB and MSV.

**Chapter V** summarizes a comprehensive study on the outer membrane protein composition of members of three chlamydial families. An *in silico* pipeline for the prediction of outer membrane proteins, outer membrane lipoproteins and lipoproteins was developed, evaluated and applied to the genomes of *Parachlamydia acanthamoebae*, *Simkania negevensis* and *Waddlia chondrophila*. Fractions enriched in outer membrane proteins after sarkosyl-treatment of purified chlamydiae were analyzed by highly sensitive mass spectrometry to study the actual protein composition. This showed that large numbers of MOMP-like proteins are present at high abundance in the outer membrane of *S. negevensis* and *W. chondrophila*, whereas other porins dominate the outer membrane of *P. acanthamoebae*. We provide evidence for the first case of a chlamydia, *S. negevensis*, completely missing cysteine-rich proteins in its outer membrane, which were so far thought to be indispensable for chlamydial stability. Accordingly, the cellular integrity of *S. negevensis* is not compromised by conditions that reduce disulfide-bridges of cysteine-rich proteins in contrast to the other two organisms where these proteins are highly abundant.

Authors names: **Karin Aistleitner**, Dorothea Anrather, Thomas Schott, Julia Klose, Monika Bright, Gustav Ammerer, Matthias Horn

Manuscript title: **Conserved features and major differences in the outer membrane protein composition of chlamydiae**

Reference: submitted to Environmental Microbiology

**Contributions:** KA planned the experiments, did the *in silico* prediction of outer membrane proteins in chlamydial genomes, prepared outer membrane protein fractions for mass spectrometry, did the stability assays of chlamydiae and analyzed the data. DA did the mass spectrometry measurements and helped with data interpretation. TS helped with purification of chlamydiae and outer membrane protein fractions. JK and MB analyzed samples by electron microscopy. KA drafted the manuscript, which was edited by MH.

**Chapter VI** describes the functional characterization of a novel porin family of the amoeba symbiont *Protochlamydia amoebophila*. In contrast to the *Chlamydiaceae* where MOMP is the dominant porin, the outer membrane of *P. amoebophila* is dominated by two members of a family of hypothetical proteins without characterized homologues. Computational analysis suggested the formation of beta-barrels by these proteins, a feature characteristic of porins. All four members of this protein family had a toxic effect on *Escherichia coli* upon heterologous expression in this host, suggesting the lysis of the cells caused by the formation of pores in the outer membrane. The two porins PomS and PomT were shown to be located in the outer membrane of *P. amoebophila* by immunofluorescence and immuno-transmission electron microscopy. Similar to MOMP of *Chlamydiaceae*, PomS was shown to be present in the outer membrane throughout the developmental cycle, with an increase in expression at the end of the cycle. Lipid bilayer assays with purified PomS proved the formation of an anion-selective pore with a size similar to MOMP. PomS, probably together with PomT, therefore acts as the functional equivalent of MOMP in *P. amoebophila*, representing a major difference between the *Chlamydiaceae* and this amoeba symbiont.

Authors names: **Karin Aistleitner**, Christian Heinz, Alexandra Hörmann, Eva Heinz, Jacqueline Montanaro, Frederik Schulz, Elke Maier, Peter Pichler, Roland Benz, Matthias Horn

Manuscript title: **Identification and characterization of a novel porin family highlights a major difference in the outer membrane of chlamydial symbionts and pathogens**

Reference: PLoS One 2013;8(1):e55010

**Contributions:** KA designed the experiments, purified PomS from chlamydiae and further analyzed its expression and location by SDS-PAGE, Western blot analysis and immunofluorescence analysis. CH and EH established the protocol for the purification of PomS. FS and AH helped with the toxicity assay, the cloning and heterologous expression of porins and AH quantified the expression of PomS via qPCR assay. JM did the immuno-TEM. Functional analysis of PomS by planar lipid bilayer assays was done by EM and RB. PP analyzed PomS fractions by mass spectrometry. The draft manuscript was prepared by KA and edited by MH.



# **Chapter III**

## **Architecture and host interface of environmental chlamydiae revealed by electron cryotomography**

Environmental Microbiology 2014

16(2):417-429

## **Architecture and host interface of environmental chlamydiae revealed by electron cryotomography**

<sup>1,3,4</sup>Martin Pilhofer, <sup>1,5</sup>Karin Aistleitner, <sup>3</sup>Mark S. Ladinsky, <sup>5</sup>Lena König, <sup>2,5</sup>Matthias Horn, <sup>2,3,4</sup>Grant J. Jensen

Running head: Chlamydial architecture and host interface

<sup>1</sup>contributed equally

<sup>2</sup>corresponding authors

<sup>3</sup>Division of Biology, California Institute of Technology, Pasadena, CA, 91125, USA

<sup>4</sup>Howard Hughes Medical Institute, Pasadena, CA, 91125, USA

<sup>5</sup>Division of Microbial Ecology, University of Vienna, Vienna, A-1090, Austria

Contact:

Grant J. Jensen: phone +1 626 395 8827, fax +1 395 5730, email [jensen@caltech.edu](mailto:jensen@caltech.edu)

Matthias Horn: phone +43 1 4277 76608, fax +43 1 4277 876601, email [horn@microbial-ecology.net](mailto:horn@microbial-ecology.net)

## Summary

Chlamydiae comprise important pathogenic and symbiotic bacteria, which alternate between morphologically and physiologically different life stages during their developmental cycle. Using electron cryotomography, we characterize the ultrastructure of the developmental stages of three environmental chlamydiae: *Parachlamydia acanthamoebae*, *Protochlamydia amoebophila*, and *Simkania negevensis*. We show that chemical fixation and dehydration alter the cell shape of *Parachlamydia* and that the crescent body is not a developmental stage, but an artifact of conventional electron microscopy. We further reveal type III secretion systems of environmental chlamydiae at macromolecular resolution, and find support for a chlamydial needle-tip protein. Imaging bacteria inside their host cells by cryotomography for the first time, we observe marked differences in inclusion morphology and development as well as host organelle recruitment between the three chlamydial organisms, with *Simkania* inclusions being tightly enveloped by the host endoplasmic reticulum. The study demonstrates the power of electron cryotomography to reveal structural details of bacteria-host interactions that are not accessible using traditional methods.

## Introduction

All chlamydiae share an obligate intracellular life style and depend on a eukaryotic host for replication [2]. Chlamydial ancestors adapted to this life inside a host more than 700 million years ago, probably thriving in ancient protists [3-5]. For a long time *Chlamydiae* were thought to consist of only human and certain animal pathogens (the *Chlamydiaceae*). In the past two decades a novel class of "environmental" chlamydiae have been identified in contaminated cell cultures, in an aborted bovine fetus, in fish gills, and as symbionts of arthropods and amoebae [6-16]. While pathogenic chlamydiae are a homogeneous phylogenetic group, the genomes of environmental chlamydiae are more diverse [17,18]. It is still unclear to what extent this genomic variation manifests as variations in cell structure.

The biphasic chlamydial life cycle starts with the infection of a host cell by the elementary body (EB) [2]. After uptake by the host, the EB resides inside a host-derived vacuole (termed "inclusion") [19] and differentiates into a reticulate body (RB), the replicative developmental stage. The RB then divides several times by binary fission before re-differentiating into EBs, which leave the host cell by lysis or exocytosis to start a new round of infection [2,20,21]. An additional infectious developmental stage, the sickle-shaped crescent body, was reported for a number of environmental chlamydiae [1,22,23].

Once inside their host, chlamydiae perturb the organelle organization of the host cell in various ways. *C. trachomatis* inclusions, for instance, cause fragmentation of the Golgi [24], which facilitates the acquisition of cholesterol and sphingomyelin [25,26]. They also recruit the host's rough endoplasmic reticulum (rER), eventually resulting in a translocation of rER proteins into the inclusion [27]. Mitochondria are recruited to the inclusions of *Chlamydia psittaci* and *Waddlia chondrophila* [28-31].

Internalization, inclusion development and host-organelle recruitment are all mediated by the secretion of effector proteins into the inclusion membrane and/or host cytoplasm by the type III secretion (T3S) system [32]. While the genes that encode this needle-like secretion system are present in all chlamydial genomes [17], T3S structures have not been seen in environmental chlamydiae and few structural details are known about the T3S systems of pathogenic chlamydiae [27,33,34].

Studying chlamydial cell biology is challenging because of their obligate intracellular lifestyle and the lack of routine genetic tools [35-38]. While many insights have come from conventional electron microscopy (EM) studies, the chemical fixation, dehydration, plastic embedding, thin sectioning and



heavy-metal staining involved can lead to membrane artifacts, misleading representations of the nucleoid structure or loss of entire cellular components [39]. Here we investigated three environmental chlamydiae, *Protochlamydia amoebophila*, *Parachlamydia acanthamoebae* and *Simkania negevensis*, by electron cryotomography (ECT), which allows cells to be imaged in a near-native, "frozen-hydrated" state. This approach revealed not only new structural details of these obligate intracellular bacteria at macro-molecular resolution and in three dimensions, but also provided new perspectives on the bacteria-host interface.

## Results

### Developmental stages of environmental chlamydiae

To investigate the ultrastructure of isolated cells, chlamydiae were purified from amoeba cultures, plunge-frozen on EM grids, and imaged intact. Twenty-five, twenty and twenty tomograms were collected on purified *Simkania*, *Parachlamydia* and *Protochlamydia* cells, respectively. EBs and RBs could be distinguished by their size, morphology and the granularity of their cytoplasm. EBs were coccoid and had diameters of 450 nm (*Simkania*, +/-22, n=9), 678 nm (*Parachlamydia*, +/-32, n=5) and 625 nm (*Protochlamydia*, +/-170, n=5) (Figure 1 A, D, G). RBs were more pleomorphic and larger (667 nm, *Simkania*, +/-46, n=5; 838 nm, *Parachlamydia*, +/-135, n=4; 884 nm, *Protochlamydia*, +/-88, n=6) (Figure 1 C, F, I). EBs exhibited regions of concentrated filamentous material (presumably condensed DNA), with different texture from the rest of the EB cytoplasm. Smaller but otherwise similar regions were also occasionally seen in RBs. Due to an irregularly shaped outer membrane, the thickness of the RB periplasm was more variable than that seen in EBs. Large numbers of ribosomes were found throughout the cytoplasm of both EBs and RBs except in the region of the putatively condensed DNA within EBs. We also observed cells with features characteristic of both developmental stages (Figure 1 B, E, H), including multiple small patches of condensed DNA, probably representing intermediate stages in the process of differentiation or re-differentiation.

Previous studies using conventional EM have reported that some chlamydiae exhibit crescent shapes, and these "crescent bodies" were suggested to represent an infectious life stage of *Simkania*, *Parachlamydia* and *Protochlamydia* [1,22,23]. Surprisingly, while our tomograms of intact as well as cryosectioned cells (see below) allowed for the identification of EBs, RBs and intermediate stages (Figure 1), we never saw any crescent bodies (Figure 1, Figure 2 A, B, Figure 3-5,). We therefore explored if crescent bodies could be an artifact of chemical fixation and dehydration/embedding.

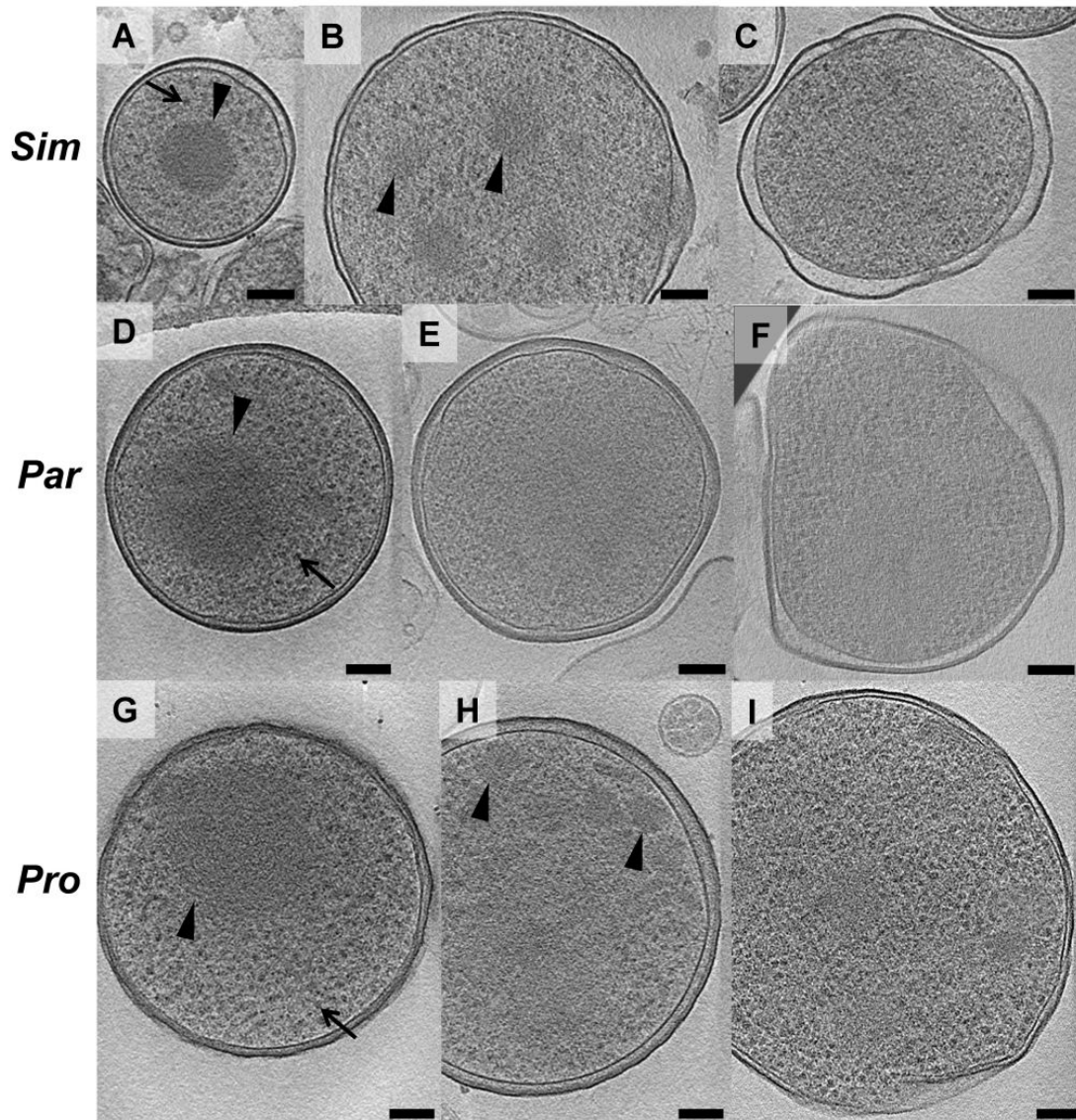


**Figure 1: Developmental stages of environmental chlamydiae.** *Simkania* (A-C), *Parachlamydia* (D-F) and *Protochlamydia* (G-I) cells were purified from asynchronously infected amoeba cultures, plunge-frozen and imaged by ECT. EBs (A, D, G) and RBs (C, F, I) were identified by differences in cell size, cell shape, thickness of periplasm and cytoplasmic granularity. EBs had a smaller diameter, a spherical shape, a uniformly thin periplasm, a condensed nucleoid (arrowheads) and a large number of ribosomes (arrows). RBs had a larger cell size, a polymorphic shape, a periplasm with varying thickness, a wavier outer membrane, and a large number of ribosomes. Intermediate stages are shown in B, E, H. Shown are slices through cryotomograms. Bars, 100 nm.

*Parachlamydia* cells were purified from asynchronous amoeba cultures and split into two aliquots. One sample was processed with procedures similar to the original study describing crescent bodies [1]: cells were fixed with glutaraldehyde and osmium tetroxide, dehydrated, plastic-embedded, thin-sectioned, stained and imaged at room temperature. Crescent bodies made up  $47 \pm 10$  % of all putative chlamydial cells ( $n=813$ ) and had the typical shape and dimensions reported previously [1] (arrows in Figure 2 C, D). The second sample was treated in the same way, except that the osmolarity and fixative concentration in the fixation buffer was reduced. Crescent bodies were still present, but only at a frequency of  $2 \pm 2$  % ( $n=1355$ ) (Figure 2 E). Osmolarity and fixative concentration therefore

influence the abundance of crescent bodies. This was further supported by scanning EM of purified chlamydial cells, where buffers with higher osmolarity and higher fixative concentration also resulted in an increased percentage of crescent bodies (Figure 2F).

To distinguish between the effects of fixation and dehydration/plastic embedding, two further aliquots of purified cells were cryo-preserved (i.e. plunge-frozen) and imaged in a frozen-hydrated state in an electron cryomicroscope. No crescent bodies were found in projection images of 584 cells, which were directly plunge-frozen after purification (Movie S1). When cells were fixed with glutaraldehyde and osmium tetroxide before plunge-freezing, crescent bodies were still absent (data not shown). Lysed cells were observed in some cases, but none of those had a typical crescent shape or continuous intact membranes, which are characteristic for crescent bodies. We conclude that crescent bodies are an artifact of the combined effect of chemical fixation and dehydration/embedding.

### **Architecture of inclusions**

Next, chlamydiae were imaged inside their host. Since ECT is limited to thin (less than ~500 nm) samples, asynchronously infected amoeba cultures were pelleted, mixed with cryoprotectant, high-pressure frozen, sectioned at cryo-temperatures (150 nm section thickness) and then imaged. Twenty-one, four and twenty-seven tomograms were collected of vitreous cryosections of *Simkania*-, *Parachlamydia*- and *Protochlamydia*-infected amoebae, respectively. For comparison, we also collected tomograms of parallel samples prepared by high-pressure freezing, freeze-substitution, plastic-embedding, thin sectioning and staining.

First, the localization of chlamydiae inside their host was investigated. Intracellular bacterial cells were always seen surrounded by an inclusion membrane and never directly in the cytoplasm (Figures 3-4 and Movies S2, S3, S4). Single-celled inclusions and inclusions packed with up to 17 chlamydial cells were observed in amoebae infected with *Simkania* (Figure 3 A-F) or *Parachlamydia* (Figure 3 G-L). RBs were the predominant stage within the inclusions, some of them dividing by binary fission. In contrast, 92% (n=52) of the inclusions in amoebae infected with *Protochlamydia* contained a single bacterial cell (Figure 4 A, D, E). The 8% of inclusions harboring more than one bacterium were not roundish and tightly packed with bacteria, as seen for *Parachlamydia* and *Simkania* (Figure 3); they rather appeared like inclusions in the process of starting separation, with membranes contracting in between the bacteria (Figure 4 B, C), or in a stage where two single-cell inclusions were connected by a narrow membrane tube. The percentage of single-cell inclusions in all cases might actually be

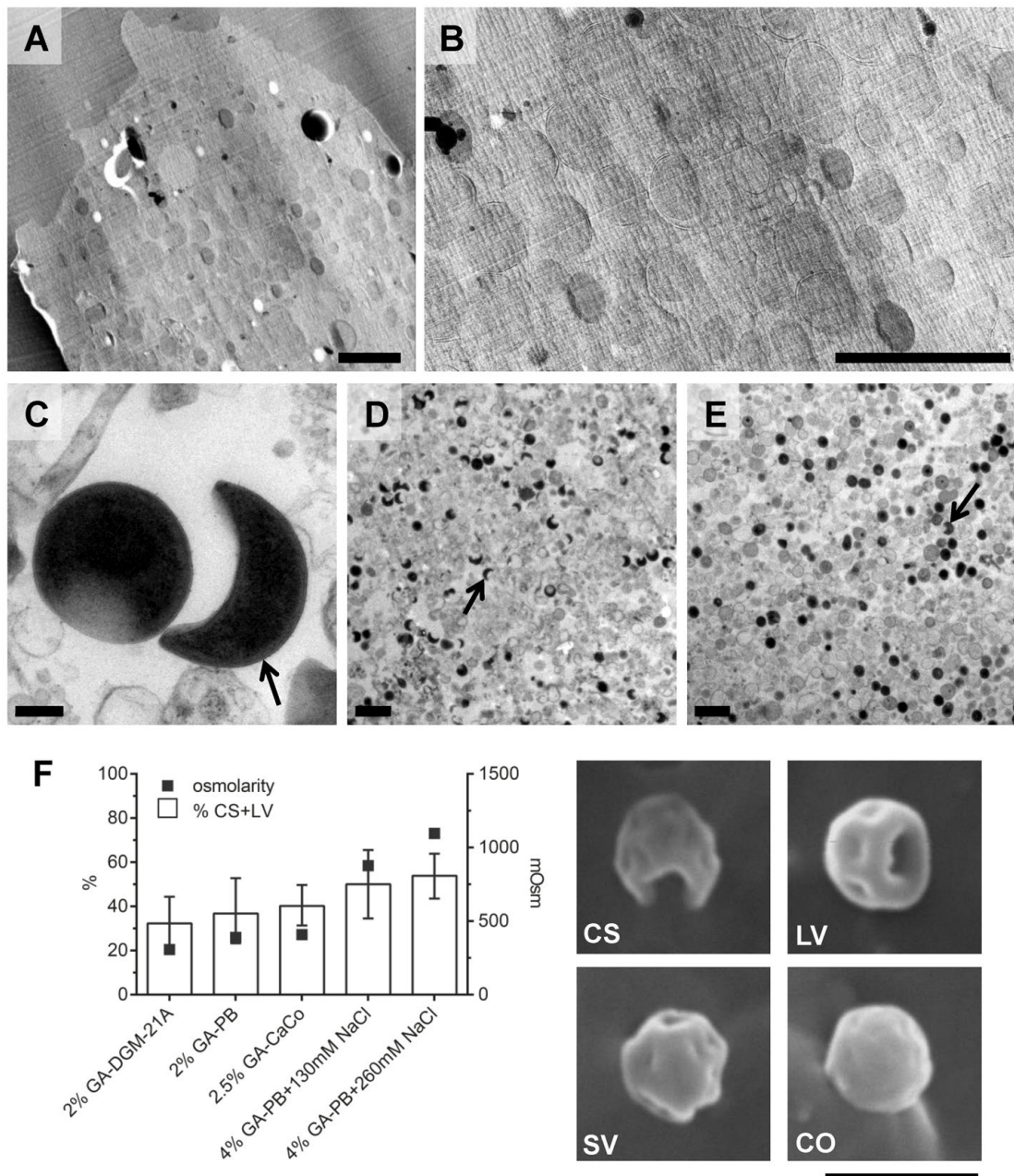


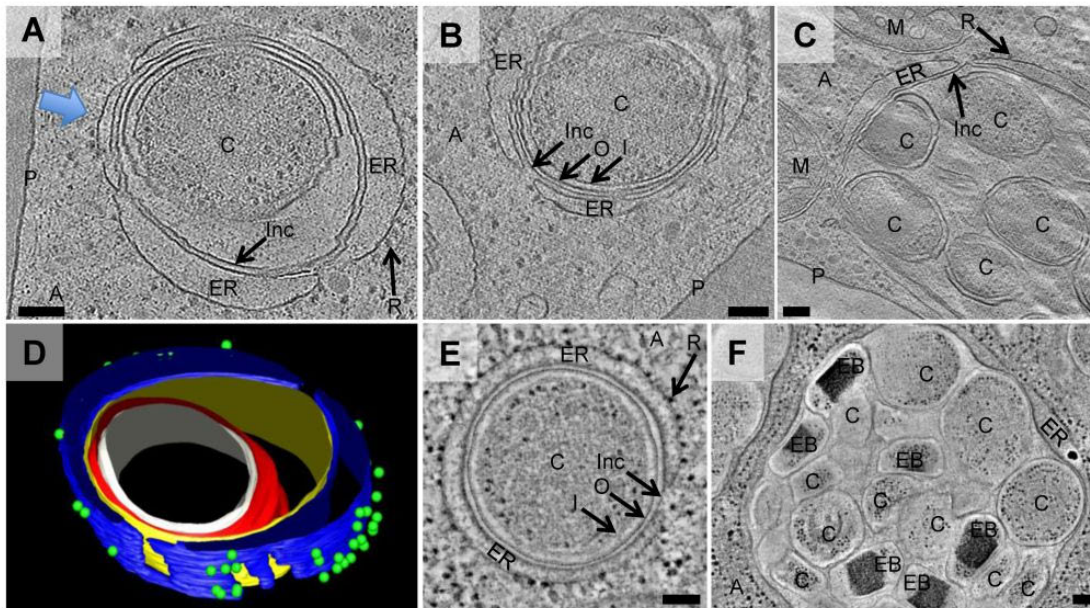
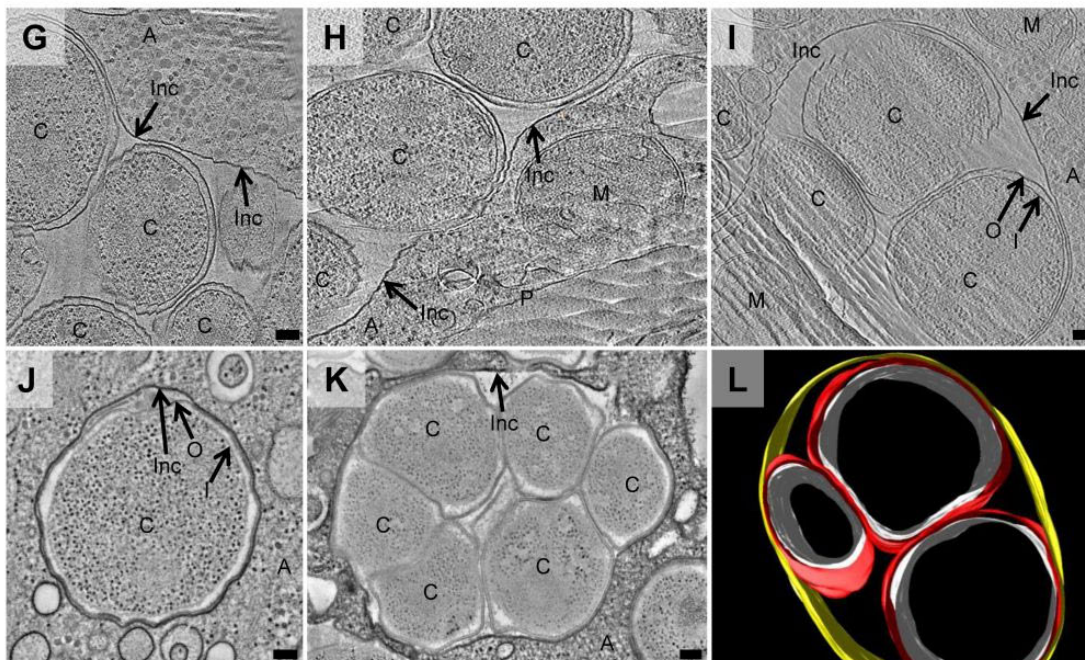
**Figure 2: Crescent bodies are not a developmental stage, but rather artifacts of conventional EM.** Crescent bodies were not observed in cryotomograms of either plunge-frozen (Figure 1, Movie S1) or cryosectioned cells (Figure 3, 4). A 2D overview image of an infected amoeba cell only showed roundish structures, representing chlamydial cells or mitochondria (A, B enlarged). In contrast, when purified *Parachlamydia* cells were fixed, dehydrated, plastic-embedded and imaged as in [1], crescent bodies (C, D arrows) were observed frequently ( $47\% \pm 10$ ). The use of a low-osmolarity, low-fixative concentration buffer resulted in far fewer ( $2\% \pm 2$ ) crescent bodies (E). Higher osmolarity and higher fixative concentration also resulted in higher percentages of crescent bodies or cells with large invaginations as observed by scanning electron microscopy (F); the graph displays the percentage of purified *Parachlamydia* cells forming crescent shapes or large invaginations after fixation with different buffers (error bars indicate the 95% confidence intervals of percentages; buffer osmolarity is indicated on the right vertical axis). Representative scanning electron microscopy images of purified *Parachlamydia* cells with different degrees of invagination are shown. “CS” crescent shape, “LV” large invaginations, “SV” small invaginations, “CO” coccoid, “GA” glutaraldehyde, “PB” phosphate buffer, “CaCo” cacodylate buffer. Bars 2  $\mu$ m (A, B, D, E, F) or 200 nm (C).

slightly lower than noted since extensions of the inclusions above and below the section cannot be visualized. Interestingly, we observed a difference in cell shape between *Simkania* EBs imaged inside densely packed inclusions within their host versus after purification. While EBs imaged inside these inclusions were frequently rod-shaped or elongated (cells labeled "EB" in Figure 3 F and Figure 5 A), purified EBs were always spherical (Figure 1 A). *Parachlamydia* and *Protochlamydia* EBs, in contrast, were always coccoid (Figure 1 D, G and cells labeled "EB" in Figure 5 B, C). RBs of all species had a somewhat polymorphic, spherical shape inside the host cell.

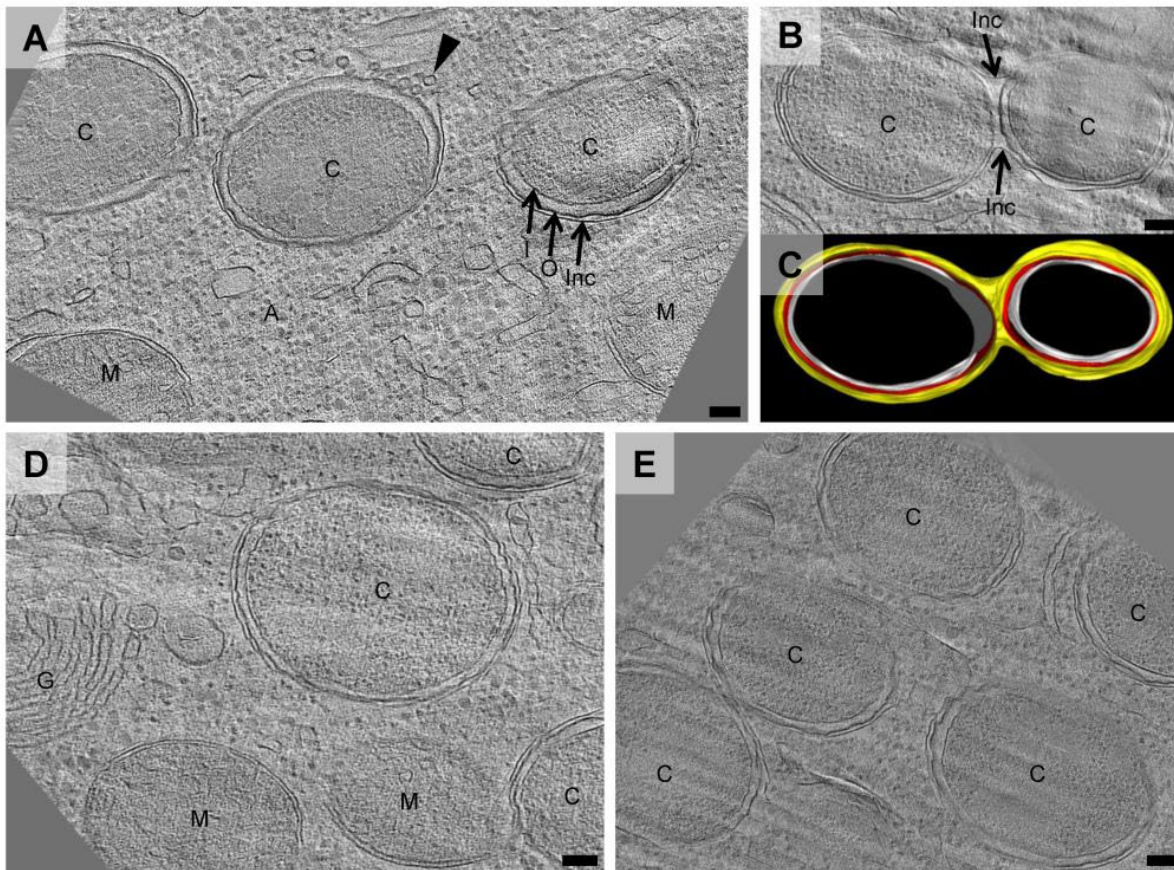
### **Recruitment of endoplasmic reticulum by *Simkania***

Chlamydiae associate not only with the inclusion membrane, but some also recruit and reshape entire host organelles. We found that inclusions of *Simkania* were always enveloped by an additional membranous structure (Figure 3 A-F). The granularity inside the cisternae-like membrane sacs was different from the rest of the eukaryotic cytoplasm, suggesting that they were part of a separate compartment. The ER-like membrane architecture and the presence of many ribosomes on the cytoplasmic side of the distal membrane identified the compartment as rough ER. Segmentations showed that the inclusions were not entirely surrounded by the rough ER, however, leaving small patches of direct connections between inclusion and amoeba cytoplasm (Figure 3 D). The rough ER was found associated with single- (Figure 3 A, B, E) and multi-cellular inclusions filled with EBs and RBs (Figure 3 C, F), indicating that ER recruitment occurs early after internalization and remains throughout the intracellular stage.

In contrast to *Simkania*, no direct association of *Parachlamydia* or *Protochlamydia* inclusions and any host organelle was detected. Mitochondria were occasionally observed in their vicinity (Figure 3 G-L, Figure 4 A-E), but a specific co-localization was not suggested by fluorescent labeling of mitochondria (Figure S1).

**Sim****Par**

**Figure 3: *Simkania* and *Parachlamydia* form multicellular inclusions, but only *Simkania* inclusions recruit the host endoplasmic reticulum.** To investigate *Simkania* (A-F) and *Parachlamydia* (G-L) inside their host, infected amoeba cultures were high-pressure frozen, cryosectioned and imaged by ECT (cryotomographic slices are shown in A-C, G-I). For comparison, another sample was high-pressure frozen, freeze-substituted, plastic-embedded, stained and imaged at room temperature (tomographic slices are shown in E, F, J, K). *Simkania* and *Parachlamydia* cells "C" were found inside uni- (A, B, E, J) and multi- (C, F, G, H, K, L) cellular inclusions ("Inc" inclusion membrane, "I" chlamydial inner membrane, "O" chlamydial outer membrane, "P" amoeba plasma membrane, "A" amoeba cytoplasm, "M" mitochondrion). Every *Simkania* inclusion (A-F) was observed in close association with cisternae-like ribosome ("R")-studded structures, likely host rER ("ER"). The host ER almost entirely enveloped the inclusion (3D-model of A in D, blue arrow indicating viewing direction; see also Movie S2). Note that membranes in close proximity (e.g. "Inc" and rER membrane in E) cannot be identified as two separate membranes in conventional EM images (E, F). L is a 3D-model of I (Movie S3). Colors in models: white "I", red "O", yellow "Inc", blue "ER", green "R". Bars, 100 nm.

**Pro**

**Figure 4: *Protochlamydia* inclusions divide with chlamydial cells.** (A, B, D, E) are cryotomographic slices of cryosectioned amoeba cells infected with *Protochlamydia*. In contrast to *Simkania* and *Parachlamydia*, *Protochlamydia* cells "C" were found only inside unicellular inclusions, or in bicellular inclusions which were either in the process of division or fusion ("Inc" inclusion membrane, "I" chlamydial inner membrane, "O" chlamydial outer membrane, "P" amoeba plasma membrane, "A" amoeba cytoplasm, "G" Golgi, "M" mitochondria). In some cases, the inclusion membrane showed budding vesicles (arrowhead), suggesting more active inclusion membrane dynamics than in *Simkania* or *Parachlamydia*. C is a 3D-model of B (white "I", red "O", yellow "Inc"; Movie S3).

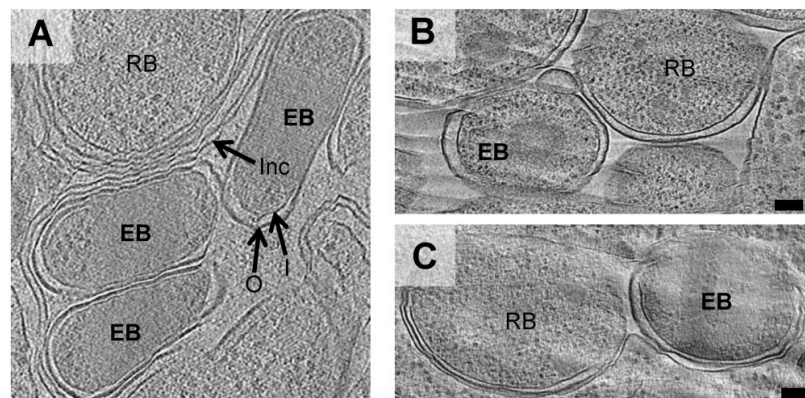


**Figure 5: *Simkania* EBs show an elongated cell shape in densely packed inclusions inside the host cell.** (A-C) show cryotomographic slices of cryosectioned amoebae infected with *Simkania*, *Parachlamydia* or *Protochlamydia* in which EBs could be identified by the granularity of the cytoplasm. In contrast to the coccoid shape of purified EBs (Figure 1), *Simkania* EBs inside host cells (A and Figure 3 F) were sometimes elongated. *Protochlamydia* and *Parachlamydia* EBs were always coccoid, both purified (Figure 1) and inside amoebae (B and C, respectively). Bars, 100 nm.

## Secretion systems

Translocation of chlamydial effector proteins into the inclusion membrane and into the host cytoplasm is crucial for chlamydiae to shape their intracellular environment. In a cryotomogram of a *Simkania* EB we observed a structure with characteristics typical of a T3S apparatus (Figure 6 A, B) [40]. A density in the periplasm was found to be similar to T3S basal bodies and connected to an extracellular needle-like structure. The needle (length 63 nm, diameter 9 nm) seemed to be engaged with a membranous structure, possibly a remnant of the host cell. The dimensions of the apparatus were similar to projections seen on the surface of infectious *Chlamydia psittaci* cells [34].

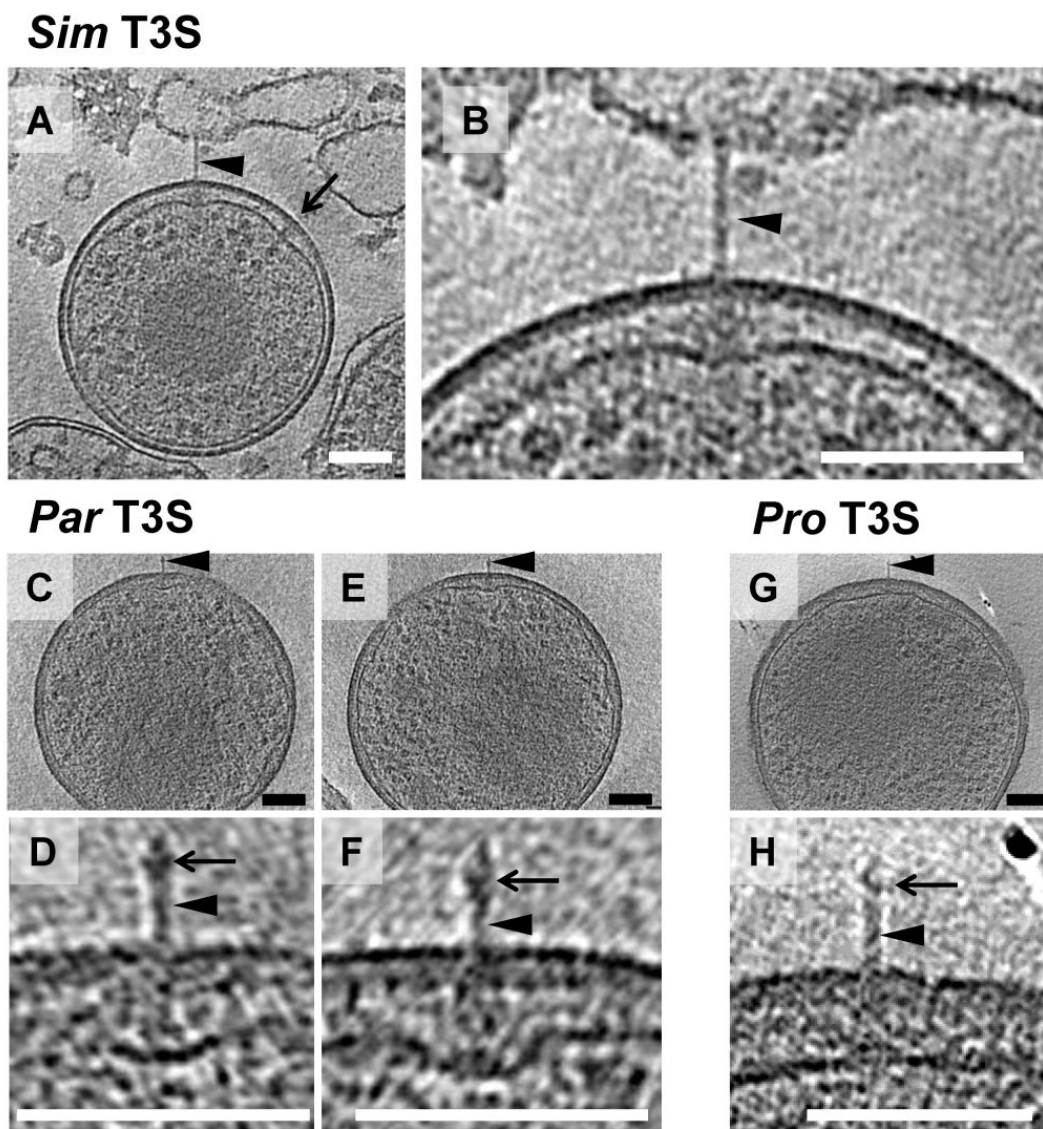


**Figure 6: Type III secretion systems.** Shown are slices through cryotomograms of purified *Simkania* (A and B enlarged), *Parachlamydia* (C, E and D, F enlarged) and *Protochlamydia* (G and H enlarged) EBs. All species show T3S structures (arrowheads in A-H). A pronounced widening of the periplasm was observed in *Simkania* (B) and *Parachlamydia* (D, F) to accommodate the T3S basal body. Often, such widening with periplasmic densities was observed in the absence of a needle in *Simkania* EBs (arrow in A and Figure S2), suggesting some needles are sheared off during purification. *Parachlamydia* and *Protochlamydia* T3S needles exhibited a bulge (arrows in D, F, H) where needle-tip proteins have been found in other bacteria.



Interestingly, the otherwise relatively narrow distance between the inner and outer membrane (13 nm) in *Simkania* EBs required a bulging (41 nm) of the cytoplasmic membrane to accommodate the basal body. Such widening of the periplasm was observed frequently in the same and other EBs (Figure 6 A and Figure S2). Basal body-like densities inside these bulges indicate that they likely represented T3S structures as well, but the corresponding needles were probably sheared off during purification. A pronounced widening of the periplasmic space was also reported for T3S structures of *Chlamydia trachomatis* [27].

Putative T3S systems in *Parachlamydia* showed a similar bulging of the periplasm in the region of the basal body (36-44 nm rather than 17 nm) (Figure 6 C-F). The needle structure was substantially different compared to *Simkania*, with a length of 38-42 nm, a diameter of 6-7 nm and a widening (12 nm) of the needle 7 nm from its tip (Figure 6 D, F). A T3S-like structure found on a *Protochlamydia* EB comprised a 52-nm long, 7-nm diameter needle, and may have also had a widening close to the needle tip (Figure 6 G, H). Periplasmic bulging was not observed, however, as the width of the periplasm in *Protochlamydia* was already ~40 nm.

## Discussion

### EBs and RBs in a life-like state

Early conventional EM studies suggested that the DNA in EBs is condensed [41], which was later found to be mediated by histone-like proteins [42]. However, nucleoid structure in particular is prone to artifacts introduced by fixation, dehydration and staining in conventional EM [39]. While a more recent ECT study imaged *C. trachomatis* cells preserved in a near-native, frozen-hydrated state, such ultrastructural details were unfortunately not resolved probably due to instrumental limitations [43]. Again plunge-freezing cells, but using higher electron energies and energy filtration, here we have confirmed that EB genomes are indeed densely packed. Our finding of ribosomes in EBs is consistent with the notion that they are metabolically active to some degree [44] [45] rather than completely dormant [46]. Besides size differences of EBs and RBs not observed before for environmental chlamydiae, another distinguishing feature between the developmental stages we noted was the variable periplasmic width in RBs. This is consistent with the notion that lower abundances of stabilizing cysteine-rich proteins in RBs result in more flexible outer membranes [47]. Similarly, the more flexible shape and deformation of *Simkania* EBs inside host cells compared to *Protochlamydia* and *Parachlamydia*, might be a consequence of differences in cell envelope architecture, such as the absence of the cysteine-rich proteins which *Simkania* lacks in contrast to all other chlamydiae [17].

### **Crescent bodies are an artifact**

While crescent-shaped cells had been seen previously and thought to represent a distinct developmental stage [1,22,23], here we showed that they are artifacts of conventional EM methods. While no crescent bodies have been reported for the pathogenic *Chlamydiaceae*, EBs with peculiar stellate outlines were found occasionally. The previous hypothesis that this morphology could be attributed to EM preparation methods as well [48] is supported by our results. The reason for crescent bodies not being observed in *Chlamydiaceae* could be differences in their outer membrane protein composition compared to environmental chlamydiae [17,49], leading to different effects during chemical fixation and dehydration/embedding.

Trapezoidal, dumbbell-shaped and elongated intracellular *Simkania* EBs have also been described in the past [50-52]. While we found elongated morphologies especially in cells tightly packed in inclusions, trapezoidal and dumbbell-shaped forms were never seen, suggesting that those are also artifacts. Conventional EM studies of other environmental chlamydiae EBs have reported head-and-tail, star and rod shapes [13,15,53]. It remains unclear whether these morphologies are natural.

Shapes of bacteria from other phyla have also been reported to be affected by chemical fixation and dehydration. For instance, crescent shaped cells were observed for *Gemmata obscuriglobus* [54], a member of the chlamydial sister-phylum *Planctomycetes*, and the mollicute *Acholeplasma laidlawii* [55], showing that fixation conditions must be chosen carefully to preserve the cell shape and that the description of new shapes based on fixed cells should be handled with caution.

### **Diversity of the intracellular niche of environmental chlamydiae**

Most chlamydiae are known to reside inside the host-derived membranous inclusion after host cell invasion [19], but *Parachlamydia* and *Simkania* have also been reported to be localized directly in the cytoplasm [1,7]. Here, intracellular chlamydiae were always seen surrounded by an inclusion membrane, supporting the importance of this host-bacterium interface for intracellular survival and replication. Inclusions in *Protochlamydia* infections were exclusively unicellular, but *Simkania* and *Parachlamydia* cells were more commonly found in multicellular inclusions.

Some chlamydial species are known to recruit and reshape entire host organelles including mitochondria, Golgi stacks or the endoplasmic reticulum (ER) [24,27-29,31]. We found that *Simkania* inclusions are almost entirely enveloped by the rough ER (Figure 3), adding additional layers to the host-bacterial interface. In this way *Simkania* might use a similar strategy as the facultative intracellular pathogens *Legionella pneumophila* and *Brucella abortus* [56-58]. However, in contrast to

*L. pneumophila* and *B. abortus* phagosomes, the *Simkania* inclusion does not fuse with ER-derived vesicles, and *Simkania* thus remains inside the inclusion. The tight association of the *Simkania* inclusion with the ER could nevertheless provide similar benefits such as prevention from fusing with lysosomes. Interestingly, the abilities to recruit ER and to replicate in human and insect cells coincide in *Simkania* [59,60] and members of the pathogenic chlamydiae [27], but are absent in *Parachlamydia* and *Protochlamydia*.

Species-specific differences in inclusion morphology and recruitment of host organelles are likely due to the presence of different effector proteins in the inclusion membrane [61-63]. Adaptation to different hosts likely drove the diversification of environmental chlamydiae [17,18].

### **Type III secretion systems**

Translocation of chlamydial effector proteins through the elaborate cell envelope and the inclusion membrane requires a secretion system and is thought to be accomplished by the type III secretion (T3S) system. T3S systems are encoded in all known chlamydial genomes [17,32] and T3S proteins were detected during all stages of infection in members of the pathogenic chlamydiae [64]. For the first time, we detected T3S-like structures in environmental chlamydiae, providing evidence for its conservation and crucial role in the infectious life cycle of modern and likely ancient chlamydiae. Fewer T3S-like structures were observed by ECT in environmental chlamydiae than by conventional transmission electron microscopy in pathogenic chlamydiae [65,66].

T3S needle tip proteins in other bacteria are known to be highly adapted to the host [67]. It has been unclear whether the chlamydial T3S needle harbors a tip protein at all. To date only one candidate for a chlamydial needle tip protein has been identified, but it remains unclear whether it rather functions as an effector [68,69]. The sub-terminal widening of the needle in *Parachlamydia* and *Protochlamydia* seen here indicates that the chlamydial T3S apparatus likely does include a needle tip protein. Interestingly, T3S structures were not seen on purified or cryosectioned RBs, perhaps because the juxtaposition of the RB outer membrane and inclusion membrane effects the length of the needle.

### **Imaging bacteria-host interactions in a near-native state**

Finally, this is the first study to image bacteria *inside their host* in a near-native, frozen-hydrated state. In addition to avoiding and uncovering artifacts, this approach provided novel insights into the

nature of the host-bacterial interface. Because amoebae can also serve as hosts for important pathogens such as *Legionella pneumophila*, *Vibrio cholerae*, mycobacteria, *Francisella tularensis*, *Pseudomonas aeruginosa*, and *Helicobacter pylori* as well as bacterial symbionts like *Amoebophilus asiaticus*, *Paracaedibacter symbiosus* or *Procabacter acanthamoebae* [70,71], our approach should prove helpful in the study of many other important bacteria-host interactions in the future.

## Experimental procedures

### Cultivation of organisms and staining of mitochondria

*Acanthamoeba castellanii* UWC1 infected with *Parachlamydia acanthamoebae* UV7 or *Simkania negevensis* and *A. castellanii* Neff infected with *Protochlamydia amoebophila* UWE25 were cultivated in TSY (trypticase soy broth with yeast extract) medium (30 g/L trypticase soy broth, 10 g/L yeast extract, pH 7.3) at 20°C. Amoebal growth was monitored by light microscopy and medium was exchanged every 3-6 days. The presence and identity of the chlamydial symbionts was checked regularly by fluorescence *in situ* hybridization (FISH) combined with 4',6-diamidino-2-phenylindole staining of infected cultures using specific probes for the respective symbiont as described previously [71]. In addition, the identity of the symbionts was verified by isolation of DNA from cultures followed by amplification and sequencing of the 16S rRNA genes. For staining of mitochondria, *A. castellanii* infected with chlamydial symbionts were incubated with 2 µM MitoTracker Orange CMTMRos in TSY for 45 min. Cells were fixed with 4% paraformaldehyde, followed by FISH with specific probes.

### Purification of chlamydiae

Infected *A. castellanii* cultures were harvested by centrifugation (7,197 × g, 10 min), washed in Page's Amoebic Saline (PAS) [72], centrifuged and resuspended in PAS. Amoeba cells were ruptured by vortexing with an equal volume of glass beads for 3 minutes. Glass beads and cell debris were removed by centrifugation (5 min, 300 × g). The supernatant was filtered through a 1.2 µm filter and centrifuged at maximum speed for 10 min. The obtained pellet was resuspended in PAS.

### Conventional transmission EM

To analyze the impact of fixation and to compare the effect of different fixation buffers on the morphology of *Parachlamydia*, chlamydiae were purified from their amoeba hosts, and the sample

was divided into three parts. One part was immediately plunge-frozen (see below). The second part was fixed in 4% glutaraldehyde in phosphate buffered saline (PBS, 130 mM NaCl, 10 mM Na<sub>x</sub>PO<sub>4</sub>; pH 7.2 – 7.4) for one hour, washed in PBS and further fixed in 1% osmium tetroxide in PBS for one hour followed by two washing steps. The third part was fixed in the same way as the second sample, except that 2% glutaraldehyde in phosphate buffer (10 mM Na<sub>x</sub>PO<sub>4</sub>; pH 7.2 – 7.4) was used as first fixative and that the 10 mM phosphate buffer replaced PBS in the following washing and fixation steps. Samples were dehydrated in ethanol and acetone through a graded series, embedded in Epon-Araldite (Electron Microscopy Sciences, Port Washington, PA), thin-sectioned with a UC6 ultramicrotome (Leica, Vienna, Austria), and stained with uranyl acetate and lead citrate. 2D images were recorded on a Tecnai T12 TEM (FEI, Eindhoven, the Netherlands).

For room temperature EM of high-pressure frozen/freeze substituted samples, infected amoeba cells were high-pressure frozen (see below). The frozen domes were transferred under liquid nitrogen to cryotubes containing 2% or 0.04% glutaraldehyde in acetone. The tubes were placed in a AFS Freeze-Substitution machine (Leica) and freeze-substituted at –90°C for 60 h, then warmed to –20°C over 10 h. Cells were rinsed 3× with cold acetone, then post-fixed with 2.5% osmium tetroxide in acetone at –20°C for 24 h. The samples were then warmed to 4°C over 2 h, rinsed 3× with cold acetone, and embedded in Epon-Araldite resin (Electron Microscopy Sciences). Following polymerization, semi-thin (200 nm) sections were cut with a UC6 ultramicrotome (Leica) and placed on Formvar-coated, copper/rhodium 1 mm slot grids (Electron Microscopy Sciences). Sections were stained with uranyl acetate and lead citrate and imaged in a Tecnai T12 TEM (FEI). Dual-axis tilt-series were acquired using SerialEM [73], then subsequently calculated and analyzed using IMOD [74] on an Apple MacPro computer.

### **Plunge-freezing**

For plunge-freezing, copper/rhodium EM grids (R2/2 or R2/1, Quantifoil, Jena, Germany) were glow-discharged for 1 min. A 20×-concentrated bovine serum albumin-treated solution of 10 nm colloidal gold (Sigma, St. Lois, MO) was added to purified chlamydiae (1:4 v/v) immediately before plunge freezing. A 4-μl droplet of the mixture was applied to the EM grid, then automatically blotted and plunge-frozen into a liquid ethane-propane mixture [75] using a Vitrobot (FEI Company) [76].

### **Cryosectioning**

*A. castellanii* cells continuously infected with either *Simkania*, *Parachlamydia* or *Protochlamydia* were mixed with uninfected amoeba cells at a ratio of 1:1 and incubated for 24 hours. For

*Parachlamydia*, the ratio of infected to uninfected cells was 5:1. Amoebae were harvested (7,197 x g, 10 min) and the pellet was mixed with 40% dextran (w/v) in PAS. The samples were transferred to brass planchettes and rapidly frozen in a HPM010 high-pressure freezing machine (Bal-Tec, Leica). Cryosectioning of the vitrified samples was done as previously described [77,78]. Semi-thin (90–200 nm) cryosections were cut at  $-145^{\circ}\text{C}$  or  $-160^{\circ}\text{C}$  with a  $25^{\circ}$  Cryo diamond knife (Diatome, Biel, Switzerland), transferred to grids (continuous-carbon coated 200-mesh copper grids or 700-mesh uncoated copper grids), and stored in liquid nitrogen.

## ECT

Images were collected using a Polara 300 kV FEG transmission electron microscope (FEI Company) equipped with an energy filter (slit width 20 eV; Gatan, Pleasanton, CA) on a lens-coupled 4 kx4 k UltraCam charge-coupled device (CCD) (Gatan) or K2 Summit direct electron detector (Gatan). Pixels on the CCD represented 0.95 nm (22,500x) or 0.63 nm (34,000x) at the specimen level. Typically, tilt series were recorded from  $-60^{\circ}$  to  $+60^{\circ}$  with an increment of  $1^{\circ}$  at 10  $\mu\text{m}$  under-focus. The cumulative dose of a tilt-series was 180–220  $\text{e}^{-}/\text{\AA}^2$  (for whole cells) or 100–150  $\text{e}^{-}/\text{\AA}^2$  (for cryosections). UCSF Tomo [79] was used for automatic acquisition of tilt-series and 2D projection images. Three-dimensional reconstructions were calculated using the IMOD software package [74] or Raptor [80]. Tomograms of cryosections were reconstructed using IMOD's patch tracking to generate the aligned stack [74]. Tomograms were visualized and segmented using 3dMOD [74].

## SEM

Glass coverslips (12 mm diameter) were cleaned in acidic ethanol, dried for one hour at  $60^{\circ}\text{C}$  and coated with 0.01% poly-L-Lysine solution for 10 min. 200  $\mu\text{l}$  of purified *Parachlamydia* in the respective buffer were spotted onto the dry coverslip. After 10 min non-attached cells were removed and remaining cells were fixed for one hour at room temperature using the following fixatives: 2 % glutaraldehyde in 10 mM phosphate buffer (pH 7.2), 2.5 % glutaraldehyde in 3 mM cacodylate buffer (pH 7.2), 2% glutaraldehyde in DGM-21A defined medium [44], 4% glutaraldehyde in 10 mM phosphate buffer with 130 mM NaCl and 4% glutaraldehyde in 10 mM phosphate buffer with 260 mM NaCl. After three washing steps (5 min each) in the respective buffer, cells were further fixed in 1% osmium tetroxide in the respective buffer for one hour at room temperature and washed again three times. Samples were dehydrated in acetone and chemically dried in hexamethyldisilazane. Glass slides were gold coated for 160 sec using default settings (Agar sputter coater B7340) and

analyzed using a Philips XL-30 ESEM. For analysis 10 or more random SEM images with 36 or more individual putative bacterial cells in total were taken. Roundish or crescent shaped objects with a diameter of 0.5-1  $\mu\text{m}$  were counted as bacterial cells. Each cell was then classified into one out of four morphological types (crescent shape, large invaginations, small invaginations, coccoid) and the percentage of each type was determined. Osmolarity measurements of buffers and fixatives were performed using an Advanced Micro 3MO plus osmometer (Block Scientific, New York, NY). Samples and standards were measured three times each.

### **Acknowledgments**

This work was funded by the Austrian Science Fund FWF (Y277-B03 to MH), the European Research Council (ERC StG “EvoChlamy” to MH), the Caltech Center for Environmental Microbiology Interactions (to GJJ, MP), and a gift from the Gordon and Betty Moore Foundation to Caltech.

### **Conflict of interest statement**

The authors declare no conflict of interest.

## References

1. Greub G, Raoult D (2002) Crescent bodies of *Parachlamydia acanthamoebae* and its life cycle within *Acanthamoeba polyphaga*: an electron micrograph study. *Appl Environ Microbiol* 68: 3076-3084.
2. Horn M (2008) Chlamydiae as symbionts in eukaryotes. *Ann Rev Microbiol* 62.
3. Horn M, Collingro A, Schmitz-Esser S, Beier CL, Purkhold U, et al. (2004) Illuminating the evolutionary history of chlamydiae. *Science* 304: 728-730.
4. Kamneva OK, Knight SJ, Liberles DA, Ward NL (2012) Analysis of genome content evolution in pvc bacterial super-phylum: assessment of candidate genes associated with cellular organization and lifestyle. *Genome Biology and Evolution* 4: 1375-1390.
5. Subtil A, Collingro A, Horn M (2013) Tracing back to primordial chlamydiae, extinct parasites of plants? . *Trends Plant Science* in press.
6. Rourke AW, Davis RW, Bradley TM (1984) A light and electron microscope study of epitheliocystis in juvenile steelhead trout, *Salmo gairdneri* Richardson. *Journal of Fish Diseases* 7: 301-309.
7. Michel R, Hauröder-Philippczyk B, Müller K-D, Weishaar I (1994) *Acanthamoeba* from human nasal mucosa infected with an obligate intracellular parasite. *European Journal of Protistology* 30: 104-110.
8. Rurangirwa FR, Dilbeck PM, Crawford TB, McGuire TC, McElwain TF (1999) Analysis of the 16S rRNA gene of microorganism WSU 86-1044 from an aborted bovine foetus reveals that it is a member of the order *Chlamydiales*: proposal of *Waddliaceae* fam. nov., *Waddlia chondrophila* gen. nov., sp. nov. *Int J Syst Bacteriol* 49: 577-581.
9. Amann R, Springer N, Schonhuber W, Ludwig W, Schmid EN, et al. (1997) Obligate intracellular bacterial parasites of acanthamoebae related to *Chlamydia* spp. *Appl Environ Microbiol* 63: 115-121.
10. Horn M, Wagner M, Muller KD, Schmid EN, Fritsche TR, et al. (2000) *Neochlamydia hartmannellae* gen. nov., sp. nov. (*Parachlamydiaceae*), an endoparasite of the amoeba *Hartmannella vermiformis*. *Microbiology* 146 ( Pt 5): 1231-1239.
11. Kahane SEM, Friedman MG (1995) Evidence that the novel microorganism 'Z' may belong to a new genus in the family *Chlamydiaceae*. *FEMS Microbiol Lett* 126: 203-208.
12. Draghi A, 2nd, Popov VL, Kahl MM, Stanton JB, Brown CC, et al. (2004) Characterization of "*Candidatus* Piscichlamydia salmonis" (order *Chlamydiales*), a chlamydia-like bacterium associated with epitheliocystis in farmed Atlantic salmon (*Salmo salar*). *J Clin Microbiol* 42: 5286-5297.
13. Kostanjsek R, Strus J, Drobne D, Avgustin G (2004) '*Candidatus* Rhabdochlamydia porcellionis', an intracellular bacterium from the hepatopancreas of the terrestrial isopod *Porcellio scaber* (Crustacea: Isopoda). *Int J Syst Evol Microbiol* 54: 543-549.
14. Fritsche TR, Horn M, Wagner M, Herwig RP, Schleifer KH, et al. (2000) Phylogenetic diversity among geographically dispersed *Chlamydiales* endosymbionts recovered from clinical and environmental isolates of *Acanthamoeba* spp. *Appl Environ Microbiol* 66: 2613-2619.
15. Karlsen M, Nylund A, Watanabe K, Helvik JV, Nylund S, et al. (2008) Characterization of '*Candidatus* Clavochlamydia salmonicola': an intracellular bacterium infecting salmonid fish. *Environ Microbiol* 10: 208-218.



16. Thomas V, Casson N, Greub G (2006) *Criblamydia sequanensis*, a new intracellular *Chlamydiales* isolated from Seine river water using amoebal co-culture. *Environ Microbiol* 8: 2125-2135.
17. Collingro A, Tischler P, Weinmaier T, Penz T, Heinz E, et al. (2011) Unity in Variety—The Pan-Genome of the *Chlamydiae*. *Molecular Biology and Evolution* 28: 3253-3270.
18. Bertelli C, Collyn F, Croxatto A, Ruckert C, Polkinghorne A, et al. (2010) The *Waddlia* genome: a window into chlamydial biology. *PLoS ONE* 5: e10890.
19. Hackstadt T, Fischer ER, Scidmore MA, Rockey DD, Heinzen RA (1997) Origins and functions of the chlamydial inclusion. *Trends in Microbiology* 5: 288-293.
20. Abdelrahman YM, Belland RJ (2005) The chlamydial developmental cycle. *FEMS Microbiol Rev* 29: 949-959.
21. Hybiske K, Stephens RS (2007) Mechanisms of host cell exit by the intracellular bacterium *Chlamydia*. *Proc Natl Acad Sci U S A* 104: 11430-11435.
22. Lamothe F, Greub G (2010) Amoebal pathogens as emerging causal agents of pneumonia. *FEMS Microbiology Reviews* 34: 260-280.
23. Nakamura S, Matsuo J, Hayashi Y, Kawaguchi K, Yoshida M, et al. (2010) Endosymbiotic bacterium *Protochlamydia* can survive in acanthamoebae following encystation. *Environ Microbiol Rep* 2: 611-618.
24. Heuer D, Lipinski AR, Machuy N, Karlas A, Wehrens A, et al. (2009) *Chlamydia* causes fragmentation of the Golgi compartment to ensure reproduction. *Nature* 457: 731-735.
25. Hackstadt T, Scidmore MA, Rockey DD (1995) Lipid metabolism in *Chlamydia trachomatis*-infected cells: directed trafficking of Golgi-derived sphingolipids to the chlamydial inclusion. *Proc Natl Acad Sci U S A* 92: 4877-4881.
26. Carabeo RA, Mead DJ, Hackstadt T (2003) Golgi-dependent transport of cholesterol to the *Chlamydia trachomatis* inclusion. *Proc Natl Acad Sci U S A* 100: 6771-6776.
27. Dumoux M, Clare DK, Saibil HR, Hayward RD (2012) Chlamydiae Assemble a Pathogen Synapse to Hijack the Host Endoplasmic Reticulum. *Traffic* 13: 1612-1627.
28. Matsumoto A, Bessho H, Uehira K, Suda T (1991) Morphological studies of the association of mitochondria with chlamydial inclusions and the fusion of chlamydial inclusions. *J Electron Microsc (Tokyo)* 40: 356-363.
29. Peterson EM, de la Maza LM (1988) Chlamydia parasitism: ultrastructural characterization of the interaction between the chlamydial cell envelope and the host cell. *J Bacteriol* 170: 1389-1392.
30. Friis RR (1972) Interaction of L Cells and *Chlamydia psittaci*: Entry of the Parasite and Host Responses to Its Development. *J Bacteriol* 110: 706-721.
31. Croxatto A, Greub G (2010) Early intracellular trafficking of *Waddlia chondrophila* in human macrophages. *Microbiology* 156: 340-355.
32. Peters J, Wilson DP, Myers G, Timms P, Bavoil PM (2007) Type III secretion a la *Chlamydia*. *Trends Microbiol* 15: 241-251.
33. Nichols BA, Setzer PY, Pang F, Dawson CR (1985) New view of the surface projections of *Chlamydia trachomatis*. *J Bacteriol* 164: 344-349.

34. Matsumoto A (1979) Recent progress of electron microscopy in microbiology and its development in future: from a study of the obligate intracellular parasites, chlamydia organisms. *J Electron Microsc*, 28: 57-64.
35. Binet R, Maurelli AT (2009) Transformation and isolation of allelic exchange mutants of *Chlamydia psittaci* using recombinant DNA introduced by electroporation. *Proc Natl Acad Sci U S A* 106: 292-297.
36. Wang Y, Kahane S, Cutcliffe LT, Skilton RJ, Lambden PR, et al. (2011) Development of a transformation system for *Chlamydia trachomatis*: restoration of glycogen biosynthesis by acquisition of a plasmid shuttle vector. *PLoS Pathog* 7: e1002258.
37. Kari L, Goheen MM, Randall LB, Taylor LD, Carlson JH, et al. (2011) Generation of targeted *Chlamydia trachomatis* null mutants. *Proc Natl Acad Sci U S A* 108: 7189-7193.
38. Nguyen BD, Valdivia RH (2012) Virulence determinants in the obligate intracellular pathogen *Chlamydia trachomatis* revealed by forward genetic approaches. *Proc Natl Acad Sci U S A* 109: 1263-1268.
39. Pilhofer M, Ladinsky MS, McDowall AW, Jensen GJ (2010) Chapter 2 - Bacterial TEM: New Insights from Cryo-Microscopy. In: Thomas M-R, editor. *Methods in Cell Biology: Academic Press*. pp. 21-45.
40. Marlovits TC, Kubori T, Sukhan A, Thomas DR, Galán JE, et al. (2004) Structural Insights into the Assembly of the Type III Secretion Needle Complex. *Science* 306: 1040-1042.
41. Moulder JW (1966) The relation of the psittacosis group (Chlamydiae) to bacteria and viruses. *Annu Rev Microbiol* 20: 107-130.
42. Barry CE, Hayes SF, Hackstad tT (1992) Nucleoid condensation in *Escherichia coli* that express a chlamydial histone homolog. *Science* 256: 377-379.
43. Huang Z, Chen M, Li K, Dong X, Han J, et al. (2010) Cryo-electron tomography of *Chlamydia trachomatis* gives a clue to the mechanism of outer membrane changes. *Journal of Electron Microscopy* 59: 237-241.
44. Haider S, Wagner M, Schmid MC, Sixt BS, Christian JG, et al. (2010) Raman microspectroscopy reveals long-term extracellular activity of chlamydiae. *Molecular Microbiology* 77: 687-700.
45. Sixt BS, Siegl A, Müller C, Watzka M, Wultsch A, et al. (2013) Metabolic features of *Protochlamydia amoebophila* elementary bodies - a link between activity and infectivity in Chlamydiae. *PLoS pathogens* in press
46. Hatch TP, Miceli M, Silverman JA (1985) Synthesis of protein in host-free reticulate bodies of *Chlamydia psittaci* and *Chlamydia trachomatis*. *J Bacteriol* 162: 938-942.
47. Hatch TP, Miceli M, Sublett JE (1986) Synthesis of disulfide-bonded outer membrane proteins during the developmental cycle of *Chlamydia psittaci* and *Chlamydia trachomatis*. *J Bacteriol* 165: 379-385.
48. Matsumoto A (1988) Structural characteristics of chlamydial bodies; Barron AL, editor. Boca Raton FL: CRC Press.
49. Heinz E, Tischler P, Rattei T, Myers G, Wagner M, et al. (2009) Comprehensive in silico prediction and analysis of chlamydial outer membrane proteins reflects evolution and life style of the *Chlamydiae*. *BMC Genomics* 10: 634.
50. Henning K, Zöller L, Hauröder B, Hotzel H, Michel R (2007) *Hartmannella vermiformis* (Hartmannellidae) harboured a hidden chlamydia-like endosymbiont. *Endocytobiosis Cell Res* 18: 1-10.

51. Kahane S, Dvoskin B, Mathias M, Friedman MG (2001) Infection of *Acanthamoeba polyphaga* with *Simkania negevensis* and *S. negevensis* survival within amoebal cysts. *Appl Environ Microbiol* 67: 4789-4795.
52. Michel R, Müller KD, Zöller L, Walochnik J, Hartmann M, et al. (2005) Free-living amoebae serve as a host for the *Chlamydia*-like bacterium *Simkania negevensis*. *Acta Protozoologica* 44: 113-121.
53. Lienard J, Croxatto A, Prod'hom G, Greub G (2011) *Estrella lausannensis*, a new star in the Chlamydiales order. *Microbes and Infection* 13: 1232-1241.
54. Lindsay MR, Webb RI, Hosmer HM, Fuerst JA (1995) Effects of fixative and buffer on morphology and ultrastructure of a freshwater planctomycete, *Gemmata obscuriglobus*. *J Microbiol Methods* 21: 45-54.
55. Lemcke RM (1972) Osmolar Concentration and Fixation of Mycoplasmas. *J Bacteriol* 110: 1154-1162.
56. Swanson MS, Isberg RR (1995) Association of *Legionella pneumophila* with the macrophage endoplasmic reticulum. *Infection and Immunity* 63: 3609-3620.
57. Abu Kwaik Y, Gao LY, Stone BJ, Venkataraman C, Harb OS (1998) Invasion of protozoa by *Legionella pneumophila* and its role in bacterial ecology and pathogenesis. *Appl Environ Microbiol* 64: 3127-3133.
58. Roy CR (2002) Exploitation of the endoplasmic reticulum by bacterial pathogens. *Trends Microbiol* 10: 418-424.
59. Kahane S, Fruchter D, Dvoskin B, Friedman MG (2007) Versatility of *Simkania negevensis* infection in vitro and induction of host cell inflammatory cytokine response. *J Infect* 55: e13-21.
60. Sixt BS, Hiess B, König L, Horn M (2012) Lack of Effective Anti-Apoptotic Activities Restricts Growth of *Parachlamydiaceae* in Insect Cells. *PLoS ONE* 7: e29565.
61. Betts HJ, Wolf K, Fields KA (2009) Effector protein modulation of host cells: examples in the *Chlamydia* spp. arsenal. *Current Opinion in Microbiology* 12: 81-87.
62. Heinz E, Rockey DD, Montanaro J, Aistleitner K, Wagner M, et al. (2010) Inclusion Membrane Proteins of *Protochlamydia amoebophila* UWE25 Reveal a Conserved Mechanism for Host Cell Interaction among the *Chlamydiae*. *J Bacteriol* 192: 5093-5102.
63. Rockey DD, Grosenbach D, Hruby DE, Peacock MG, Heinzen RA, et al. (1997) *Chlamydia psittaci* IncA is phosphorylated by the host cell and is exposed on the cytoplasmic face of the developing inclusion. *Mol Microbiol* 24: 217-228.
64. Fields KA, Mead DJ, Dooley CA, Hackstadt T (2003) *Chlamydia trachomatis* type III secretion: evidence for a functional apparatus during early-cycle development. *Mol Microbiol* 48: 671-683.
65. Matsumoto A (1982) Electron microscopic observations of surface projections on *Chlamydia psittaci* reticulate bodies. *J Bacteriol* 150: 358-364.
66. Wilson DP, Timms P, McElwain DL, Bavoil PM (2006) Type III secretion, contact-dependent model for the intracellular development of chlamydia. *Bull Math Biol* 68: 161-178.
67. Abby SS, Rocha EPC (2012) The Non-Flagellar Type III Secretion System Evolved from the Bacterial Flagellum and Diversified into Host-Cell Adapted Systems. *PLoS Genet* 8: e1002983.
68. Markham AP, Jaafar ZA, Kemege KE, Middaugh CR, Hefty PS (2009) Biophysical Characterization of *Chlamydia trachomatis* CT584 Supports Its Potential Role as a Type III Secretion Needle Tip Protein. *Biochemistry* 48: 10353-10361.

69. Stone CB, Sugiman-Marangos S, Bulir DC, Clayden RC, Leighton TL, et al. (2012) Structural Characterization of a Novel *Chlamydia pneumoniae* Type III Secretion-Associated Protein, Cpn0803. PLoS ONE 7: e30220.
70. Horn M, Wagner M (2004) Bacterial endosymbionts of free-living amoebae. J Eukaryot Microbiol 51: 509-514.
71. Schmitz-Esser S, Toenshoff ER, Haider S, Heinz E, Hoenninger VM, et al. (2008) Diversity of Bacterial Endosymbionts of Environmental *Acanthamoeba* Isolates. Appl Environl Microbiol 74: 5822-5831.
72. Page FC (1976) An illustrated key to freshwater and soil amoebae. Ambleside: Freshwater Biological Association.
73. Mastronarde DN (2005) Automated electron microscope tomography using robust prediction of specimen movements. J Struct Biol 152: 36-51.
74. Kremer JR, Mastronarde DN, McIntosh JR (1996) Computer visualization of three-dimensional image data using IMOD. J Struct Biol 1996/01/01: 71-76.
75. Tivol WF, Briegel A, Jensen GJ (2008) An improved cryogen for plunge freezing. Microsc Microanal 14: 375-379.
76. Iancu CV, Tivol WF, Schooler JB, Dias DP, Henderson GP, et al. (2006) Electron cryotomography sample preparation using the Vitrobot. Nat Protocols 1: 2813-2819.
77. Ladinsky MS (2010) Chapter Eight - Micromanipulator-Assisted Vitreous Cryosectioning and Sample Preparation by High-Pressure Freezing. In: Grant JJ, editor. Methods in Enzymology: Academic Press. pp. 165-194.
78. Ladinsky MS, Pierson JM, McIntosh JR (2006) Vitreous cryo-sectioning of cells facilitated by a micromanipulator. Journal of Microscopy 224: 129-134.
79. Zheng SQ, Keszthelyi B, Branlund E, Lyle JM, Braunfeld MB, et al. (2007) UCSF tomography: an integrated software suite for real-time electron microscopic tomographic data collection, alignment, and reconstruction. J Struct Biol 157: 138-147.
80. Amat F, Moussavi F, Comolli LR, Elidan G, Downing KH, et al. (2008) Markov random field based automatic image alignment for electron tomography. J Struct Biol 161: 260-275.

## Supplementary information

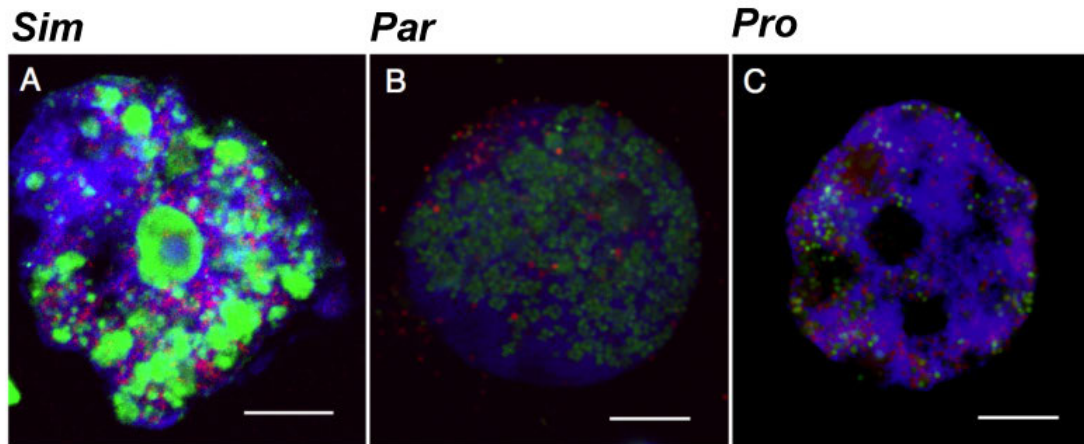


**Figure S1. *Simkania*, *Parachlamydia* and *Protochlamydia* do not recruit mitochondria to their inclusions.** MitoTracker staining of mitochondria (red) was combined with detection of chlamydiae (green) and the amoeba host (blue) by fluorescence *in situ* hybridization. No significant clustering of mitochondria around inclusions of *Simkania* (A), *Parachlamydia* (B) or *Protochlamydia* (C) was detected in *A. castellanii*. Bars 10  $\mu$ m.

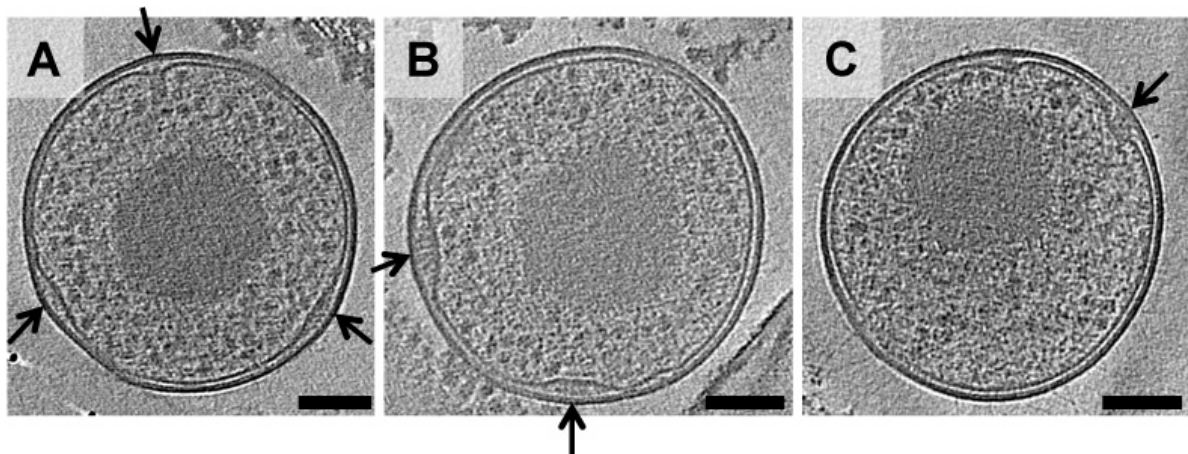


**Figure S2. More examples of putative *Simkania* T3S structures with sheared-off needles.**

Shown are slices through cryotomograms of purified *Simkania*. Often, a widening of the periplasm and basal body-like densities were observed in the absence of a T3S needle, suggesting some needles are sheared off during purification. Bar 100 nm.

**Movie S1. Crescent bodies are not seen in projection images of plunge-frozen *Parachlamydia* cells.**

<http://onlinelibrary.wiley.com/store/10.1111/1462-2920.12299/asset/supinfo/emi12299-sup-0002-m1.mov?v=1&s=2470e62d3f4abc9c003dca3675549b6fe369a45c>

**Movie S2. Cryotomogram and 3D model of the *Simkania* inclusion from Figure 3D.**

<http://onlinelibrary.wiley.com/store/10.1111/1462-2920.12299/asset/supinfo/emi12299-sup-0003-m2.mov?v=1&s=2ebeb341fff5d08bcbe135275cad02bef65175>

**Movie S3. Cryotomogram and 3D model of the *Parachlamydia* inclusion from Figure 3L.**

<http://onlinelibrary.wiley.com/store/10.1111/1462-2920.12299/asset/supinfo/emi12299-sup-0004-m3.mov?v=1&s=fb35774e566b8adff5e8f61a3d52939c90d7b872>

**Movie S4. Cryotomogram and 3D model of the *Protochlamydia* inclusion from Figure 4.**

<http://onlinelibrary.wiley.com/store/10.1111/1462-2920.12299/asset/supinfo/emi12299-sup-0005-m4.mov?v=1&s=642c9435e847d759dc86a64a3bd76a57228c0101>



# **Chapter IV**

## **Discovery of chlamydial peptidoglycan reveals bacteria with murein sacculi but without FtsZ**

Nature Communications 2013; 4:2856.

## **Discovery of chlamydial peptidoglycan reveals bacteria with murein sacculi but without FtsZ**

<sup>1,3,4</sup>Martin Pilhofer, <sup>1,5</sup>Karin Aistleitner, <sup>6</sup>Jacob Biboy, <sup>7</sup>Joe Gray, <sup>8</sup>Erkin Kuru, <sup>8</sup>Edward Hall, <sup>8</sup>Yves V. Brun, <sup>8</sup>Michael S. VanNieuwenhze, <sup>6</sup>Waldemar Vollmer, <sup>2,5</sup>Matthias Horn, <sup>2,3,4</sup>Grant J. Jensen

<sup>1</sup>contributed equally

<sup>2</sup>corresponding authors

<sup>3</sup>Division of Biology, California Institute of Technology, Pasadena, CA, 91125, USA

<sup>4</sup>Howard Hughes Medical Institute

<sup>5</sup>Division of Microbial Ecology, University of Vienna, Vienna, A-1090, Austria

<sup>6</sup>Institute for Cell and Molecular Biosciences, The Centre for Bacterial Cell Biology, Newcastle University, Newcastle upon Tyne, NE2 4AX, United Kingdom

<sup>7</sup>Institute for Cell and Molecular Biosciences, Pinnacle Laboratory, Newcastle University, Newcastle upon Tyne, NE2 4AX, United Kingdom

<sup>8</sup>Indiana University, Bloomington, IN, 47405, USA

Contact:

Grant J. Jensen: [jensen@caltech.edu](mailto:jensen@caltech.edu)

Matthias Horn: [horn@microbial-ecology.net](mailto:horn@microbial-ecology.net)



## **Abstract**

Chlamydiae are important pathogens and symbionts with unique cell biological features. They lack the cell-division protein FtsZ, and the existence of peptidoglycan (PG) in their cell wall has been highly controversial. FtsZ and PG together function in orchestrating cell division and maintaining cell shape in almost all other bacteria. Using electron cryotomography, mass spectrometry and fluorescent labeling dyes, here we show that some environmental chlamydiae have cell wall sacculi consisting of a novel PG type. Treatment with fosfomicin (a PG synthesis inhibitor) leads to lower infection rates and aberrant cell shapes, suggesting that PG synthesis is crucial for the chlamydial life cycle. Our findings demonstrate for the first time the presence of PG in a member of the *Chlamydiae*. They also present a unique example of a bacterium with a PG sacculus but without FtsZ, challenging the current hypothesis that it is the absence of a cell wall that renders FtsZ non-essential.

## Introduction

*Chlamydiae* are members of the *Planctomycetes-Verrucomicrobia-Chlamydiae* (PVC) bacterial superphylum [1]. Like most other bacteria, some PVC bacteria are already known to possess peptidoglycan (PG), that is, chains of alternating N-acetylglucosamine and N-acetylmuramic acid sugars crosslinked by short peptides. PVC bacteria display striking eukaryote-like and archaea-like cell biological features, promoting hypothesis on PVC ancestors' role in cellular evolution [2,3]. In *Verrucomicrobia* like in almost all other bacteria, septal PG synthesis is orchestrated by the FtsZ cytoskeleton [4,5]. *Planctomycetes* lack both PG and FtsZ [5]. This fits to the notion that PG-loss renders FtsZ dispensable, like in mycoplasmas [6] or L-form bacilli [7]. While from genome sequences it is clear that chlamydiae do not possess FtsZ, the presence or absence of chlamydial PG has been highly controversial. One early study reported the colorimetric detection of muramic acid in chlamydiae [8], but more reliable chromatographic methods subsequently failed to confirm this result [9,10]. All attempts to purify chlamydial sacculi have failed [11,12] and also no periplasmic density layers have been detected between inner and outer membranes by electron microscopy (including for instance [13-15]). The absence of PG in chlamydiae is surprising, however, since despite their highly reduced genomes, a nearly complete pathway for the synthesis of PG is present in the genomes of all chlamydiae ([16]). In addition, several of the chlamydial PG biosynthetic enzymes have been characterized and shown to be functional *in vitro* and in complementation assays [17-22].

Here we look for the evidence of PG cell walls in two diverse and deeply rooting chlamydiae [23], *Protochlamydia amoebophila* and *Simkania negevensis*. Through electron cryotomography (ECT), biochemical purification, enzymatic digestion, mass spectrometry (MS), fluorescence microscopy and antibiotic treatment, we show that *P. amoebophila* are indeed surrounded by sacculi containing a new type of PG. In contrast, no evidence of PG is found in *S. negevensis*. These results prove that some chlamydiae do in fact synthesize PG sacculi, explaining the presence of PG-synthetic genes, but raising new questions about the identity and purpose of the modifications and the mechanisms of cell division in the absence of FtsZ.

## Results

### Electron cryotomography of the chlamydial cell envelope

We imaged the environmental chlamydiae *Simkania negevensis* and *Protochlamydia amoebophila* by electron cryotomography (ECT) to resolve the structure of these diverse and deeply rooting members of the chlamydial phylum in a near-native state. Bacteria were purified from amoeba cultures, plunge-frozen, and 25 and 20 tomograms were collected of intact cells (Figure 1). Density profiles of the cell envelope of *Simkania* and *Protochlamydia* were different. Four layers were resolved in *Simkania* envelopes (Figure 1 B, C), and five layers were resolved in the envelope of *Protochlamydia* (Figure 1 E, F). Because the individual leaflets of lipid bilayers can be resolved in some cryotomograms, especially when the images are taken close to focus, in the case of *Simkania*, it is unclear whether the four layers represent the two leaflets of the outer and inner membranes ("O" and "A" being the two leaflets of the outer membrane, and layers "B" and "I" being the two leaflets of the inner membrane), or whether one or more of these layers are non-membranous. The facts that layers O and A have fairly similar contrast and are consistently spaced even through the undulations, are consistent with them being two leaflets of a single bilayer membrane. Their separation (~5 nm), however, is much larger than typical phospholipid bilayer membranes, whose

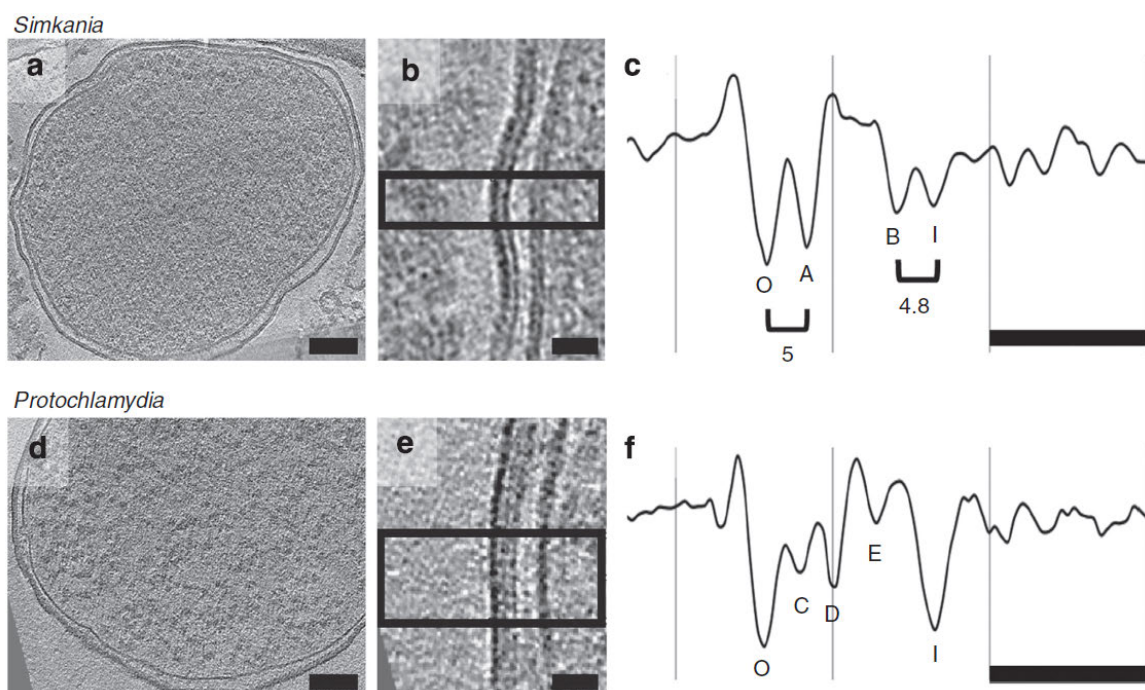


**Figure 1: Chlamydial cell envelopes are multi-layered.** *Simkania* (A-C) and *Protochlamydia* (D-F) cells were purified from asynchronously infected amoeba cultures, plunge-frozen and imaged by ECT. Shown are tomographic slices through reticulate bodies (A, D and B, E enlarged) and corresponding density profiles (C, F) of the cell envelopes. Profiles are enlarged, aligned and cropped relative to the outer membrane. Distances between peaks (in nm) are indicated. In contrast to the *Simkania* profile, the *Protochlamydia* profile resembles those of other bacteria with peptidoglycan cell walls (see text for a full discussion of each profile and layer). Bar, 100 nm in A, D and 20 nm in B, C, E, F.

two density peaks (from the phospholipid head groups) are only 3.7-4 nm apart [24]. Similarly, *Simkania* layers B and I may be the two leaflets of a single membrane, since they have similar contrast and a consistent spacing, but again they appear too far apart. In contrast to the *Simkania* envelope, the profile of *Protochlamydia* surprisingly resembled those of other Gram-negative bacteria with peptidoglycan cell walls [25-27]. Between the *Protochlamydia* outer and inner membranes (labeled "O" and "I", respectively) appeared to be three additional layers (labeled "C"- "E"). The similar-looking three layers in *Treponema pallidum* (from the outside in) were identified as proteinaceous (lipoproteins), peptidoglycan, and again proteinaceous [26]. By analogy this suggests that layer C is composed of lipoproteins (perhaps connecting the outer membrane to the cell wall) and other outer-membrane-associated proteins, layer D is cell wall, and layer E is composed of lipoproteins and inner-membrane-associated proteins (perhaps including the penicillin binding proteins - PBPs - responsible for cell wall synthesis, the lipoprotein OmcA as well as the cysteine-rich protein OmcB). While other interpretations remain possible (cysteine-rich disulphide-cross-linked envelope proteins have been suggested to be the functional equivalent of PG in chlamydiae [28]), the most important and clear observation was that *Protochlamydia* exhibit a distinct periplasmic layer (D).

### **Purification and imaging of sacculi**

In order to explore whether any of the observed periplasmic layers consisted of peptidoglycan (PG), we attempted to purify sacculi by boiling chlamydial cells (obtained from asynchronously infected amoeba cultures) in 4% sodium dodecyl sulfate. Strikingly, in three independent experiments, we observed sacculus-like structures in preparations from *Protochlamydia* (Figure 2, A-D), but not *Simkania* (two experiments, not shown). *Protochlamydia* sacculi diameters (679 nm +/-34 s.d. n=10) and morphologies matched the size and shape of intact cells. *Protochlamydia* sacculi had one or two 5-7 nm thick layers (arrowheads in Figure 2 E), plus mesh-like (up to 30 nm long) high-density aggregates attached to the outside (arrows in Figure 2 D).

### **Digestion and biochemical analyses of sacculi**

To check for the presence of peptidoglycan in the purified sacculi, we digested the samples with cellosyl, a glycan strand-cleaving peptidoglycan muramidase. Cellosyl released soluble material from insoluble sacculi, which was reduced with sodium borohydride and analyzed by high pressure liquid

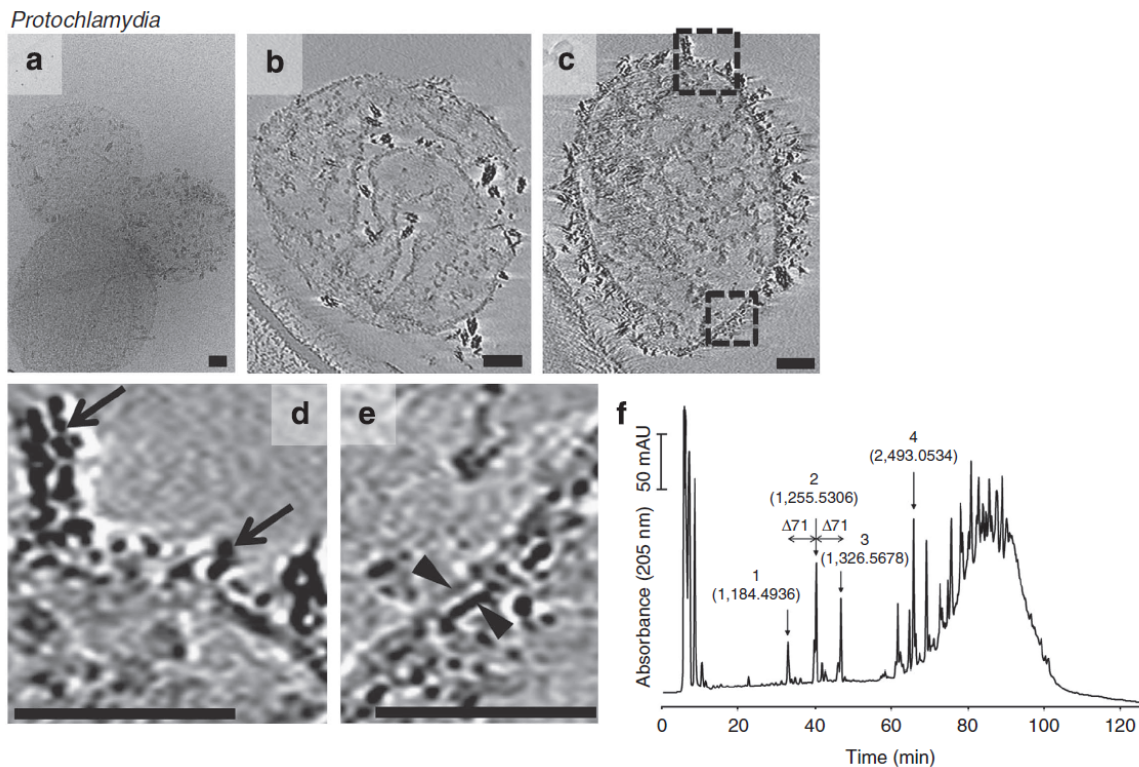


**Figure 2: *Protochlamydia* synthesize purifiable sacculi which contain peptidoglycan.** Cryoprojections (A) and tomographic slices (B-E) through sacculi-like structures purified from *Protochlamydia* cells. Similar structures were not obtained from *Simkania*. Sacculi had one or two layers (arrowheads) plus short high-density filaments (arrows) on the outside (C enlarged in D, E). Sacculi were digested, reduced and separated by high-pressure liquid chromatography (F). Mass spectrometry analysis of peaks 1-3 (neutral masses indicated in Da) indicated the presence of modified peptidoglycan (see also Table 1 and Supplementary Fig. S1). Bars, 100 nm.

chromatography (HPLC) using conditions for separating muropeptides [29]. The chromatogram (Figure 2 F) showed three main peaks in the monomeric region (20-50 min) and many peaks after 60 min that are poorly separated at higher retention time (>75 min) forming a "hump", which is typical for highly cross-linked and/or incompletely digested PG material [30]. The retention times and overall pattern of cellosyl digestion products were different from those of muropeptide mixtures obtained from various Gram-positive and Gram-negative bacteria.

To characterize this material, the three main cellosyl products in the monomeric region and one well-separated main product at the beginning of the "hump" region were analyzed by mass spectrometry (MS). The determined neutral masses of the earlier three products were higher than what would be expected for monomeric muropeptides, but the masses of products 1 and 2 and of products 2 and 3 differed by 71 Da, a typical feature of monomeric muropeptides with a tri-, tetra- and pentapeptide, respectively, due to the presence of none, one or two D-alanine residues (Figure 2 F). In MS/MS analysis the three muropeptides fragmented in a similar way showing that they are related (Supplementary Fig. S1, Table 1). For all three peaks, we observed mass differences to the parent ion

Fraction No <sup>a</sup> / muro-peptide	Fragment	Mass of fragments, H <sup>+</sup> form (m/z)		Proposed structure
		determined	calculated	
1	A	1167.3447	1167.4908	[M+H] <sup>+</sup> -H <sub>2</sub> O
	B	1056.3231	1056.5014	[M+H] <sup>+</sup> -129
	C	982.3848	982.4220	[M+H] <sup>+</sup> -GlcNAc
	D	853.3392	853.4220	[M+H] <sup>+</sup> -129-GlcNAc
	E	705.3032	705.3059	[M+H] <sup>+</sup> -GlcNAcMurNAc(r)
	F	634.3148	634.2688	[M+H] <sup>+</sup> -GlcNAcMurNAc(r)Ala
	G	505.2668	505.2262	[M+H] <sup>+</sup> -GlcNAcMurNAc(r)AlaGlu
2	A	1238.3288	1238.5255	[M+H] <sup>+</sup> -H <sub>2</sub> O
	B	1127.4075	1127.5361	[M+H] <sup>+</sup> -129
	C	1053.3859	1053.4567	[M+H] <sup>+</sup> -GlcNAc
	D	924.3934	924.4567	[M+H] <sup>+</sup> -129-GlcNAc
	E	776.3376	776.3406	[M+H] <sup>+</sup> -GlcNAcMurNAc(r)
	F	705.3202	705.3035	[M+H] <sup>+</sup> -GlcNAcMurNAc(r)Ala
	G	576.3141	576.2609	[M+H] <sup>+</sup> -GlcNAcMurNAc(r)AlaGlu
3	A	1309.4104	1309.5684	[M+H] <sup>+</sup> -H <sub>2</sub> O
	B	1198.3875	1198.5790	[M+H] <sup>+</sup> -129
	C	1124.3796	1124.4996	[M+H] <sup>+</sup> -GlcNAc
	D	995.3871	995.4996	[M+H] <sup>+</sup> -129-GlcNAc
	E	847.3485	847.3835	[M+H] <sup>+</sup> -GlcNAcMurNAc(r)
	F	776.3356	776.3464	[M+H] <sup>+</sup> -GlcNAcMurNAc(r)Ala
	G	647.3268	647.3038	[M+H] <sup>+</sup> -GlcNAcMurNAc(r)AlaGlu
Tetra From <i>C. jejuni</i>	A	946.4128	946.3869	[M+Na] <sup>+</sup> -H <sub>2</sub> O
	B	n.d.	835.4202	[M+Na] <sup>+</sup> -129
	C	761.3908	761.3181	[M+Na] <sup>+</sup> -GlcNAc
	D	n.d.	632.3181	[M+Na] <sup>+</sup> -129-GlcNAc
	E	484.3317	484.2019	[M+Na] <sup>+</sup> -GlcNAcMurNAc(r)
	F	413.2619	413.1648	[M+Na] <sup>+</sup> -GlcNAcMurNAc(r)Ala
	G	284.3200	284.1222	[M+Na] <sup>+</sup> -GlcNAcMurNAc(r)AlaGlu

**Table 1. Fragmentation masses from fractions of reduced *P. amoebophila* muropeptides.** Fraction numbers correspond to peak numbers in Figure 2 F. Fragments correspond to fragments in Supplementary Fig. S1. The parental ion ([M+H]<sup>+</sup> or [M+Na]<sup>+</sup>) of each muropeptide fragments to ions lacking either water, an unknown modification with 129 Da, a GlcNAc residue, 129 Da and GlcNAc, a GlcNAcMurNAc(r) disaccharide (r, indicates reduction to muramitol), GlcNAcMurNAc(r)Ala or GlcNAcMurNAc(r)AlaGlu (column Proposed structure). Tetra, reduced disaccharide tetrapeptide muropeptide fraction from *Campylobacter jejuni* [31]; The Na<sup>+</sup> containing ion with m/z 964.4202 was fragmented; n.d., not detected.

corresponding to the loss GlcNAc, GlcNAcMurNAc(r) (r, indicates reduction to *N*-acetylmuramitol), GlcNAcMurNAc(r)-L-alanine and GlcNAcMurNAc(r)-L-alanine-D-glutamate, confirming that products 1-3 are all modified muropeptides. The neutral masses of the *Protochlamydia* products 1, 2 and 3 were all 314.12 Da larger than the masses of the reduced monomeric muropeptides (with tri-, tetra-

or pentapeptide) from Gram-negative bacteria [32], however, suggesting the presence of a common modification in the *Protochlamydia* muropeptides. The neutral mass of product 4 was consistent with a peptide cross-linked dimer of product 2. Additional mass differences that occurred in all fragmentation spectra indicated the presence of the same and as yet unknown modifications with 129 and 203 Da, respectively, explaining the higher mass of *Protochlamydia* muropeptides 1-3 compared to the monomeric muropeptides of *E. coli*.

To investigate whether PG or protein was a major component of *Protochlamydia* sacculi, purified sacculi were subjected to lysozyme and DTT treatment, respectively. Only the incubation with lysozyme resulted in a degradation of sacculi, as observed by negative stain electron microscopy (Supplementary Fig. S2).

### **Fluorescent imaging of D-alanine incorporation *in vivo***

To further confirm the presence of PG in *Protochlamydia* sacculi, we tested whether fluorescently labeled amino acids (FDAA; here labeled D-alanine) [33] would be incorporated into chlamydial cells *in vivo*. Incubation of amoeba cultures continuously infected with *Protochlamydia* (including reticulate bodies, elementary bodies, and transitional stages) with FDAA (HADA and BADA) resulted in multiple strong and chlamydial cell-sized signals inside amoeba cells (Figure 3 A-D, Supplementary Fig. S3 A). In many cases the FDAA labeling in infected amoebae overlapped with staining of the chlamydial cells by DAPI or chlamydiae-specific fluorescence *in situ* hybridization (FISH). Not all cells stained by FISH/DAPI show a corresponding FDAA signal because chlamydial cells are in different developmental stages, including non-replicating elementary bodies. No signals were detected when uninfected amoebae were incubated with FDAA (Supplementary Fig. S3 D, E), or when infected amoebae were incubated with DMSO only (not shown). Interestingly, purified *Protochlamydia* elementary bodies that cannot undergo cell division (and are therefore probably not actively synthesizing new PG) also did not show labeling upon incubation with FDAA (Supplementary Fig. S3 B, C), indicating that PG synthesis takes place during *Protochlamydia* replication inside the host. Amoeba cultures infected with *Simkania*, on the other hand, showed no signals (BADA) or signals similar to the background level (HADA) upon labeling with FDAAs (Supplementary Fig. S4 A, B), confirming the absence of purifiable sacculi. Purified *Simkania* cells were not labeled by either dye (Supplementary Fig. S4 C, D).

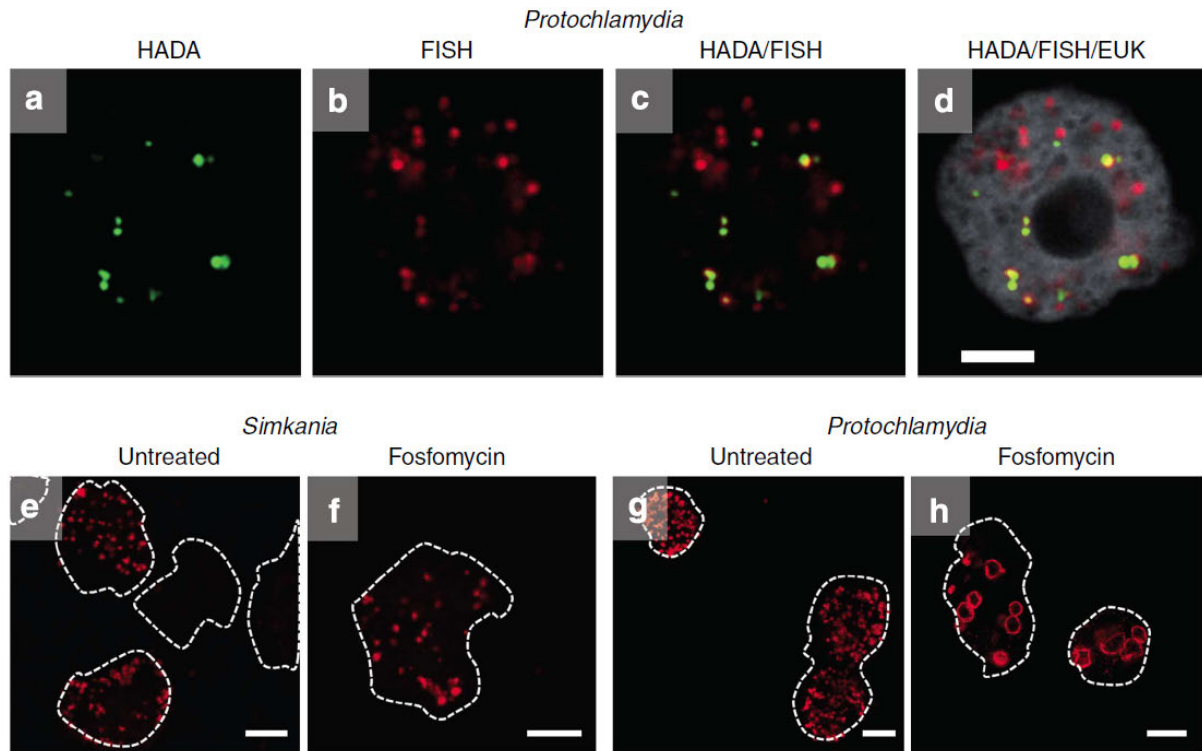


**Figure 3: *Protochlamydia* incorporate D-alanine *in vivo* and are sensitive to fosfomycin.** *Protochlamydia*-infected amoebae (A-D) but not purified *Protochlamydia* cells (Supplementary Fig. S2) or uninfected amoeba cells (Supplementary Fig. S2) stained positively for new peptidoglycan synthesis with fluorescently labeled D-alanine dyes HADA (A) and BADA (Supplementary Fig. S2), confirming the synthesis of peptidoglycan in actively-growing *Protochlamydia*. Specific FISH staining of chlamydial cells (B, overlay with A shown in C) and the eukaryotic host (D, shows overlay with C) are shown. The treatment of *Protochlamydia*-infected amoeba cultures (amoeba cell outlines in white) with cell wall synthesis-targeting fosfomycin (H, control shown in G) resulted in a dramatic decrease in infection rate and aberrant/larger chlamydial cell shapes (shown are immunofluorescent stainings of chlamydial outer membrane proteins), suggesting a crucial role of PG in the *Protochlamydia* life cycle. Fosfomycin did not affect *Simkania* (F, control shown in E). Bars, 5  $\mu\text{m}$  in D, 10  $\mu\text{m}$  in E-H.

### Monitoring *Protochlamydia* sensitivity to cell wall antibiotics

Due to the high conservation of PG throughout the bacterial domain of life, many antibacterial drugs target PG synthesis. The so-called “chlamydial anomaly” [34] is that despite the fact that PG has not been detected in pathogenic chlamydiae, these organisms are sensitive to cell wall-targeting beta-lactam antibiotics. Penicillin, for instance, leads to the formation of enlarged aberrant cells [35,36] and blocks the conversion between developmental stages [37]. Environmental chlamydiae, in contrast, are resistant to beta-lactams [38,39] - possibly due to putative beta-lactamases encoded in their genomes. To explore the role of the PG sacculus in the *Protochlamydia* life cycle, we used an alternative PG synthesis-targeting antibiotic (fosfomycin) to treat infected amoeba cells. The addition of 500  $\mu\text{g}/\text{ml}$  fosfomycin to *Protochlamydia*-infected amoeba cultures led to a significant decrease in infection rate (20.2%  $\pm$  8 infected amoebae for fosfomycin-treated cultures vs. 95.8%  $\pm$  2.2 infected amoebae for untreated cultures;  $p < 0.0001$ , unpaired t-test). *Protochlamydia* cells within treated



cultures were also up to eight-times larger than normal (diameters of up to 6  $\mu\text{m}$ ) (Figure 3 G, H). Lower fosfomycin concentrations (25  $\mu\text{g}/\text{ml}$  and 100  $\mu\text{g}/\text{ml}$ ) induced the formation of fewer aberrant forms and did not affect the infection rate (not shown). Fosfomycin-treatment of *Simkania*-infected amoeba cultures led to only a slight decrease in infection rate (59.9%  $\pm$  5.6 infected amoebae for fosfomycin-treated cultures vs. 67%  $\pm$  1.7 infected amoebae for untreated cultures) and no differences in cell size were detected (Figure 3 E, F).

## Discussion

We conclude that *Protochlamydia* synthesize sacculi consisting of peptidoglycan that (i) can be hydrolyzed by cellosyl, (ii) contains monomeric and cross-linked muropeptides and (iii) carries yet unknown modifications at virtually every subunit. Because transglycosylases have not been found in chlamydial genomes (Supplementary Table S1) [16], and some other PG-possessing bacteria [40,41] also lack known transglycosylases, some other enzyme/s must be capable of synthesizing glycan strands. Fluorescent imaging of D-Ala incorporation *in vivo* and monitoring of cell wall antibiotic sensitivity suggest that the *Protochlamydia* PG sacculus plays an important role in cell cycle and shape. The presence of sacculi in *Protochlamydia* but not in *Simkania* matches the less complete set of synthetic genes in the latter: *Simkania*, as well as pathogenic chlamydiae, lack an undecaprenyl-diphosphate phosphatase (UppP), and alanine/glutamine racemases (Alr, Murl) (Supplementary Table S1) [16,42,43].

The presence of PG sacculi in *Protochlamydia* and chlamydiae's sister phylum *Verrucomicrobia* [44], together with the more complete PG synthesis pathway in basal chlamydial lineages, make it likely that the last common chlamydial ancestor was able to synthesize a PG sacculus as well. In addition to proving that some chlamydia do in fact synthesize PG, our discovery of a PG sacculus challenges the previous speculations that chlamydiae synthesize a small ring of PG only during cell division [45]. This might still be true for *Simkania* and pathogenic chlamydiae, and our data prompts a reconsideration of whether these organisms lack PG entirely (and the effects of beta-lactams are pleiotropic) or if they synthesize novel PG structures, which are not purified by the standard sacculus preparation protocols. Finally, the detection of a PG-containing sacculus in *Protochlamydia* challenges the view that FtsZ is essential in PG-possessing bacteria [4,6,7], because to our knowledge, *Protochlamydia* is the first example of a bacterium *with* a PG cell wall, but *without* FtsZ. Studying the cell division mechanism and septal PG-synthesis in this organism could help clarify the role of FtsZ.

*Protochlamydia* could represent an intermediate evolutionary stage in the transition to PG- and FtsZ-independency.

## Methods

### Cultivation of organisms

*Acanthamoeba castellanii* Neff infected with *Protochlamydia amoebophila* UWE25 or *A. castellanii* UWC1 infected with *Simkania negevensis* was cultivated in TSY medium (30 g/L trypticase soy broth, 10 g/L yeast extract, pH 7.3) at 20°C. Amoebal growth was monitored by light microscopy and medium was exchanged every 3-6 days. The presence and identity of the chlamydial symbionts was verified by isolation of DNA from cultures followed by amplification and sequencing of the 16S rRNA genes. In addition, fluorescence *in situ* hybridization (FISH) using specific probes combined with 4',6-diamidino-2-phenylindole (DAPI) staining of infected cultures was performed using specific probes for the respective symbiont as described previously [46]. Amoebae infected with chlamydiae were allowed to attach on slides and were fixed with 4% formaldehyde at 20 °C. Cells were hybridized for 1.5 h at 46 °C at a formamide concentration of 25% with the *Protochlamydia*-specific probe E25-454 (5'-GGA TGT TAG CCA GCT CAT-3') or the *Simkania*-specific probe Simneg-183 (5'-CAG GCT ACC CCA GCT CTC-3') and the probe EUB338. Subsequently, cells were stained with DAPI (0.5 µg ml<sup>-1</sup> in PBS) for 5 min, and slides were analysed using an epifluorescence microscope.

### Purification of chlamydiae

Infected *A. castellanii* cultures were harvested by centrifugation (7,197 × g, 10 min), washed in Page's Amoebic Saline (PAS) [47], centrifuged and resuspended in PAS. Amoeba cells were disrupted by vortexing with an equal volume of glass beads for 3 minutes. Glass beads and cell debris were removed by centrifugation (5 min, 300 × g). The supernatant was filtered through a 1.2 µm filter and centrifuged at maximum speed for 10 min. The obtained pellet was resuspended in PAS.

### Plunge-freezing

For plunge-freezing, copper/rhodium electron microscopy (EM) grids (R2/2 or R2/1, Quantifoil) were glow-discharged for 1 min. A 20×-concentrated bovine serum albumin-treated solution of 10 nm colloidal gold (Sigma) was added to purified chlamydiae or sacculi (1:4 v/v) immediately before

plunge freezing. A 4- $\mu$ l droplet of the mixture was applied to the EM grid, then automatically blotted and plunge-frozen into a liquid ethane-propane mixture [48] using a Vitrobot (FEI Company) [49].

### **Electron cryotomography**

Images were collected using a Polara 300 kV FEG transmission electron microscope (FEI Company) equipped with an energy filter (slit width 20 eV; Gatan) on a lens-coupled 4 k $\times$ 4 k UltraCam CCD (Gatan). Pixels on the CCD represented 0.95 nm (22,500 $\times$ ) or 0.63 nm (34,000 $\times$ ) at the specimen level. Typically, tilt series were recorded from  $-60^\circ$  to  $+60^\circ$  with an increment of  $1^\circ$  at 10  $\mu$ m under-focus. The cumulative dose of a tilt-series was 180–220 e $^-$ / $\text{\AA}^2$ . UCSF Tomo [50] was used for automatic acquisition of tilt-series and 2D projection images. Three-dimensional reconstructions were calculated using the IMOD software package [51] or Raptor [52]. Tomograms were visualized using 3dMOD [51]. Density profiles were generated using ImageJ.

### **Fluorescent labeling of peptidoglycan**

Newly synthesized peptidoglycan was labeled using fluorescent D-amino acids [33]. *A. castellanii* cells continuously infected with *Protochlamydia* or *Simkania* were harvested and resuspended in a mixture of TSY and PAS (1:1). Cells were incubated with 1.5 mM HADA (hydroxy coumarin-carbonyl-amino-D-alanine) [33] or BADA (4,4-Difluoro-5,7-Dimethyl-4-Bora-3a,4a-Diaza-s-Indacene-3-Propionic Acid-3-amino-D-alanine) for 6 h with gentle shaking. Cells were pelleted, washed three times and fixed with 4% PFA followed by FISH using chlamydia-specific probe Chls-0523 or DAPI-staining. As a control, uninfected amoebae and purified chlamydiae were treated in the same way.

### **Antibiotic treatment of infected amoebae cultures**

*A. castellanii* were seeded into the wells of a multi-well dish and infected with purified *Simkania* and *Protochlamydia* elementary bodies [53]. After centrifugation at 600  $\times$  g for 10 min, the medium was exchanged for TSY supplemented with fosfomycin (0, 25, 100 or 500  $\mu$ g ml $^{-1}$ , respectively). Medium was exchanged once at 48 h post infection. Cells were fixed with methanol at 96 h post infection followed by immunofluorescence analysis using either anti-PomS antibodies [53] or anti-*Simkania* antibodies raised against purified chlamydiae. The number of infected amoebae was counted for each treatment.

### Preparation and composition analysis of sacculi

Chlamydial cells were purified from 1.8 L (*Protochlamydia*) and 3 L (*Simkania*) of infected amoeba culture and, depending on the amount of harvested cells, resuspended in 2.6 ml to 5.2 ml 4% SDS (w/v). After shipping (over night, room temperature), the suspensions were dripped into 4% SDS (preheated to 90°C, 6 ml final volume) and stirred for 2.5 h at 90°C. Sacculi were pelleted (30 min, 135,000 × g) in a TLA-100.3 rotor (Beckman Coulter), washed 4× in 3 ml water, resuspended in 150 µl water and supplemented with 0.02% (w/v) sodium azide. Muropeptides were released from the PG by an overnight incubation with the muramidase Cellosyl (Hoechst, Frankfurt am Main, Germany) on a thermal shaker at 37°C and 800 rpm. The sample was boiled for 10 min and centrifuged for 10 min at 13,500 × g. The muropeptides present in the supernatant were reduced with sodium borohydride and separated on a 250×4.6 mm 3 µm Prontosil 120-3-C18 AQ reversed phase column (Bischoff, Germany) at 55 °C using a 135 min gradient from 50 mM sodium phosphate pH 4.31 to 75 mM sodium phosphate pH 4.95, 15% methanol and a flow rate of 0.5 ml min<sup>-1</sup> [29]. Muropeptide fractions were collected, concentrated in a SpeedVac, acidified by 1% trifluoroacetic acid, and analyzed by offline electrospray mass spectrometry on a Finnigan LTQ-FT mass spectrometer (ThermoElectron, Bremen, Germany) in positive ion mode using mass scans over the mass range from  $m/z=300$  to  $m/z=1,900$  at a typical spray voltage of 1.1–1.5 kV [32]. Parent ion scans were acquired with an FT MS resolution setting of 100,000 (at  $m/z=400$ ) with a typical mass accuracy of 3 ppm. MS/MS scans were performed in the ion trap, which has a typical mass accuracy for the fragment ion of ±0.3 Da. MS spectra were deconvoluted to generate uncharged masses using the QualBrowser program (ThermoElectron, Bremen, Germany) [32].

### Negative stain electron microscopy of treated sacculi preparations

Purified sacculi were incubated at 37°C for 12 h in 20 µl total volume with either lysozyme (10 mg/ml), dithiothreitol (5 mM) or phosphate buffered saline. Samples were applied to a Formvar-coated, carbon-coated, glow-discharged copper EM grid (Electron Microscopy Sciences). Samples were aspirated, stained with 1.5% uranylacetate and imaged on an FEI Tecnai T12 electron microscope.

## References

1. Wagner M, Horn M (2006) The Planctomycetes, Verrucomicrobia, Chlamydiae and sister phyla comprise a superphylum with biotechnological and medical relevance. *Current Opinion in Biotechnology* 17: 241-249.
2. Devos DP, Reynaud EG (2010) Evolution. Intermediate steps. *Science* 330: 1187-1188.
3. Reynaud EG, Devos DP (2011) Transitional forms between the three domains of life and evolutionary implications. *Proc Biol Sci* 278: 3321-3328.
4. Erickson HP, Anderson DE, Osawa M (2010) FtsZ in Bacterial Cytokinesis: Cytoskeleton and Force Generator All in One. *Microbiol Mol Biol Rev* 74: 504-528.
5. Pilhofer M, Rappl K, Eckl C, Bauer AP, Ludwig W, et al. (2008) Characterization and Evolution of Cell Division and Cell Wall Synthesis Genes in the Bacterial Phyla Verrucomicrobia, Lentisphaerae, Chlamydiae, and Planctomycetes and Phylogenetic Comparison with rRNA Genes. *J Bacteriol* 190: 3192-3202.
6. Lluch-Senar M, Querol E, Pinol J (2010) Cell division in a minimal bacterium in the absence of ftsZ. *Mol Microbiol* 78: 278-289.
7. Leaver M, DomA-nguez-Cuevas P, Coxhead JM, Daniel RA, Errington J (2009) Life without a wall or division machine in *Bacillus subtilis*. *Nature* 457: 849-853.
8. Perkins HR, Allison AC (1963) Cell-wall Constituents of *Rickettsiae* and Psittacosis-Lymphogranuloma Organisms. *Journal of General Microbiology* 30: 469-480.
9. Garrett AJ, Harrison MJ, Manire GP (1974) A Search for the Bacterial Mucopeptide Component, Muramic Acid, in *Chlamydia*. *Journal of General Microbiology* 80: 315-318.
10. Fox A, Rogers JC, Gilbert J, Morgan S, Davis CH, et al. (1990) Muramic acid is not detectable in *Chlamydia psittaci* or *Chlamydia trachomatis* by gas chromatography-mass spectrometry. *Infect Immun* 58: 835-837.
11. Caldwell HD, Kromhout J, Schachter J (1981) Purification and partial characterization of the major outer membrane protein of *Chlamydia trachomatis*. *Infect Immun* 31: 1161-1176.
12. Barbour AG, Amano K, Hackstadt T, Perry L, Caldwell HD (1982) *Chlamydia trachomatis* has penicillin-binding proteins but not detectable muramic acid. *Journal of Bacteriology* 151: 420-428.
13. Matsumoto A (1979) Recent progress of electron microscopy in microbiology and its development in future: from a study of the obligate intracellular parasites, chlamydia organisms. *J Electron Microsc*, 28: 57-64.
14. Tamura A, Matsumoto A, Manire GP, Higashi N (1971) Electron Microscopic Observations on the Structure of the Envelopes of Mature Elementary Bodies and Developmental Reticulate Forms of *Chlamydia psittaci*. *J Bacteriol* 105: 355-360.
15. Huang Z, Chen M, Li K, Dong X, Han J, et al. (2010) Cryo-electron tomography of *Chlamydia trachomatis* gives a clue to the mechanism of outer membrane changes. *Journal of Electron Microscopy* 9: 237-241.
16. McCoy AJ, Maurelli AT (2006) Building the invisible wall: updating the chlamydial peptidoglycan anomaly. *Trends Microbiol* 14: 70-77.

17. McCoy AJ, Maurelli AT (2005) Characterization of *Chlamydia* MurC-Ddl, a fusion protein exhibiting D-alanyl-D-alanine ligase activity involved in peptidoglycan synthesis and D-cycloserine sensitivity. *Mol Microbiol* 57: 41-52.
18. McCoy AJ, Sandlin RC, Maurelli AT (2003) In vitro and in vivo functional activity of *Chlamydia* MurA, a UDP-N-acetylglucosamine enolpyruvyl transferase involved in peptidoglycan synthesis and fosfomycin resistance. *J Bacteriol* 185: 1218-1228.
19. Hesse L, Bostock J, Dementin S, Blanot D, Mengin-Lecreux D, et al. (2003) Functional and Biochemical Analysis of *Chlamydia trachomatis* MurC, an Enzyme Displaying UDP-N-Acetylmuramate:Amino Acid Ligase Activity. *J Bacteriol* 185: 6507-6512.
20. Patin D, Bostock J, Blanot D, Mengin-Lecreux D, Chopra I (2009) Functional and biochemical analysis of the *Chlamydia trachomatis* ligase MurE. *J Bacteriol* 191: 7430-7435.
21. Patin D, Bostock J, Chopra I, Mengin-Lecreux D, Blanot D (2012) Biochemical characterisation of the chlamydial MurF ligase, and possible sequence of the chlamydial peptidoglycan pentapeptide stem. *Archives of Microbiology* 194: 505-512.
22. Henrichfreise B, Schiefer A, Schneider T, Nzukou E, Poellinger C, et al. (2009) Functional conservation of the lipid II biosynthesis pathway in the cell wall-less bacteria *Chlamydia* and *Wolbachia*: why is lipid II needed? *Mol Microbiol* 73: 913-923.
23. Horn M (2008) Chlamydiae as symbionts in eukaryotes. *Annual Review of Microbiology* 62: 113-131.
24. Leforestier A, Lemercier N, Livolant F (2012) Contribution of cryoelectron microscopy of vitreous sections to the understanding of biological membrane structure. *Proc Natl Acad Sci U S A* 109: 8959-8964.
25. Tocheva EI, Li Z, Jensen GJ (2010) Electron cryotomography. *Cold Spring Harb Perspect Biol* 2: a003442.
26. Liu J, Howell JK, Bradley SD, Zheng Y, Zhou ZH, et al. (2010) Cellular architecture of *Treponema pallidum*: novel flagellum, periplasmic cone, and cell envelope as revealed by cryo electron tomography. *J Mol Biol* 403: 546-561.
27. Tocheva EI, Matson EG, Morris DM, Moussavi F, Leadbetter JR, et al. (2011) Peptidoglycan remodeling and conversion of an inner membrane into an outer membrane during sporulation. *Cell* 146: 799-812.
28. Hatch T (1996) Disulfide cross-linked envelope proteins: the functional equivalent of peptidoglycan in chlamydiae? *J Bacteriol* 178: 1-5.
29. Glauner B (1988) Separation and quantification of muropeptides with high-performance liquid chromatography. *Anal Biochem* 172: 451-464.
30. de Jonge BL, Tomasz A (1993) Abnormal peptidoglycan produced in a methicillin-resistant strain of *Staphylococcus aureus* grown in the presence of methicillin: functional role for penicillin-binding protein 2A in cell wall synthesis. *Antimicrob Agents Chemother* 37: 342-346.
31. Firdich E, Biboy J, Adams C, Lee J, Ellermeier J, et al. (2012) Peptidoglycan-modifying enzyme Pgp1 is required for helical cell shape and pathogenicity traits in *Campylobacter jejuni*. *PLoS Pathog* 8: e1002602.
32. Bui NK, Gray J, Schwarz H, Schumann P, Blanot D, et al. (2009) The peptidoglycan sacculus of *Myxococcus xanthus* has unusual structural features and is degraded during glycerol-induced myxospore development. *J Bacteriol* 191: 494-505.

33. Kuru E, Hughes HV, Brown PJ, Hall E, Tekkam S, et al. (2012) In Situ probing of newly synthesized peptidoglycan in live bacteria with fluorescent D-amino acids. *Angew Chem Int Ed Engl* 51: 12519-12523.
34. Moulder JW (1993) Why is *Chlamydia* sensitive to penicillin in the absence of peptidoglycan? *Infect Agents Dis* 2: 87-99.
35. Matsumoto A, Manire GP (1970) Electron Microscopic Observations on the Effects of Penicillin on the Morphology of *Chlamydia psittaci*. *Journal of Bacteriology* 101: 278-285.
36. Skilton RJ, Cutcliffe LT, Barlow D, Wang Y, Salim O, et al. (2009) Penicillin Induced Persistence in *Chlamydia trachomatis*: High Quality Time Lapse Video Analysis of the Developmental Cycle. *PLoS ONE* 4: e7723.
37. Beatty WL, Morrison RP, Byrne GI (1994) Persistent chlamydiae: from cell culture to a paradigm for chlamydial pathogenesis. *Microbiological Reviews* 58: 686-699.
38. Maurin M, Bryskier A, Raoult D (2002) Antibiotic susceptibilities of *Parachlamydia acanthamoeba* in amoebae. *Antimicrob Agents Chemother* 46: 3065-3067.
39. Kahane S, Gonen R, Sayada C, Elion J, Friedman MG (1993) Description and partial characterization of a new chlamydia-like microorganism. *FEMS Microbiol Letters* 109: 329-334.
40. McPherson DC, Popham DL (2003) Peptidoglycan Synthesis in the Absence of Class A Penicillin-Binding Proteins in *Bacillus subtilis*. *Journal of Bacteriology* 185: 1423-1431.
41. Arbeloa A, Segal H, Hugonnet J-E, Josseaume N, Dubost L, et al. (2004) Role of Class A Penicillin-Binding Proteins in PBP5-Mediated  $\beta$ -Lactam Resistance in *Enterococcus faecalis*. *Journal of Bacteriology* 186: 1221-1228.
42. Horn M, Collingro A, Schmitz-Esser S, Beier CL, Purkhold U, et al. (2004) Illuminating the evolutionary history of chlamydiae. *Science* 304: 728-730.
43. Collingro A, Tischler P, Weinmaier T, Penz T, Heinz E, et al. (2011) Unity in Variety—The Pan-Genome of the *Chlamydiae*. *Molecular Biology and Evolution* 28: 3253-3270.
44. Hedlund BP, Gosink JJ, Staley JT (1996) Phylogeny of *Prostheco bacter*, the fusiform caulobacters: Members of a recently discovered division of the Bacteria. *International Journal of Systematic Bacteriology* 46: 960-966.
45. Brown WJ, Rockey DD (2000) Identification of an antigen localized to an apparent septum within dividing chlamydiae. *Infect Immun* 68: 708-715.
46. Schmitz-Esser S, Toenshoff ER, Haider S, Heinz E, Hoenninger VM, et al. (2008) Diversity of Bacterial Endosymbionts of Environmental *Acanthamoeba* Isolates. *Applied and Environmental Microbiology* 74: 5822-5831.
47. Page FC (1976) An illustrated key to freshwater and soil amoebae. Ambleside: Freshwater Biological Association.
48. Tivol WF, Briegel A, Jensen GJ (2008) An improved cryogen for plunge freezing. *Microsc Microanal* 14: 375-379.
49. Iancu CV, Tivol WF, Schooler JB, Dias DP, Henderson GP, et al. (2006) Electron cryotomography sample preparation using the Vitrobot. *Nat Protocols* 1: 2813-2819.

50. Zheng SQ, Keszthelyi B, Branlund E, Lyle JM, Braunfeld MB, et al. (2007) UCSF tomography: an integrated software suite for real-time electron microscopic tomographic data collection, alignment, and reconstruction. *J Struct Biol* 157: 138-147.
51. Kremer JR, Mastronarde DN, McIntosh JR (1996) Computer visualization of three-dimensional image data using IMOD. *J Struct Biol* 1996/01/01: 71-76.
52. Amat F, Moussavi F, Comolli LR, Elidan G, Downing KH, et al. (2008) Markov random field based automatic image alignment for electron tomography. *J Struct Biol* 161: 260-275.
53. Aistleitner K, Heinz C, Hörmann A, Heinz E, Montanaro J, et al. (2013) Identification and Characterization of a Novel Porin Family Highlights a Major Difference in the Outer Membrane of Chlamydial Symbionts and Pathogens. *PLoS ONE* 8: e55010.
54. McCoy AJ, Maurelli AT (2006) Building the invisible wall: updating the chlamydial peptidoglycan anomaly. *Trends Microbiol* 14: 70-77.
55. Lovering AL, Safadi SS, Strynadka NCJ (2012) Structural Perspective of Peptidoglycan Biosynthesis and Assembly. *Annual Review of Biochemistry* 81: 451-478.
56. Chopra I, Storey C, Falla TJ, Pearce JH (1998) Antibiotics, peptidoglycan synthesis and genomics: the chlamydial anomaly revisited. *Microbiology* 144 ( Pt 10): 2673-2678.
57. McCoy AJ, Adams NE, Hudson AO, Gilvarg C, Leustek T, et al. (2006) l,l-diaminopimelate aminotransferase, a trans-kingdom enzyme shared by *Chlamydia* and plants for synthesis of diaminopimelate/lysine. *Proceedings of the National Academy of Sciences* 103: 17909-17914.

### **Acknowledgments**

This work was funded by the Austrian Science Fund FWF (Y277-B03 to MH), the European Research Council (ERC StG “EvoChlamy” to MH), NIH grant GM094800B (to GJJ), the Caltech Center for Environmental Microbiology Interactions (to GJJ, MP), a gift from the Gordon and Betty Moore Foundation to Caltech, the BBSRC (BB/I020012/1 to WV), NIH grant AI059327 (to MSV) and NIH grant GM051986 (to YVB). We thank Elitza Tocheva for discussions on the preparation of sacculi.

### **Author contributions**

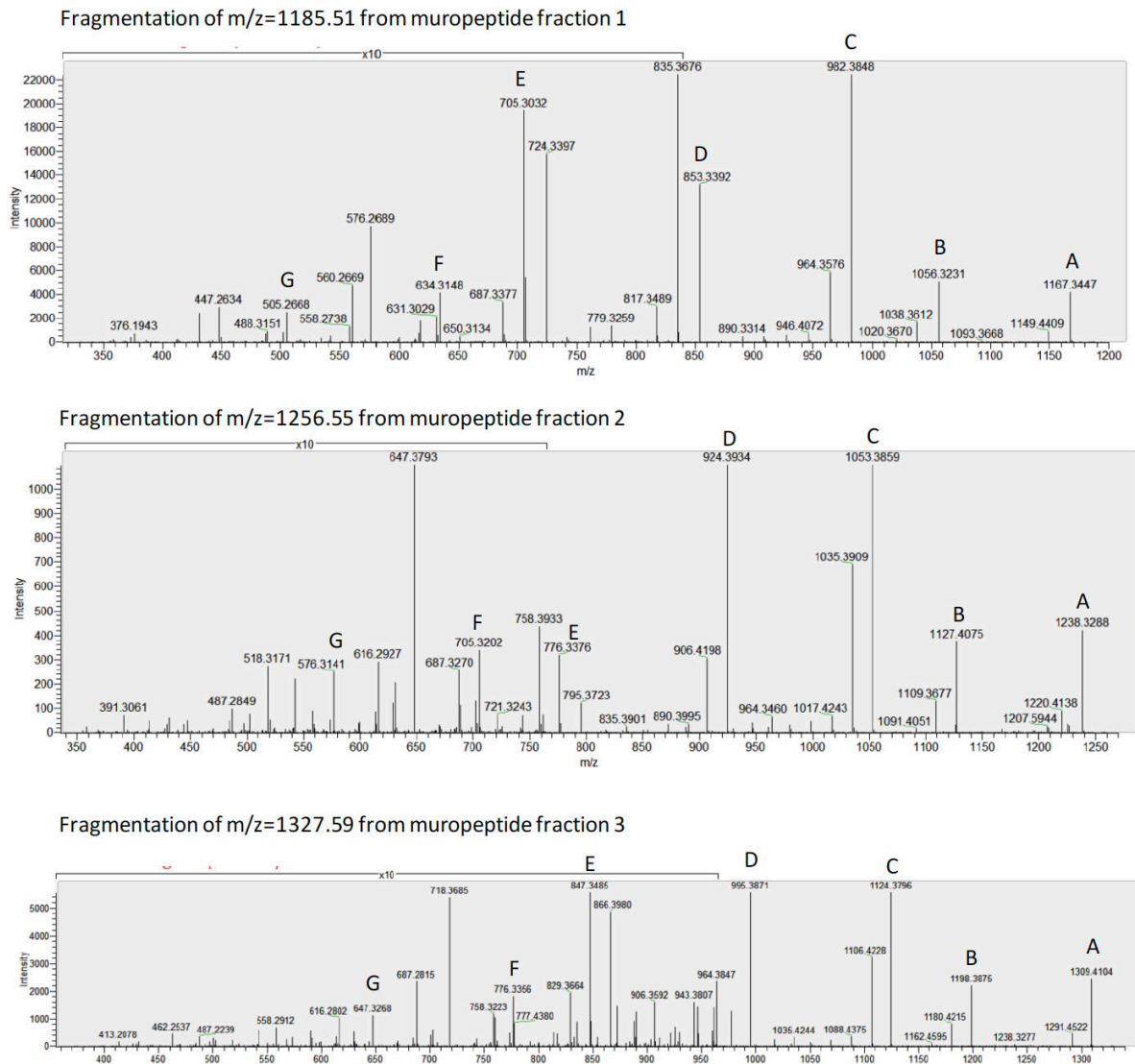
MP initiated the study. MP and KA performed all experiments except HPLC/MS analyses of sacculi, which were done by JB, JG, and WV. EK, EH, YVB, and MSV provided the FDAA dyes and advice on the FDAA labeling experiments. MP, KA, WV, MH, and GJJ designed the experiments and wrote the manuscript.

### **Competing financial interests**

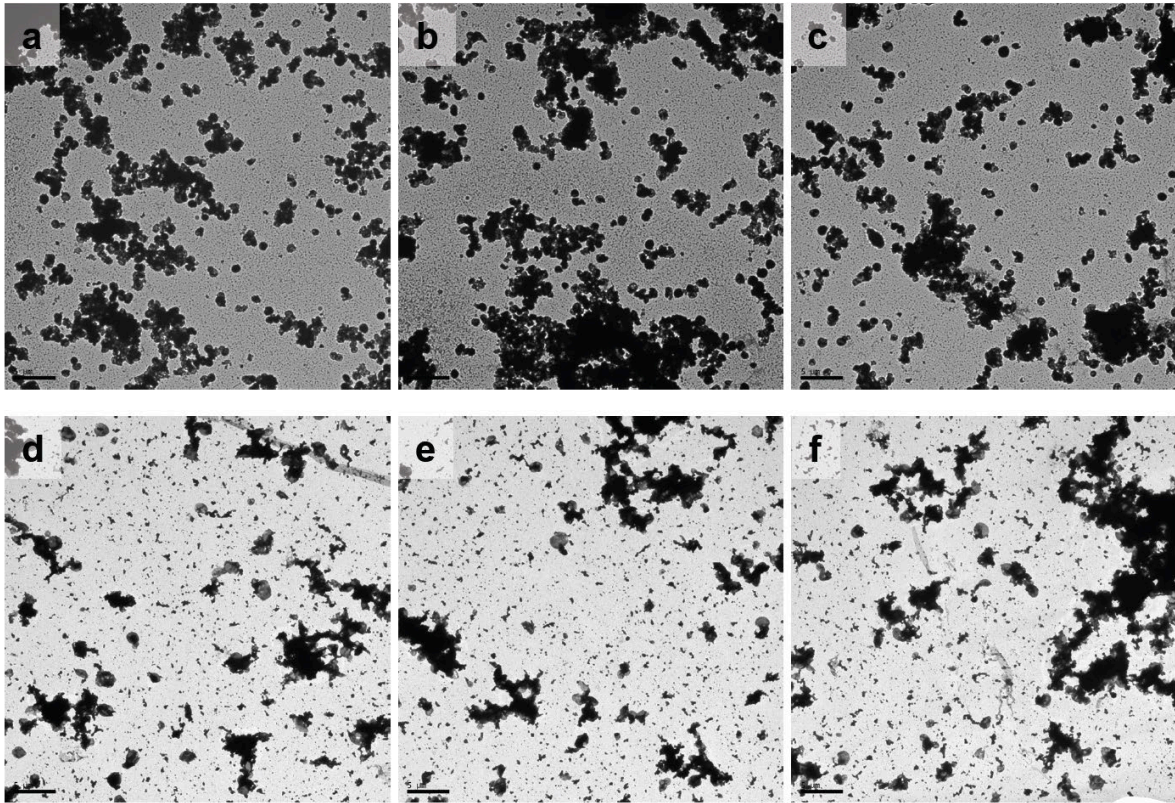
The authors declare no competing financial interests.



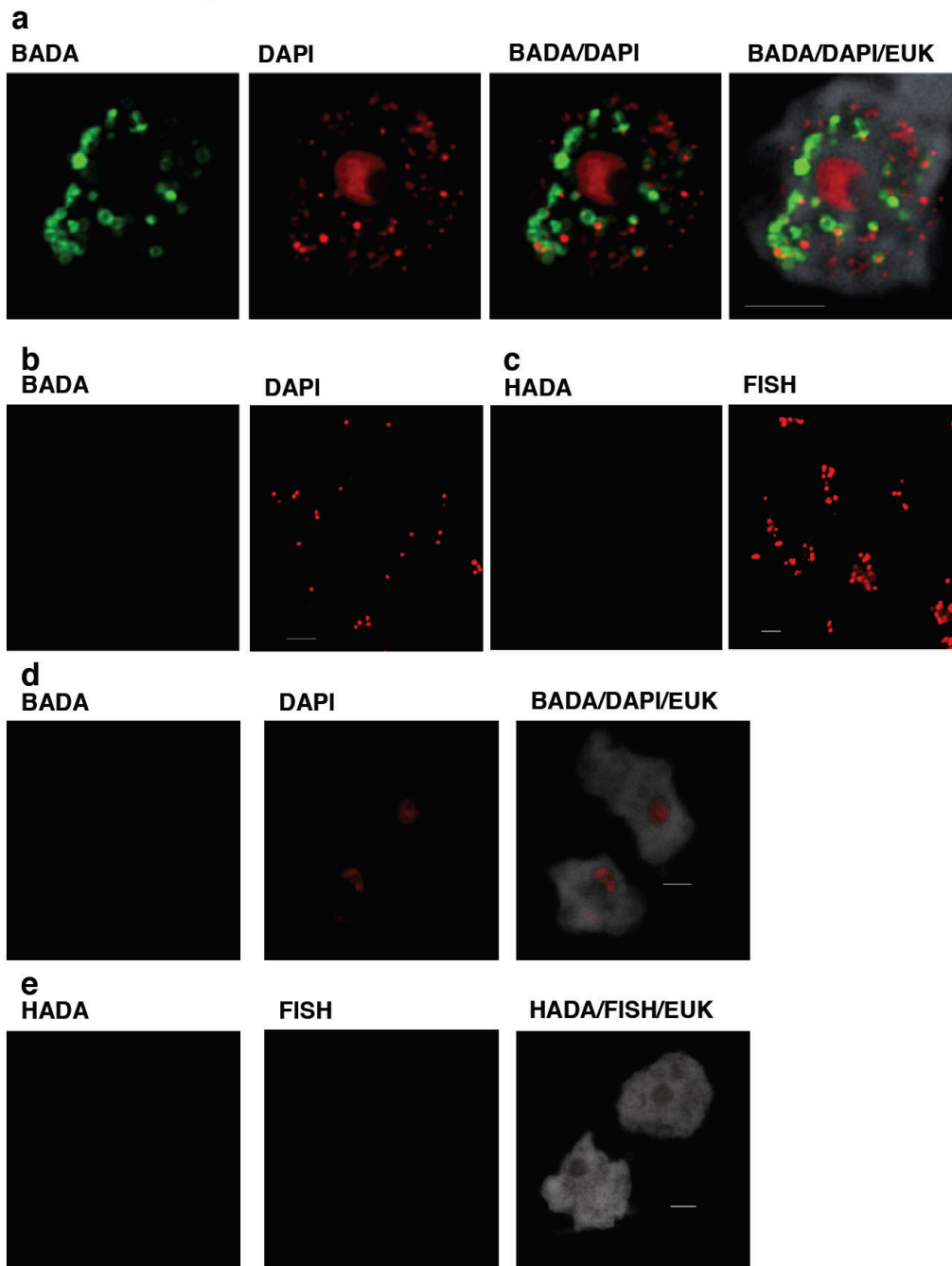
## Supplementary material



**Supplementary Figure S1. *Protochlamydia* HPLC fractions 1-3 contain modified muuropeptides.** MS/MS analysis of the three *Protochlamydia* muuropeptides (Figure 2 E) show similar fragmentation patterns. The masses of the fragment ions A-G are consistent with modified muuropeptides, whereby two modifications add an extra mass of 314 Da compared to the canonical muuropeptides with tri-, tetra- and pentapeptide, respectively.



**Supplementary Figure S2. *Protochlamydia* sacculi are degraded by lysozyme.** Representative negative stain EM images of *Protochlamydia* sacculi. The undigested control sample (A-C) contained many coccoid sacculi. After digestion with lysozyme (D-F), only few intact sacculi and degraded material was detected. Bars, 5 $\mu$ m.

***Protochlamydia***

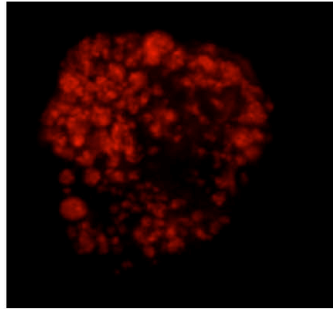
**Supplementary Figure S3. Fluorescent D-amino acids label intracellular but not purified *Protochlamydia* cells or uninfected amoebae.** Shown is an amoeba cell infected with *Protochlamydia* and stained by DAPI to detect chlamydial cells and fluorescently labeled D-alanine [33] (BADA) to detect sites of PG synthesis (A). BADA results in multiple strong signals (some of them halo-shaped). Because FISH/DAPI never stains all chlamydial cells inside amoebae, not all FDAA signals have a corresponding signal. Purified chlamydial cells (B, C) or uninfected amoebae (D, E) showed no signal with HADA (C, E) and BADA (B, D). Note that chlamydiae cannot divide in host-free media, and thus would not incorporate FDAA. Amoeba cells are stained (white) with eukaryote-specific FISH in A, D and E. Bars, 5  $\mu$ m.

***Simkania*****a**

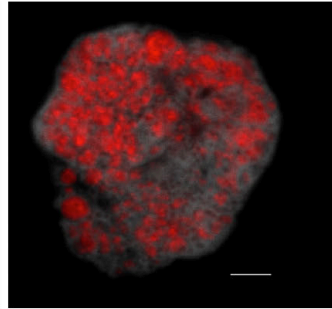
HADA



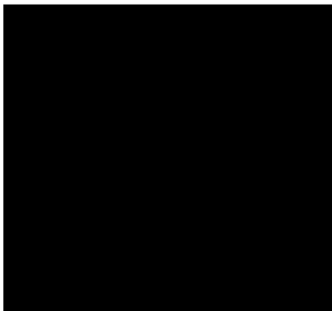
FISH



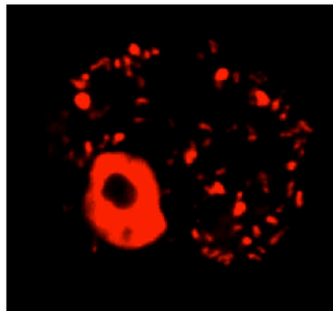
HADA/FISH/EUK

**b**

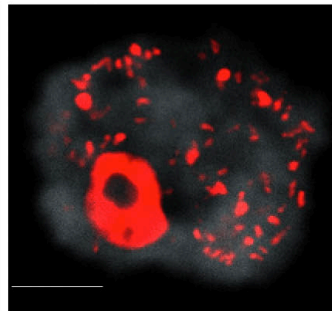
BADA



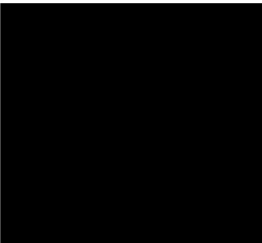
DAPI



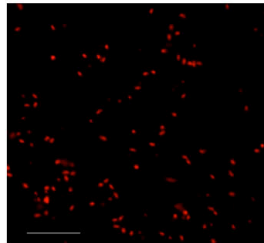
BADA/DAPI/EUK

**c**

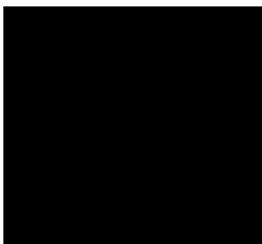
BADA



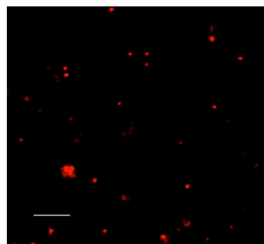
DAPI

**d**

HADA



FISH



**Supplementary Figure S4. Fluorescent D-amino acids label neither intracellular, nor purified *Simkania* cells.** Shown are amoeba cells infected with *Simkania* (A, B) and stained by FISH or DAPI to detect chlamydial cells and fluorescently labeled D-alanine [33] (HADA in A, BADA in B). BADA labeling showed no signals. When labeled with HADA, no signals were visible with the image acquisition settings used for *Protochlamydia*; in images recorded at maximum sensitivity few *Simkania* cells showed very weak signals (just above the detection limit) for HADA. Purified *Simkania* elementary bodies (C, D) are not stained by FDAA labeling. Amoeba cells are stained (white) with eukaryote-specific FISH in A, B. Bars, 5  $\mu$ m.

**Supplementary Table S1: PG synthesis genes in chlamydial genomes.**

Protein <sup>A</sup>	Function	Comment
<b>MurA</b>	UDP-N-acetylglucosamine 1-carboxyvinyltransferase	<i>Chlamydiaceae</i> are resistant to fosfomycin due to replacement of Cys115-> Asp in MurA [54]
<b>MurB</b>	UDP-N-acetylmuramate dehydrogenase	
<b>MurC<sup>B</sup></b>	UDP-N-acetylmuramate alanine ligase	MurC of <i>C. trachomatis</i> uses L-alanine, L-serine and glycine with comparable efficiency <i>in vitro</i> [19]
<b>MurD</b>	UDP-N-acetylmuramoylalanine D-glutamate ligase	
<b>MurE</b>	UDP-N-acetylmuramoyl-L-alanyl-D-glutamate 2,6-diaminopimelate ligase	MurE of chlamydiae has Arg at position 416, typical of m-DAP specific enzymes [55]
<b>MurF</b>	UDP-N-acetylmuramoyl-tripeptide D-alanyl-D-alanine ligase	
<b>MraY</b>	Phospho-N-acetylmuramoyl pentapeptide transferase	
<b>MurG</b>	N-acetylglucosaminyl transferase	
<b>Class A HMW PBPs</b>	Bifunctional transpeptidase/transglycosylase	
<b>Class B HMW PBPs</b>		
PBP2 (PBP1)	Transpeptidase	In contrast to environmental chlamydiae, members of the <i>Chlamydiaceae</i> are susceptible to beta-lactams
PBP3 (PBP2)	Transpeptidase	
<b>LMW PBP</b>		
PBP6 (PBP3)	D-alanyl-D-alanine carboxypeptidase	
<b>Alr</b>	Alanine racemase	Chlamydiae possess DagA, a D-alanine glycine permease
<b>MurI</b>	Glutamate racemase	
<b>Ddl<sup>B</sup></b>	D-alanine-D-alanine ligase	Although <i>Chlamydiaceae</i> lack Alr, Ddl of <i>C. trachomatis</i> uses D-Ala as a substrate [17]
<b>UppP</b>	Undecaprenyl-diphosphate phosphatase	<i>Chlamydiaceae</i> lack UppP, but are sensitive to Bacitracin [56]
<b>m-DAP pathway</b>	Synthesis of m-DAP	Like plants and cyanobacteria chlamydiae use the aminotransferase pathway for generation of m-DAP [57]

<sup>A</sup> Genes for proteins highlighted in dark blue are absent from the genomes of all chlamydiae. Proteins highlighted in light blue are encoded in the genomes of *Protochlamydia* and *Parachlamydia*, but not in pathogenic chlamydiae (*Chlamydiaceae*) and *Simkania*. Underlined Proteins were characterized previously [18-22]. GlcNac, N-acetylglucosamine; MurNAc, N-acetyl muramic acid; HMW PBP, high molecular weight penicillin binding protein; LMW PBP, low molecular weight penicillin binding protein; UPP, Undecaprenyl-diphosphate; m-DAP, meso-diamino pimelic acid

<sup>B</sup> MurC and Ddl are encoded as fusion protein in *Chlamydiaceae*



# **Chapter V**

## **Conserved features and major differences in the outer membrane protein composition of chlamydiae**

submitted to Environmental Microbiology

## **Conserved features and major differences in the outer membrane protein composition of chlamydiae**

Karin Aistleitner<sup>1</sup>, Dorothea Anrather<sup>2</sup>, Thomas Schott<sup>1</sup>, Julia Klose<sup>3</sup>, Monika Bright<sup>3</sup>, Gustav Ammerer<sup>2</sup>, Matthias Horn<sup>1</sup>

<sup>1</sup>Department of Microbiology and Ecosystem Science, University of Vienna, Vienna, Austria

<sup>2</sup>Department of Biochemistry, Max-F.-Perutz Laboratories, University of Vienna, Vienna, Austria

<sup>3</sup>Department of Limnology and Oceanography, University of Vienna, Vienna, Austria

Running head: Variations in chlamydial outer membrane composition

Contact:

Matthias Horn: phone +43 1 4277 76608, fax +43 1 4277 876601, email horn@microbial-ecology.net



## Summary

Chlamydiae are a highly successful group of obligate intracellular bacteria infecting a variety of eukaryotic hosts. Outer membrane proteins involved in attachment to and uptake into host cells, and cross-linking of these proteins via disulfide bonds are key features of the biphasic chlamydial developmental cycle. In this study, we used a consensus approach to predict outer membrane proteins in the genomes of members of three chlamydial families. By analyzing outer membrane protein fractions of purified chlamydiae with highly sensitive mass spectrometry, we show that the protein composition of the outer membrane differs largely between these organisms. The outer membrane of *Simkania negevensis* is dominated by a family of 35 MOMP-like proteins, but lacks proteins with homology to cell wall-stabilizing cysteine-rich proteins, which are present in all other chlamydiae. In agreement with this, the cellular integrity of *Parachlamydia* and *Waddlia* where these proteins are highly abundant, but not of *Simkania*, is impaired by conditions that reduce disulfide bonds of cysteine-rich outer membrane proteins. The observed differences in the protein composition of the outer membrane among members of divergent chlamydial families suggest different stabilities of these organisms in the environment, probably due to adaption to different niches or transmission routes.

## Introduction

Chlamydiae are a group of obligate intracellular bacteria whose members colonize a variety of eukaryotic hosts, ranging from amoebae to insects, reptiles, birds and mammals, including humans [1]. All chlamydiae switch between two morphologically and metabolically distinct stages during their developmental cycle. This cycle starts with the adhesion of the extracellular, infectious elementary body (EB) to a host cell, followed by the uptake and differentiation into a reticulate body (RB) inside a host-derived vacuole [2]. RBs divide several times before they re-differentiate into EBs and exit from the host cell [1,3,4]. Both developmental stages are well adapted to serve their designated purpose. EBs, which need to persist in the environment in order to infect new host cells, are extremely stable [5,6] and have only limited metabolic capabilities [6-8], but are preloaded with effector proteins that are crucial for infection [9]. In contrast, RBs are very efficient in the acquisition of nutrients from the host cell to fuel their fast metabolic turnover during replication, but are not infectious and more fragile than EBs [6]. These differences in stability, infectivity and substrate uptake are linked to changes in the protein composition of the outer membrane, but also to changes in the redox-state of the cysteine-residues of these proteins during the progression of the developmental cycle [10,11]. The importance of cysteine residues for chlamydial development is illustrated by the observation that cysteine-deprivation inhibits re-differentiation of RBs to EBs [12].

Because of their significance for human health and the important role of outer membrane proteins (OMPs) for vaccine development [13], the OMP composition of members of the *Chlamydiaceae*, comprising human pathogens like *Chlamydia trachomatis* and *C. pneumoniae*, has been extensively studied. The most abundant protein in the outer membrane of the *Chlamydiaceae* is the major outer membrane protein (MOMP) which makes up ~60% of the protein content of the outer membrane in EBs [14] and functions as porin [15]. The permeability of the outer membrane is partly controlled by the oxidation state of the disulfide-bridges between the cysteine-residues of MOMP, with drastically enhanced pore-forming activity after their reduction [15]. The remarkable rigidity of chlamydial EBs is thought to be the result of extensive disulfide-bridge formation between two cysteine-rich OMPs, OmcA and OmcB, which represent together with MOMP the main constituents of the chlamydial outer membrane complex (COMC) [10]. These disulfide-bridges are reduced after entry into the host cell accompanied by a decrease in the amount of OmcA and OmcB in RBs [16,17], leading to a more flexible and fragile life stage. Also the redox state of certain proteins of the type three secretion system is linked to the developmental cycle and was suggested to regulate its activity [18].

A recent study that analyzed the outer membrane composition of the amoeba symbiont *Protochlamydia amoebophila*, a member of the *Parachlamydiaceae*, showed that some, but not all of

these main components are conserved among chlamydiae [19,20]. Proteins homologous to OmcA and OmcB were also found at high abundance in *Protochlamydia*, suggesting a common mechanism for the stabilization of the cell wall in different chlamydial families. In contrast, no protein with similarity to MOMP was found in this organism [20]. Instead, a novel family of highly abundant porins represents the functional replacement of MOMP in *Protochlamydia* [21]. Sequencing and analyses of the genomes of members of other chlamydial families suggested an even higher diversity with respect to OMPs [22,23].

In this study, we analyzed the OMP composition of members of three chlamydial families originating from very different sources and showing different host ranges. *Parachlamydia acanthamoebae* was isolated from activated sludge [24], *Waddlia chondrophila* from an aborted bovine foetus [25] and *Simkania negevensis* was discovered in a contaminated mammalian cell culture [26]. We used a combination of *in silico* tools for the prediction of OMPs in the genomes of these organisms, experimentally enriched OMPs from purified chlamydiae and analyzed these fractions by highly sensitive mass spectrometry. We show that there are major differences in their outer membrane protein composition and that *Simkania* lacks cysteine-rich proteins in its outer membrane, a feature so far assumed to be essential for all chlamydiae to stabilize their outer membrane.

## Experimental procedures

### Cultivation, purification and transmission electron microscopy of chlamydiae

*Acanthamoeba castellanii* UWC1 infected with *P. acanthamoebae* UV7, *S. negevensis* or *W. chondrophila* 2032/99 were grown in trypticase soy broth with yeast extract (30 g/L trypticase soy broth, 10 g/L yeast extract, pH 7.2) at 20°C. Chlamydiae were purified from their amoeba hosts as previously described [20] with some modifications. Infected amoebae were harvested and the pellet was resuspended in 6.5 ml SPG/g wet weight (SPG, sucrose-phosphate-glutamate buffer; 75 g/L sucrose, 0.52 g/L KH<sub>2</sub>PO<sub>4</sub>, 1.53 g/L Na<sub>2</sub>HPO<sub>4</sub>×2H<sub>2</sub>O, 0.75 g/L glutamic acid). cOmplete, EDTA-free Protease Inhibitor Cocktail (Roche) was added and the host cells were broken using a Dounce homogenizer. Intact host cells and host debris were removed by centrifugation (300 x g, 10 min, 4°C) and filtration through 5 µm and 1.2 µm filters. Elementary bodies were enriched by sequential ultracentrifugation steps: first, the suspension was layered on 35% gastrografin and centrifuged at 55 000 x g for 45 min at 4°C. The pellet was resuspended in SPG. This was followed by two additional centrifugation steps using a sucrose/gastrografin gradient (50% sucrose overlaid with 30% gastrografin) and a gastrografin gradient (46% gastrografin overlaid with 40% gastrografin) (both 55

000 x g, 2h, 4°C). Between the centrifugation steps, the suspension was homogenized using needles (diameter 0.90 and 0.45 mm). After the last centrifugation step, cell pellets representing enriched EBs were resuspended in SPG and either used directly or stored at -80°C until further use. For transmission electron microscopy, EBs or sarkosyl-treated samples (see below) were fixed with 2% glutaraldehyde in 10 mM phosphate buffer (pH 7.2) for 1 hour at room temperature, rinsed in the phosphate buffer 3 times for 10 min each, followed by fixation with 2% osmium tetroxide in 10 mM phosphate buffer. Samples were dehydrated in an ascending series of ethanol and embedded in LV resin. Ultra-thin sections (70 nm) were cut using a Leica EM UC7 ultramicrotome, stained with 0.5% uranyl acetate and 3% lead citrate or 2.5% gadolinium and 3% lead citrate and imaged with a Zeiss EM 902 transmission electron microscope.

### **PCR and sequencing**

For re-sequencing of MOMP-like genes, DNA-fragments spanning both adjacent genes were amplified with specific primer pairs (SNE\_A08780\_F, 5'-ATG AGA AAC TGG CTT ATT-3'/SNE\_A08790\_R, 5'-TTAGAAATCGAAGCGACC-3'; and SNE\_A02800\_F, 5'-TTA GAA GTC AAA GCG GAA-3'/SNE\_A02810\_R, 5'-ATG TCT GGG CAA GGA ACTT-3') and Sanger-sequenced using the BigDye Terminator Cycle Sequencing Kit v3.1 and an ABI 3130xl Genetic Analyzer (Applied Biosystems, Foster City, CA, USA) according to the manufacturer's instructions.

### **Enrichment of chlamydial OMPs**

Three different detergents were tested for the enrichment of chlamydial OMPs: N-laurylsarcosine (sarkosyl), which selectively solubilizes inner membrane proteins [27] leaving proteins of the chlamydial outer membrane to form an insoluble pellet [14]; n-octyl polyoxyethylene (n-POE), which solubilizes OMPs; and Triton X-114 used for the enrichment of OMPs via phase separation [28]. For treatment with sarkosyl, purified chlamydiae were resuspended in 2% sarkosyl in phosphate buffered saline (PBS) with protease inhibitor. The suspension was sonicated five times for 2 min. 5 mM MgCl<sub>2</sub> and 50 U benzonase (Novagen) were added followed by incubation at 37°C for one hour with vigorous shaking. Samples were centrifuged (18 000 x g, 10 min) and the sarkosyl treatment was repeated for the pellet. The resulting sarkosyl-insoluble pellet was resuspended in protein loading buffer containing 400 mM dithiothreitol (DTT) unless indicated otherwise. For treatment with n-POE, purified chlamydiae were resuspended in 100 µl POP05-buffer (0.087 g/L EDTA, 5.84 g/L NaCl, 300 mM Na<sub>x</sub>PO<sub>4</sub>, 0.5% n-POE; pH 6.5) with 100 mM DTT per 3 mg EBs (wet weight) and incubated for 1 h

at 37°C on a rocking platform [21]. After removal of insoluble material (18 000 × g, 10 min, 4°C), ice-cold acetone was added to the supernatant and proteins were precipitated for 1 h at –20°C, followed by another centrifugation step (18 000 × g, 10 min, 4°C). The resulting pellet was resuspended in protein loading buffer. For treatment with Triton X-114, purified chlamydiae were resuspended in 250 µl ice-cold 2% Triton X-114 in phosphate buffer (pH 8.0), sonicated for 10 min and put on ice. Phases were separated by heating to 90°C in a water bath followed by centrifugation (400 × g, 10 min, 37°C). The aqueous upper phase was removed, 250 µl phosphate buffer was added to the lower phase and the extraction was repeated. 15 µl of the lower phase were mixed with 5 µl protein loading buffer. After addition of protein loading buffer, samples were heated to 95°C for 5 min and proteins were separated by 1D gel electrophoresis using either self-cast 12.5% SDS-PAGE gels or 10% Mini-PROTEAN TGX gels for samples subjected to mass spectrometry. Gels were stained with colloidal coomassie and destained with water.

### **In-gel digestion of protein fractions**

Each lane of the stained gel was cut into 10-14 sections, chopped, washed with 50 mM ammonium bicarbonate (ABC, pH 8.5), and dried with acetonitrile (ACN). Disulfide bonds were reduced with DTT (200 µl of 10 mM DTT for 30 min at 56°C). DTT was washed off and cysteines were alkylated by incubation with 100 µl 54 mM iodoacetamide for 20 min at room temperature in the dark. Gel pieces were dried with ACN, swollen in 10 ng/µl trypsin (recombinant, proteomics grade, Roche) in 50 mM ABC and incubated over night at 37°C. The reaction was stopped by adding formic acid to a final concentration of approximately 1% and peptides were extracted by sonication.

### **In-solution digestion of protein fractions**

The protein pellet was solubilized in 40 ml solubilization buffer (8 M urea, 100 mM Tris-HCl, pH 8.0) by sonication for 5 min. Reduction and alkylation were performed as described elsewhere [29]. Proteins were digested with LysC (Wako Chemicals; 1:25 of the estimated amount of protein) for three hours at 30°C. Samples were diluted with 50 mM ABC to a concentration of 0.8 M urea followed by tryptic digestion (recombinant, proteomics grade, Roche; 1:30 of the estimated amount of protein) at 37°C overnight. Detergents were removed with Pierce Detergent Removal Spin Columns (Thermo Scientific) according to the manufacturer's protocol. The eluates were acidified, desalted on STRATA-X columns (Phenomenex) and concentrated on the speed-vac.

### LC-MS/MS analysis

Peptides were separated on an UltiMate 3000 nano HPLC or an RSLC system (Dionex, Thermo Fisher Scientific). Digests were loaded on a trapping column (PepMap C18, 5 µm particle size, 300 µm i.d. x 5 mm, Thermo Fisher Scientific) equilibrated with 0.1% trifluoroacetic acid (TFA) and separated on an analytical column (PepMap C18, 2 µm, 75 µm i.d. x 150-250 mm, Thermo Fisher Scientific) applying a 60-180 minutes linear gradient from 1.6% up to 32% ACN with 0.1% formic acid followed by a washing step with up to 72% ACN. The HPLC was directly coupled to an LTQ-Orbitrap Velos mass spectrometer (Thermo Fisher Scientific) equipped with a nanoelectrospray ionization source (Proxeon, Thermo Fisher Scientific). The mass spectrometer was operated in the data-dependent mode: 1 full scan (resolution 60000) with lock mass enabled was followed by maximal 12 MS/MS scans in the LTQ. The lock mass was set at the signal of polydimethylcyclsiloxane at  $m/z$  445.120025. Monoisotopic precursor selection was enabled and singly charged signals were excluded from fragmentation. The collision energy was set at 35%, Q-value at 0.25 and the activation time at 10 ms. Fragmented ions were put on an exclusion list for up to 120 s depending on the gradient length.

### Interpretation of MS data

Raw spectra were interpreted by Mascot 2.2.04 (Matrix Science) using Mascot Daemon 2.2.2. Spectra were searched against a database containing the sequences of *Protochlamydia amoebophila* UWE25 [30], *Waddlia chondrophila* WSU 86-1044 [23], *Waddlia chondrophila* 2032/99, *Parachlamydia acanthamoebae* UV7, *Simkania negevensis* [22], *Acanthamoeba castellanii* Neff [31] and sequences of common contaminants. The parameters were set as following: the peptide tolerance was set to 5 ppm, MS/MS tolerance to 0.8 Da, carbamidomethylcysteine as static modification and oxidation of methionine as a variable modification. Trypsin was selected as the protease and two missed cleavages were allowed. MASCOT results were loaded into Scaffold (Ver. 3.6.2; Proteome Software). Protein identifications were accepted when a minimum of two peptides were identified with a probability greater than 95% as assigned by the Protein Prophet algorithm [32] resulting in a false discovery rate of 0.0% on the protein and peptide level. Relative protein abundance in one lane was determined over all gel sections by calculating the normalized spectral abundance factor (NSAF) for proteins with a minimum of five spectra [33] if equal amounts of the gel pieces of one lane were loaded. For bands rich in protein only a fraction of the corresponding digests were injected into the LC-MS system in order to avoid overloading. The protein abundance in the corresponding lanes was calculated based on the total ion current and differences in the injected amount of the digests were adjusted by multiplication. Proteins were sorted according to their abundance and the mean rank between the two biological replicates was calculated. This showed that 32, 42 and 34 of the 50 most

abundant proteins overlapped between both biological replicates in *Parachlamydia*, *Simkania* and *Waddlia*, respectively.

### **Osmotic stability in the presence of reducing agent**

Chlamydiae were purified from their host cells as previously described [34]. In brief, asynchronously infected amoebae were harvested and broken by vortexing with glass beads. Cell debris and intact amoebae were removed by centrifugation followed by two filtration steps (5  $\mu\text{m}$  and 1.2  $\mu\text{m}$ ). The suspension was split into aliquots, spun down and the resulting pellets were resuspended in one of the following buffers either with or without 5 mM DTT: 10 mM phosphate buffer (pH 7.2), 10 mM phosphate buffer with 170 mM NaCl or 10 mM phosphate buffer with 480 mM NaCl. Cell suspensions were incubated at 37°C with gentle shaking. The optical density (OD<sub>600</sub>) was measured at 0, 10, 20, 40 and 60 min after start of the incubation. All measurements were done in three biological replicates.

### ***In silico* prediction of the subcellular localization of chlamydial proteins**

For the prediction of OMPs in the genomes of *Simkania*, *Parachlamydia* and *Waddlia* a combination of different prediction tools was used (Fig. 1). For *Waddlia*, genomes of both strain WSU 86-1044, representing a closed genome, and strain 2032/99, representing the strain used in the experimental part of this study and for which a nearly complete genome is available, were analyzed, and a consensus list of OMPs was built. The subcellular localization of proteins was predicted using PSORTb v3.0 [35], CELLO [36] and SOSUI-GramN [37]; beta-barrel OMPs were predicted using BOMP including the BLAST-option [38], MCMBB [39] and TMBETADISC-RBF using PSSM features [40]; lipoproteins were predicted using LIPO [41] and LipoP [42]; transmembrane helices were predicted using Phobius [43] and TMHMM v.2.0 [44]. Signal peptides were predicted using SignalP 4.0 [45]. Criteria for the prediction of OMPs were evaluated using a dataset of 529 proteins of Gram-negative bacteria with known subcellular location [46]. Parameters were optimized by changing the number of positive predictions required for the assignment of a protein as OMP and calculating the accuracy (percent of correct predictions), sensitivity (percent of true positive predictions), specificity (percent of true negative predictions) and the Matthews correlation coefficient (Table S1). Prediction parameters were further adjusted by using a test set of chlamydial proteins of known location, consisting of 24 OMPs and 25 proteins with other subcellular locations (Table S2). The optimized parameters were then used to predict OMPs, outer membrane lipoproteins and lipoproteins in the genomes of *Parachlamydia*, *Simkania*, *Waddlia*, *Protochlamydia* and *C. trachomatis* D/UW-3/CX.

Positive results by a lipoprotein prediction tool overruled any beta-barrel prediction, since the prediction of lipoproteins was previously shown to be highly specific [42]. Whether a lipoprotein is attached to the inner or the outer membrane of Gram-negative bacteria depends on the presence of aspartic acid in position +2 relative to the cleavage site [47]. However, this rule is not universal for all bacteria [48,49]. Since predictions by subcellular localization and lipoprotein prediction tools were contradictory for several proteins, we decided to annotate proteins only as outer or inner membrane lipoproteins if there was additional support by localization prediction tools and to annotate the others generally as 'lipoprotein'.

Alpha-transmembrane helices are a feature characteristic for inner membrane proteins, and all proteins with more than one helix predicted by TMHMM or Phobius were from the list of OMPs. We allowed for one helix as signal peptides are sometimes incorrectly predicted as transmembrane helices by prediction tools. To further improve prediction results, proteins with an overall of at least 2 positive predictions were re-evaluated using HHOMP with a threshold of >90% to predict a protein as OMP [50], and the list of OMPs was manually revised. Structure predictions for selected proteins were performed using I-TASSER [51].

The subcellular localization of all non-OMPs in the genomes was predicted based on a consensus prediction by PSORTb, CELLO and SOSUI-GramN: if at least two of these tools agreed on the same subcellular localization, the protein was assigned to this compartment; otherwise, the localization was stated as 'Unknown'.

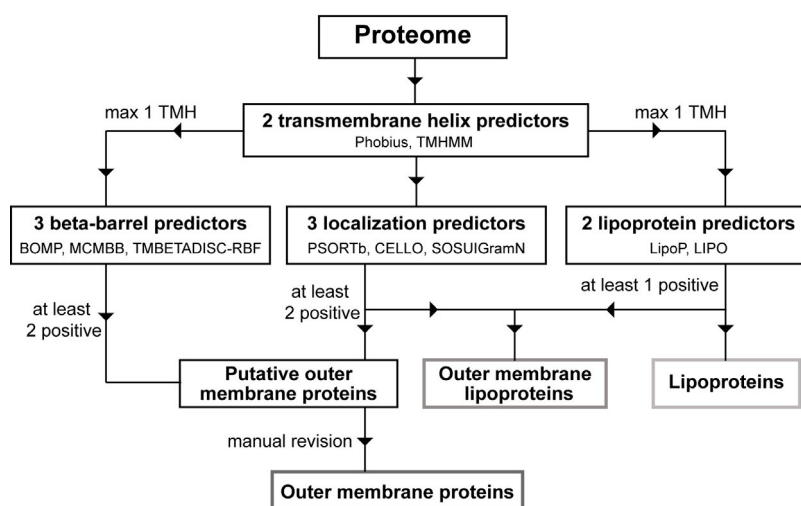


**Figure 1: Workflow for the prediction of outer membrane proteins in the proteomes of chlamydiae.** A combination of *in silico* tools was used for the prediction of the subcellular location, possible beta-barrel conformation or the presence of lipoprotein signal peptides and transmembrane helices (TMH) of chlamydial proteins. The prediction performance was optimized by the calculation of statistical parameters for protein sets of known localization (Table S1). The list of putative outer membrane proteins was manually revised by taking into account probabilities calculated with the outer membrane prediction tool HHOMP and by searching the existing literature.



## Results

### A consensus approach for *in silico* prediction of chlamydial OMPs

Most OMPs share features specific for this group of proteins and various *in silico* tools exist for their identification in genomes based on alternating hydrophobicity patterns, amino acid composition, N- and C- terminal patterns, or homology detection. We used three subcellular localization (PSORTb, CELLO, SOSUI-GramN), three beta-barrel conformation (BOMP, MCMBB, TMBETADISC-RBF) and two lipoprotein (LIPO and LipoP) prediction tools to identify OMPs in the genomes of *Parachlamydia*, *Simkania* and *Waddlia* (Fig. S1). There were striking differences in the numbers of predicted OMPs for the different tools. For example, the beta-barrel prediction tool MCMBB predicted 724 proteins as beta-barrel proteins in the genome of *Parachlamydia*, in contrast to 92 proteins predicted by TMBETADISC-RBF and only 38 by BOMP (Fig. S1). Similarly, while LipoP predicted 44 lipoproteins in the genome of *Parachlamydia*, only 6 were predicted by LIPO and only two of these proteins were consistently predicted by both methods (Fig. S1). On the other hand, PSORTb predicted only 9 OMPs in *Waddlia*, quite likely missing many OMPs.

To increase the confidence of our predictions, we decided to establish a consensus prediction approach based on the combination of different tools as this has been shown to enhance the prediction performance [46,52-54]. We evaluated the prediction performance using an existing set of proteins of known location [46] showing that very stringent criteria were ideal for the identification of OMPs in this protein set as indicated by high accuracy, recall, specificity and Matthews correlation coefficient (Table S1). However, this published dataset included only one chlamydial OMP. Therefore, we set up a second, smaller test set consisting of 49 chlamydial proteins of known location, including 24 OMPs (Table S2). The percentage of correct predictions dropped for this set of proteins for all prediction criteria tested, mainly due to a lower percentage of true positive predictions (Table S1). Based on the evaluation of prediction parameters with the chlamydial dataset, we chose the following criteria: at least two positive predictions by localization prediction tools or beta-barrel prediction tools for predicting OMPs; an additional prediction by a lipoprotein prediction tool for outer membrane lipoproteins; and at least one positive prediction by a lipoprotein prediction tool for lipoproteins in general (Fig. 1).

To further evaluate our consensus prediction approach, OMPs were predicted in the genomes of *C. trachomatis* and *Protochlamydia*, two organisms for which experimental data is available on the protein composition of the outer membrane. 32 and 44 OMPs were predicted for *C. trachomatis* and *Protochlamydia*, respectively (Table S3). 24 and 27 of the predicted OMPs are in agreement with

predictions in an earlier study [19], while 11 and 16 have been detected experimentally in the outer membrane previously [20,55,56]. Four known OMPs (PmpA, OprB, CTL0541 and the 15 kDa cysteine-rich protein) of *C. trachomatis* were missed by our computational approach.

Application of our *in silico* consensus approach for the prediction of OMPs to the genomes of *Parachlamydia*, *Simkania* and *Waddlia* lead to the identification of 64, 84 and 50 putative OMPs (including outer membrane lipoproteins), respectively (Table S4).

### Optimization of the enrichment of OMPs from purified chlamydiae

Most OMPs make up only a small fraction of the overall protein content of a cell, and different methods exist for their enrichment. We evaluated three popular methods for the enrichment of OMPs by treating purified *Simkania* EBs with sarkosyl, n-POE or Triton X-114. Band patterns were similar after treatment with sarkosyl and n-POE, but differed for Triton X-114 (Fig. 2). Mass spectrometry analysis of in-gel digests of proteins showed that sarkosyl and n-POE both worked well for the enrichment of OMPs – although *Simkania* might be more tightly associated with host organelles than other chlamydiae (Mehlitz et al., 2014) – as this class of proteins was strongly enriched and included the most abundant proteins for both treatments (Fig. 3). Although OMPs were also present in the Triton X-114-treated sample, cytoplasmic proteins and proteins of the amoeba host were much more abundant than for the other two detergents (Fig. 3). 53 predicted OMPs were identified with all three detergents, but nine were only found after treatment with sarkosyl or n-POE (Fig. S2, Table S5). For *Parachlamydia*, the enrichment of OMPs was not as efficient as for *Simkania*

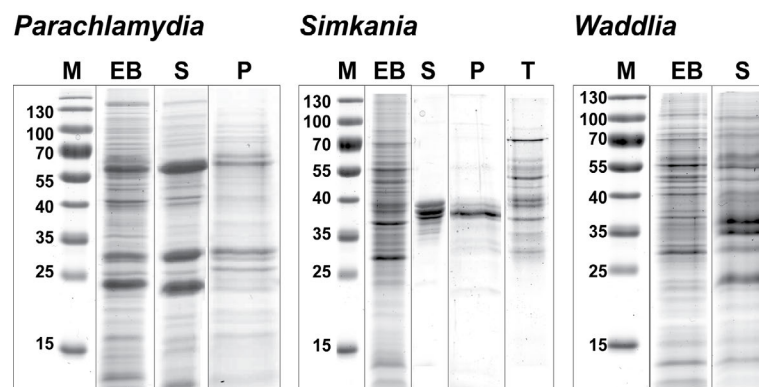


**Figure 2: Enrichment of outer membrane proteins of *Parachlamydia*, *Simkania* and *Waddlia* EBs using different detergents.** Band patterns in SDS PAGE gels after treatment with sarkosyl (lanes labelled S) differ between *Simkania* and the other two organisms, suggesting different protein compositions of the outer membrane of these organisms. Treatment of *Simkania* EBs with sarkosyl or n-POE (lanes labelled P) results in similar patterns in contrast to treatment with Triton X-114 (lane labelled T).

Molecular mass of marker proteins in kDa is indicated on the left; M, marker; EB, purified EBs of the respective organism.

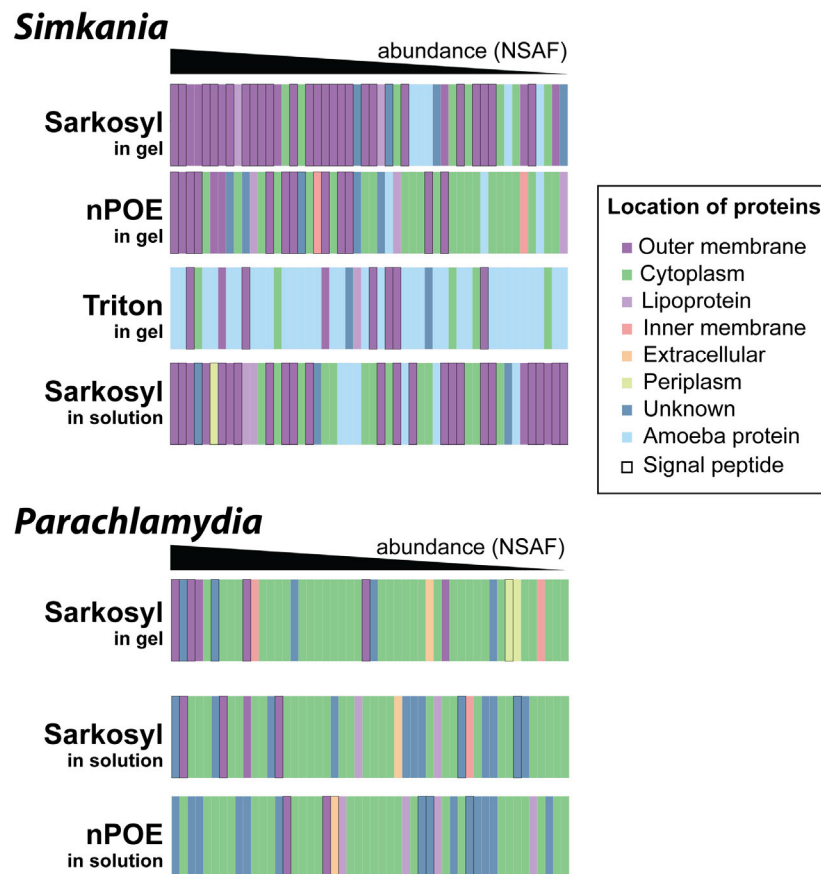


**Figure 3: Comparison of different extraction methods and digestion protocols for spectrometry-based detection of outer membrane proteins.**

The 50 most abundant proteins and their predicted locations are shown for each approach. Proteins were quantified and ranked by calculating the normalized spectral abundance factor (NSAF).

(Fig. 3), but still more cell envelope proteins were identified in the sarkosyl-treated sample compared to n-POE (Fig 3). Based on these results, we decided to use sarkosyl for the enrichment of OMPs in all further experiments.

After enrichment OMPs must be effectively solubilized for further analysis, which is challenging for hydrophobic proteins. We compared two sample preparation procedures after sarkosyl-treatment of purified *Simkania* and *Parachlamydia* cells: solubilization of proteins by the strong anionic detergent SDS followed by 1D gelelectrophoresis and in-gel digests and denaturation of proteins in urea followed by in-solution digests. 27 OMPs were detected only upon in-gel, but not upon in-solution digests for *Simkania*, including several MOMP-like proteins (Table S5). For both *Parachlamydia* and *Simkania*, OMPs were more frequently detected after in-gel digests compared to in-solution digests (Fig. 3). Based on these results, we decided to use the more sensitive in-gel digest in all further experiments.

### Enrichment of OMPs by sarkosyl

Treatment of purified EBs with sarkosyl resulted in the enrichment of cell envelopes devoid of cytoplasmic content for all three organisms as shown by transmission electron microscopy (Fig 4). Envelopes of *Parachlamydia* and *Waddlia* maintained the shape of intact EBs, whereas envelopes of *Simkania* were more flexible in shape and often broken open (Fig 4). 1D gel electrophoresis of the obtained fractions showed that the band patterns were strikingly different between *Simkania* and the other two organisms (Fig. 2). For *Simkania*, the complexity of the sample was substantially reduced after treatment with sarkosyl, resulting in only few bands at a molecular mass of ~40 kDa on SDS-PAGE gels. Proteins in specific bands were also enriched after treatment with sarkosyl for *Parachlamydia* and *Waddlia*, but overall band patterns were much more complex than those observed for *Simkania*. These differences in band patterns also corresponded to the number of proteins identified by mass spectrometry after in-gel digests of proteins (Table S6). For *Simkania*, 123

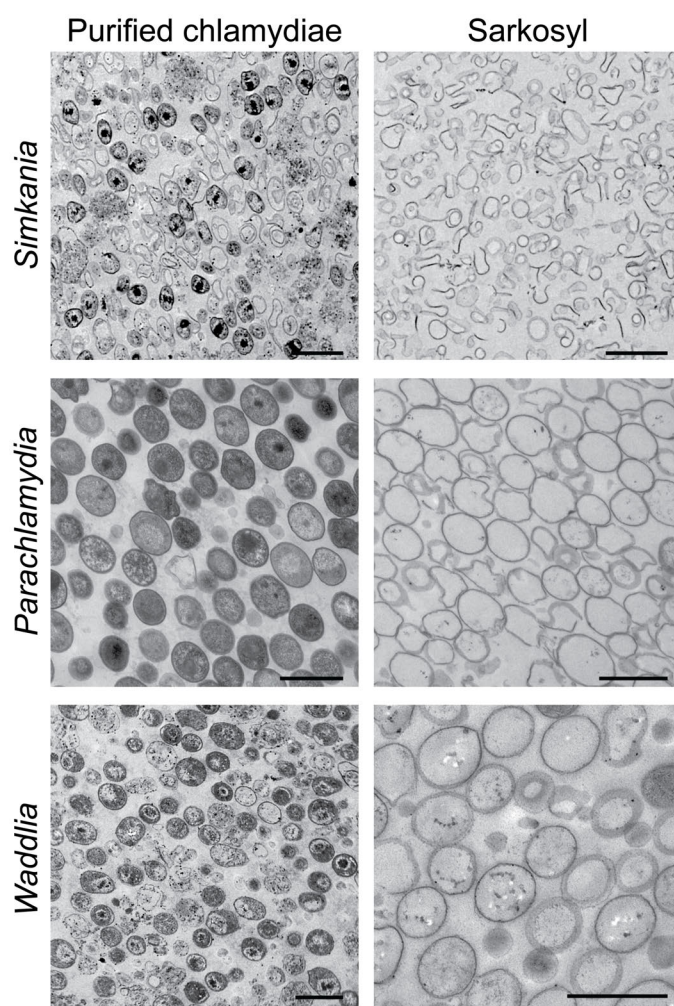


**Figure 4: Treatment of environmental chlamydiae with sarkosyl leads to an enrichment of cell envelopes.**

Transmission electron microscopy of purified EBs before (left panel) and after (right panel) treatment with sarkosyl shows the successful depletion of cytoplasmic content. Bars, 1  $\mu\text{m}$ .

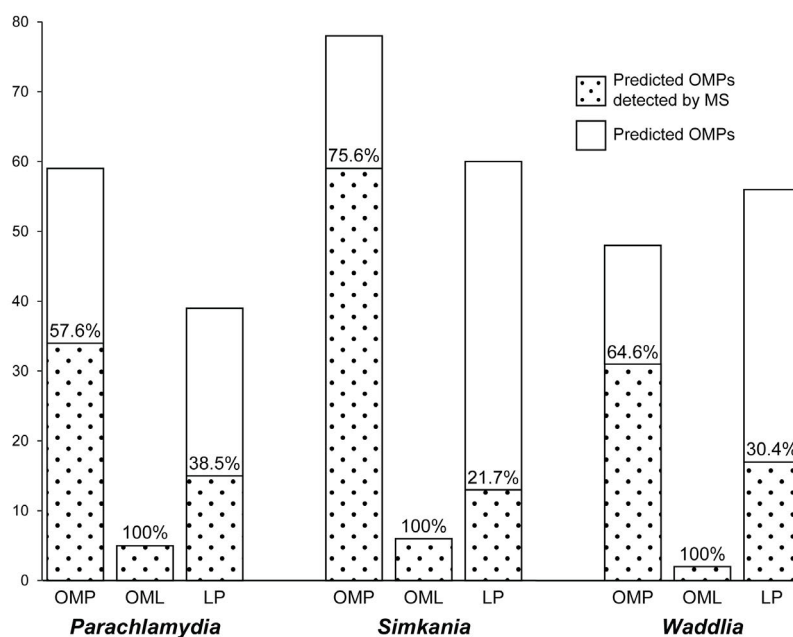


**Figure 5: Numbers of experimentally verified predicted outer membrane and lipoproteins of *Parachlamydia*, *Simkania* and *Waddlia***

More than half of all predicted outer membrane proteins (OMP) and all outer membrane lipoproteins (OML) were detected by mass spectrometry in outer membrane protein fractions of all three organisms. Only proteins that were identified in both biological replicates were considered. The percentage of predicted proteins that were detected by mass spectrometry is indicated. LP, lipoproteins.

chlamydial proteins were identified in both biological replicates, and 65 of these were predicted OMPs with an additional 13 being predicted lipoproteins. For *Parachlamydia*, 825 chlamydial proteins were detected, including 39 predicted OMPs and 15 lipoproteins. In fractions of *Waddlia*, 921 chlamydial proteins were identified, 33 of them being predicted OMPs and 17 lipoproteins. These represent 58%, 76% and 65% of all predicted OMPs of *Parachlamydia*, *Simkania* and *Waddlia*, respectively, as well as all outer membrane lipoproteins predicted in the genomes of these organisms (Fig. 5).

For all three chlamydiae, OMPs were the most abundant proteins in the enriched fractions based on relative quantification by the normalized spectral abundance factor (NSAF) (Table S7). However, while all of the twenty most abundant proteins were either predicted OMPs or lipoproteins for *Simkania*, this was only the case for five and seven proteins for *Parachlamydia* and *Waddlia*. Other OMPs detected for *Parachlamydia* and *Waddlia* were present in much lower amounts, suggesting that these proteins are either not abundant in EBs or that they were not enriched by the applied method.

**Many MOMP-like proteins dominate the outer membrane of *Simkania* and *Waddlia***

The most abundant protein in the outer membrane of the *Chlamydiaceae* is the porin MOMP [14]. In the genomes of *Simkania* and *Waddlia* large protein families with homology to MOMP are present (37 and 11 MOMP-like proteins, respectively) [22,23]. Proteins of this rather divergent family share between 20-40% sequence identity with each other in *Simkania* and between 15-25% identity in *Waddlia*. Exceptions are pairs or triplets of MOMP-like proteins that are encoded adjacent to each other in the genomes, which show considerably higher sequence identity with each other (up to 81% sequence identity in *Simkania* and 35-80% identity in *Waddlia*). In our study, we detected all MOMP-like proteins in OMP fractions of the respective organism by mass spectrometry. The outer membrane of *Simkania* was clearly dominated by this protein family. The seven most abundant and 17 of the 20 most abundant proteins belonged to the MOMP-like protein family in this organism (Table S7). All MOMP-like proteins of *Simkania* except four had a predicted molecular mass of ~ 40 kDa, suggesting that the dominant bands detected in OMP fractions on SDS-PAGE gels represent this group of proteins (Fig. 2). The four MOMP-like proteins with a predicted lower molecular mass were encoded by adjacent genes. Re-sequencing of the respective genome region revealed sequencing errors in the original genome sequence that wrongly introduced stop codons in both cases. When we searched for spectra corresponding to the corrected parts of the sequences, we found matches for both full-length proteins in the database (Fig. S3). In fact, these two MOMP-like proteins were among the twenty most abundant proteins in outer membrane fractions of *Simkania*.

Proteins in bands of ~34-38 kDa were also strongly enriched in sarkosyl-treated protein fractions of *Waddlia* compared to untreated EBs (Fig. 2). This molecular mass range matches MOMP-like proteins that were highly abundant in OMP fractions of *Waddlia*, with four MOMP-like proteins among the ten most abundant proteins detected by mass spectrometry. For the majority of MOMP-like proteins (30 out of 37) of *Simkania*, but only for one protein of *Waddlia*, a beta-barrel conformation was predicted (Table S4), suggesting a possible role as porin in the outer membrane similar to MOMP [15]. A single MOMP-like protein was also detected in OMP fractions of *Parachlamydia*, but at much lower abundance compared to other predicted outer membrane components. Instead, three hypothetical proteins, PUV\_27500, PUV\_11160 and PUV\_07550, were the most abundant proteins in OMP fractions of this organism. PUV\_27500 is homologous to the OMP pc0004 of *Protochlamydia* [20] and to the 76 kDa *C. pneumoniae* protein which was described as an EB surface antigen [57]. The function of all three hypothetical proteins is unknown, but BOMP and TMBETADISC-RBF predicted a beta-barrel conformation for PUV\_27500. A beta-barrel conformation was also predicted by the structure prediction tool I-TASSER for PUV\_07550, indicating a possible function as porin.

### **Autotransporter and secretion systems**

Autotransporters, which are classified as type V secretion systems [58], are widely distributed among Gram-negative bacteria and many of them have a role in virulence [59]. *Simkania* is the only chlamydia besides the *Chlamydiaceae* that encodes proteins belonging to the polymorphic membrane protein family, autotransporters with an important role during attachment to the host in the *Chlamydiaceae* [60]. Three homologues of PmpB are encoded in the genome of *Simkania* and all are predicted to form beta-barrel structures in the outer membrane. Interestingly, subcellular localization tools predicted both a location in the outer membrane and extracellularly for these proteins, in agreement with the fact that they consist of an integral outer membrane as well as a secreted part. Peptides corresponding to all three *Simkania* autotransporters were detected by mass spectrometry, and quantification based on the NSAF suggested that they are present in similar amounts in the outer membrane. In *Parachlamydia*, two proteins have highest similarity to autotransporters of *Proteobacteria*. For PUV\_1000, formation of a beta-barrel structure and location in the outer membrane or extracellularly was predicted, similar to the Pmps of *Simkania*. Although PUV\_3300 was predicted to form a beta-barrel by only one of three tools, HHOMP predicted it with high confidence as OMP. However, both proteins were only present in low amounts in outer membrane fractions. A protein, which is annotated as putative autotransporter in the genome of *Waddlia* (wcv\_0271) [23], was also detected at low abundance by mass spectrometry. However, in contrast to the autotransporters of *Simkania* and *Parachlamydia*, neither a location in the outer membrane nor the formation of a beta-barrel structure was predicted for this protein with the *in silico* tools used in this study.

For all three organisms, structural components and chaperones of the type III secretion system were detected in OMP fractions, in agreement with a previous study reporting the presence of these needle-like structures on EBs of *Simkania* and *Parachlamydia* [34]. *Simkania* encodes an additional type IV secretion system in its genome [22], but no structural components of this apparatus were detected in outer membrane fractions.

### ***Simkania* lacks cysteine-rich outer membrane proteins**

Cysteine-rich proteins play an important role in the stabilization of the chlamydial cell envelope and are major components of the COMC of *Protochlamydia* and members of the *Chlamydiaceae* [10,20]. In agreement, also the most abundant proteins in outer membrane fractions of *Parachlamydia* and *Waddlia* showed high cysteine contents. MOMP-like proteins, which dominate the outer membrane of *Waddlia*, contain 3.5-5.3% cysteine residues. The two most abundant OMPs of *Parachlamydia*,

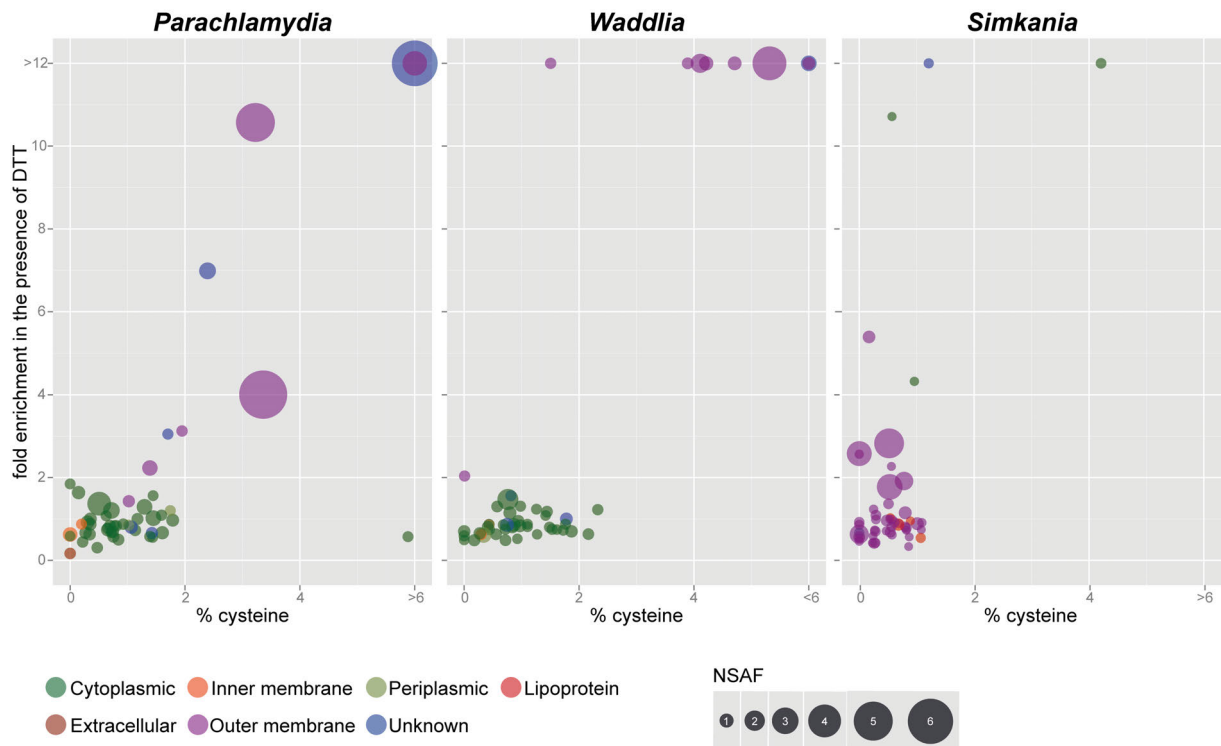


**Figure 6: Abundant outer membrane proteins of *Parachlamydia* and *Waddlia*, but not of *Simkania*, have a high cysteine content and are enriched in SDS-PAGE gels in the presence of reducing agent.**

The percentage of cysteines per protein is plotted against fold enrichment in the presence versus absence of the reducing agent dithiothreitol (DTT). The fold enrichment was calculated by dividing the respective percent spectral counts determined by mass spectroscopy. The 50 most abundant proteins (based on quantification by NSAF) in the presence of reducing agent are shown.

PUV\_27500 and PUV\_07550, show a cysteine content of more than 3%. Homologues of the cysteine-rich protein OmcB were highly abundant in both organisms, with a cysteine content of 7.6% in *Parachlamydia* and 9.4% in *Waddlia*. In addition, two homologous proteins with a molecular mass of ~22 kDa and high cysteine content (10.5% for PUV\_11160 of *Parachlamydia* and 6.9% for wcw\_0272 of *Waddlia*) were strongly enriched in outer membrane fractions of both organisms (Fig. 2). Although our *in silico* prediction approach could not assign a location to these proteins, their high abundance in outer membrane fractions and the presence of a signal peptide suggest a location in the cell envelope.

No homologue of OmcB is encoded in the genome of *Simkania*, and in striking contrast to all other chlamydiae investigated so far, no detected OMP of *Simkania* showed a cysteine content higher than 1.8%. In fact, MOMP-like proteins, the most abundant protein component in the outer membrane of *Simkania*, show a percentage of cysteine ranging from 0 to 1.1%, far below the cysteine content of MOMP-like proteins of *Waddlia*. Overall, the average cysteine content of predicted OMPs of *Simkania* was 0.54%, comparable to *Escherichia coli* K-12 (0.51% based on OMP prediction by (Heinz, Tischler et al. 2009)). In contrast, OMPs of *Parachlamydia* and *Waddlia* encoded for an average of



1.3% and 2% cysteine, respectively. The cysteine content of all proteins encoded in the genome was similar for all three chlamydiae (1.2% for *Simkania*, 1.4% for *Parachlamydia* and *Waddlia*) and comparable to *Escherichia coli* K-12 or *Legionella pneumophila* (both 1.3%).

### **Pinpointing the COMC of *Parachlamydia* and *Waddlia***

For *Parachlamydia* and *Waddlia* high numbers of cytoplasmic proteins were detected among the 50 most abundant proteins in samples after sarkosyl-treatment. To identify true components of the COMC in these organisms, we compared OMP fractions treated with or without the reducing agent DTT by mass spectrometry. For each protein, an enrichment factor was calculated by dividing the percent spectral counts in the presence of DTT by the percent spectral counts in the absence of DTT. Many dominant OMPs of *Parachlamydia* and *Waddlia* were strongly depleted in the absence of DTT (Fig. 6, Table S8) demonstrating their participation in formation of the COMC. The cysteine-rich protein OmcB, a putative long-chain fatty acid transport protein and eight of the 11 MOMP-like proteins were not detected at all in gels in the absence of DTT for *Waddlia*. The three MOMP-like proteins that were detected under both conditions were the most abundant OMPs under reducing conditions and were at least 57-fold enriched in the presence of DTT. In *Parachlamydia*, OmcB was enriched 126-fold under reducing conditions, and the cysteine-rich protein PUV\_11160 was enriched more than 70-fold. In contrast, all MOMP-like proteins and all other components of the outer membrane except one were present at similar levels in both *Simkania* samples. The protein SNE\_A20110, which is probably involved in protein secretion, showed a five-fold enrichment in the presence of DTT despite its low cysteine content (0.17%). In addition, one protein of unknown location with a cysteine content of 1.2%, and two cytoplasmic proteins were enriched between 10 to 12-fold in fractions under reducing conditions in *Simkania*.

### **Stability of chlamydiae under reducing conditions**

To test whether the observed differences in outer membrane protein composition also affect the stability of the organisms, purified *Simkania*, *Parachlamydia* and *Waddlia* cells were incubated in buffers of different osmolarities in the absence or presence of reducing agent. For *Simkania*, the integrity of cells decreased slowly for all incubations, and no differences associated with the presence of DTT were observed (Fig. 7). The presence of DTT had only a minor influence during incubations under high osmolarity conditions for *Parachlamydia* and *Waddlia*. However, when these chlamydiae were incubated under low osmolarity conditions, cells lysed rapidly in the presence but not in the absence of DTT.

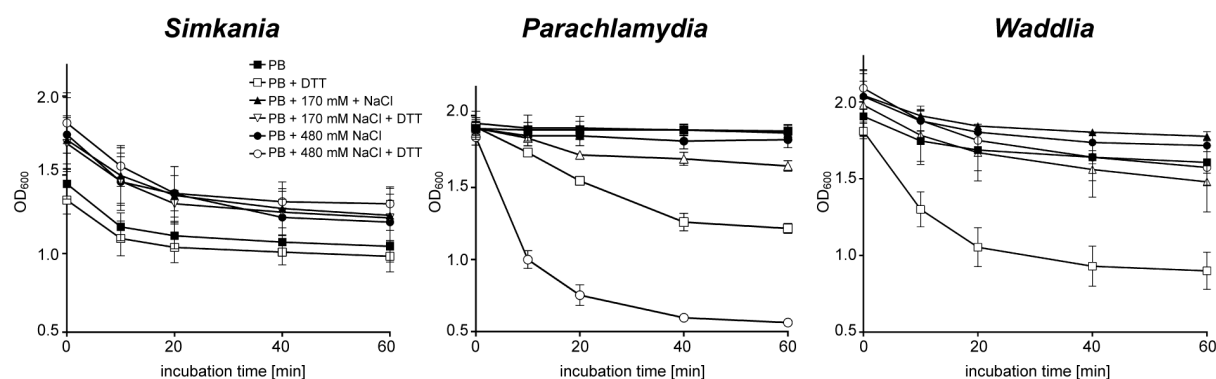


**Figure 7: The stability of *Parachlamydia* and *Waddlia*, but not of *Simkania*, is affected by reducing conditions.**

Changes in cell density of purified chlamydiae (measured as OD<sub>600</sub>) during incubation in host-free buffers of different osmolarities in the presence (empty symbols) or absence (filled symbols) of DTT are shown. The cell density decreased rapidly for *Parachlamydia* or *Waddlia* under low osmolarity conditions in the presence of DTT. No differences were seen for incubations of *Simkania* in the presence or absence of reducing agent. PB, phosphate buffer; DTT, dithiothreitol;

## Discussion

### Challenges in the prediction and enrichment of chlamydial OMPs

In this study we characterized the protein composition of the outer membrane of members of three chlamydial families using a combination of *in silico* localization predictions and highly sensitive mass spectrometry analysis. The *in silico* analyses showed large discrepancies in the number and identity of predicted OMPs between the different tools. In general, predictions were more heterogeneous for chlamydial proteins compared to a published protein testset for Gram-negative bacteria that was used for a first evaluation of the prediction parameters. In comparison, also signal peptides were identified less frequently for predicted OMPs of chlamydiae than for OMPs in the testset (33%-60% of chlamydial OMPs vs. 70% of OMPs in the testset). One possibility is that this is caused by inaccurate gene predictions in chlamydial genomes. However, it more likely arises from the large phylogenetic distance of chlamydiae to the *Proteobacteria*, which are commonly used in the training of Gram-negative specific versions of *in silico* prediction tools. Consistent with this, ambiguous *in silico* predictions were also encountered in a recent study that searched for OMPs in members of the chlamydial sister phyla *Planctomycetes* and *Verrucomicrobia* [61].

A major challenge in the preparation of outer membrane fractions is the minimization of contaminating proteins from other cellular compartments. Cellular sub-fractions represent rather an enrichment of proteins from the respective compartment than a sharp separation from other cellular compartments. Thus although OMPs can be enriched by treatment with detergents, co-purification of non-OMPs is unavoidable [62-65], particularly when highly sensitive mass spectrometry methods are used. We indeed detected high numbers of low abundant proteins from all other cellular

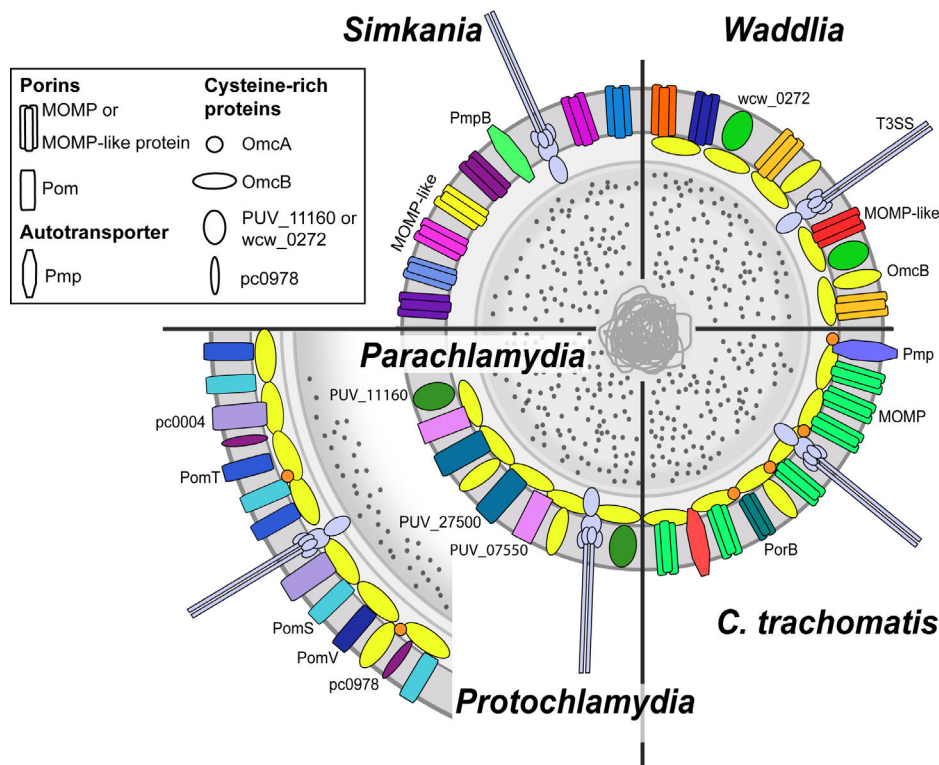


**Figure 8: A model of the outer membranes of members of four different chlamydial families shows conserved features, but also highlights major differences in the outer membrane composition.**

The stabilizing cysteine-rich protein OmcB is present in *Parachlamydia*, *Protochlamydia*, *Waddlia* and *C. trachomatis*, but absent from *Simkania*. MOMP and MOMP-like proteins dominate the outer membrane of *Simkania*, *Waddlia* and *C. trachomatis*, but not of *Parachlamydia* and *Protochlamydia*. The model includes only the most dominant proteins. T3SS, type three secretion system.

compartments in the outer membrane fractions, especially for *Parachlamydia* and *Waddlia* (Figure 3). The efficiency of the OMP enrichment differed largely between *Simkania* and the other two organisms. In *Simkania*, all but two of the 50 most abundant proteins were predicted to be associated with the outer membrane, and 63% of all detected proteins represented predicted OMPs or lipoproteins. This is a performance comparable to or better than achieved in other outer membrane proteome studies [66-69]. The same enrichment protocol was much less efficient for *Parachlamydia* and *Waddlia* and consistent with a recent study on immunogenic proteins of *Waddlia* [70]. In outer membrane fractions of these organisms, non-OMPs such as ribosomal proteins, elongation factors and heat-shock proteins were detected in high amounts. Ribosomal proteins often are a major contaminant in outer membrane fractions due to their high abundance and hydrophobicity. In addition, protein aggregates and large complexes like GroEL can co-precipitate with membrane fractions during high-speed centrifugation [66]. However, electron microscopy clearly showed a depletion of cytoplasmic contents after sarkosyl-treatment for all three organisms similar to other studies (Fig. 4)[20,55]. The differences between *Simkania* vs. *Parachlamydia* and

*Waddlia* could result from lower abundance of OMPs in the latter organisms or from structural differences of the cell walls that hindered a better enrichment of OMPs.

### **Major differences in the outer membrane protein composition**

We found remarkable differences in the most abundant protein components of the outer membrane between members of different chlamydial families, but also between members of the same family (Fig. 8). *Parachlamydia* and *Protochlamydia*, both members of the *Parachlamydiaceae*, differ from other chlamydiae in that they do not share MOMP or MOMP-like proteins as the most abundant protein and major porin in their cell envelope. In addition, the major porin also differs between the two *Parachlamydiaceae*, in contrast to the *Chlamydiaceae* which all share MOMP as the most abundant porin in their outer membrane [71]. PomS and PomT are the dominant OMPs in *Protochlamydia* [20], and the function of PomS as porin has been demonstrated recently [21]. The outer membrane of *Parachlamydia* is dominated by three hypothetical proteins (PUV\_27500, PUV\_11160, PUV\_07550), and for two of these a beta-barrel conformation has been predicted suggesting a function as porin. Interestingly, *Parachlamydia* encodes both a homologue of MOMP and a member of the Pom family, but these proteins were only detected at low abundance, suggesting that they do not play a major role in the outer membrane of *Parachlamydia*.

In contrast to members of the *Chlamydiaceae* that encode a single copy of MOMP and the MOMP-homologue PorB [72], the outer membrane of *Simkania* and *Waddlia* is dominated by large numbers of MOMP-like proteins. Of the 84 predicted OMPs of *Simkania*, 35 belonged to the family of MOMP-like proteins, and they account for more than half of all OMPs that were detected by mass spectrometry. In *Waddlia*, MOMP-like proteins represent a third of all detected OMPs. Expanded OMP families are also found in other bacteria, for example the Hop family of *Helicobacter pylori* [73] or the OMP-1/MSP2/P44 family of the obligate intracellular tick-borne pathogens *Anaplasma marginale* [74] and *Ehrlichia chaffeensis* [75]. All 22 full-length paralogs of the OMP-1/MSP2/P44-family were detected in a proteomic analysis of *E. chaffeensis* and *A. phagocytophilum* [76]. Members of this protein family are differentially expressed between infections of vertebrate and invertebrate hosts [77,78] or at different temperatures [79]. It was suggested that the porin activity of these proteins regulates nutrient uptake during intracellular development, for example by feeding the incomplete citric acid cycle in these organisms [80]. The role of the individual members of the MOMP-like families of *Simkania* and *Waddlia* is unclear. However, similar to *E. chaffeensis*, expression levels could vary between different hosts or in the course of the developmental cycle.

For *C. trachomatis*, it was suggested that the folding of two loops towards the outer membrane surface by intramolecular disulfide-bonds regulates the entrance of various molecules through the MOMP channel [81]. As cysteine is completely or nearly absent in most MOMP-like proteins of *Simkania*, expression of different sets of proteins during the developmental cycle could substitute for the regulation via disulfide-bridges. Differential expression of MOMP-like proteins in *Simkania* and *Waddlia* could thus help in the adaptation to different osmolarity conditions inside and outside the host cell, confer host-specificity during adhesion or help in the evasion of the immune system.

Diversification in the OMP composition can also be seen for autotransporter, a group of proteins that is associated with virulence in many Gram-negative bacteria. Autotransporters are represented by the Pmp-family in the *Chlamydiaceae*, which are present in 9 (*C. trachomatis*) to 21 (*C. pneumoniae*) copies in their genomes. They are suggested to be involved in the adhesion to host cells [82] and to confer tissue-specificity [60]. Pmps are remarkably absent from the outer membranes of other chlamydiae, with the exception of three PmpB homologues in *Simkania*. However, *Parachlamydia* and *Waddlia* both express putative autotransporters with highest similarity to proteobacterial autotransporters. These variations in proteins that are putatively involved in attachment likely represent an adaptation to an environmental life style and might facilitate the attachment to different host cells.

### **The exception proves the rule - the cell wall of *Simkania* is not stabilized by disulfide-linked proteins**

The cell envelope of all chlamydiae studied so far is enforced by the COMC, a mesh consisting of intra- and intermolecular cysteine cross-linked proteins [10]. Reduction and oxidation of the disulfide bonds of proteins in the COMC during the chlamydial developmental cycle strongly influence stability, permeability and probably also infectivity of chlamydiae [11,15,18]. Not all OMPs are necessarily components of the COMC. For example, PmpD can be extracted from intact EBs with gentle detergents in the absence of reducing agents, showing that it is not a true component of the COMC [55,83]. Strong depletion of several cysteine-rich proteins under non-reducing conditions indicated that these proteins are true components of the COMC in *Parachlamydia* and *Waddlia*. These included the cysteine-rich protein OmcB in both organisms and the MOMP-like proteins of *Waddlia*. All of these proteins share cysteine-rich clusters of CxCxC, CxxC, CC or CxxCxxC signature sequences that are essential in the cross-linking of chlamydial OMPs [23,81].

*Simkania* is the first member of the *Chlamydiae* that entirely lacks homologues of known chlamydial cysteine-rich proteins or other cysteine-rich proteins in its cell envelope. In contrast to MOMP or

MOMP-like proteins of other chlamydiae, only two of the 35 MOMP-like proteins of *Simkania* (SNE\_A02860 and SNE\_A14850) encode two cysteines in close vicinity to each other. Although the genome of *Simkania* encodes some, mostly small proteins with high cysteine content, none of these proteins was detected by mass spectrometry. In addition, the stability of *Simkania* cells was not altered in the presence of reducing agent in contrast to *Parachlamydia* and *Waddlia*, strongly arguing against a stabilizing role of disulfide-bridges in the *Simkania* cell envelope. It has been previously suggested that in contrast to other chlamydiae both developmental stages of *Simkania* are infectious [84], which might be a consequence of the lack of strongly cross-linked proteins in their outer membrane. The absence of stabilizing cysteine-rich proteins could also explain the earlier observation that *Simkania* EBs seem to be more flexible and are deformed inside tightly packed inclusions in contrast to *Parachlamydia* and *Protochlamydia* [34].

The increased osmotic fragility of *Parachlamydia* and *Waddlia* in the presence of reducing agents is similar to that of *C. trachomatis*, where cysteine-rich proteins stabilize the cell wall [16,85]. This suggests that *Parachlamydia*, *Protochlamydia*, and *Waddlia* also stabilize their cell envelope through cross-linking of cysteine-rich proteins. Additional cysteine-rich proteins absent in the *Chlamydiaceae* [20] may be used as an additional enforcement of the cell wall in those organisms. This is supported by the observed high stability of *Parachlamydia* under low osmolarity conditions up to 48 hours (data not shown) in contrast to *C. trachomatis* and *Simkania* [86]. Interestingly, a higher stability was reported for *Simkania* in drinking water compared to *C. trachomatis*, raising the question how *Simkania* stabilizes its cell wall in the absence of cysteine-rich proteins. Peptidoglycan has recently been detected for the first time in some chlamydiae [87,88], but no evidence for the presence of this structure was found in *Simkania*.

## Conclusion

In contrast to the *Chlamydiaceae*, *Parachlamydia*, *Protochlamydia*, *Waddlia*, and *Simkania* infect free-living amoebae. This environmental transmission route and life style might require specific adaptations in the cell envelope and the ability to persist longer under host-free conditions. These differences contribute to the success of chlamydiae as obligate intracellular bacteria with a uniquely broad host spectrum. The original host of *Simkania* is not known since it was discovered as a cell culture contaminant. However, its atypical cell envelope suggests a natural habitat with probably high osmolarity conditions where cysteine-rich proteins became dispensable.

## Acknowledgments

We thank Ilias Lagkouvardos for help with data visualization, Lena Koenig and Elena Toenshoff for advice on electron microscopy, Ingrid Kolar for technical assistance on preparation of the electron microscopy specimens, and the Core Facility of Cell Imaging and Ultrastructural Research, Faculty of Life Sciences, University of Vienna, for their support. This work was funded by the Austrian Science Fund FWF (Y277-B03 to MH) and the European Research Council (ERC StG “EvoChlamy” to MH). Additional support from the University of Vienna to KA is acknowledged.

## Conflict of interest statement

The authors declare no conflict of interest.

## References

1. Horn M (2008) Chlamydiae as symbionts in eukaryotes. *Annu Rev Microbiol* 62: 113-131.
2. Hackstadt T, Fischer ER, Scidmore MA, Rockey DD, Heinzen RA (1997) Origins and functions of the chlamydial inclusion. *Trends in Microbiology* 5: 288-293.
3. Hybiske K, Stephens RS (2007) Mechanisms of host cell exit by the intracellular bacterium *Chlamydia*. *Proc Natl Acad Sci USA* 104: 11430-11435.
4. Abdelrahman YM, Belland RJ (2005) The chlamydial developmental cycle. *FEMS Microbiol Rev* 29: 949-959.
5. Tamura A, Higashi N (1963) Purification and chemical composition of meningopneumonitis virus. *Virology* 20: 596-604.
6. Omsland A, Sager J, Nair V, Sturdevant DE, Hackstadt T (2012) Developmental stage-specific metabolic and transcriptional activity of *Chlamydia trachomatis* in an axenic medium. *Proc Natl Acad Sci U S A* 109: 19781-19785.
7. Haider S, Wagner M, Schmid MC, Sixt BS, Christian JG, et al. (2010) Raman microspectroscopy reveals long-term extracellular activity of Chlamydiae. *Mol Microbiol* 77: 687-700.
8. Sixt BS, Siegl A, Müller C, Watzka M, Wulsch A, et al. (2013) Metabolic Features of *Protochlamydia amoebophila* Elementary Bodies – A Link between Activity and Infectivity in *Chlamydiae*. *PLoS Pathog* 9: e1003553.
9. Clifton DR, Fields KA, Grieshaber SS, Dooley CA, Fischer ER, et al. (2004) A chlamydial type III translocated protein is tyrosine-phosphorylated at the site of entry and associated with recruitment of actin. *Proc Natl Acad Sci U S A* 101: 10166-10171.
10. Hatch TP (1996) Disulfide cross-linked envelope proteins: the functional equivalent of peptidoglycan in chlamydiae? *J Bacteriol* 178: 1-5.

11. Hatch TP, Allan I, Pearce JH (1984) Structural and Polypeptide Differences between Envelopes of Infective and Reproductive Life-Cycle Forms of *Chlamydia* Spp. *Journal of Bacteriology* 157: 13-20.
12. Allan I, Hatch TP, Pearce JH (1985) Influence of cysteine deprivation on chlamydial differentiation from reproductive to infective life-cycle forms. *J Gen Microbiol* 131: 3171-3177.
13. Hafner LM, Wilson DP, Timms P Development status and future prospects for a vaccine against *Chlamydia trachomatis* infection. *Vaccine*.
14. Caldwell HD, Kromhout J, Schachter J (1981) Purification and partial characterization of the major outer membrane protein of *Chlamydia trachomatis*. *Infect Immun* 31: 1161-1176.
15. Bavoil P, Ohlin A, Schachter J (1984) Role of disulfide bonding in outer membrane structure and permeability in *Chlamydia trachomatis*. *Infect Immun* 44: 479-485.
16. Hatch TP, Miceli M, Sublett JE (1986) Synthesis of disulfide-bonded outer membrane proteins during the developmental cycle of *Chlamydia psittaci* and *Chlamydia trachomatis*. *J Bacteriol* 165: 379-385.
17. Newhall WJ, 5th (1987) Biosynthesis and disulfide cross-linking of outer membrane components during the growth cycle of *Chlamydia trachomatis*. *Infect Immun* 55: 162-168.
18. Betts-Hampikian HJ, Fields KA (2011) Disulfide bonding within components of the *Chlamydia* type III secretion apparatus correlates with development. *J Bacteriol* 193: 6950-6959.
19. Heinz E, Tischler P, Rattei T, Myers G, Wagner M, et al. (2009) Comprehensive in silico prediction and analysis of chlamydial outer membrane proteins reflects evolution and life style of the *Chlamydiae*. *BMC Genomics* 10: 634.
20. Heinz E, Pichler P, Heinz C, op den Camp HJM, Toenshoff ER, et al. (2010) Proteomic analysis of the outer membrane of *Protochlamydia amoebophila* elementary bodies. *PROTEOMICS* 10: 4363-4376.
21. Aistleitner K, Heinz C, Hörmann A, Heinz E, Montanaro J, et al. (2013) Identification and Characterization of a Novel Porin Family Highlights a Major Difference in the Outer Membrane of Chlamydial Symbionts and Pathogens. *PLoS ONE* 8: e55010.
22. Collingro A, Tischler P, Weinmaier T, Penz T, Heinz E, et al. (2011) Unity in variety--the pan-genome of the Chlamydiae. *Mol Biol Evol* 28: 3253-3270.
23. Bertelli C, Collyn F, Croxatto A, Rückert C, Polkinghorne A, et al. (2010) The *Waddlia* Genome: A Window into Chlamydial Biology. *PLoS ONE* 5: e10890.
24. Collingro A, Poppert S, Heinz E, Schmitz-Esser S, Essig A, et al. (2005) Recovery of an environmental chlamydia strain from activated sludge by co-cultivation with *Acanthamoeba* sp. *Microbiology* 151: 301-309.
25. Rurangirwa FR, Dilbeck PM, Crawford TB, McGuire TC, McElwain TF (1999) Analysis of the 16S rRNA gene of microorganism WSU 86-1044 from an aborted bovine foetus reveals that it is a member of the order *Chlamydiales*: proposal of *Waddliaceae* fam. nov., *Waddlia chondrophila* gen. nov., sp. nov. *Int J Syst Bacteriol* 49: 577-581.
26. Kahane S, Gonen R, Sayada C, Elion J, Friedman MG (1993) Description and partial characterization of a new chlamydia-like microorganism. *FEMS Microbiol Lett* 109: 329-333.
27. Filip C, Fletcher G, Wulff JL, Earhart CF (1973) Solubilization of the Cytoplasmic Membrane of *Escherichia coli* by the Ionic Detergent Sodium-Lauryl Sarcosinate. *J Bacteriol* 115: 717-722.



28. Arnold T, Linke D (2008) The Use of Detergents to Purify Membrane Proteins. Current Protocols in Protein Science: John Wiley & Sons, Inc.
29. Cipak L, Gupta S, Rajovic I, Jin Q-W, Anrather D, et al. (2013) Crosstalk between casein kinase II and Ste20-related kinase Nak1. Cell Cycle 12: 884-888.
30. Horn M, Collingro A, Schmitz-Esser S, Beier CL, Purkhold U, et al. (2004) Illuminating the evolutionary history of chlamydiae. Science 304: 728-730.
31. Clarke M, Lohan A, Liu B, Lagkouvardos I, Roy S, et al. (2013) Genome of *Acanthamoeba castellanii* highlights extensive lateral gene transfer and early evolution of tyrosine kinase signaling. Genome Biology 14: R11.
32. Nesvizhskii AI, Keller A, Kolker E, Aebersold R (2003) A statistical model for identifying proteins by tandem mass spectrometry. Anal Chem 75: 4646-4658.
33. Collier TS, Sarkar P, Franck WL, Rao BM, Dean RA, et al. (2010) Direct comparison of stable isotope labeling by amino acids in cell culture and spectral counting for quantitative proteomics. Anal Chem 82: 8696-8702.
34. Pilhofer M, Aistleitner K, Ladinsky MS, Konig L, Horn M, et al. (2014) Architecture and host interface of environmental chlamydiae revealed by electron cryotomography. Environ Microbiol 16: 417-429.
35. Yu NY, Wagner JR, Laird MR, Melli G, Rey S, et al. (2010) PSORTb 3.0: improved protein subcellular localization prediction with refined localization subcategories and predictive capabilities for all prokaryotes. Bioinformatics 26: 1608-1615.
36. Yu C-S, Lin C-J, Hwang J-K (2004) Predicting subcellular localization of proteins for Gram-negative bacteria by support vector machines based on n-peptide compositions. Protein Science 13: 1402-1406.
37. Imai K, Asakawa N, Tsuji T, Akazawa F, Ino A, et al. (2008) SOSUI-GramN: high performance prediction for sub-cellular localization of proteins in Gram-negative bacteria. Bioinformation 2: 417-421.
38. Berven FS, Flikka K, Jensen HB, Eidhammer I (2004) BOMP: a program to predict integral beta-barrel outer membrane proteins encoded within genomes of Gram-negative bacteria. Nucleic Acids Res 32: W394-399.
39. Bagos PG, Liakopoulos TD, Hamodrakas SJ (2004) Finding beta-barrel outer membrane proteins with a markov chain model. WSEAS Transactions on Biology and Biomedicine 2: 186-189.
40. Ou YY, Gromiha MM, Chen SA, Suwa M (2008) TMBETADISC-RBF: Discrimination of beta-barrel membrane proteins using RBF networks and PSSM profiles. Comput Biol Chem 32: 227-231.
41. Berven FS, Karlsen OA, Straume AH, Flikka K, Murrell JC, et al. (2006) Analysing the outer membrane subproteome of *Methylococcus capsulatus* (Bath) using proteomics and novel biocomputing tools. Archives of Microbiology 184: 362-377.
42. Juncker AS, Willenbrock H, Von Heijne G, Brunak S, Nielsen H, et al. (2003) Prediction of lipoprotein signal peptides in Gram-negative bacteria. Protein Sci 12: 1652-1662.
43. Kall L, Krogh A, Sonnhammer EL (2007) Advantages of combined transmembrane topology and signal peptide prediction--the Phobius web server. Nucleic Acids Res 35: W429-432.
44. Krogh A, Larsson B, von Heijne G, Sonnhammer EL (2001) Predicting transmembrane protein topology with a hidden Markov model: application to complete genomes. J Mol Biol 305: 567-580.

45. Petersen TN, Brunak S, von Heijne G, Nielsen H (2011) SignalP 4.0: discriminating signal peptides from transmembrane regions. *Nat Meth* 8: 785-786.
46. T Ek, Burchmore R, Herzyk P, Davies R (2012) Predicting the outer membrane proteome of *Pasteurella multocida* based on consensus prediction enhanced by results integration and manual confirmation. *BMC Bioinformatics* 13: 63.
47. Yamaguchi K, Yu F, Inouye M (1988) A single amino acid determinant of the membrane localization of lipoproteins in *E. coli*. *Cell* 53: 423-432.
48. Seydel A, Gounon P, Pugsley AP (1999) Testing the '+2 rule' for lipoprotein sorting in the *Escherichia coli* cell envelope with a new genetic selection. *Molecular Microbiology* 34: 810-821.
49. Lewenza S, Mhlanga MM, Pugsley AP (2008) Novel inner membrane retention signals in *Pseudomonas aeruginosa* lipoproteins. *J Bacteriol* 190: 6119-6125.
50. Remmert M, Linke D, Lupas AN, Soding J (2009) HHomp--prediction and classification of outer membrane proteins. *Nucleic Acids Res* 37: W446-451.
51. Roy A, Kucukural A, Zhang Y (2010) I-TASSER: a unified platform for automated protein structure and function prediction. *Nat Protocols* 5: 725-738.
52. Shen Y, Burger G (2007) 'Unite and conquer': enhanced prediction of protein subcellular localization by integrating multiple specialized tools. *BMC Bioinformatics* 8: 420.
53. Horler RSP, Butcher A, Papangelopoulos N, Ashton PD, Thomas GH (2009) EchoLOCATION: an in silico analysis of the subcellular locations of *Escherichia coli* proteins and comparison with experimentally derived locations. *Bioinformatics* 25: 163-166.
54. Goudenege D, Avner S, Lucchetti-Miganeh C, Barloy-Hubler F (2010) CoBaltDB: Complete bacterial and archaeal orfeomes subcellular localization database and associated resources. *BMC Microbiology* 10: 88.
55. Liu X, Afrane M, Clemmer DE, Zhong G, Nelson DE (2010) Identification of *Chlamydia trachomatis* outer membrane complex proteins by differential proteomics. *J Bacteriol* 192: 2852-2860.
56. Birkelund S, Morgan-Fisher M, Timmerman E, Gevaert K, Shaw AC, et al. (2009) Analysis of proteins in *Chlamydia trachomatis* L2 outer membrane complex, COMC. *FEMS Immunol Med Microbiol* 55: 187-195.
57. Perez Melgosa M, Kuo CC, Campbell LA (1994) Isolation and characterization of a gene encoding a *Chlamydia pneumoniae* 76-kilodalton protein containing a species-specific epitope. *Infect Immun* 62: 880-886.
58. Henderson IR, Cappello R, Nataro JP (2000) Autotransporter proteins, evolution and redefining protein secretion. *Trends in Microbiology* 8: 529-532.
59. Grijpstra J, Arenas J, Rutten L, Tommassen J (2013) Autotransporter secretion: varying on a theme. *Res Microbiol* 164: 562-582.
60. Gomes JP, Nunes A, Bruno WJ, Borrego MJ, Florindo C, et al. (2006) Polymorphisms in the nine polymorphic membrane proteins of *Chlamydia trachomatis* across all serovars: evidence for serovar Da recombination and correlation with tissue tropism. *J Bacteriol* 188: 275-286.

61. Speth DR, van Teeseling MC, Jetten MS (2012) Genomic analysis indicates the presence of an asymmetric bilayer outer membrane in planctomycetes and verrucomicrobia. *Front Microbiol* 3: 304.
62. Lee EY, Bang JY, Park GW, Choi DS, Kang JS, et al. (2007) Global proteomic profiling of native outer membrane vesicles derived from *Escherichia coli*. *PROTEOMICS* 7: 3143-3153.
63. Walters MS, Mobley HL (2009) Identification of uropathogenic *Escherichia coli* surface proteins by shotgun proteomics. *J Microbiol Methods* 78: 131-135.
64. Cao Y, Bazemore-Walker CR (2014) Proteomic profiling of the surface-exposed cell envelope proteins of *Caulobacter crescentus*. *J Proteomics* 97: 187-194.
65. Koßmehl S, Wöhlbrand L, Drüppel K, Feenders C, Blasius B, et al. (2013) Subcellular protein localization (cell envelope) in *Phaeobacter inhibens* DSM 17395. *PROTEOMICS* 13: 2743-2760.
66. Thein M, Sauer G, Paramasivam N, Grin I, Linke D (2010) Efficient subfractionation of gram-negative bacteria for proteomics studies. *J Proteome Res* 9: 6135-6147.
67. Gesslbauer B, Poljak A, Handwerker C, Schüler W, Schwendenwein D, et al. (2012) Comparative membrane proteome analysis of three *Borrelia* species. *PROTEOMICS* 12: 845-858.
68. Chung JW, Ng-Thow-Hing C, Budman LI, Gibbs BF, Nash JHE, et al. (2007) Outer membrane proteome of *Actinobacillus pleuropneumoniae*: LC-MS/MS analyses validate in silico predictions. *PROTEOMICS* 7: 1854-1865.
69. Cao Y, Johnson HM, Bazemore-Walker CR (2012) Improved enrichment and proteomic identification of outer membrane proteins from a Gram-negative bacterium: focus on *Caulobacter crescentus*. *PROTEOMICS* 12: 251-262.
70. Lienard J, Croxatto A, Gervais A, Posfay-Barbe K, Baud D, et al. (2014) Undressing of *Waddlia chondrophila* to enrich its outer membrane proteins to develop a new species-specific ELISA. *New Microbes and New Infections* 2: 13-24.
71. Raulston JE (1995) Chlamydial envelope components and pathogen-host cell interactions. *Mol Microbiol* 15: 607-616.
72. Kubo A, Stephens RS (2000) Characterization and functional analysis of PorB, a *Chlamydia* porin and neutralizing target. *Mol Microbiol* 38: 772-780.
73. Alm RA, Bina J, Andrews BM, Doig P, Hancock RE, et al. (2000) Comparative genomics of *Helicobacter pylori*: analysis of the outer membrane protein families. *Infect Immun* 68: 4155-4168.
74. Brayton KA, Kappmeyer LS, Herndon DR, Dark MJ, Tibbals DL, et al. (2005) Complete genome sequencing of *Anaplasma marginale* reveals that the surface is skewed to two superfamilies of outer membrane proteins. *Proc Natl Acad Sci U S A* 102: 844-849.
75. Ohashi N, Zhi N, Zhang Y, Rikihisa Y (1998) Immunodominant major outer membrane proteins of *Ehrlichia chaffeensis* are encoded by a polymorphic multigene family. *Infect Immun* 66: 132-139.
76. Lin M, Kikuchi T, Brewer HM, Norbeck AD, Rikihisa Y (2011) Global proteomic analysis of two tick-borne emerging zoonotic agents: *Anaplasma phagocytophilum* and *Ehrlichia chaffeensis*. *Front Microbiol* 2: 24.

77. Unver A, Rikihisa Y, Stich RW, Ohashi N, Felek S (2002) The omp-1 major outer membrane multigene family of *Ehrlichia chaffeensis* is differentially expressed in canine and tick hosts. *Infection and Immunity* 70: 4701-4704.
78. Noh SM, Brayton KA, Knowles DP, Agnes JT, Dark MJ, et al. (2006) Differential expression and sequence conservation of the *Anaplasma marginale* msp2 gene superfamily outer membrane proteins. *Infect Immun* 74: 3471-3479.
79. Unver A, Ohashi N, Tajima T, Stich RW, Grover D, et al. (2001) Transcriptional analysis of p30 major outer membrane multigene family of *Ehrlichia canis* in dogs, ticks, and cell culture at different temperatures. *Infect Immun* 69: 6172-6178.
80. Huang H, Wang X, Kikuchi T, Kumagai Y, Rikihisa Y (2007) Porin activity of *Anaplasma phagocytophilum* outer membrane fraction and purified P44. *J Bacteriol* 189: 1998-2006.
81. Yen T-Y, Pal S, de la Maza LM (2005) Characterization of the Disulfide Bonds and Free Cysteine Residues of the *Chlamydia trachomatis* Mouse Pneumonitis Major Outer Membrane Protein. *Biochemistry* 44: 6250-6256.
82. Crane DD, Carlson JH, Fischer ER, Bavoil P, Hsia R-c, et al. (2006) *Chlamydia trachomatis* polymorphic membrane protein D is a species-common pan-neutralizing antigen. *Proc Natl Acad Sci U S A* 103: 1894-1899.
83. Swanson KA, Taylor LD, Frank SD, Sturdevant GL, Fischer ER, et al. (2009) *Chlamydia trachomatis* polymorphic membrane protein D is an oligomeric autotransporter with a higher-order structure. *Infect Immun* 77: 508-516.
84. Kahane S, Kimmel N, Friedman MG (2002) The growth cycle of *Simkania negevensis*. *Microbiology* 148: 735-742.
85. Hackstadt T, Todd WJ, Caldwell HD (1985) Disulfide-mediated interactions of the chlamydial major outer membrane protein: role in the differentiation of chlamydiae? *J Bacteriol* 161: 25-31.
86. Kahane S, Platzner N, Dvoskin B, Itzhaki A, Friedman MG (2004) Evidence for the Presence of *Simkania negevensis* in Drinking Water and in Reclaimed Wastewater in Israel. *Appl Environ Microbiol* 70: 3346-3351.
87. Liechti GW, Kuru E, Hall E, Kalinda A, Brun YV, et al. (2014) A new metabolic cell-wall labelling method reveals peptidoglycan in *Chlamydia trachomatis*. *Nature* 506: 507-510.
88. Pilhofer M, Aistleitner K, Biboy J, Gray J, Kuru E, et al. (2013) Discovery of chlamydial peptidoglycan reveals bacteria with murein sacculi but without FtsZ. *Nat Commun* 4.

## Supplementary material

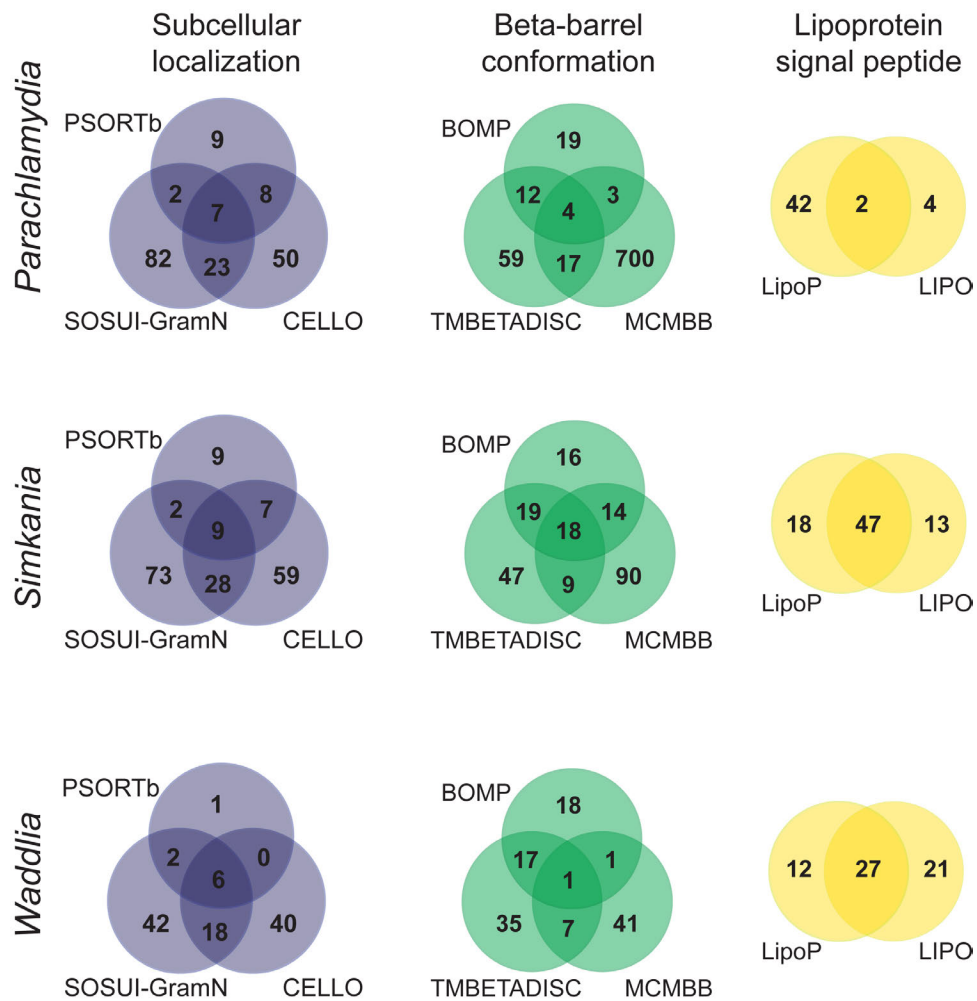


**Figure S1: Comparison of outer membrane proteins predicted by different *in silico* tools.**

The number of outer membrane proteins predicted for *Simkania*, *Parachlamydia* and *Waddlia* by subcellular localization predictors (PSORTb, SOSUI-GramN and CELLO), predictors of beta-barrel conformation (BOMP, TMBETADISC-RBF and MCMBB) and lipoproteins (LipoP and LIPO) is shown. The number of proteins predicted by individual prediction tools and the number of overlapping predictions between these tools is shown.

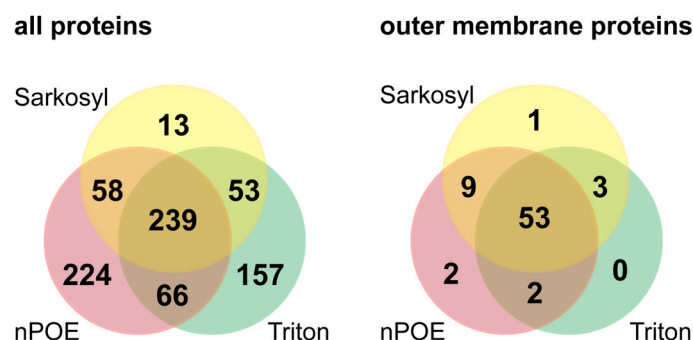


**Figure S2: Numbers of *Simkania* proteins identified by mass spectrometry using different detergents for the enrichment of outer membrane proteins**

For all three detergents, a high number of non-outer membrane proteins was identified in addition to the enriched outer membrane proteins. Compared to sarkosyl, treatment with n-octylpolyoxyethylene (nPOE) and TritonX-114 (Triton) resulted in higher numbers of non-outer membrane proteins. Almost all predicted outer membrane proteins were identified in fractions obtained with either of the three detergents.

new SSSDYVNRPVLPTTIIPTLAFALTAFDRISAHWDLDFNVI  
SNE\_A2810 SSSDYVNRPVLPYNYHSNTRFCIDRI  
SNE\_A2800 MTAFDRISAHWDLDFNVI

new WSINGAPLTGITNSRASWDITFHNVNFEIGRNSYLSQYL  
SNE\_A08780 WSINGAPLTGITNSRASLGYYISQCEF  
SNE\_A08790 MNFEIGRNSYLSQYL

**Figure S3: Mass spectrometry analysis confirms the corrected sequences of two MOMP-like proteins**

Two MOMP-like proteins were predicted in the genome to be split into two parts as result of sequencing errors introducing stop codons. Re-sequencing of these genes resulted in corrected sequences without stop codons, and spectra corresponding to the corrected sequences were found in both cases. Corrected parts of the sequence are indicated in orange; parts of the sequence for which spectra were identified by mass spectrometry are highlighted in grey. “new” indicates the corrected sequence;

**Table S1: Evaluation of prediction parameters for the consensus prediction of outer membrane proteins**

The number of positive predictions required by each class of predictors in order to classify a protein as outer membrane protein was optimized by calculating the accuracy (percent of correct predictions), sensitivity (percent of true positive predictions), specificity (percent of true negative predictions) and the Matthews correlation coefficient (MCC) for a set of proteins with known localization (protein set 1, from Ekomon et al. 2012) and a set of chlamydial proteins (protein set 2) of known localization (see Table S2). “+” indicates a positive prediction by one prediction tool. Parameters giving the best performance for each protein set are highlighted in grey.

	Localization predictors	Beta-barrel predictors	Lipoprotein predictors	Accuracy	Sensitivity	Specificity	MCC
<b>Protein set 1</b>							
	++	++	+	0.929	1	0.923	0.7
	++	++	++	0.947	1	0.942	0.751
	++	+++	+	0.962	0.976	0.961	0.799
	++	+++	++	0.981	0.976	0.981	0.885
	+++	++	+	0.931	0.929	0.932	0.678
	+++	++	++	0.949	0.929	0.95	0.734
	+++	+++	+	0.958	0.857	0.967	0.748
	+++	+++	++	0.977	0.857	0.988	0.845
<b>Protein set 2</b>							
	+++	+++	+	0.78	0.583	0.962	0.594
	+++	++	++	0.74	0.5	0.962	0.526
	++	+++	+	0.816	0.667	0.96	0.658
	++	+++	++	0.816	0.667	0.96	0.658
	++	++	+	0.878	0.792	0.96	0.765
	++	++	++	0.878	0.792	0.96	0.765
	++	++	+*	0.878	0.75	1	0.778

\*...manually curated

Table S2: Set of chlamydial proteins of known location used to evaluate the consensus prediction approach

gi identifier	Protein	organism	References
<b>Outer membrane proteins</b>			
157060526	MOMP	<i>Chlamydia trachomatis</i>	Caldwell, H.D., and Judd, R.C. (1982) <i>Infect Immun.</i> <b>38</b> (3): 960-968.
78714101	PorB	<i>Chlamydia trachomatis</i>	Kubo, A., and Stephens, R.S. (2000) <i>Mol Microbiol</i> <b>38</b> (4): 772-780.
165978620	PmpC	<i>Chlamydia trachomatis</i>	Gomes, J.P. et al. (2005) <i>Microbes Infect.</i> <b>7</b> (3): 410-420.
16753066	hypothetical protein	<i>Chlamydophila pneumoniae</i>	Perez Melgosa, M., Kuo, C.C., and Campbell, L.A. (1994) <i>Infect Immun.</i> <b>62</b> (3): 880-886.
7189126	OmcB	<i>Chlamydophila pneumoniae</i>	Moelleken, K., and Hegemann, J.H. (2008) <i>Mol Microbiol.</i> <b>67</b> (2): 403-419.
29834155	type III secretion protein SctC	<i>Chlamydophila caviae</i> GPIC	Beeckman, D., et al (2008) <i>Vet Res.</i> <b>39</b> (27)
29839846	Mip	<i>Chlamydophila caviae</i> GPIC	Rockey, D.D. et al. (1996) <i>Microbiology</i> <b>142</b> (4):945-953.
46447123	PomS	<i>Protochlamydia amoebophila</i>	Aistleitner, K. et al. (2013) <i>PLoS ONE</i> <b>8</b> (1): e55010.
46446711	PomT	<i>Protochlamydia amoebophila</i>	Aistleitner, K. et al. (2013) <i>PLoS ONE</i> <b>8</b> (1): e55010.
339626043	OprB	<i>Chlamydia trachomatis</i>	Birkelund, S. et al. (2009) <i>FEMS Immunol Med Microbiol.</i> <b>55</b> (2): 187-195.
385244762	YscC	<i>Chlamydia trachomatis</i>	Birkelund, S. et al. (2009) <i>FEMS Immunol Med Microbiol.</i> <b>55</b> (2): 187-195.
82547791	PmpD	<i>Chlamydia trachomatis</i>	Crane, D.D. et al. (2006) <i>Proc Natl Acad Sci U S A</i> <b>103</b> (6): 1894-1899.
62198507	PmpB	<i>Chlamydia trachomatis</i>	Liu , X. et al. (2010) <i>J Bacteriol.</i> <b>192</b> (11): 2852-2860.
62198631	PmpG	<i>Chlamydia trachomatis</i>	Mygind, P.H. et al. (2000) <i>FEMS Microbiol Lett.</i> <b>186</b> (2): 163-169.
165978716	PmpH	<i>Chlamydia trachomatis</i>	Mygind, P.H. et al. (2000) <i>FEMS Microbiol Lett.</i> <b>186</b> (2): 163-169.
3255936	Omp4	<i>Chlamydophila pneumoniae</i>	Knudsen, K. et al.(1999) <i>Infect Immun.</i> <b>67</b> (1): 375-383.
3255935	Omp5	<i>Chlamydophila pneumoniae</i>	Knudsen, K. et al.(1999) <i>Infect Immun.</i> <b>67</b> (1): 375-383.
46399892	OmcA	<i>Protochlamydia amoebophila</i>	Heinz, E. et al. (2010) <i>Proteomics</i> <b>10</b> (24): 4363-4376.
46446250	OmcB	<i>Protochlamydia amoebophila</i>	Heinz, E. et al. (2010) <i>Proteomics</i> <b>10</b> (24): 4363-4376.
46399279	hypothetical protein	<i>Protochlamydia amoebophila</i>	Heinz, E. et al. (2010) <i>Proteomics</i> <b>10</b> (24): 4363-4376.



46401160	hypothetical protein	<i>Protochlamydia amoebophila</i>	Heinz, E. et al. (2010) <i>Proteomics</i> <b>10</b> (24): 4363-4376.
46447189	hypothetical protein	<i>Protochlamydia amoebophila</i>	Heinz, E. et al. (2010) <i>Proteomics</i> <b>10</b> (24): 4363-4376.
385244329	OmpH	<i>Chlamydia trachomatis</i>	
376282551	MIP	<i>Chlamydia trachomatis</i>	Neff, L. et al. (2007) <i>J Bacteriol.</i> <b>189</b> (13): 4739-4748.
<b>Cytoplasmic proteins</b>			
339626069	DnaK	<i>Chlamydia trachomatis</i>	Birkelund, S., Lundemose, A.G., and Christiansen, G. (1990) <i>Infect Immun.</i> <b>58</b> (7): 2098-2104.
15604874	Phospholipase D endonuclease	<i>Chlamydia trachomatis</i>	Nelson, D.E. et al. (2006) <i>Infect Immun.</i> <b>74</b> (1): 73-80.
3329217	Hsp60	<i>Chlamydia trachomatis</i>	Nelson, D.E. et al. (2006) <i>Infect Immun.</i> <b>74</b> (1): 73-80.
270285161	30S ribosomal protein S1	<i>Chlamydia muridarum</i> Nigg	
76167711	Euo	<i>Chlamydia trachomatis</i>	Zhang, L., Douglas, A.L., and Hatch, T.P. (1998) <i>Infect Immun.</i> <b>66</b> (3): 1167-1173.
347975614	Hc1	<i>Chlamydia trachomatis</i>	
15835394	DNA polymerase I	<i>Chlamydia muridarum</i> Nigg	
15605036	DNA-directed RNA polymerase subunit beta	<i>Chlamydia trachomatis</i>	
15836411	SET domain-containing protein	<i>Chlamydophila pneumoniae</i>	Murata, M. et al. (2007) <i>Microbiology</i> <b>153</b> (2): 585-592.
237802613	DNA gyrase subunit A	<i>Chlamydia trachomatis</i>	
255310842	Holliday junction DNA helicase RuvB	<i>Chlamydia trachomatis</i>	
376282804	DnaG	<i>Chlamydia trachomatis</i>	
<b>Periplasmic proteins</b>			
73811687	YgtA	<i>Chlamydia trachomatis</i>	Miller, J.D. et al.. (2009) <i>Microbiology</i> <b>155</b> (9): 2884-2894.
81789859	DsbH	<i>Chlamydophila pneumoniae</i>	Hung, K.-C., Mac, T.-T., and Ulmer, T. (2007) <i>Biomol NMR Assign.</i> <b>1</b> (2): 195-196.
<b>Inner membrane proteins</b>			
15605283	BrnQ	<i>Chlamydia trachomatis</i>	Braun, P.R. et al. (2008) <i>J Bacteriol.</i> <b>190</b> (5): 1822-1830.
15835466	SctS	<i>Chlamydia muridarum</i>	

15834984	SctV	<i>Chlamydia muridarum</i>	
38174867	Ntt1	<i>Protochlamydia amoebophila</i>	Haferkamp, I. et al. (2004) <i>Nature</i> <b>432</b> (7017): 622-625.
<b>Extracellular proteins</b>			
15618622	FHA domain-containing protein	<i>Chlamydophila pneumoniae</i>	Müller, N. et al. (2008) <i>Med Microbiol Immunol.</i> <b>197</b> (4): 387-396.
15618618	hypothetical protein	<i>Chlamydophila pneumoniae</i>	Müller, N. et al. (2008) <i>Med Microbiol Immunol.</i> <b>197</b> (4): 387-396.
15605529	hypothetical protein	<i>Chlamydia trachomatis</i>	Qi, M. et al.(2011) <i>J Bacteriol.</i> <b>193</b> (10): 2498-2509.
15605032	hypothetical protein	<i>Chlamydia trachomatis</i>	Lei, L. et al. (2011) <i>Microb Pathog.</i> <b>51</b> (3): 101-109.
380250608	CopN	<i>Chlamydia trachomatis</i>	Fields, K.A., and Hackstadt, T. (2000) <i>Mol Microbiol.</i> <b>38</b> (5):: 1048-1060.
15605352	CT621	<i>Chlamydia trachomatis</i>	Hobolt-Pedersen et al. (2009) <i>FEMS Immunol Med Microbiol.</i> <b>57</b> (1): 46-58.
15605166	hypothetical protein	<i>Chlamydia trachomatis</i>	Li, Z. et al. (2011) <i>Sci China Life Sci.</i> <b>54</b> (11): 1048-1054.

**Table S3: Outer membrane proteins, outer membrane lipoproteins and lipoproteins predicted in the proteomes of *Protochlamydia amoebophila* UWE25 and *Chlamydia trachomatis* D/UW-3/CX.**

Proteins highlighted in grey were experimentally detected in outer membrane fractions of *Protochlamydia* (Heinz, E. et al., 2010) or of *C. trachomatis* (Liu et al., 2010). For comparison, the location of proteins predicted by pCOMP (Heinz et al., 2009) is shown. For HHOMP, the probability for the protein to be an outer membrane protein is indicated. CP, cytoplasmic; EC, extracellular; IM, inner membrane; PP, periplasmic; OM, outer membrane; UK, unknown; LP, lipoprotein; OMP, outer membrane protein

***Protochlamydia amoebophila* UWE25**

gi identifier	Locus tag	Protein description	Subcellular localization			Beta barrel conformation			Lipoprotein		Signal peptide		Predicted by pCOMP as
			PSORTb	CELLO	SOSUI - GramN	BOMP	MCMBB	TMBETADISC-RBF	LipoP	LIPO	SignalP	HHOMP	
<b>Outer membrane proteins</b>													
46445670	pc0036	hypothetical protein	OM	EC	OM	1	0.033	no	no	no			OMP
46445708	pc0074	hypothetical protein	UK	UK	UK	no	0.064	yes	no	no			OMP
46445727	pc0093	hypothetical protein	CP	OM	EC	no	<0	yes	no	no		96.83%	
46445924	pc0290	cation efflux system membrane protein C	UK	OM	UK	0	<0	yes	no	no			OMP (putative)
46446186	pc0552	outer membrane protein	UK	OM	OM	no	<0	yes	no	no			OMP (putative)
46446187	pc0553	hypothetical protein	UK	OM	OM	no	0.01	no	no	no			
46446209	pc0575	hypothetical protein	CP	CP	OM	no	<0	yes	no	no	yes	96.84%	
46446241	pc0607	hypothetical protein	CP	OM	OM	no	<0	no	no	no	yes		OMP
46446269	pc0635	outer membrane protein TolC	UK	CP	OM	0	<0	yes	no	no			OMP (putative)
46446309	pc0675	hypothetical protein	OM	OM	OM	3	0.018	yes	no	no	yes		OMP

Outer membrane proteins of environmental chlamydiae

46446343	pc0709	hypothetical protein	EC	UK	UK	1	0.021	no	no	no			
46446344	pc0710	hypothetical protein	EC	UK	CP	1	0.017	no	no	no			
46446348	pc0714	hypothetical protein	EC	OM	EC	3	0.043	no	no	no			
46446373	pc0739	rhs core protein with extension	CP	OM	EC	3	<0	yes	no	no	yes		OMP
46446424	pc0790	hypothetical protein	EC	EC	IM	3	0.029	no	no	no			OMP
46446504	pc0870	hypothetical protein	UK	OM	OM	1	<0	yes	no	no	yes		
46446572	pc0938	hypothetical protein	UK	EC	OM	1	0.044	no	no	no			OMP
46446578	pc0944	hypothetical protein	OM	OM	CP	no	<0	no	no	no			LP (putative)
46446606	pc0972	hypothetical protein	UK	UK	CP	no	0.039	yes	no	no			
46446704	pc1070	hypothetical protein	OM	OM	OM	no	0.008	no	no	no			
46446705	pc1071	hypothetical protein	UK	OM	OM	no	0.014	yes	no	no			OMP
46446925	pc1291	serine proteinase	PP	OM	OM	no	0.008	yes	no	no	yes		
46447014	pc1380	hypothetical protein	OM	OM	EC	no	0.036	no	no	no			OMP
46447017	pc1383	hypothetical protein	UK	OM	OM	1	0.037	no	no	no			
46447109	pc1475	component D of type II secretion pathway	OM	OM	EC	no	<0	yes	no	no			OMP (putative)
46447123	pc1489	hypothetical protein (PomS)	OM	OM	OM	5	0.013	yes	no	no	yes		OMP
46447154	pc1520	periplasmic immunogenic protein	PP	UK	UK	no	0.005	yes	no	no	yes		
46447360	pc1726	outer membrane protein Omp85	OM	OM	OM	1	<0	yes	no	no			OMP (putative)
46447383	pc1749	hypothetical protein	OM	OM	IM	no	<0	yes	no	no		100.00%	OMP (putative)
46447384	pc1750	hypothetical protein	OM	OM	IM	no	0.007	yes	no	no			
46447484	pc1850	translocation protein TolB	PP	OM	OM	no	<0	yes	no	no	yes		LP (putative)
46447496	pc1862	hypothetical protein	UK	EC	EC	1	0.041	no	no	no	yes		OMP
46447501	pc1867	hypothetical protein	UK	OM	IM	2	<0	yes	no	no	yes		
46447513	pc1879	hypothetical protein	UK	OM	IM	1	<0	yes	no	no			
46447519	pc1885	hypothetical protein	UK	OM	OM	1	<0	no	no	no	yes		OMP
46447532	pc1898	protein of the general secretion pathway	OM	OM	CP	no	<0	yes	no	no			LP (putative)
46447604	pc1970	hypothetical protein	UK	OM	OM	no	<0	yes	no	no			
46447608	pc1974	hypothetical protein	UK	OM	OM	no	<0	no	no	no	yes		
<b>Outer membrane lipoproteins</b>													
46446240	pc0606	peptidoglycan-associated lipoprotein	OM	UK	PP	no	0.027	yes	yes	yes			LP

## Chapter V

46446250	pc0616	60 kDa cysteine-rich outer membrane protein	OM	OM	PP	0	<0	yes	yes	no			LP
46446529	pc0895	outer membrane protein	OM	OM	IM	no	0.004	yes	yes	no			LP
46446711	pc1077	hypothetical protein (PomT)	OM	OM	OM	4	<0	yes	no	yes	yes		OMP
46447136	pc1502	oligo/dipeptide-binding protein oppA	UK	OM	OM	no	<0	no	yes	yes			LP (putative)
46447494	pc1860	hypothetical protein	OM	OM	OM	4	<0	yes	yes	yes	yes		LP
<b>Lipoproteins</b>													
46445635	pc0001	hypothetical protein	IM	UK	PP	no	<0	no	no	yes			
46445715	pc0081	hypothetical protein	CP	CP	EC	no	<0	no	yes	yes			LP
46445820	pc0186	polysaccharide export protein wza	UK	UK	PP	0	<0	no	yes	yes	yes		LP
46445839	pc0205	type III secretion protein SctJ	UK	UK	IM	no	<0	no	yes	yes			LP
46445890	pc0256	ABC transporter periplasmic substrate-binding protein ytgA	IM	CP	UK	no	<0	no	yes	yes			LP
46445925	pc0291	hypothetical protein	UK	UK	CP	no	<0	no	yes	no			LP
46446004	pc0370	hypothetical protein	UK	EC	PP	no	<0	no	yes	yes			LP
46446017	pc0383	MIP	UK	PP	PP	no	<0	no	no	yes	yes		OMP (putative)
46446025	pc0391	hypothetical protein	CP	CP	CP	no	<0	no	yes	yes	yes		LP
46446087	pc0453	ABC transporter substrate binding protein yaeC	IM	UK	PP	no	<0	no	yes	yes	yes		
46446132	pc0498	hypothetical protein	CP	CP	UK	no	<0	no	yes	yes	yes		LP
46446156	pc0522	hypothetical protein	UK	CP	IM	no	<0	no	no	yes	yes		
46446411	pc0777	hypothetical protein	CP	CP	CP	no	<0	no	yes	yes			LP
46446477	pc0843	hypothetical protein	UK	CP	UK	no	<0	no	yes	yes	yes		LP
46446508	pc0874	spermidine/putrescine-binding protein	PP	UK	PP	no	<0	no	yes	yes	yes		LP
46446510	pc0876	hypothetical protein	UK	CP	CP	no	<0	no	yes	no			
46446644	pc1010	hypothetical protein	CP	CP	PP	no	<0	no	no	yes			
46446719	pc1085	hypothetical protein	CP	CP	CP	no	<0	no	no	yes			
46446725	pc1091	hypothetical protein	UK	CP	PP	no	<0	no	no	yes	yes		
46446736	pc1102	aspartate-semialdehyde dehydrogenase	CP	UK	OM	no	<0	no	no	yes			
46446787	pc1153	hypothetical protein	UK	UK	PP	no	<0	no	no	yes			
46446805	pc1171	hypothetical protein	UK	CP	PP	no	0.011	no	yes	yes			LP

46446853	pc1219	outer membrane protein of AcrAB(MexAB)-OprM multidrug efflux pump	UK	CP	CP	no	<0	yes	yes	yes			LP
46446927	pc1293	hypothetical protein	EC	CP	UK	no	<0	no	no	yes			
46447063	pc1429	hypothetical protein	UK	PP	PP	no	<0	no	no	yes	yes		
46447081	pc1447	hypothetical protein	UK	UK	OM	no	<0	no	no	yes	yes		
46447110	pc1476	hypothetical protein	UK	CP	EC	no	<0	no	no	yes	yes		
46447206	pc1572	tylosin resistance protein	UK	CP	CP	no	<0	no	no	yes			
46447222	pc1588	ADP-D-beta-heptose epimerase, hldD	CP	CP	CP	no	<0	no	no	yes			
46447293	pc1659	hypothetical protein	UK	CP	EC	no	<0	no	yes	no			LP
46447334	pc1700	hypothetical protein	CP	CP	UK	no	<0	no	no	yes			
46447393	pc1759	superoxide dismutase (Cu-Zn)	PP	PP	PP	no	<0	no	no	yes	yes		
46447455	pc1812	hypothetical protein	UK	UK	OM	no	<0	no	no	yes			
46447485	pc1851	peptidoglycan-associated lipoprotein (pal)	OM	CP	PP	no	<0	no	yes	yes	yes		LP
46447533	pc1899	hypothetical protein	CP	UK	IM	no	<0	no	no	yes			
46447638	pc2004	hypothetical protein	CP	UK	IM	no	<0	no	no	yes			

***Chlamydia trachomatis* D/UW-3/CX**

gi identifier	Locus tag	Protein description	Subcellular localization			Beta barrel conformation			Lipoprotein		Signal peptide	Predicted by pCOMP as
			PSORTb	CELLO	SOSUI-GramN	BOMP	MCMBB	TMBETADISC-RBF	LipoP	LIPO	SignalP	
<b>Outer membrane proteins</b>												
15604749	CT_031	hypothetical protein	UK	CP	CP	no	0.018	yes	no	no		
15604768	CT_049	hypothetical protein	EC	OM	EC	no	0.014	yes	no	no		
15604770	CT_051	hypothetical protein	UK	EC	EC	no	0.02	yes	no	no		OMP (putative)
15604850	CT_131	hypothetical protein	OM	OM	IM	no	<0	no	no	no		
15604861	CT_142	hypothetical protein	UK	OM	EC	no	0.012	yes	no	no		OMP
15604872	CT_153	hypothetical protein	OM	OM	CP	no	<0	no	no	no		OMP (putative)
15604962	CT_241	Omp85	OM	OM	OM	1	0.004	yes	no	no	yes	OMP
15605074	CT_351	hypothetical protein	UK	OM	OM	no	<0	no	no	no		OMP
15605116	CT_391	hypothetical protein	UK	OM	OM	no	<0	no	no	no		

15605138	CT_413	Putative outer membrane protein B (PmpB)	OM	EC	EC	no	0.024	yes	no	no	yes		OMP
15605139	CT_414	Putative outer membrane protein C (PmpC)	OM	UK	EC	no	0.017	yes	no	no	yes		OMP
15605152	CT_425	hypothetical protein	CP	OM	OM	no	<0	no	no	no			
15605169	CT_443	60kDa Cysteine-Rich OMP (OmcB)	OM	OM	OM	0	<0	yes	no	no			OMP
15605301	CT_572	general secretion protein D	OM	OM	UK	no	<0	yes	no	no			LP (putative)
15605350	CT_619	hypothetical protein	OM	OM	EC	no	0.014	no	no	no			
15605351	CT_620	hypothetical protein	IM	OM	OM	no	0.009	no	no	no			OMP (putative)
15605353	CT_622	CHLPN 76kDa Homolog	EC	UK	EC	no	0.036	yes	no	no			
15605354	CT_623	CHLPN 76kDa Homolog	UK	OM	OM	1	0.007	yes	no	no	yes		OMP
15605407	CT_674	probable Yop proteins translocation protein C (PulD/YscC)	OM	OM	OM	no	<0	yes	no	no			OMP (putative)
15605414	CT_681	Major Outer Membrane Protein	OM	OM	OM	2	<0	yes	no	no	yes		OMP
15605444	CT_711	hypothetical protein	UK	OM	OM	no	0.001	no	no	no			
15605446	CT_713	Outer Membrane Protein Analog (PorB)	OM	OM	OM	1	<0	yes	no	no	yes		OMP
15605605	CT_869	Putative Outer Membrane Protein E (PmpE)	OM	UK	EC	1*	<0	yes	no	no			OMP
15605606	CT_870	Putative Outer Membrane Protein F (PmpF)	OM	OM	EC	no	0.015	yes	no	no	yes		OMP
15605607	CT_871	Putative Outer Membrane Protein G (PmpG)	OM	UK	OM	1	0.016	yes	no	yes	yes		OMP
15605608	CT_872	Putative Outer Membrane Protein H (PmpH)	EC	UK	OM	1	0.01	yes	no	no	yes		OMP
15605610	CT_874	Putative Outer Membrane Protein I (PmpI)	EC	OM	EC	4	<0	yes	no	no			OMP
<b>Outer membrane lipoproteins</b>													
15604725	CT_007	hypothetical protein	UK	OM	CP	4	<0	yes	yes	yes			OMP
15604974	CT_253	hypothetical protein	UK	OM	OM	no	<0	no	yes	yes	yes		LP (putative)
15605270	CTDEC_0541	FKBP-type peptidyl-prolyl cis-trans isomerases 1	OM	UK	OM	0	<0	yes	yes	yes			OMP (putative)
15605330	CTDEC_0600	Peptidoglycan-associated lipoprotein (Pal)	OM	CP	OM	no	<0	yes	yes	yes	yes		LP

Outer membrane proteins of environmental chlamydiae

15605546	CT_812	Putative Outer Membrane Protein D	OM	UK	OM	2	<0	yes	yes	yes	yes		OMP
<b>Lipoproteins</b>													
15604786	CT_067	Solute Protein Binding Family	IM	CP	CP	no	<0	no	yes	yes	yes		LP
15604796	CT_077	hypothetical protein	UK	PP	PP	no	<0	no	yes	yes	yes		LP
15604811	CT_092	GTP Binding Protein	CP	CP	CP	no	<0	no	yes	yes			
15604824	CT_105	hypothetical protein	EC	OM	EC	no	<0	yes	yes	no			LP
15604858	CT_139	Oligopeptide Binding Protein	UK	UK	PP	no	<0	no	yes	yes			LP
15604895	CT_175	Oligopeptide binding protein permease	UK	CP	PP	no	<0	no	yes	no			LP
15604918	CT_198	Oligopeptide Binding Protein	PP	UK	PP	no	<0	no	yes	yes	yes		LP
15605024	CT_303	hypothetical protein	UK	UK	IM	1	<0	no	yes	no			LP
15605073	CT_350	hypothetical protein	UK	UK	PP	no	<0	no	yes	yes	yes		
15605105	CTDEC_0381	Arginine-binding protein	UK	CP	PP	no	<0	yes	yes	yes	yes		LP
15605170	CT_444	9kDa-Cysteine-Rich Lipoprotein (OmcA)	UK	PP	PP	no	<0	no	yes	yes	yes		OMP
15605171	CT_444.1	hypothetical protein	UK	UK	PP	no	<0	no	yes	yes			LP
15605192	CT_465	hypothetical protein	IM	UK	PP	no	<0	no	yes	no	yes		
15605277	CT_548	hypothetical protein	UK	UK	PP	no	<0	no	yes	yes			LP
15605288	CT_559	Yop proteins translocation lipoprotein J	UK	UK	IM	no	<0	yes	yes	no	yes		LP (putative)
15605387	CT_654	hypothetical protein	UK	UK	PP	no	<0	no	yes	yes			LP (putative)
15605467	CT_734	hypothetical protein	UK	UK	PP	no	<0	no	yes	yes	yes		LP (putative)
15605503	CT_770	Acyl Carrier Protein Synthase	CP	CP	PP	no	<0	no	yes	yes			

Known outer membrane proteins of *C. trachomatis* not predicted as outer membrane proteins in this study

gi identifier	Locus tag	Protein description	Subcellular localization			Beta barrel conformation			Lipoprotein		Signal peptide	Predicted by pCOMP as	Predicted location in this study	comments
			PSORTb	CELLO	SOSUI-GramN	BOMP	MCMBB	TMBETADISC-RBF	LipoP	LIPO	SignalP			
15605137	CTDEC_0412	PmpA	UK	EC	IM	no	<0	yes	no	no		OMP	UK	
15605168	CT_442	15kDa Cysteine-Rich Protein	OM	OM	UK	0	<0	yes	no	no		OMP	OMP	2 TMHs
15605096	CTDEC_0372	OprB	EC	OM	CP	no	<0	no	no	no		OMP	UK	
15605114	CT_389	CTL0645	CP	CP	OM	no	<0	no	no	no	yes		CP	



**Table S4: Outer membrane proteins, outer membrane lipoproteins and lipoproteins predicted in the proteomes of *Parachlamydia acanthamoebae*, *Simkania negevensis* and *Waddlia chondrophila* in the *in silico* consensus prediction approach; CP, cytoplasmic; EC, extracellular; IM, inner membrane; PP, periplasmic; OM, outer membrane; UK, unknown;**

***Parachlamydia acanthamoebae* UV7**

gi identifier	Locus tag		Subcellular localization			Beta barrel conformation			Lipoprotein		Signal peptide	HHOMP
			PSORTb	CELLO	SOSUI-GramN	BOMP	MCMBB	TMBETADISC-RBF	LipoP	LIPO	SignalP	
<b>Outer membrane proteins</b>												
338174013	PUV_00190	hypothetical protein	OM	OM	OM	no	<0	no	no	no		
338174039	PUV_00450	hypothetical protein	OM	OM	CP	no	0	no	no	no		
338174157	PUV_01630	hypothetical protein	IM	OM	OM	no	<0	no	no	no		
338174161	PUV_01670	outer membrane protein oprM	OM	OM	OM	no	<0	no	no	no		
338174166	PUV_01720	hypothetical protein	OM	OM	UK	3	<0	no	no	no	yes	
338174171	PUV_01770	hypothetical protein	UK	CP	CP	no	0	no	no	no		
338174184	PUV_01900	hypothetical protein	UK	OM	OM	no	0.018	no	no	no		
338174185	PUV_01910	hypothetical protein	UK	CP	EC	0	0	no	no	no	yes	
338174324	PUV_03300	hypothetical protein	UK	UK	OM	no	<0	no	no	no	yes	100.0%
338174336	PUV_03420	hypothetical protein	UK	OM	OM	no	0.108	no	no	no	yes	
338174355	PUV_03610	carboxy-terminal	IM	CP	CP	no	0	no	no	no		
338174452	PUV_04580	hypothetical protein	OM	OM	EC	1	<0	no	no	no	yes	
338174483	PUV_04890	hypothetical protein	CP	OM	CP	no	0	no	no	no		
338174565	PUV_05710	type III secretion outer membrane ring component	OM	OM	CP	no	<0	no	no	no		
338174567	PUV_05730	type III secretion outer membrane ring component	OM	OM	OM	no	<0	no	no	no		
338174587	PUV_05930	hypothetical protein	OM	EC	OM	1	0.007	no	no	no		
338174677	PUV_06830	tail-specific protease	IM	OM	OM	no	<0	no	no	no	yes	
338174705	PUV_07110	hypothetical protein	UK	UK	UK	no	0.001	no	no	no		
338174738	PUV_07440	hypothetical protein	IM	UK	OM	no	<0	no	no	no		
338174749	PUV_07550	hypothetical protein	UK	OM	EC	no	0	no	no	no	yes	100.0%
338174816	PUV_08220	hypothetical protein	IM	OM	OM	no	<0	no	no	no		97.04%

Outer membrane proteins of environmental chlamydiae

338174817	PUV_08230	hypothetical protein	OM	OM	PP	0	<0	no	no	no		
338174833	PUV_08390	hypothetical protein	EC	OM	OM	1	0.009	no	no	no		
338174862	PUV_08680	hypothetical protein	UK	OM	OM	no	<0	no	no	no		
338174985	PUV_09910	hypothetical protein	OM	OM	OM	1	<0	no	no	no	yes	
338174994	PUV_10000	hypothetical protein	UK	EC	OM	2	<0	no	no	no	yes	
338175011	PUV_10170	OmcB	OM	OM	PP	no	<0	no	no	no		
338175086	PUV_10920	hypothetical protein	UK	UK	CP	no	0	no	no	no		
338175122	PUV_11280	hypothetical protein	UK	OM	CP	1	<0	no	no	no		
338175178	PUV_11840	hypothetical protein	UK	OM	OM	no	0	no	no	no	yes	
338175388	PUV_13940	hypothetical protein	UK	OM	OM	no	<0	no	no	no		
338175478	PUV_14840	hypothetical protein	UK	OM	IM	1	<0	no	no	no		
338175569	PUV_15750	hypothetical protein	CP	CP	PP	no	0.038	no	no	no	yes	
338175677	PUV_16830	hypothetical protein	UK	OM	CP	no	0	no	no	no		
338175773	PUV_17790	outer membrane protein oprM	OM	UK	PP	no	<0	no	no	no		
338175826	PUV_18320	hypothetical protein	UK	CP	OM	4	<0	no	no	no	yes	100.0%
338175829	PUV_18350	hypothetical protein	UK	CP	CP	no	0	no	no	no		99.4%
338175855	PUV_18610	hypothetical protein	OM	OM	EC	no	<0	no	no	no		
338175881	PUV_18870	hypothetical protein	UK	OM	OM	no	<0	no	no	no		
338175919	PUV_19250	hypothetical protein	UK	OM	OM	no	<0	no	no	no	yes	
338176016	PUV_20220	hypothetical protein	UK	UK	OM	no	0	no	no	no	yes	
338176053	PUV_20590	hypothetical protein	UK	OM	OM	3	<0	no	no	no	yes	90.4%
338176057	PUV_20630	hypothetical protein	OM	OM	OM	3	0	no	no	no	yes	
338176146	PUV_21520	hypothetical protein	UK	OM	OM	no	<0	no	no	no	yes	
338176216	PUV_22220	hypothetical protein	UK	UK	UK	no	0	no	no	no		
338176334	PUV_23400	hypothetical protein	CP	OM	OM	3	<0	no	no	no		
338176384	PUV_23900	hypothetical protein	UK	OM	OM	no	<0	no	no	no		
338176434	PUV_24400	hypothetical protein	UK	CP	CP	no	<0	no	no	no		
338176480	PUV_24860	hypothetical protein	CP	EC	IM	3	0	no	no	no	yes	100.0%
338176486	PUV_24920	hypothetical protein	UK	OM	IM	3	<0	no	no	no	yes	
338176513	PUV_25190	hypothetical protein	OM	UK	IM	no	<0	no	no	no		
338176516	PUV_25220	hypothetical protein	CP	OM	PP	no	0	no	no	no	yes	100.0%
338176617	PUV_26230	hypothetical protein	EC	OM	EC	3	<0	no	no	no		
338176698	PUV_27040	hypothetical protein	CP	OM	OM	no	<0	no	no	no		

## Chapter V

338176719	PUV_27250	hypothetical protein	UK	CP	CP	no	0	no	no	no		
338176727	PUV_27330	hypothetical protein	UK	OM	OM	no	<0	no	no	no		
338176743	PUV_27490	hypothetical protein	OM	OM	PP	3	<0	no	no	no	yes	
338176744	PUV_27500	hypothetical protein	UK	OM	EC	2	0	no	no	no	yes	
338176766	PUV_27720	hypothetical protein	CP	OM	OM	no	0	no	no	no		
<b>Outer membrane lipoproteins</b>												
338174079	PUV_00850	hypothetical protein	OM	OM	OM	no	<0	no	yes	no	yes	
338175289	PUV_12950	mOMP-like family protein	CP	OM	OM	1	<0	no	yes	no		
338175723	PUV_17290	hypothetical protein	OM	UK	OM	no	<0	no	yes	no		
338176096	PUV_21020	solvent efflux pump outer membrane protein srpC	OM	OM	OM	no	0	no	yes	no		
338176612	PUV_26180	hypothetical protein	OM	OM	OM	no	0.001	no	yes	no	yes	
<b>Lipoproteins</b>												
338174014	PUV_00200	hypothetical protein	CP	UK	EC	no	<0	no	yes	no	yes	
338174087	PUV_00930	hyperosmotically inducible periplasmic protein	UK	PP	OM	no	<0	no	yes	no		
338174104	PUV_01100	peptidoglycan-associated lipoprotein	UK	CP	PP	no	<0	no	yes	no		
338174137	PUV_01430	type III secretion periplasmic lipoprotein	OM	UK	IM	no	<0	no	yes	no		
338174193	PUV_01990	hypothetical protein	CP	CP	PP	no	0.014	no	yes	no	yes	
338174207	PUV_02130	metal-binding lipoprotein TC_0338	IM	CP	OM	no	0	no	yes	no	yes	
338174216	PUV_02220	polysaccharide export protein wza	CP	UK	PP	0	<0	no	yes	no		
338174318	PUV_03240	hypothetical protein	UK	CP	PP	no	0.029	no	yes	no		
338174419	PUV_04250	hypothetical protein	UK	CP	PP	no	<0	no	yes	yes	yes	
338174604	PUV_06100	carbonic anhydrase	CP	UK	PP	no	<0	no	yes	no	yes	
338174666	PUV_06720	thioredoxin	UK	OM	PP	no	<0	no	yes	no	yes	
338174686	PUV_06920	hypothetical protein	UK	CP	PP	no	<0	no	yes	no	yes	
338174734	PUV_07400	hypothetical protein	UK	CP	PP	no	<0	no	yes	no		
338174752	PUV_07580	spermidine/putrescine-binding periplasmic protein	UK	UK	UK	no	<0	no	yes	no		
338174793	PUV_07990	hypothetical protein	UK	UK	PP	no	<0	no	yes	no	yes	
338174896	PUV_09020	thiamine biosynthesis lipoprotein ApbE	CP	UK	CP	no	0	no	yes	no		
338174998	PUV_10040	hypothetical protein	CP	CP	OM	no	<0	no	yes	no	yes	
338175064	PUV_10700	hypothetical protein	UK	UK	PP	no	0	no	no	yes	yes	
338175148	PUV_11540	hypothetical protein	CP	OM	EC	no	<0	no	yes	no		

Outer membrane proteins of environmental chlamydiae

338175166	PUV_11720	hypothetical protein	CP	EC	OM	no	0	no	yes	no		
338175223	PUV_12290	hypothetical protein	CP	UK	UK	no	<0	no	yes	no		
338175464	PUV_14700	superoxide dismutase [Cu-Zn]	PP	UK	UK	no	<0	no	yes	no	yes	
338175475	PUV_14810	hypothetical protein	IM	IM	IM	no	0	no	no	yes		
338175692	PUV_16980	type III secretion periplasmic lipoprotein	OM	UK	IM	no	<0	no	yes	no		
338175911	PUV_19170	hypothetical protein	UK	PP	OM	no	<0	no	yes	yes		
338175936	PUV_19420	hypothetical protein	UK	OM	PP	1	<0	no	yes	no	yes	
338175966	PUV_19720	protein Yqil	UK	UK	PP	no	<0	no	yes	no		
338176058	PUV_20640	hypothetical protein	UK	CP	CP	no	<0	no	yes	no		
338176089	PUV_20950	hypothetical protein	UK	UK	PP	no	<0	no	yes	no	yes	
338176122	PUV_21280	hypothetical protein	CP	CP	PP	no	<0	no	yes	no		
338176142	PUV_21480	hypothetical protein	UK	PP	OM	no	<0	no	yes	no	yes	
338176224	PUV_22300	hypothetical protein	UK	UK	PP	no	<0	no	yes	no		
338176317	PUV_23230	hypothetical protein	UK	CP	UK	no	0	no	yes	no	yes	
338176360	PUV_23660	hypothetical protein	UK	CP	CP	no	0	no	yes	no		
338176552	PUV_25580	hypothetical protein	UK	UK	CP	no	0.074	no	yes	no		
338176597	PUV_26030	hypothetical protein	UK	UK	PP	no	<0	no	yes	no		
338176668	PUV_26740	hypothetical protein	UK	UK	PP	no	<0	no	no	yes	yes	
338176711	PUV_27170	hypothetical protein	UK	CP	CP	no	<0	no	yes	no	yes	
338176764	PUV_27700	hypothetical protein	IM	PP	PP	no	<0	no	yes	no	yes	

*Simkania negevensis*

gi identifier	Locus tag		Subcellular localization			Beta barrel conformation			Lipoprotein		Signal peptide	HHOMP
			PSORTb	CELLO	SOSUI-GramN	BOMP	MCMBB	TMBETADISC-RBF	LipoP	LIPO	SignalIP	
<b>Outer membrane proteins</b>												
338731814	SNE_B24380	hypothetical protein	CP	CP	CP	no	<0	no	no	no	yes	100.0%
338731881	SNE_B25050	hypothetical protein	UK	UK	OM	5	<0	no	no	no		98.5%
338731883	SNE_B25070	hypothetical protein	UK	OM	OM	no	<0	no	no	no		
338731911	SNE_A00150	hypothetical protein	UK	UK	IM	no	0.019	no	no	no		
338731913	SNE_A00170	hypothetical protein	UK	OM	OM	no	<0	no	no	no	yes	

338731935	SNE_A00390	hypothetical protein	UK	OM	OM	4	0.037	no	no	no	yes	
338731937	SNE_A00410	major outer membrane protein	IM	OM	EC	1	0.012	no	no	no	yes	
338731938	SNE_A00420	major outer membrane protein	UK	UK	CP	no	0.012	no	no	no		95.24%
338731959	SNE_A00630	polymorphic outer membrane B	UK	EC	OM	4*	0.055	no	no	no	yes	
338731963	SNE_A00670	hypothetical	CP	OM	OM	no	<0	no	no	no		
338731971	SNE_A00750	MOMP-like family protein	OM	OM	OM	5	0.01	no	no	no		
338731972	SNE_A00760	hypothetical protein	UK	OM	OM	no	<0	no	no	no		
338731978	SNE_A00820	MOMP-like family protein	UK	OM	OM	no	0.008	no	no	no		
338731979	SNE_A00830	hypothetical protein	OM	OM	OM	1	<0	no	no	no	yes	
338732010	SNE_A01140	hypothetical protein	OM	PP	OM	no	<0	no	no	no		
338732061	SNE_A01660	hypothetical protein	OM	OM	OM	no	<0	no	no	no		
338732099	SNE_A02040	hypothetical protein	UK	UK	EC	no	0.005	no	no	no		
338732101	SNE_A02060	MOMP-like family protein	UK	OM	OM	4	0.003	no	no	no	yes	
338732121	SNE_A02260	MOMP-like family protein	OM	OM	OM	3	0.04	no	no	no	yes	
338732147	SNE_A02520	hypothetical protein	UK	UK	PP	2	0.002	no	no	no	yes	
338732170	SNE_A02750	hypothetical protein	UK	UK	UK	no	0.023	no	no	no		
338732171	SNE_A02760	MOMP-like family protein	UK	CP	OM	2	<0	no	no	no	yes	
338732173	SNE_A02780	MOMP-like family protein	UK	OM	OM	4	<0	no	no	no	yes	
338732179	SNE_A02840	MOMP-like family protein	OM	OM	EC	5	<0	no	no	no	yes	
338732181	SNE_A02860	MOMP-like family protein	UK	EC	EC	1	<0	no	no	no	yes	97.4%
338732182	SNE_A02870	MOMP-like family protein	UK	OM	OM	2	<0	no	no	no	yes	
338732238	SNE_A03430	hypothetical protein	OM	OM	PP	4	<0	no	no	no	yes	
338732346	SNE_A04510	hypothetical protein	OM	CP	IM	no	<0	no	no	no		100.0%
338732404	SNE_A05090	MOMP-like family protein	OM	OM	OM	5	0.027	no	no	no	yes	
338732415	SNE_A05200	polymorphic outer membrane B	UK	EC	OM	4*	0.061	no	no	no	yes	
338732416	SNE_A05210	hypothetical protein	EC	EC	IM	3	0.017	no	no	no	yes	
338732484	SNE_A05890	hypothetical protein	IM	EC	OM	1	0.022	no	no	no		
338732533	SNE_A06380	hypothetical protein	PP	EC	EC	4	<0	no	no	no	yes	100.0%
338732549	SNE_A06540	carbohydrate-selective porin, OprB family	OM	OM	CP	4	0.011	no	no	no	yes	
338732634	SNE_A07390	hypothetical	UK	EC	EC	1	0.006	no	no	no	yes	
338732638	SNE_A07430	MOMP-like family protein	UK	EC	OM	no	<0	no	no	no	yes	
338732639	SNE_A07440	MOMP-like family protein	UK	OM	OM	4	<0	no	no	no		

Outer membrane proteins of environmental chlamydiae

338732676	SNE_A07810	hypothetical protein	OM	OM	OM	no	0.004	no	no	no		
338732690	SNE_A07950	MOMP-like family protein	UK	OM	OM	5	0.003	no	no	no	yes	
338732701	SNE_A08060	MOMP-like family protein	UK	OM	IM	4	<0	no	no	no	yes	97.6%
338732702	SNE_A08070	MOMP-like family protein	UK	OM	IM	no	<0	no	no	no		97.52%
338732712	SNE_A08170	putative outer membrane Omp85	OM	OM	OM	4	0.003	no	no	no	yes	
338732745	SNE_A08500	MOMP-like family protein	UK	OM	OM	4	0.01	no	no	no	yes	
338732757	SNE_A08620	hypothetical protein	UK	UK	IM	no	<0	no	no	no	yes	97.44%
338732777	SNE_A08820	MOMP-like family protein	CP	OM	OM	no	<0	no	no	no	yes	
338732778	SNE_A08830	MOMP-like family protein	UK	OM	OM	1	0.01	no	no	no	yes	
338732791	SNE_A08960	hypothetical protein	UK	OM	OM	no	<0	no	no	no	yes	
338732858	SNE_A09630	hypothetical protein	UK	OM	UK	no	0.007	no	no	no		
338732896	SNE_A10010	MOMP-like family protein	UK	UK	OM	4	<0	no	no	no	yes	
338732953	SNE_A10580	peptidase S9, prolyl oligopeptidase active site region	UK	OM	OM	no	<0	no	no	no	yes	
338733007	SNE_A11120	hypothetical protein	EC	OM	EC	no	0.017	no	no	no		
338733016	SNE_A11210	MOMP-like family protein	UK	OM	OM	1	<0	no	no	no	yes	
338733073	SNE_A11780	hypothetical protein	IM	UK	OM	1	<0	no	no	no	yes	
338733205	SNE_A13100	hypothetical protein	IM	UK	OM	3	0.005	no	no	no		
338733241	SNE_A13460	hypothetical protein	UK	OM	OM	no	<0	no	no	no		
338733367	SNE_A14720	polymorphic outer membrane B	EC	EC	EC	3	0.068	no	no	no		
338733380	SNE_A14850	MOMP-like family protein	CP	OM	OM	4	<0	no	no	no		
338733381	SNE_A14860	MOMP-like family protein	UK	OM	OM	4	0.015	no	no	no	yes	
338733428	SNE_A15330	hypothetical protein	UK	UK	OM	no	<0	no	no	no	yes	97.31%
338733478	SNE_A15830	hypothetical protein	CP	OM	UK	no	<0	no	no	no		100.0%
338733707	SNE_A18120	MOMP-like family protein	UK	OM	EC	5	0.015	no	no	no	yes	
338733823	SNE_A19280	hypothetical protein	EC	UK	OM	1	0.017	no	no	no	yes	
338733835	SNE_A19400	hypothetical protein	UK	UK	EC	no	0.029	no	no	no		
338733906	SNE_A20110	hypothetical protein	OM	OM	OM	no	0.001	no	no	no	yes	
338733966	SNE_A20710	MOMP-like family protein	UK	OM	OM	4	0.016	no	no	no		
338733988	SNE_A20930	hypothetical protein	OM	OM	IM	4	<0	no	no	no		100.0%
338733989	SNE_A20940	hypothetical protein	UK	EC	PP	1	0.065	no	no	no	yes	
338734078	SNE_A21830	hypothetical protein	CP	OM	PP	1	<0	no	no	no	yes	
338734198	SNE_A23030	hypothetical protein	OM	OM	CP	3	<0	no	no	no		
338734232	SNE_A23370	MOMP-like family protein	OM	OM	IM	4	<0	no	no	no	yes	

338734234	SNE_A23390	MOMP-like family protein	IM	OM	EC	1	0.017	no	no	no	yes	
338734236	SNE_A23410	MOMP-like family protein	OM	OM	OM	5	0.022	no	no	no	yes	
338734237	SNE_A23420	MOMP-like family protein	UK	OM	OM	4	0.007	no	no	no	yes	
338734262	SNE_A23670	hypothetical protein	CP	UK	PP	1	<0	no	no	no		
338734267	SNE_A23720	hypothetical protein	UK	OM	OM	1	<0	no	no	no		
338734277	SNE_A23820	hypothetical protein	UK	OM	OM	no	<0	no	no	no	yes	98.5%
338732175_new		MOMP-like family protein	UK	UK	OM	1	0.011	no	no	no		
338732773_new		MOMP-like family protein	UK	OM	OM	4	0.014	no	no	no	yes	
<b>Outer membrane lipoproteins</b>												
338731826	SNE_B24500	outer membrane efflux protein	OM	IM	IM	no	no	no	yes	yes	yes	
338732172	SNE_A02770	MOMP-like family protein	UK	OM	OM	4	<0	no	yes	no	yes	
338732558	SNE_A06630	outer membrane protein	OM	UK	OM	no	<0	no	yes	yes		
338733019	SNE_A11240	putative outer membrane factor (OMF) family efflux porin	OM	OM	EC	1	0.006	no	yes	no		
338733489	SNE_A15940	MOMP-like family protein	UK	OM	OM	5	<0	no	yes	no	yes	
338734235	SNE_A23400	MOMP-like family protein	UK	OM	OM	1	0.017	no	yes	no	yes	
<b>Lipoproteins</b>												
338731815	SNE_B24390	chemiosmotic efflux system B B	UK	UK	CP	no	<0	yes	yes	yes		
338731825	SNE_B24490	hypothetical protein	UK	CP	PP	no	<0	no	yes	yes		
338731827	SNE_B24510	multicopper oxidase domain-containing protein	PP	PP	PP	no	<0	no	yes	no	yes	
338731851	SNE_B24750	hypothetical protein	UK	CP	CP	no	<0	no	yes	yes		
338731888	SNE_B25120	hypothetical protein	UK	UK	PP	no	<0	no	yes	yes	yes	
338731901	SNE_A00050	hypothetical protein	UK	UK	CP	no	<0	no	yes	no		
338731920	SNE_A00240	peptidyl-prolyl cis-trans isomerase Mip	UK	CP	CP	no	<0	no	yes	no		
338731936	SNE_A00400	NTE family ylbK	EC	CP	PP	no	<0	no	yes	yes	yes	
338731973	SNE_A00770	hypothetical protein	CP	CP	IM	no	<0	no	yes	yes		
338731981	SNE_A00850	hypothetical protein	CP	OM	IM	no	<0	yes	yes	yes		
338732016	SNE_A01200	hypothetical protein	UK	UK	PP	no	0.042	no	yes	yes		
338732019	SNE_A01230	hypothetical protein	CP	CP	CP	no	<0	no	yes	yes	yes	
338732020	SNE_A01240	peptidoglycan-associated lipoprotein	OM	CP	PP	no	<0	yes	yes	yes	yes	
338732021	SNE_A01250	tolB	PP	UK	PP	no	<0	yes	yes	no		
338732073	SNE_A01780	alkaline phosphatase synthesis sensor phoR	IM	UK	IM	no	<0	no	yes	no		

Outer membrane proteins of environmental chlamydiae

338732126	SNE_A02310	putative polysaccharide export Wza	CP	UK	PP	0	<0	no	yes	yes		
338732150	SNE_A02550	hypothetical protein	IM	UK	OM	no	<0	no	yes	yes	yes	
338732188	SNE_A02930	type III secretion periplasmic lipoprotein	UK	OM	IM	no	<0	yes	yes	yes	yes	
338732194	SNE_A02990	hypothetical protein	UK	UK	OM	no	<0	no	no	yes	yes	
338732195	SNE_A03000	amino acid ABC transporter periplasmic amino acid-binding protein	UK	UK	PP	no	<0	no	yes	yes		
338732214	SNE_A03190	hypothetical protein	UK	UK	OM	no	<0	no	yes	yes	yes	
338732248	SNE_A03530	hypothetical protein	PP	CP	UK	no	<0	no	yes	no		
338732345	SNE_A04500	membrane-fusion protein, component of multidrug efflux system	IM	UK	UK	no	<0	yes	yes	yes		
338732356	SNE_A04610	hypothetical protein	UK	UK	UK	no	<0	no	yes	yes		
338732395	SNE_A05000	putative N-acetylmuramoyl-L-alanine amidase	UK	UK	PP	no	<0	no	yes	yes	yes	
338732407	SNE_A05120	metal-binding lipoprotein	IM	CP	CP	no	<0	no	yes	yes		
338732493	SNE_A05980	hypothetical protein	CP	CP	CP	no	<0	no	yes	yes		
338732530	SNE_A06350	pyridoxine/pyridoxamine 5'-phosphate oxidase	CP	CP	PP	no	<0	no	yes	no	yes	
338732554	SNE_A06590	3-phytase	UK	EC	OM	no	<0	no	yes	yes		
338732700	SNE_A08050	hypothetical protein	UK	UK	EC	no	<0	no	yes	yes		
338732704	SNE_A08090	hypothetical protein	UK	UK	UK	no	<0	no	yes	no	yes	
338732943	SNE_A10480	oligopeptide-binding OppA	UK	CP	PP	no	<0	no	yes	yes		
338732944	SNE_A10490	oligopeptide-binding OppA	UK	CP	EC	no	<0	no	yes	yes		
338732946	SNE_A10510	putative RND efflux system outer membrane lipoNodT	UK	UK	OM	no	<0	yes	yes	yes	yes	
338732963	SNE_A10680	hypothetical protein	CP	CP	CP	no	<0	no	yes	yes		
338732965	SNE_A10700	oligopeptide-binding OppA	UK	CP	PP	no	<0	no	yes	yes	yes	
338732966	SNE_A10710	oligopeptide-binding OppA	UK	CP	PP	no	<0	yes	yes	yes		
338732975	SNE_A10800	hypothetical protein	UK	UK	IM	no	<0	yes	no	yes		
338733006	SNE_A11110	hypothetical protein	UK	UK	UK	no	<0	no	yes	no		
338733018	SNE_A11230	multidrug resistance mdtA	IM	UK	OM	no	<0	yes	yes	yes		
338733107	SNE_A12120	hypothetical protein	UK	UK	EC	no	<0	no	yes	yes	yes	
338733154	SNE_A12590	hypothetical protein	UK	UK	OM	no	<0	no	yes	yes		
338733335	SNE_A14400	hypothetical protein	CP	CP	CP	no	<0	no	yes	yes		
338733337	SNE_A14420	serpin-like protein	IM	UK	PP	no	<0	no	yes	no		



Chapter V

338733375	SNE_A14800	hypothetical protein	UK	CP	CP	no	<0	no	yes	yes		
338733392	SNE_A14970	hypothetical protein	UK	CP	PP	no	<0	no	yes	no	yes	
338733394	SNE_A14990	hypothetical protein	UK	CP	CP	no	<0	no	yes	yes		
338733485	SNE_A15900	hypothetical protein	CP	CP	PP	no	<0	no	yes	no	yes	
338733524	SNE_A16290	hypothetical protein	UK	UK	UK	no	<0	no	yes	yes		
338733614	SNE_A17190	hypothetical protein	CP	CP	IM	no	<0	no	yes	no		
338733616	SNE_A17210	hypothetical protein	UK	OM	CP	no	<0	no	no	yes	yes	
338733690	SNE_A17950	hypothetical protein	UK	CP	EC	no	<0	no	yes	yes	yes	
338733691	SNE_A17960	hypothetical protein	UK	CP	EC	no	<0	no	yes	yes		
338733789	SNE_A18940	hypothetical protein	CP	CP	IM	no	<0	no	yes	yes		
338733812	SNE_A19170	hypothetical protein	CP	CP	CP	no	<0	no	yes	yes		
338733909	SNE_A20140	hypothetical protein	UK	CP	OM	no	<0	no	yes	no	yes	
338734053	SNE_A21580	hypothetical protein	UK	OM	CP	no	<0	yes	yes	yes		
338734091	SNE_A21960	hypothetical protein	UK	CP	UK	no	<0	no	yes	yes		
338734212	SNE_A23170	oligopeptide-binding OppA	PP	PP	PP	no	<0	no	yes	yes	yes	
338734223	SNE_A23280	hypothetical protein	CP	CP	EC	no	<0	no	yes	yes		

***Waddlia chondrophila***

gi identifier	Locus tag	Protein description	Subcellular localization			Beta barrel conformation			Lipoprotein		Signal peptide	
			PSORTb	CELLO	SOSUI-GramN	BOMP	MCMBB	TMBETADISC-RBF	LipoP	LIPO	SignalP	HHOMP
<b>Outer membrane proteins</b>												
297620275	wcw_0029	hypothetical protein	UK	UK	UK	no	0.005	no	no	no		
297620283	wcw_0037	hypothetical protein	CP	CP	UK	1	<0	no	no	no		
297620304	wcw_0059	hypothetical protein	IM	OM	OM	4	<0	no	no	no	yes	
297620308	wcw_0063	hypothetical protein	UK	OM	OM	no	<0	no	no	no	yes	
297620309	wcw_0064	hypothetical protein	OM	OM	OM	no	<0	no	no	no	yes	
297620310	wcw_0065	hypothetical protein	UK	OM	OM	4	<0	no	no	no	yes	
297620399	wcw_0155	hypothetical protein	UK	OM	CP	no	0.03	no	no	no	yes	
297620409	wcw_0165	hypothetical protein	UK	OM	OM	no	<0	no	no	no		
297620418	wcw_0174	putative rhs family protein	UK	OM	OM	3	<0	no	no	no	yes	

Outer membrane proteins of environmental chlamydiae

297620631	wcw_0390	putative rhs family protein	EC	OM	OM	3	<0	no	no	no	yes	
297620694	wcw_0453	putative rhs family protein	CP	OM	OM	3	<0	no	no	no		
297620700	wcw_0459	putative rhs family protein	CP	UK	CP	1	<0	no	no	no		
297620857	wcw_0620	putative rhs family protein	UK	OM	EC	3	<0	no	no	no		
297620886	wcw_0649	putative periplasmic immunogenic protein	PP	PP	OM	no	0.027	no	no	no	yes	
297620916	wcw_0680	hypothetical protein	UK	OM	OM	no	0.003	no	no	no	yes	
297620968	wcw_0732	putative long-chain fatty acid transport precursor	OM	UK	UK	2	<0	no	no	no		
297620971	wcw_0735	putative long-chain fatty acid transport precursor	UK	EC	OM	1	0.009	no	no	no	yes	
297621009	wcw_0773	putative secreted protein	UK	OM	OM	no	<0	no	no	no	yes	
297621014	wcw_0778	hypothetical protein	UK	OM	OM	no	<0	no	no	no		
297621126	wcw_0895	hypothetical protein	UK	OM	OM	4	<0	no	no	no		
297621168	wcw_0938	hypothetical protein	UK	EC	OM	no	<0	no	no	no	yes	97.58%
297621169	wcw_0939	hypothetical protein	UK	UK	OM	4	<0	no	no	no	yes	97.53%
297621173	wcw_0943	putative rhs family protein	OM	OM	OM	3	<0	no	no	no	yes	
297621218	wcw_0989	hypothetical protein	UK	OM	OM	no	<0	no	no	no	yes	
297621251	wcw_1023	putative rhs family protein	UK	OM	PP	3	<0	no	no	no	yes	
297621274	wcw_1046	hypothetical protein	UK	UK	CP	no	0.008	no	no	no		
297621312	wcw_1086	hypothetical protein	UK	OM	OM	no	<0	no	no	no		
297621326	wcw_1100	hypothetical protein	UK	UK	IM	2	0.007	no	no	no		
297621388	wcw_1162	putative 60 kDa cysteine-rich outer membrane	OM	OM	OM	0	<0	no	no	no	yes	
297621393	wcw_1167	hypothetical protein	CP	OM	OM	1	<0	no	no	no		
297621417	wcw_1191	Outer membrane assembly factor yaeT precursor	OM	OM	OM	1	<0	no	no	no	yes	
297621441	wcw_1215	hypothetical protein	OM	OM	OM	1	<0	no	no	no		
297621493	wcw_1272	hypothetical protein	UK	UK	OM	4	<0	no	no	no	yes	97.68%
297621494	wcw_1273	hypothetical protein	UK	UK	OM	1	<0	no	no	no	yes	97.66%
297621536	wcw_1315	hypothetical protein	UK	OM	OM	no	<0	no	no	no		
297621584	wcw_1364	putative rhs family protein	CP	OM	OM	3	<0	no	no	no		
297621613	wcw_1394	putative long-chain fatty acid transport protein	UK	UK	OM	1	<0	no	no	no		
297621747	wcw_1529	FKBP-type peptidyl-prolyl cis-trans isomerase	OM	UK	OM	0	<0	no	no	no	yes	
297621790	wcw_1573	hypothetical protein	UK	CP	EC	no	0.002	no	no	no		
297621816	wcw_1602	hypothetical protein	UK	UK	CP	no	0.022	no	no	no		
297621836	wcw_1622	putative type III secretion protein SctC	OM	OM	OM	no	<0	no	no	no		
297621928	wcw_1715	putative outer membrane efflux protein	UK	CP	CP	no	<0	no	no	no		100.0%

Chapter V

297622042	wcw_1834	putative rhs family protein	UK	OM	OM	3	<0	no	no	no	yes	
297622051	wcw_1843	hypothetical protein	UK	CP	CP	2	<0	no	no	no	yes	97.65%
297622052	wcw_1844	hypothetical protein	UK	CP	OM	2	<0	no	no	no	yes	97.6%
297622064	wcw_1856	putative rhs family protein	UK	OM	OM	no	<0	no	no	no	yes	
337292490	WCH_DC18990	putative uncharacterized protein	IM	OM	OM	no	<0	no	no	no		
337293792	WCH_CN15720	putative uncharacterized protein	UK	PP	OM	no	0.023	no	no	no		
<b>Outer membrane lipoproteins</b>												
297622025	wcw_1817	putative outer membrane factor (OMF) family efflux porin	UK	OM	PP	0	<0	no	no	yes		
297622034	wcw_1826	putative outer membrane efflux protein	OM	UK	OM	no	<0	no	yes	yes		
<b>Lipoproteins</b>												
297620274	wcw_0028	putative peptidyl-prolyl cis-trans isomerase Mip precursor	UK	UK	OM	no	<0	no	yes	no		
297620306	wcw_0061	putative capsule polysaccharide export precursor	CP	UK	PP	0	<0	no	yes	yes		
297620366	wcw_0122	Sodium-type flagellar motY precursor	UK	CP	PP	no	<0	no	yes	yes		
297620430	wcw_0186	hypothetical protein	UK	UK	PP	no	<0	no	yes	yes	yes	
297620499	wcw_0255	hypothetical protein	UK	CP	CP	no	<0	no	yes	no		
297620597	wcw_0354	putative N-acetylmuramoyl alanine amidase	CP	CP	PP	no	<0	no	yes	yes		
297620613	wcw_0372	hypothetical protein	CP	UK	CP	no	<0	no	yes	yes		
297620632	wcw_0391	hypothetical protein	UK	PP	PP	no	<0	no	yes	yes	yes	
297620634	wcw_0393	hypothetical protein	UK	PP	PP	no	0.014	no	yes	yes	yes	
297620704	wcw_0463	hypothetical protein	UK	UK	OM	no	<0	no	yes	yes		
297620765	wcw_0525	hypothetical protein	UK	CP	CP	no	<0	no	yes	no		
297620838	wcw_0601	hypothetical protein	UK	CP	PP	no	<0	no	no	yes		
297620878	wcw_0641	hypothetical protein	CP	CP	CP	no	<0	no	no	yes		
297621151	wcw_0921	spermidine/putrescine-binding potD precursor	PP	CP	CP	no	<0	no	yes	yes		
297621158	wcw_0928	hypothetical protein	UK	CP	PP	no	<0	no	yes	no		
297621171	wcw_0941	hypothetical protein	UK	CP	IM	no	<0	no	yes	no		
297621172	wcw_0942	hypothetical protein	UK	CP	UK	no	<0	no	yes	yes		
297621211	wcw_0982	hypothetical protein	CP	UK	OM	no	<0	no	yes	no	yes	
297621224	wcw_0995	hypothetical protein	CP	CP	CP	no	<0	no	no	yes		

## Outer membrane proteins of environmental chlamydiae

297621246	wcw_1018	hypothetical protein	UK	UK	PP	no	<0	no	no	yes		
297621250	wcw_1022	hypothetical protein	UK	PP	PP	no	0.007	no	yes	no		
297621357	wcw_1131	hypothetical protein	CP	CP	CP	no	<0	no	no	yes		
297621386	wcw_1160	putative cysteine-rich outer membrane protein OmcA	UK	UK	UK	no	<0	no	yes	yes	yes	
297621400	wcw_1174	Thiamine biosynthesis lipoapbE precursor	UK	CP	PP	no	<0	no	yes	yes	yes	
297621420	wcw_1194	putative secreted protein	UK	UK	IM	no	<0	no	yes	no		
297621445	wcw_1219	hypothetical protein	CP	CP	CP	no	<0	no	yes	no		
297621453	wcw_1227	putative copper/zinc superoxide dismutase	PP	CP	PP	no	<0	no	yes	yes		
297621457	wcw_1231	putative amine oxidoreductase	CP	CP	CP	no	<0	no	no	yes		
297621463	wcw_1237	FAD dependent oxidoreductase	CP	CP	PP	no	<0	no	no	yes		
297621739	wcw_1521	hypothetical protein	UK	UK	EC	no	<0	no	no	yes		
297621759	wcw_1541	hypothetical protein	CP	EC	PP	no	<0	no	yes	yes		
297621767	wcw_1549	hypothetical protein	CP	CP	OM	no	<0	no	yes	yes		
297621857	wcw_1643	FKBP-type peptidyl-prolyl cis-trans isomerase	UK	UK	CP	0	<0	no	no	yes		
297621927	wcw_1714	hypothetical protein	UK	CP	PP	no	<0	no	yes	yes		
297621963	wcw_1753	hypothetical protein	CP	UK	CP	no	<0	no	yes	no		
297622009	wcw_1801	hypothetical protein	CP	UK	OM	no	<0	no	yes	no		
297622010	wcw_1802	hypothetical protein	CP	CP	CP	no	<0	no	no	yes		
297622047	wcw_1839	hypothetical protein	CP	UK	PP	no	<0	no	yes	yes		
297622135	wcw_1930	hypothetical protein	CP	OM	EC	no	<0	no	yes	yes		
297622178	wcw_1976	hypothetical protein	CP	EC	CP	no	<0	no	yes	yes		
337292491	WCH_DC19000	unknown protein	UK	EC	OM	no	<0	no	yes	no		
337292911	WCH_AU05480	putative uncharacterized protein	UK	UK	CP	no	<0	no	yes	yes		
337293547	WCH_AD02780	unknown protein	UK	CP	PP	no	<0	no	no	yes	yes	
337293798	WCH_CN15810	putative rhs family protein	UK	PP	EC	no	<0	no	no	yes		
337293801	WCH_AX06730	hypothetical protein	UK	PP	UK	no	<0	no	yes	yes	yes	
337293823	WCH_AX06730	hypothetical protein	UK	PP	PP	no	<0	no	yes	yes	yes	
337293885	WCH_AA00280	putative uncharacterized protein	UK	CP	CP	no	<0	no	yes	no		
337293934	WCH_DD19350	putative uncharacterized protein	UK	CP	IM	no	<0	no	yes	yes		
337293935	WCH_DD19360	putative uncharacterized protein	UK	CP	IM	no	<0	no	yes	yes		
337293936	WCH_DD19370	putative uncharacterized protein	UK	CP	IM	no	<0	no	yes	yes		
337293937	WCH_DD19380	putative uncharacterized protein	UK	CP	IM	no	<0	no	yes	yes		
337293938	WCH_DD19390	putative uncharacterized protein	UK	CP	IM	no	<0	no	yes	yes		

## Chapter V

---

337294104	WCH_AW06200	putative uncharacterized protein	UK	CP	OM	no	<0	no	yes	yes		
337294238	WCH_CA13570	ABC-type transporter, substrate-binding lipoprotein	IM	CP	UK	no	<0	no	yes	no		
337294286	WCH_DB18760	putative uncharacterized protein	UK	CP	IM	no	<0	no	yes	yes		
337294287	WCH_DB18770	putative uncharacterized protein	CP	CP	IM	no	<0	no	yes	yes		

**Table S5: Outer membrane proteins of *Simkania* detected by mass spectrometry after extraction with sarkosyl, n-octylpolyoxyethylene (nPOE) or TritonX-114 (Triton)**

Shown are proteins detected after in-gel digests of protein fractions. Proteins not detected after in-solution digests of sarkosyl-treated samples are highlighted in grey.

gi identifier	Locus tag	Protein description	Molecular mass	Unique peptides Sarkosyl	Spectral counts Sarkosyl	Unique peptides nPOE	Spectral counts nPOE	Unique peptides Triton	Spectral counts Triton
<b>Sarkosyl, nPOE and TritonX-114</b>									
338731826	SNE_B24500	outer membrane efflux protein	53 kDa	14	33	14	43	7	23
338731881	SNE_B25050	hypothetical protein	38 kDa	8	33	8	58	3	3
338731935	SNE_A00390	hypothetical protein	47 kDa	15	57	16	68	7	11
338731938	SNE_A00420	major outer membrane protein	27 kDa	9	14	8	10	4	4
338731959	SNE_A00630	polymorphic outer membrane protein B	152 kDa	18	96	15	84	5	9
338731979	SNE_A00830	hypothetical protein	43 kDa	10	50	14	79	3	3
338732099	SNE_A02040	hypothetical protein	46 kDa	14	62	19	117	4	6
338732101	SNE_A02060	MOMP-like family protein	41 kDa	11	70	13	93	7	16
338732121	SNE_A02260	MOMP-like family protein	37 kDa	11	57	6	19	2	6
338732147	SNE_A02520	hypothetical protein	36 kDa	8	159	11	231	5	29
338732171	SNE_A02760	MOMP-like family protein	43 kDa	18	125	18	155	6	22
338732173	SNE_A02780	MOMP-like family protein	45 kDa	13	167	17	278	6	52
338732179	SNE_A02840	MOMP-like family protein	40 kDa	12	85	12	87	2	2
338732181	SNE_A02860	MOMP-like family protein	43 kDa	14	131	15	101	7	34
338732182	SNE_A02870	MOMP-like family protein	42 kDa	11	102	17	112	4	24
338732238	SNE_A03430	hypothetical protein	65 kDa	17	55	16	58	3	4
338732404	SNE_A04510	MOMP-like family protein	47 kDa	21	217	22	337	11	78
338732415	SNE_A05090	polymorphic outer membrane protein B	177 kDa	14	114	14	140	8	18
338732416	SNE_A05210	hypothetical protein	70 kDa	2	19	3	13	2	6
338732533	SNE_A06380	hypothetical protein	41 kDa	8	45	8	51	4	12

338732549	SNE_A06540	carbohydrate-selective porin, OprB family	50 kDa	14	70	19	120	4	7
338732638	SNE_A07430	MOMP-like family protein	42 kDa	14	276	16	253	7	69
338732639	SNE_A07440	MOMP-like family protein	45 kDa	13	269	20	501	6	52
338732690	SNE_A07950	MOMP-like family protein	41 kDa	13	113	18	134	5	31
338732701	SNE_A08060	MOMP-like family protein	40 kDa	8	65	13	90	3	6
338732702	SNE_A08070	MOMP-like family protein	40 kDa	9	69	11	85	3	7
338732712	SNE_A08170	putative outer membrane protein Omp85	91 kDa	47	213	48	316	28	65
338732745	SNE_A08500	MOMP-like family protein	44 kDa	17	132	15	106	7	28
338732757	SNE_A08620	hypothetical protein	40 kDa	10	44	15	81	6	10
338732777	SNE_A08820	MOMP-like family protein	46 kDa	16	83	16	93	6	12
338732778	SNE_A08830	MOMP-like family protein	44 kDa	19	89	17	94	2	6
338732791	SNE_A08960	hypothetical protein	82 kDa	22	56	23	86	6	6
338732896	SNE_A10010	MOMP-like family protein	41 kDa	15	124	18	152	8	26
338732953		peptidase S9, prolyl oligopeptidase active site region	75 kDa	7	9	14	78	3	5
338733016	SNE_A11120	MOMP-like family protein	38 kDa	14	96	14	98	5	10
338733073	SNE_A11780	hypothetical protein	19 kDa	5	17	6	23	4	5
338733367	SNE_A14720	polymorphic outer membrane protein B	275 kDa	20	95	20	102	7	12
338733380	SNE_A14850	MOMP-like family protein	42 kDa	10	71	14	91	3	11
338733381	SNE_A14860	MOMP-like family protein	40 kDa	14	120	16	219	7	54
338733489	SNE_A15330	MOMP-like family protein	43 kDa	17	112	16	123	2	2
338733707	SNE_A18120	MOMP-like family protein	44 kDa	16	404	13	522	10	77
338733823	SNE_A19280	hypothetical protein	102 kDa	10	24	18	130	3	13
338733906	SNE_A20110	hypothetical protein	194 kDa	98	849	62	215	52	122
338733966	SNE_A20710	MOMP-like family protein	41 kDa	25	862	24	578	10	77
338733988	SNE_A20930	hypothetical protein	66 kDa	22	78	21	99	7	7
338733989	SNE_A20940	hypothetical protein	462 kDa	14	51	13	37	6	6

Outer membrane proteins of environmental chlamydiae

338734232	SNE_A23370	MOMP-like family protein	41 kDa	14	52	14	49	3	3
338734234	SNE_A23390	MOMP-like family protein	42 kDa	10	49	15	59	3	11
338734235	SNE_A23400	MOMP-like family protein	46 kDa	11	52	14	64	2	8
338734236	SNE_A23410	MOMP-like family protein	43 kDa	26	1182	26	1131	11	171
338734237	SNE_A23420	MOMP-like family protein	43 kDa	30	825	30	866	14	118
338732175_new		new sequence MOMP-like protein	39 kDa	17	550	21	841	11	105
338732773_new		new sequence MOMP-like protein	39 kDa	10	105	12	125	5	25
<b>Sarkosyl and nPOE</b>									
338731937	SNE_A00410	major outer membrane protein	29 kDa	9	24	10	22		
338731971	SNE_A00750	MOMP-like family protein	42 kDa	6	25	5	16		
338731978	SNE_A00820	MOMP-like family protein	39 kDa	5	9	3	9		
338732172	SNE_A02770	MOMP-like family protein	39 kDa	12	38	13	60		
338732676	SNE_A07810	hypothetical protein	49 kDa	4	4	7	16		
338733205	SNE_A13100	hypothetical protein	36 kDa	4	6	4	14		
338733428	SNE_A15330	hypothetical protein	46 kDa	7	22	9	49		
338734198	SNE_A23030	hypothetical protein	81 kDa	4	11	5	14		
338734277	SNE_A23820	hypothetical protein	36 kDa	2	3	5	11		
<b>nPOE and TritonX-114</b>									
338731883	SNE_B25070	hypothetical protein	44 kDa			10	51	3	6
338733007	SNE_A11120	hypothetical protein	75 kDa			8	16	2	2
338731814	SNE_B24380	hypothetical protein	48 kDa	11	15			7	9
338733019		putative outer membrane factor (OMF) family efflux porin	55 kDa	17	49			5	7
338733478	SNE_A15830	hypothetical protein	54 kDa	13	28			6	8
<b>Sarkosyl only</b>									
338732558	SNE_A06630	outer membrane protein	53 kDa	12	21				
<b>nPOE only</b>									
338731972	SNE_A00760	hypothetical protein	321 kDa			3	3		
338732858	SNE_A09630	hypothetical protein	30 kDa			3	4		



**Table S6: Outer membrane proteins, outer membrane lipoproteins and lipoproteins detected by mass spectrometry in outer membrane protein fractions of *Simkania*, *Parachlamydia* and *Waddlia* after treatment with sarkosyl**

Proteins detected with at least two unique peptides in both biological replicates are listed. For *Waddlia*, locus tags for both strain WSU86-1044 and 2032/99 are listed. The protein identified by mass spectrometry is indicated by bold letters for *Waddlia*. Signal peptides were predicted by SignalP.

***Parachlamydia acanthamoebae* UV7**

gi identifier	Locus tag	Protein description	Molecular mass	Unique peptides repl1	Unique peptides repl2	Spectral counts repl 1	Spectral counts repl2	% cysteine	Signal peptide	
<b>Outer membrane proteins</b>										
338174157	PUV_01630	hypothetical protein	32 kDa	11	15	22	18	0.70%		
338174161	PUV_01670	outer membrane proteinoprM	54 kDa	12	10	23	17	0.83%		
338174166	PUV_01720	hypothetical protein	208 kDa	38	18	88	46	1.10%	yes	
338174185	PUV_01910	hypothetical protein	48 kDa	11	11	18	17	0.48%	yes	
338174324	PUV_03300	hypothetical protein	91 kDa	11	4	24	13	1.41%	yes	
338174355	PUV_03610	carboxy-terminal	74 kDa	38	28	114	80	0.15%		
338174452	PUV_04580	hypothetical protein	64 kDa	6	11	24	58	2.69%	yes	
338174483	PUV_04890	hypothetical protein	53 kDa	9	5	11	8	1.46%		
338174565	PUV_05710	type III secretion outer membrane ring component	106 kDa	11	9	22	22	0.42%		
338174567	PUV_05730	type III secretion outer membrane ring component	105 kDa	6	10	14	12	0.52%		
338174677	PUV_06830	tail-specific protease	77 kDa	15	5	31	7	0.15%	yes	
338174738	PUV_07440	hypothetical protein	34 kDa	7	9	18	19	2.03%		
338174749	PUV_07550	hypothetical protein	31 kDa	23	21	1517	1585	3.23%	yes	
338174816	PUV_08220	hypothetical protein	129 kDa	16	7	21	6	0.52%		

Outer membrane proteins of environmental chlamydiae

338174817	PUV_08230		hypothetical protein	68 kDa	16	6	28	9	1.17%	
338174833	PUV_08390		hypothetical protein	60 kDa	11	9	12	12	0.00%	
338174862	PUV_08680		hypothetical protein	48 kDa	29	27	602	824	1.39%	
338174985	PUV_09910		hypothetical protein	89 kDa	46	38	401	411	1.02%	yes
338174994	PUV_10000		hypothetical protein	91 kDa	11	9	21	27	1.29%	yes
338175011	PUV_10170		OmcB	68 kDa	37	32	1173	3520	7.63%	
338175178	PUV_11840		hypothetical protein	36 kDa	21	20	139	253	0.00%	yes
338175388	PUV_13940		hypothetical protein	103 kDa	43	37	134	161	0.33%	
338175773	PUV_17790		outer membrane protein OprM	44 kDa	16	8	40	13	0.26%	
338175826	PUV_18320		hypothetical protein	35 kDa	16	15	209	208	1.95%	yes
338175829	PUV_18350		hypothetical protein	47 kDa	18	18	76	49	1.73%	
338175855	PUV_18610		hypothetical protein	76 kDa	36	27	72	53	0.15%	
338175881	PUV_18870		hypothetical protein	23 kDa	15	11	45	29	3.06%	
338175919	PUV_19250		hypothetical protein	87 kDa	29	16	62	22	1.09%	yes
338176146	PUV_21520		hypothetical protein	45 kDa	6	4	6	10	2.22%	yes
338176384	PUV_23900		hypothetical protein	51 kDa	11	11	24	29	0.89%	
338176434	PUV_24400		hypothetical protein	55 kDa	13	6	18	8	1.47%	
338176513	PUV_25190		hypothetical protein	47 kDa	21	17	49	26	0.49%	
338176516	PUV_25220		hypothetical protein	39 kDa	15	10	17	10	2.07%	yes
338176744	PUV_27500		hypothetical protein	54 kDa	53	47	2503	4430	3.36%	yes
<b>Outer membrane lipoproteins</b>										
338174079	PUV_00850		hypothetical protein	53 kDa	12	12	24	27	1.08%	yes
338175289	PUV_12950		mOMP-like family protein	42 kDa	11	11	54	66	2.67%	
338175723	PUV_17290		hypothetical protein	54 kDa	16	15	25	39	0.64%	
338176096	PUV_21020		solvent efflux pump outer membrane proteinsrpC	56 kDa	24	18	52	53	0.81%	
338176612	PUV_26180		hypothetical protein	56 kDa	12	9	19	17	0.61%	yes
<b>Lipoproteins</b>										

338174087	PUV_00930		hyperosmotically inducible periplasmic protein	17 kDa	19	6	116	116	0.63%	
338174137	PUV_01430		type III secretion periplasmic lipoprotein	35 kDa	19	18	41	41	0.62%	
338174207	PUV_02130		metal-binding lipoprotein TC_0338	39 kDa	11	8	20	20	1.16%	yes
338174216	PUV_02220		polysaccharide export protein wza	39 kDa	10	10	40	40	1.44%	
338174318	PUV_03240		hypothetical protein	45 kDa	7	7	9	9	2.22%	
338174604	PUV_06100		carbonic anhydrase	23 kDa	10	5	33	33	1.43%	yes
338174752	PUV_07580		spermidine/putrescine-binding periplasmic protein	39 kDa	10	9	22	22	0.87%	
338174896	PUV_09020		thiamine biosynthesis lipoproteinApbE	39 kDa	6	3	10	10	2.05%	
338175166	PUV_11720		hypothetical protein	36 kDa	12	2	20	20	1.24%	
338175464	PUV_14700		superoxide dismutase [Cu-Zn]	19 kDa	14	3	22	22	2.25%	yes
338175692	PUV_16980		type III secretion periplasmic lipoprotein	34 kDa	13	12	41	41	0.66%	
338175911	PUV_19170		hypothetical protein	15 kDa	10	6	54	54	0.72%	
338176142	PUV_21480		hypothetical protein	40 kDa	12	8	17	17	1.39%	yes
338176711	PUV_27170		hypothetical protein	54 kDa	22	23	62	62	1.26%	yes
338176764	PUV_27700		hypothetical protein	53 kDa	21	17	34	34	0.43%	yes

*Simkania negevensis*

gi identifier	locus tag		Protein description	Molecular mass	Unique peptides repl1	Unique peptides repl2	Spectral counts repl1	Spectral counts repl2	% cysteine	Signal peptide
<b>Outer membrane proteins</b>										
338731881	SNE_B25050		hypothetical protein	38 kDa	8	8	45	33	1.78%	
338733073	SNE_A11780		hypothetical protein	19 kDa	6	5	20	17	1.18%	yes
338733380	SNE_A14850		MOMP-like family protein	42 kDa	13	10	94	71	1.09%	

Outer membrane proteins of environmental chlamydiae

338731979	SNE_A00830		hypothetical protein	43 kDa	17	10	81	50	1.08%	yes
338732639	SNE_A07440		MOMP-like family protein	45 kDa	23	13	374	269	1.01%	
338732757	SNE_A08620		hypothetical protein	40 kDa	22	10	156	44	0.86%	yes
338732171	SNE_A02760		MOMP-like family protein	43 kDa	25	18	187	125	0.82%	yes
338732533	SNE_A06380		hypothetical protein	41 kDa	11	8	74	45	0.82%	yes
338733823	SNE_A19280		hypothetical protein	102 kDa	17	10	77	24	0.81%	yes
338732638	SNE_A07430		MOMP-like family protein	42 kDa	25	14	283	276	0.80%	yes
338733707	SNE_A18120		MOMP-like family protein	44 kDa	18	16	251	404	0.78%	yes
338732416	SNE_A05200		hypothetical protein	70 kDa	4	2	11	19	0.77%	yes
338733988	SNE_A20930		hypothetical protein	66 kDa	30	22	110	78	0.69%	
338731959	SNE_A00630		polymorphic outer membrane protein B	152 kDa	25	18	69	96	0.61%	yes
338733016	SNE_A11120		MOMP-like family protein	38 kDa	16	14	128	96	0.61%	yes
338731978	SNE_A00820		MOMP-like family protein	39 kDa	10	5	18	9	0.58%	
338732702	SNE_A08070		MOMP-like family protein	40 kDa	7	9	84	69	0.57%	
338732701	SNE_A08060		MOMP-like family protein	40 kDa	19	8	131	65	0.57%	yes
338734232	SNE_A23370		MOMP-like family protein	41 kDa	13	14	27	52	0.56%	yes
338732690	SNE_A07950		MOMP-like family protein	41 kDa	13	13	165	113	0.56%	yes
338732181	SNE_A02860		MOMP-like family protein	43 kDa	18	14	227	131	0.54%	yes
338732238	SNE_A03430		hypothetical protein	65 kDa	23	17	66	55	0.53%	yes
338734237	SNE_A23420		MOMP-like family protein	43 kDa	34	30	559	825	0.53%	yes
338734236	SNE_A23410		MOMP-like family protein	43 kDa	23	26	482	1182	0.52%	yes
338732745	SNE_A08500		MOMP-like family protein	44 kDa	19	17	112	132	0.51%	yes
338733428	SNE_A15330		hypothetical protein	46 kDa	6	7	44	22	0.50%	yes
338732404	SNE_A04510		MOMP-like family protein	47 kDa	29	21	271	217	0.48%	yes
338731814	SNE_B24380		hypothetical protein	48 kDa	31	11	73	15	0.48%	yes
338732099	SNE_A02040		hypothetical protein	46 kDa	18	14	105	62	0.47%	
338732415	SNE_A05090		polymorphic outer membrane protein B	177 kDa	16	14	62	114	0.47%	yes

338733478	SNE_A15830		hypothetical protein	54 kDa	24	13	56	28	0.42%	
338731937	SNE_A00410		major outer membrane protein	29 kDa	15	9	100	24	0.39%	yes
338733367	SNE_A14720		polymorphic outer membrane protein B	275 kDa	22	20	101	95	0.37%	
338733205	SNE_A13100		hypothetical protein	36 kDa	5	4	14	6	0.31%	
338734277	SNE_A23820		hypothetical protein	36 kDa	3	2	9	3	0.31%	yes
338732773_new			new sequence MOMP-like protein	39 kDa	13	10	115	105	0.29%	
338732179	SNE_A02840		MOMP-like family protein	40 kDa	15	12	103	85	0.29%	yes
338732896	SNE_A10010		MOMP-like family protein	41 kDa	19	15	214	124	0.28%	yes
338733381	SNE_A14860		MOMP-like family protein	40 kDa	20	14	349	120	0.28%	yes
338732101	SNE_A02060		MOMP-like family protein	41 kDa	14	11	115	70	0.27%	yes
338734234	SNE_A23390		MOMP-like family protein	42 kDa	15	10	94	49	0.27%	yes
338732173	SNE_A02780		MOMP-like family protein	45 kDa	27	13	483	167	0.26%	yes
338732777	SNE_A08820		MOMP-like family protein	46 kDa	16	16	81	83	0.25%	yes
338732549	SNE_A06540		carbohydrate-selective porin, OprB family	50 kDa	26	14	204	70	0.23%	yes
338733989	SNE_A20940		hypothetical protein	462 kDa	9	14	14	51	0.19%	yes
338733906	SNE_A20110		hypothetical protein	194 kDa	57	98	188	849	0.17%	yes
338734198	SNE_A23030		hypothetical protein	81 kDa	21	4	42	11	0.14%	
338731935	SNE_A00390		hypothetical protein	47 kDa	26	15	126	57	0.00%	yes
338731938	SNE_A00420		major outer membrane protein	27 kDa	14	9	37	14	0.00%	
338731971	SNE_A00750		MOMP-like family protein	42 kDa	8	6	21	25	0.00%	
338732121	SNE_A02260		MOMP-like family protein	37 kDa	21	11	147	57	0.00%	yes
338732147	SNE_A02520		hypothetical protein	36 kDa	19	8	342	159	0.00%	yes
338732182	SNE_A02870		MOMP-like family protein	42 kDa	18	11	148	102	0.00%	yes
338732676	SNE_A07810		hypothetical protein	49 kDa	14	4	36	4	0.00%	
338732712	SNE_A08170		putative outer membrane protein Omp85	91 kDa	59	47	271	213	0.00%	yes

Outer membrane proteins of environmental chlamydiae

338732778	SNE_A08830		MOMP-like family protein	44 kDa	16	19	41	89	0.00%	yes
338732791	SNE_A08960		hypothetical protein	82 kDa	29	22	116	56	0.00%	yes
338733966	SNE_A20710		MOMP-like family protein	41 kDa	24	25	403	862	0.00%	
338732175_new			new sequence MOMP-like protein	39 kDa	19	17	1088	550	0.00%	yes
<b>Outer membrane lipoproteins</b>										
338731826	SNE_B24500		outer membrane efflux protein	53 kDa	20	14	70	33	0.21%	yes
338732172	SNE_A02770		MOMP-like family protein	39 kDa	14	12	80	38	0.87%	yes
338732558	SNE_A06630		outer membrane protein	53 kDa	18	12	39	21	0.22%	
338733019	SNE_A11240		putative outer membrane factor (OMF) family efflux porin	55 kDa	18	17	79	49	0.41%	
338733489	SNE_A15940		MOMP-like family protein	43 kDa	18	17	170	112	0.80%	yes
338734235	SNE_A23400		MOMP-like family protein	46 kDa	13	11	108	52	0.24%	yes
<b>Lipoproteins</b>										
338731815	SNE_B24390		chemiosmotic efflux system B protein B	43 kDa	21	8	62	11	0.26%	
338731827	SNE_B24510		multicopper oxidase domain-containing protein	48 kDa	13	5	52	11	0.93%	yes
338732016	SNE_A01200		hypothetical protein	15 kDa	13	8	118	83	0.68%	
338732126	SNE_A02310		putative polysaccharide export protein Wza	39 kDa	13	3	32	5	0.28%	
338732150	SNE_A02550		hypothetical protein	24 kDa	4	3	8	5	1.37%	yes
338732214	SNE_A03190		hypothetical protein	13 kDa	8	5	22	18	0.89%	yes
338732946	SNE_A10510		putative RND efflux system outer membrane lipoprotein NodT	55 kDa	28	18	51	23	0.21%	yes
338733018	SNE_A11230		multidrug resistance protein mdtA	42 kDa	16	14	65	56	0.54%	
338733107	SNE_A12120		hypothetical protein	42 kDa	21	19	252	114	1.07%	yes

338733154	SNE_A12590		hypothetical protein	17 kDa	11	7	13	9	1.32%	
338733375	SNE_A14800		hypothetical protein	20 kDa	7	2	7	2	1.21%	
338733909	SNE_A20140		hypothetical protein	36 kDa	11	9	48	21	1.27%	yes
338734053	SNE_A21580		hypothetical protein	22 kDa	7	2	8	3	0.50%	

***Waddlia chondrophila***

gi identifier	Locus tag WSU 86-1044	Locus tag 20322/99	Protein description	Molecular mass	Unique peptides repl1	Unique peptides repl2	Spectral counts repl1	Spectral counts repl2	% cysteine	Signal peptide
<b>Outer membrane proteins</b>										
297620304	<b>wcw_0059</b>	WCH_CT17220	MOMP-like family protein	42 kDa	12	13	123	294	4.81%	yes
297620310	<b>wcw_0065</b>	WCH_CT17280	MOMP-like family protein	39 kDa	7	7	326	1347	4.21%	yes
297620409	<b>wcw_0165</b>	WCH_CN15940	hypothetical protein	83 kDa	12	15	21	31	0.27%	
297620857	<b>wcw_0620</b>	WCH_BJ08770	putative rhs family protein	197 kDa	17	6	26	7	1.40%	
297620886	<b>wcw_0649</b>	WCH_AG04060	putative periplasmic immunogenic protein	25 kDa	4	4	17	15	0.00%	yes
297620916	<b>wcw_0680</b>	WCH_AG04220	hypothetical protein	40 kDa	12	15	58	69	0.28%	yes
297621126	<b>wcw_0895</b>	WCH_AD00800	hypothetical protein	39 kDa	8	7	24	20	3.22%	
297621168	<b>wcw_0938</b>	WCH_AD01220	MOMP-like family protein	42 kDa	7	8	93	98	5.08%	yes
297621169	<b>wcw_0939</b>	WCH_AD01230	MOMP-like family protein	42 kDa	10	7	51	20	3.49%	yes
297621173	<b>wcw_0943</b>	WCH_AD01270	putative rhs family protein	210 kDa	4	2	4	2	2.02%	yes
297621218	<b>wcw_0989</b>	WCH_AD01740	hypothetical protein	31 kDa	12	7	45	17	1.49%	yes
297621326	<b>wcw_1100</b>	WCH_AD02810	hypothetical protein	21 kDa	12	14	96	660	0.00%	
297621388	<b>wcw_1162</b>	WCH_AD03430	60 kDa cysteine-rich outer membrane protein	56 kDa	27	23	370	1231	9.42%	yes
297621393	<b>wcw_1167</b>	WCH_AD03490	hypothetical protein	82 kDa	14	7	19	11	1.58%	
297621417	<b>wcw_1191</b>	WCH_BX12680	Outer membrane protein assembly factor yaeT precursor	93 kDa	37	28	121	106	2.20%	yes

Outer membrane proteins of environmental chlamydiae

297621441	<b>wcw_1215</b>	WCH_BX12460	hypothetical protein	66 kDa	14	5	15	15	0.35%	
297621494	<b>wcw_1273</b>	WCH_BX11910	MOMP-like family protein	38 kDa	6	7	25	24	4.20%	yes
297621536	<b>wcw_1315</b>	WCH_AU05370	MOMP-like family protein	41 kDa	6	11	30	65	3.49%	
297621747	<b>wcw_1529</b>	WCH_CF14220	FKBP-type peptidyl-prolyl cis-trans isomerase	28 kDa	8	15	11	40	0.40%	yes
297621836	<b>wcw_1622</b>	WCH_CF14220	putative type III secretion protein SctC	124 kDa	23	16	72	79	0.54%	
297622051	<b>wcw_1843</b>	WCH_DD19250	MOMP-like family protein	34 kDa	12	11	84	67	5.02%	yes
337292687	wcw_1394	<b>WCH_BP09860</b>	<b>putative long-chain fatty acid transport protein</b>	47 kDa	4	5	38	18	1.44%	
337292861	wcw_0063	<b>WCH_CT17260</b>	<b>MOMP-like family protein</b>	39 kDa	7	13	323	936	4.71%	yes
337292862	wcw_0064	<b>WCH_CT17270</b>	<b>MOMP-like family protein</b>	40 kDa	12	13	622	1760	4.11%	yes
337293209	wcw_0732	<b>WCH_BT11230</b>	<b>putative long-chain fatty acid transport protein</b>	51 kDa	26	18	259	464	1.51%	yes
337293540	wcw_1086	<b>WCH_AD02710</b>	<b>putative uncharacterized protein</b>	93 kDa	29	26	92	94	0.24%	
337293684	wcw_1272	<b>WCH_BX11920</b>	<b>MOMP-like family protein</b>	37 kDa	10	17	177	574	3.89%	
337293922	wcw_1844	<b>WCH_DD19230</b>	<b>MOMP-like family protein</b>	34 kDa	18	19	1263	2752	5.32%	yes
337293933	wcw_1834	<b>WCH_DD19340</b>	<b>putative rhs family protein</b>	200 kDa	5	5	7	5	1.09%	yes
337294082	wcw_1602	<b>WCH_AW05980</b>	<b>putative uncharacterized protein</b>	46 kDa	13	14	59	106	0.00%	
337294187	wcw_1715	<b>WCH_CA13060</b>	<b>putative outer membrane efflux protein</b>	54 kDa	9	4	14	8	1.05%	
<b>Outer membrane lipoproteins</b>										
297622034	<b>wcw_1817</b>	WCH_DD19440	putative outer membrane efflux protein	54 kDa	19	21	60	64	0.63%	
297622025	<b>wcw_1826</b>	WCH_DD19520	putative outer membrane factor (OMF) family efflux porin	54 kDa	13	11	28	16	1.66%	
<b>Lipoproteins</b>										
297620306	<b>wcw_0061</b>	WCH_CT17240	putative capsule polysaccharide export protein precursor	40 kDa	9	9	17	18	1.44%	



297620597	<b>wcw_0354</b>	WCH_AH04240	putative N-acetylmuramoyl alanine amidase	26 kDa	16	15	42	53	0.87%	
297620704	<b>wcw_0463</b>	WCH_BJ08840	hypothetical protein	43 kDa	18	8	57	40	2.27%	
297620878	<b>wcw_0641</b>	WCH_AA00050	hypothetical protein	33 kDa	2	2	3	2	2.45%	
297621151	<b>wcw_0921</b>	WCH_AD0105	spermidine/putrescine-binding potD proteinprecursor	39 kDa	5	2	5	2	1.18%	
297621211	<b>wcw_0982</b>	WCH_AD01670	hypothetical protein	67 kDa	10	7	15	11	1.48%	yes
297621453	<b>wcw_1227</b>	WCH_BX12340	putative copper/zinc superoxide dismutase	22 kDa	7	6	44	37	1.46%	
297621457	<b>wcw_1231</b>	WCH_BX12300	putative amine oxidoreductase	47 kDa	13	4	20	8	1.92%	
297621759	<b>wcw_1541</b>	WCH_CF14110	hypothetical protein	37 kDa	28	23	118	159	1.23%	
297621927	<b>wcw_1714</b>	WCH_CA13050	hypothetical protein	18 kDa	15	4	37	3	1.26%	
297622178	<b>wcw_1976</b>	WCH_CJ14630	hypothetical protein	49 kDa	12	11	22	39	0.70%	
337292466	wcw_0122	<b>WCH_BB08040</b>	<b>peptidoglycan-associated lipoprotein</b>	29 kDa	13	9	62	9	2.02%	
337292818	wcw_0028	<b>WCH_CT16830</b>	<b>macrophage infectivity potentiator</b>	35 kDa	3	2	4	2	0.66%	
337293928	wcw_1839	<b>WCH_DD19290</b>	<b>putative uncharacterized protein</b>	28 kDa	16	9	33	26	1.70%	
337294124	wcw_1643	<b>WCH_AW06400</b>	<b>macrophage infectivity potentiator</b>	29 kDa	9	12	19	25	1.17%	
337294286	wcw_1832	<b>WCH_DB18760</b>	<b>putative uncharacterized protein</b>	21 kDa	6	2	9	2	0.55%	

**Table S7: The fifty most abundant proteins detected in outer membrane protein fractions of *Parachlamydia*, *Simkania* and *Waddlia***

Quantification of proteins is based on ranks obtained by calculating the normalized spectral abundance factor (NSAF) or the total ion current (TIC) if varying amounts of bands were injected. The mean rank of two replicates is shown. Proteins with a predicted location in the outer membrane are highlighted in grey. Signal peptides were predicted with SignalP. CP, cytoplasmic; EC, extracellular; IM, inner membrane; PP, periplasmic; OM, outer membrane; UK, unknown; LP, lipoprotein;

***Parachlamydia acanthamoebae***

Mean rank	gi identifier	Locus tag	Protein description	Molecular mass	Unique peptides 1	Unique peptides 2	Predicted location	NSAF 1	TIC 2	Signal peptide	% cysteine
1	338176744	PUV_27500	hypothetical protein	54 kDa	53	47	OM	6.4456	3.46E+10	yes	3.36%
1	338175110	PUV_11160	hypothetical protein	20 kDa	11	14	UK	6.081	3.61E+10	yes	10.50%
3	338174749	PUV_07550	hypothetical protein	31 kDa	23	21	OM	4.9813	3.43E+10	yes	3.23%
4	338175011	PUV_10170	OmcB	68 kDa	37	32	OM	2.6663	1.66E+10		7.63%
5	338175982	PUV_19880	elongation factor Tu	43 kDa	31	29	CP	2.5438	4.10E+09		0.51%
6	338175975	PUV_19810	DNA-directed RNA polymerase subunit beta	141 kDa	101	93	CP	1.4125	2.24E+09		0.72%
7	338175974	PUV_19800	DNA-directed RNA polymerase subunit beta'	155 kDa	110	96	CP	1.2531	2.11E+09		1.45%
8	338174646	PUV_06520	elongation factor G	77 kDa	61	47	CP	1.2644	1.19E+09		1.29%
8	338174862	PUV_08680	hypothetical protein	48 kDa	29	27	OM	1.221	2.04E+09		1.39%
10	338174602	PUV_06080	heat shock protein 70	71 kDa	67	63	CP	0.94924	8.26E+08		0.30%
10	338174478	PUV_04840	ATP-dependent Clp protease ATP-binding subunit	96 kDa	69	64	CP	0.80371	1.08E+09		0.35%
12	338175969	PUV_19750	chaperone protein ClpB	98 kDa	80	70	CP	0.82328	6.43E+08		0.35%
12	338175954	PUV_19600	30S ribosomal protein S1	66 kDa	59	54	CP	0.74152	9.69E+08		0.34%
12	338174985	PUV_09910	hypothetical protein	89 kDa	46	38	OM	0.70988	9.95E+08	yes	1.02%
15	338175303	PUV_13090	heat shock protein 60	58 kDa	44	38	CP	0.76617	6.97E+08		0.74%
15	338176274	PUV_22800	DNA-directed RNA polymerase subunit alpha	42 kDa	29	29	CP	0.74156	7.40E+08		0.27%

17	338175232	PUV_12380	succinate-semialdehyde dehydrogenase	50 kDa	32	31	CP	0.85492	5.91E+08	0.65%
18	338174633	PUV_06390	hypothetical protein	70 kDa	37	37	CP	0.87498	4.75E+08	1.61%
19	338174858	PUV_08640	heat shock protein 60	56 kDa	40	39	CP	0.67737	4.63E+08	0.75%
20	338174111	PUV_01170	protein translocase subunit SecA	117 kDa	75	62	CP	0.66524	4.50E+08	1.17%
21	338174164	PUV_01700	aconitate hydratase	106 kDa	57	55	CP	0.51868	6.92E+08	0.63%
22	338176292	PUV_22980	50S ribosomal protein L2	31 kDa	20	22	UK	0.69512	4.05E+08	1.42%
22	338176325	PUV_23310	V-type ATP synthase subunit alpha	67 kDa	48	46	CP	0.65285	4.27E+08	0.84%
22	338176502	PUV_25080	chaperone protein htpG	72 kDa	57	47	CP	0.64065	4.32E+08	1.13%
25	338174244	PUV_02500	insulin-degrading enzyme	112 kDa	69	61	PP	0.52067	5.05E+08	1.02%
26	338174806	PUV_08120	hypothetical protein	134 kDa	97	86	CP	0.46594	6.27E+08	0.00%
26	338174472	PUV_04780	superoxide dismutase	23 kDa	16	9	UK	0.41933	1.60E+09	0.98%
28	338174370	PUV_03760	transcription elongation factor greA	84 kDa	73	53	CP	0.60753	4.11E+08	0.69%
29	338174201	PUV_02070	heat shock protein 60	58 kDa	36	29	CP	0.51796	4.72E+08	0.71%
30	338175494	PUV_15000	hypothetical protein	86 kDa	61	51	CP	0.53015	4.38E+08	0.65%
31	338175681	PUV_16870	protein DR_1082	25 kDa	21	22	CP	0.60415	3.75E+08	0.47%
32	338174732	PUV_07380	hypothetical protein	87 kDa	55	51	CP	0.63432	3.51E+08	0.80%
33	338175470	PUV_14760	DNA gyrase subunit A	98 kDa	59	57	CP	0.57724	3.59E+08	0.92%
34	338175674	PUV_16800	hypothetical protein	116 kDa	78	65	CP	0.44054	4.67E+08	0.60%
35	338175800	PUV_18060	hypothetical protein	35 kDa	15	21	EC	0.60708	3.09E+08	0.00%
36	338175763	PUV_17690	hypothetical protein	25 kDa	13	16	UK	0.344	2.73E+09	0.00%
37	338174094	PUV_01000	hypothetical protein	22 kDa	19	13	UK	0.41966	4.44E+08	0.51%
37	338175033	PUV_10390	hypothetical protein	76 kDa	43	39	CP	0.41003	5.10E+08	1.35%
37	338174758	PUV_07640	fatty acid oxidation complex subunit alpha	80 kDa	53	43	CP	0.40816	5.68E+08	0.98%
40	338174907	PUV_09130	polyribonucleotide nucleotidyltransferase	76 kDa	41	36	CP	0.39767	5.97E+08	1.29%
41	338174424	PUV_04300	elongation factor Ts	31 kDa	26	25	CP	0.42336	4.33E+08	1.08%
42	338175951	PUV_19570	translation initiation factor IF-2	100 kDa	73	55	CP	0.53873	2.96E+08	0.77%

Outer membrane proteins of environmental chlamydiae

43	338174423	PUV_04290	30S ribosomal protein S2	30 kDa	24	24	CP	0.45542	3.68E+08		1.49%
44	338174508	PUV_05140	type III secretion translocator protein CopB	91 kDa	37	31	IM	0.41855	4.26E+08		0.00%
45	338174270	PUV_02760	aminopeptidase N	100 kDa	55	52	CP	0.54754	2.72E+08		1.59%
46	338174599	PUV_06050	NAD-specific glutamate dehydrogenase	119 kDa	76	66	CP	0.44944	3.20E+08		1.54%
47	338176364	PUV_23700	ATP-dependent zinc metalloprotease FtsH	103 kDa	70	57	IM	0.42083	3.12E+08		0.44%
48	338176289	PUV_22950	30S ribosomal protein S3	24 kDa	23	22	CP	0.55537	2.45E+08		1.39%
49	338174320	PUV_03260	hypothetical protein	169 kDa	81	52	IM	0.50923	2.68E+08		0.20%
50	338175384	PUV_13900	hypothetical protein	25 kDa	14	12	CP	0.38323	4.36E+08		0.00%

*Simkania negevensis*

Mean rank	gi identifier	Locus tag	Protein description	Molecular mass	Unique peptides 1	Unique peptides 2	Predicted location	NSAF 1	NSAF 2	Signal peptide	% cysteine
1	338734237	SNE_A23420	MOMP-like family protein	43 kDa	34	30	OM	1.4973	2.8596	yes	0.53%
1	338734236	SNE_A23410	MOMP-like family protein	43 kDa	23	26	OM	1.3095	3.5148	yes	0.52%
3	338732175_new		new sequence MOMP-like protein	39 kDa	19	17	OM	2.9113	1.8017	yes	0.00%
4	338733966	SNE_A20710	MOMP-like family protein	41 kDa	24	25	OM	1.1055	2.7256		0.00%
5	338733707	SNE_A18120	MOMP-like family protein	44 kDa	18	16	OM	0.75772	1.7014	yes	0.78%
6	338732639	SNE_A07440	MOMP-like family protein	45 kDa	23	13	OM	0.89003	0.80868		1.01%
7	338732173	SNE_A02780	MOMP-like family protein	45 kDa	27	13	OM	1.1607	0.53544	yes	0.26%
8	338732147	SNE_A02520	hypothetical protein	36 kDa	19	8	OM	0.98056	0.63105	yes	0.00%
9	338732638	SNE_A07430	MOMP-like family protein	42 kDa	25	14	OM	0.70691	0.82724	yes	0.80%
10	338732016	SNE_A01200	hypothetical protein	15 kDa	13	8	LP	0.71377	0.71952		0.68%
10	338732404	SNE_A04510	MOMP-like family protein	47 kDa	29	21	OM	0.74791	0.63607	yes	0.48%
12	338732181	SNE_A02860	MOMP-like family protein	43 kDa	18	14	OM	0.66026	0.49471	yes	0.54%
13	338733381	SNE_A14860	MOMP-like family protein	40 kDa	20	14	OM	0.90199	0.37678	yes	0.28%
14	338732171	SNE_A02760	MOMP-like family protein	43 kDa	25	18	OM	0.5782	0.45252	yes	0.82%
15	338732896	SNE_A10010	MOMP-like family protein	41 kDa	19	15	OM	0.61933	0.43396	yes	0.28%

16	338733107	SNE_A12120	hypothetical protein	42 kDa	21	19	LP	0.70987	0.37406	yes	1.07%
17	338732773_new		new sequence MOMP-like protein	39 kDa	13	10	OM	0.39883	0.46473		0.29%
18	338732690	SNE_A07950	MOMP-like family protein	41 kDa	13	13	OM	0.47254	0.37885	yes	0.56%
18	338733489	SNE_A15940	MOMP-like family protein	43 kDa	18	17	OM LP	0.44548	0.40995	yes	0.80%
20	338733016	SNE_A11120	MOMP-like family protein	38 kDa	16	14	OM	0.40627	0.43031	yes	0.61%
21	338732745	SNE_A08500	MOMP-like family protein	44 kDa	19	17	OM	0.32873	0.4423	yes	0.51%
22	338732182	SNE_A02870	MOMP-like family protein	42 kDa	18	11	OM	0.43043	0.37601	yes	0.00%
22	338732712	SNE_A08170	putative outer membrane protein Omp85	91 kDa	59	47	OM	0.37701	0.41541	yes	0.00%
24	338732906	SNE_A10110	hypothetical protein	9 kDa	8	7	UK	0.29002	0.37876		1.30%
25	338732549	SNE_A06540	carbohydrate-selective porin, OprB family	50 kDa	26	14	OM	0.47497	0.19504	yes	0.23%
26	338732701	SNE_A08060	MOMP-like family protein	40 kDa	19	8	OM	0.35631	0.24883	yes	0.57%
27	338732121	SNE_A02260	MOMP-like family protein	37 kDa	21	11	OM	0.4279	0.22916	yes	0.00%
27	338732179	SNE_A02840	MOMP-like family protein	40 kDa	15	12	OM	0.31341	0.32727	yes	0.29%
29	338732101	SNE_A02060	MOMP-like family protein	41 kDa	14	11	OM	0.3185	0.24843	yes	0.27%
30	338732702	SNE_A08070	MOMP-like family protein	40 kDa	7	9	OM	0.22425	0.2694		0.57%
31	338732757	SNE_A08620	hypothetical protein	40 kDa	22	10	OM	0.43337	0.16034	yes	0.86%
31	338733906	SNE_A20110	hypothetical protein	194 kDa	57	98	OM	0.12706	0.76324	yes	0.17%
33	338733380	SNE_A14850	MOMP-like family protein	42 kDa	13	10	OM	0.24543	0.2324		1.09%
34	338732777	SNE_A08820	MOMP-like family protein	46 kDa	16	16	OM	0.21172	0.24615	yes	0.25%
35	338731935	SNE_A00390	hypothetical protein	47 kDa	26	15	OM	0.30714	0.16733	yes	0.00%
35	338733988	SNE_A20930	hypothetical protein	66 kDa	30	22	OM	0.22937	0.20347		0.69%
37	338732099	SNE_A02040	hypothetical protein	46 kDa	18	14	OM	0.2319	0.18002		0.47%
38	338734235	SNE_A23400	MOMP-like family protein	46 kDa	13	11	OM LP	0.26295	0.16584	yes	0.24%
39	338731937	SNE_A00410	major outer membrane protein	29 kDa	15	9	OM	0.41681	0.11969	yes	0.39%
40	338734234	SNE_A23390	MOMP-like family protein	42 kDa	15	10	OM	0.25424	0.14945	yes	0.27%
41	338731979	SNE_A00830	hypothetical protein	43 kDa	17	10	OM	0.20639	0.1671	yes	1.08%
42	338732533	SNE_A06380	hypothetical protein	41 kDa	11	8	OM	0.18958	0.17843	yes	0.82%
43	338732172	SNE_A02770	MOMP-like family protein	39 kDa	14	12	OM LP	0.21604	0.15719	yes	0.87%
44	338733018	SNE_A11230	multidrug resistance protein mdtA	42 kDa	16	14	LP	0.18999	0.16491		0.54%

## Outer membrane proteins of environmental chlamydiae

45	338732214	SNE_A03190	hypothetical protein	13 kDa	8	5	LP	0.15712	0.17779	yes	0.89%
46	338733019	SNE_A11240	putative outer membrane factor (OMF) family efflux porin	55 kDa	18	17	OM LP	0.20523	0.14787		0.41%
47	338732778	SNE_A08830	MOMP-like family protein	44 kDa	16	19	OM	0.10753	0.24179	yes	0.00%
48	338732557	SNE_A06620	hypothetical protein	43 kDa	18	10	IM	0.2206	0.10563		0.77%
48	338732791	SNE_A08960	hypothetical protein	82 kDa	29	22	OM	0.19331	0.13587	yes	0.00%
50	338732238	SNE_A03430	hypothetical protein	65 kDa	23	17	OM	0.13454	0.15557	yes	0.53%

*Waddlia chondrophila*

Mean rank	gi identifier	Locus tag	Protein description	Molecular mass	Unique peptides 1	Unique peptides 2	Predicted location	NSAF 1	TIC 2	Signal peptide	% cysteine
1	337293922	WCH_DD19230	MOMP-like family protein	34 kDa	18	19	OM	4.1664	4.55E+10	yes	5.32%
2	297620822	wcw_0584	Elongation factor Tu	43 kDa	36	32	CP	2.1201	1.16E+10		0.76%
3	297620310	wcw_0065	MOMP-like family protein	39 kDa	7	7	OM	1.0305	1.39E+10	yes	4.21%
4	337292862	WCH_CT17270	MOMP-like family protein	40 kDa	12	13	OM	1.8106	1.03E+10	yes	4.11%
5	297620516	wcw_0272	hypothetical protein	22 kDa	16	13	UK	1.2396	6.99E+09	yes	6.91%
5	337293174	WCH_BT10880	putative uncharacterized protein	34 kDa	38	28	PP	1.2628	2.49E+09		0.34%
7	337292861	WCH_CT17260	MOMP-like family protein	39 kDa	7	13	OM	0.95695	1.07E+10	yes	4.71%
8	297621388	wcw_1162	putative 60 kDa cysteine-rich outer membrane protein OmcB	56 kDa	27	23	OM	0.78649	1.17E+10	yes	9.42%
9	297620550	wcw_0306	Elongation factor G	77 kDa	45	54	CP	0.9482	1.32E+09		0.86%
10	297620829	wcw_0592	DNA-directed RNA polymerase beta chain	142 kDa	108	93	CP	0.83536	1.01E+09		0.80%
11	297621699	wcw_1481	DNA-directed RNA polymerase, alpha subunit	42 kDa	32	32	CP	0.70881	1.25E+09		0.27%
12	337293684	WCH_BX11920	MOMP-like family protein	37 kDa	10	17	OM	0.6279	1.58E+09		3.89%
13	297621787	wcw_1570	30S ribosomal protein S4	24 kDa	18	19	CP	0.7984	7.43E+08		0.97%
14	297621717	wcw_1499	50S ribosomal protein L2	32 kDa	23	23	UK	0.79696	7.38E+08		1.78%
15	297621615	wcw_1396	60 kDa chaperonin	56 kDa	42	35	CP	0.705	8.38E+08		0.94%

16	297622138	wcw_1934	Elongation factor Ts	31 kDa	20	21	CP	0.61414	1.20E+09		0.72%
17	297621564	wcw_1343	Chaperonin GroEL	58 kDa	33	39	CP	0.61797	1.15E+09		0.55%
17	297620830	wcw_0593	DNA-directed RNA polymerase beta' chain	155 kDa	99	88	CP	0.6275	9.70E+08		1.44%
19	337293209	WCH_BT11230	putative long-chain fatty acid transport protein	51 kDa	26	18	OM	0.55795	1.03E+09	yes	1.51%
20	337293040	WCH_CL15100	putative ATP-dependent Clp protease ATP-binding subunit	98 kDa	60	64	CP	0.6246	7.35E+08		0.57%
21	297622057	wcw_1849	Chaperonin GroEL	58 kDa	31	30	CP	0.53832	9.12E+08		0.72%
21	297621861	wcw_1647	Transcription termination factor rho	51 kDa	31	27	CP	0.54518	7.67E+08		0.00%
23	297621437	wcw_1211	UPF0365 protein yqfA	37 kDa	20	21	IM	0.5553	7.16E+08		0.29%
24	297620371	wcw_0127	S-adenosylmethionine synthetase	43 kDa	30	27	CP	0.55227	6.81E+08		1.53%
25	297620842	wcw_0605	V-type ATP synthase, subunit A	66 kDa	48	46	CP	0.69655	4.63E+08		0.84%
26	297621697	wcw_1479	glyceraldehyde-3-P dehydrogenase	37 kDa	22	19	CP	0.52104	6.65E+08		1.76%
26	297621201	wcw_0972	Leucyl aminopeptidase	53 kDa	37	32	CP	0.63382	4.29E+08		0.41%
28	337294077	WCH_AW05930	trigger factor	50 kDa	43	33	CP	0.5185	6.22E+08		0.68%
29	297620460	wcw_0216	Na(+)-translocating NADH-quinone reductase subunit F	49 kDa	32	23	CP	0.55438	4.49E+08		2.33%
29	337294064	WCH_AW05800	putative uncharacterized protein	118 kDa	56	60	CP	0.49697	5.40E+08		1.26%
31	297621719	wcw_1501	50S ribosomal protein L4	26 kDa	26	19	CP	0.51608	5.18E+08		0.44%
32	297620826	wcw_0589	50S ribosomal protein L1	25 kDa	18	15	CP	0.44021	6.46E+08		0.00%
33	297621714	wcw_1496	30S ribosomal protein S3	24 kDa	24	19	CP	0.74179	3.37E+08		0.00%
34	297622137	wcw_1933	30S ribosomal protein S2	32 kDa	26	25	CP	0.50241	5.15E+08		1.72%
35	337293667	WCH_BQ10230	putative uncharacterized protein	39 kDa	18	22	UK	0.38016	1.20E+09		1.72%
36	297621095	wcw_0860	30S ribosomal protein S1	64 kDa	54	50	CP	0.67906	3.12E+08		0.18%
37	297620833	wcw_0596	Transaldolase	35 kDa	18	18	CP	0.42335	4.72E+08		1.27%
38	297621813	wcw_1599	ATP-dependent Clp protease ATP-binding subunit clpX	46 kDa	33	27	CP	0.41427	4.92E+08		1.45%

Outer membrane proteins of environmental chlamydiae

38	297622180	wcw_1978	bacterial DNA recombination protein recA	38 kDa	25	25	CP	0.39627	5.69E+08		0.57%
40	297621818	wcw_1604	putative type III secretion chaperone SycD/LcrH	22 kDa	18	16	CP	0.52786	3.68E+08		1.49%
41	297620921	wcw_0685	putative cell division protein FtsH	103 kDa	52	62	IM	0.47364	4.10E+08		0.43%
42	297621708	wcw_1490	50S ribosomal protein L5	21 kDa	17	16	CP	0.6206	2.96E+08		2.16%
43	297621674	wcw_1456	hypothetical protein	30 kDa	21	20	CP	0.38443	5.26E+08		1.94%
44	297621809	wcw_1594	actin-like ATPase involved in cell morphogenesis	39 kDa	22	21	CP	0.47038	3.59E+08		1.10%
45	297621326	wcw_1100	hypothetical protein	21 kDa	12	14	OM	0.53967	2.93E+08		0.00%
46	297622124	wcw_1918	putative Na(+)-translocating NADH-quinone reductase subunit A	52 kDa	30	21	CP	0.52585	3.05E+08		0.43%
47	297621706	wcw_1488	50S ribosomal protein L6	20 kDa	18	12	CP	0.40376	3.92E+08		0.00%
48	297620304	wcw_0059	MOMP-like family protein	42 kDa	12	13	OM	0.37572	4.23E+08	yes	4.81%
48	297622069	wcw_1862	Enolase	47 kDa	16	14	CP	0.40629	3.67E+08		1.16%
50	297621759	wcw_1541	hypothetical protein	37 kDa	28	23	LP	0.33929	5.76E+08		1.23%



**Table S8: Enrichment of the 50 most abundant proteins (based on quantification by NSAF) of *Parachlamydia*, *Simkania* and *Waddlia* in the presence of reducing agent compared to the absence of reducing agent**

Proteins are shown for each organism sorted by their predicted subcellular location. The fold enrichment was calculated by dividing the respective percent spectral counts determined by mass spectroscopy. n.d., not detected in fractions without DTT in the loading buffer

***Parachlamydia acanthamoebae***

	gi identifier	Protein description	NSAF	% cysteine	Enrichment DTT vs no DTT
<b>Cytoplasmic</b>					
	338176301	(3R)-hydroxymyristoyl-ACP dehydratase	0.487	0.00	1.85
	338175617	hypothetical protein PUV_16230	0.883	0.15	1.64
	338176741	hypothetical protein PUV_27470	0.488	1.44	1.56
	338175982	elongation factor Tu	2.544	0.51	1.37
	338174646	elongation factor G	1.264	1.29	1.29
	338175975	DNA-directed RNA polymerase subunit beta	1.413	0.72	1.20
	338174270	aminopeptidase N	0.548	1.59	1.09
	338174164	aconitate hydratase	0.519	0.63	1.08
	338175974	DNA-directed RNA polymerase subunit beta'	1.253	1.45	1.02
	338174478	ATP-dependent Clp protease ATP-binding subunit	0.804	0.35	1.00
	338174111	protein translocase subunit SecA	0.665	1.17	1.00
	338175645	hypothetical protein PUV_16510	0.813	1.79	0.97
	338174602	heat shock protein 70	0.949	0.30	0.92
	338175470	DNA gyrase subunit A	0.577	0.92	0.88
	338175969	chaperone protein ClpB	0.823	0.35	0.87
	338174370	transcription elongation factor greA	0.608	0.69	0.84
	338174732	hypothetical protein PUV_07380	0.634	0.80	0.83
	338175951	translation initiation factor IF-2	0.539	0.77	0.83
	338175494	hypothetical protein PUV_15000	0.530	0.65	0.78
	338175232	succinate-semialdehyde dehydrogenase	0.855	0.65	0.74
	338176502	chaperone protein htpG	0.641	1.13	0.73
	338175303	heat shock protein 60	0.766	0.74	0.70
	338174633	protein Mb0897	0.875	1.61	0.67
	338176274	DNA-directed RNA polymerase subunit alpha	0.742	0.27	0.67
	338174201	heat shock protein 60	0.518	0.71	0.67
	338175954	30S ribosomal protein S1	0.742	0.34	0.63
	338174806	hypothetical protein PUV_08120	0.466	0.00	0.59
	338176289	30S ribosomal protein S3	0.555	1.39	0.58
	338174858	heat shock protein 60	0.677	0.75	0.57
	338175281	hypothetical protein PUV_12870	0.497	5.88	0.57
	338174838	hypothetical protein PUV_08440	0.477	1.44	0.55
	338176325	V-type ATP synthase subunit alpha	0.653	0.84	0.50

Outer membrane proteins of environmental chlamydiae

	338174663	transcription termination factor Rho	0.578	0.22	0.44
	338175681	protein DR_1082	0.604	0.47	0.31
<b>Extracellular</b>					
	338175800	hypothetical protein PUV_18060	0.607	0.00	0.17
<b>Inner membrane</b>					
	338174320	hypothetical protein PUV_03260	0.509	0.20	0.88
	338175368	protein LemA	1.077	0.00	0.63
<b>Periplasmic</b>					
	338175901	protein disulfide isomerase	0.519	1.74	1.20
	338174244	insulin-degrading enzyme	0.521	1.02	0.85
<b>Outer membrane</b>					
	338175011	OmcB	2.666	7.63	126.67
	338174749	hypothetical protein PUV_07550	4.981	3.23	10.57
	338176744	hypothetical protein PUV_27500	6.446	3.36	4.00
	338175826	hypothetical protein PUV_18320	0.578	1.95	3.13
	338174862	hypothetical protein PUV_08680	1.221	1.39	2.23
	338174985	hypothetical protein PUV_09910	0.710	1.02	1.43
<b>Unknown</b>					
	338175110	hypothetical protein PUV_11160	6.081	10.50	73.44
	338175566	hypothetical protein PUV_15720	1.437	2.39	6.99
	338174268	hypothetical protein PUV_02740	0.531	1.70	3.05
	338175854	50S ribosomal protein L28	0.865	1.06	0.80
	338176292	50S ribosomal protein L2	0.695	1.42	0.66

*Simkania negevensis*

	gi identifier	Protein description	NSAF	% cysteine	Enrichment DTT vs no DTT
<b>Cytoplasmic</b>					
	338732821	hypothetical protein SNE_A09260	0.458	4.21	12.14
	338732655	50S ribosomal protein L19	0.212	0.57	10.71
	338734017	30S ribosomal protein S3	0.236	0.96	4.32
<b>Lipoprotein</b>					
	338733018	multidrug resistance protein mdtA	0.165	0.54	1.03
	338732214	hypothetical protein SNE_A03190	0.178	0.89	0.95
	338732016	hypothetical protein SNE_A01200	0.720	0.68	0.86
	338733107	hypothetical protein SNE_A12120	0.374	1.07	0.54
<b>Outer membrane</b>					
	338733906	hypothetical protein SNE_A20110	0.763	0.17	5.39
	338734236	MOMP-like family protein	3.515	0.52	2.83
	338733966	MOMP-like family protein	2.726	0.00	2.58
	338732778	MOMP-like family protein	0.242	0.00	2.56
	338734232	MOMP-like family protein	0.179	0.56	2.27
	338733707	MOMP-like family protein	1.701	0.78	1.92
	338734237	MOMP-like family protein	2.860	0.53	1.77
	338732745	MOMP-like family protein	0.442	0.51	1.36

	338732777	MOMP-like family protein	0.246	0.25	1.23
	338732638	MOMP-like family protein	0.827	0.80	1.15
	338732773_new	new sequence MOMP-like protein	0.465	0.29	1.09
	338732238	hypothetical protein SNE_A03430	0.156	0.53	1.00
	338732179	MOMP-like family protein	0.327	0.29	0.99
	338732702	MOMP-like family protein	0.269	0.57	0.99
	338732404	MOMP-like family protein	0.636	0.48	0.96
	338732712	putative outer membrane protein Omp85	0.415	0.00	0.92
	338733016	MOMP-like family protein	0.430	0.61	0.92
	338733380	MOMP-like family protein	0.232	1.09	0.91
	338733988	hypothetical protein SNE_A20930	0.203	0.69	0.89
	338732639	MOMP-like family protein	0.809	1.01	0.89
	338732182	MOMP-like family protein	0.376	0.00	0.86
	338732690	MOMP-like family protein	0.379	0.56	0.81
	338733489	MOMP-like family protein	0.410	0.80	0.81
	338732171	MOMP-like family protein	0.453	0.82	0.78
	338731979	hypothetical protein SNE_A00830	0.167	1.08	0.74
	338732533	hypothetical protein SNE_A06380	0.178	0.82	0.73
	338732101	MOMP-like family protein	0.248	0.27	0.73
	338732099	hypothetical protein SNE_A02040	0.180	0.47	0.71
	338732896	MOMP-like family protein	0.434	0.28	0.70
	338732181	MOMP-like family protein	0.495	0.54	0.68
	338732175_new	new sequence MOMP-like protein	1.802	0.00	0.63
	338732701	MOMP-like family protein	0.249	0.57	0.62
	338734235	MOMP-like family protein	0.166	0.24	0.59
	338732172	MOMP-like family protein	0.157	0.87	0.57
	338732147	hypothetical protein SNE_A02520	0.631	0.00	0.56
	338731935	hypothetical protein SNE_A00390	0.167	0.00	0.54
	338732121	MOMP-like family protein	0.229	0.00	0.46
	338733381	MOMP-like family protein	0.377	0.28	0.42
	338732549	carbohydrate-selective porin, OprB family	0.195	0.23	0.42
	338732173	MOMP-like family protein	0.535	0.26	0.41
	338732757	hypothetical protein SNE_A08620	0.160	0.86	0.33
<b>Unknown</b>					
	338732146	hypothetical protein SNE_A02510	0.372	1.21	12.46
	338732906	hypothetical protein SNE_A10110	0.379	1.30	0.67

***Waddlia chondrophila***

	gi identifier	Protein description	NSAF	% cysteine	Enrichment DTT vs no DTT
<b>Cytoplasmic</b>					
	297620822	Elongation factor Tu	2.120	0.76	1.47
	297621495	Fatty acid oxidation complex, alpha subunit FadB	0.530	0.98	1.31
	337293040	putative ATP-dependent Clp protease ATP-binding subunit	0.625	0.57	1.30

Outer membrane proteins of environmental chlamydiae

	337294064	putative uncharacterized protein	0.497	1.26	1.24
	297620460	Na(+)-translocating NADH-quinone reductase subunit F	0.554	2.33	1.22
	297620830	DNA-directed RNA polymerase beta' chain	0.628	1.44	1.18
	297620829	DNA-directed RNA polymerase beta chain	0.835	0.80	1.15
	297621492	acyl-Coenzyme A dehydrogenase family protein	0.449	1.42	1.08
	297621615	60 kDa chaperonin	0.705	0.94	0.95
	297621697	glyceraldehyde-3-P dehydrogenase	0.521	1.76	0.87
	297621809	actin-like ATPase involved in cell morphogenesis	0.470	1.10	0.87
	297622124	putative Na(+)-translocating NADH-quinone reductase subunit A	0.526	0.43	0.87
	297620550	Elongation factor G	0.948	0.86	0.86
	337294077	trigger factor	0.519	0.68	0.86
	297621787	30S ribosomal protein S4	0.798	0.97	0.83
	297621263	hypothetical protein wcw_1035	0.480	1.10	0.81
	297621201	Leucyl aminopeptidase	0.634	0.41	0.81
	297620842	V-type ATP synthase, subunit A	0.697	0.84	0.80
	297621818	putative type III secretion chaperone SycD/LcrH	0.528	1.49	0.80
	297620371	S-adenosylmethionine synthetase	0.552	1.53	0.75
	297622057	Chaperonin GroEL	0.538	0.72	0.75
	297621050	50S ribosomal protein L25	0.438	1.61	0.74
	297621719	50S ribosomal protein L4	0.516	0.44	0.74
	297622137	30S ribosomal protein S2	0.502	1.72	0.73
	297621802	hypothetical protein wcw_1585	0.748	1.87	0.70
	297621714	30S ribosomal protein S3	0.742	0.00	0.70
	297621699	DNA-directed RNA polymerase, alpha subunit	0.709	0.27	0.65
	297621708	50S ribosomal protein L5	0.621	2.16	0.63
	297621564	Chaperonin GroEL	0.618	0.55	0.63
	297620833	Transaldolase	0.423	1.27	0.63
	297621861	Transcription termination factor rho	0.545	0.00	0.59
	297620549	30S ribosomal protein S10	0.441	0.93	0.52
	297620826	50S ribosomal protein L1	0.440	0.00	0.49
	297621095	30S ribosomal protein S1	0.679	0.18	0.49
	297622138	Elongation factor Ts	0.614	0.72	0.49
<b>Inner membrane</b>					
	297620921	putative cell division protein FtsH	0.474	0.43	0.86
	297621437	UPF0365 protein yqfA	0.555	0.29	0.63
<b>Periplasmic</b>					
	337293174	putative uncharacterized protein	1.263	0.34	0.61
<b>Outer membrane</b>					
	337292861	MOMP-like family protein	0.957	4.71	n.d.
	297621388	putative 60 kDa cysteine-rich outer membrane protein	0.786	9.40	n.d.
	337293684	MOMP-like family protein	0.628	3.89	n.d.

---

	337293209	putative long-chain fatty acid transport protein	0.558	1.51	n.d.
	337292862	MOMP-like family protein	1.811	4.11	211.76
	337293922	MOMP-like family protein	4.166	5.32	146.00
	297620310	hypothetical protein wcw_0065	1.031	4.21	57.58
	297621326	hypothetical protein wcw_1100	0.540	0.00	2.04
<b>Unknown</b>					
	297620516	hypothetical protein wcw_0272	1.240	6.91	n.d.
	297620388	hypothetical protein wcw_0144	0.530	0.81	1.56
	297621717	50S ribosomal protein L2	0.797	1.78	1.00
	297621700	30S ribosomal protein S11	0.978	0.75	0.86



# **Chapter VI**

**Identification and characterization  
of a novel porin family highlights a  
major difference in the outer  
membrane of chlamydial symbionts  
and pathogens**

PLoS One 2013;8(1):e55010

## **Identification and characterization of a novel porin family highlights a major difference in the outer membrane of chlamydial symbionts and pathogens**

Karin Aistleitner<sup>1</sup>, Christian Heinz<sup>1</sup>, Alexandra Hörmann<sup>1</sup>, Eva Heinz<sup>1</sup>, Jacqueline Montanaro<sup>1</sup>, Frederik Schulz<sup>1</sup>, Elke Maier<sup>2</sup>, Peter Pichler<sup>3</sup>, Roland Benz<sup>2,4</sup>, Matthias Horn<sup>1\*</sup>

<sup>1</sup>Department of Microbial Ecology, University of Vienna, Vienna, Austria

<sup>2</sup>Rudolf-Virchow-Center, Deutsche Forschungsgemeinschaft - Research Center for Experimental Biomedicine, University of Würzburg, Würzburg, Germany

<sup>3</sup>Christian Doppler Laboratory for Mass Spectrometry, Vienna, Austria

<sup>4</sup>School of Engineering and Science, Jacobs University Bremen, Bremen, Germany

\* E-mail: [horn@microbial-ecology.net](mailto:horn@microbial-ecology.net)



**Abstract**

The *Chlamydiae* constitute an evolutionary well separated group of intracellular bacteria comprising important pathogens of humans as well as symbionts of protozoa. The amoeba symbiont *Protochlamydia amoebophila* lacks a homologue of the most abundant outer membrane protein of the *Chlamydiaceae*, the major outer membrane protein MOMP, highlighting a major difference between environmental chlamydiae and their pathogenic counterparts. We recently identified a novel family of putative porins encoded in the genome of *P. amoebophila* by *in silico* analysis. Two of these *Protochlamydia* outer membrane proteins, PomS (pc1489) and PomT (pc1077), are highly abundant in outer membrane preparations of this organism. Here we show that all four members of this putative porin family are toxic when expressed in the heterologous host *Escherichia coli*. Immunofluorescence analysis using antibodies against heterologously expressed PomT and PomS purified directly from elementary bodies, respectively, demonstrated the location of both proteins in the outer membrane of *P. amoebophila*. The location of the most abundant protein PomS was further confirmed by immuno-transmission electron microscopy. We could show that *pomS* is transcribed, and the corresponding protein is present in the outer membrane throughout the complete developmental cycle, suggesting an essential role for *P. amoebophila*. Lipid bilayer measurements demonstrated that PomS functions as a porin with anion-selectivity and a pore size similar to the *Chlamydiaceae* MOMP. Taken together, our results suggest that PomS, possibly in concert with PomT and other members of this porin family, is the functional equivalent of MOMP in *P. amoebophila*. This work contributes to our understanding of the adaptations of symbiotic and pathogenic chlamydiae to their different eukaryotic hosts.

## Introduction

Chlamydiae are a group of obligate intracellular bacteria with an extraordinarily broad host spectrum. They include important human pathogens like *Chlamydia* (aka *Chlamydomphila*) *pneumoniae* and *Chlamydia trachomatis* as well as many animal pathogens and symbionts of amoebae [2-5]. All chlamydiae share a biphasic developmental cycle in which they alternate between two developmental forms, the extremely stable and infectious elementary body (EB) and the replicative reticulate body (RB) [6]. At the beginning of the developmental cycle, EBs attach to and are taken up by the host cell. Upon entry, chlamydiae reside within a host-derived vacuole [7] where the EBs differentiate into RBs. After several rounds of replication, RBs re-differentiate into EBs and leave the host cell by either lysis of the host or exocytosis in order to infect new host cells [3,8].

During all stages of the chlamydial developmental cycle, proteins in the bacterial outer membrane play an important role. They mediate the first contact to the host cell, and once inside the host, they are involved in the uptake of nutrients and the removal of waste products. Being surface-exposed, outer membrane proteins represent promising candidates for vaccine development [9,10] and have therefore been thoroughly studied for the pathogenic chlamydiae, which have been grouped into the family *Chlamydiaceae* [11-17]. The major outer membrane protein (MOMP) and the two cysteine-rich proteins OmcA and OmcB are the most abundant proteins in the outer membrane of the *Chlamydiaceae* and together form the chlamydial outer membrane complex (COMC) [18,19]. Chlamydiae lack detectable amounts of peptidoglycan [20]. Instead, the COMC and OmcA and OmcB in particular stabilize the outer membrane by forming extensive disulfide-bonds in the osmotically stable EBs whereas these bonds are reduced in the more fragile RBs [14,21-23].

MOMP is the most abundant protein in the outer membrane of the *Chlamydiaceae* and makes up about 60% of the proteins of the COMC in EBs [19]. MOMP determines *C. trachomatis* serovars [24] and functions as a diffusion porin, a group of proteins that form channels in the outer membrane of Gram-negative bacteria, facilitating passive diffusion of small molecules [25-27]. The porin function of MOMP was first suggested by Bavoil and coworkers based on liposome swelling assays [28] and later confirmed by lipid bilayer measurements using purified native and recombinant MOMP [29,30]. MOMP shows a beta-barrel structure with a pore size of 2 nm [31] and occurs as trimer in the outer membrane [32].

In contrast to the *Chlamydiaceae*, little is known about the composition of the outer membrane of other chlamydiae. Several key mechanisms for host cell interaction, such as a type three secretion system and its effector proteins, are conserved among all chlamydiae [33-35]. Yet, the genome of the

amoeba symbiont *Protochlamydia amoebophila* encodes no homologue of MOMP [34], and antibodies targeting *Chlamydiaceae* MOMP did not bind to the outer membrane of these bacteria [36]. A recent study identified 38 outer membrane proteins of *P. amoebophila* by combining 1D and 2D gel electrophoresis of outer membrane fractions with mass spectrometry analysis [37]. The identified proteins included OmcA (pc0617) and OmcB (pc0616). Additionally, a novel protein family was identified consisting of four proteins that share an amino acid sequence identity of 22-28 % and have no functionally characterized homologues in other organisms (Table 1). Two of these proteins were frequently detected in outer membrane fractions. Both were predicted to form beta-barrels by *in silico* analysis and to contain signal peptides. Their predicted structure and their high abundance in outer membrane fractions led to the hypothesis that they function as porins and together form the COMC of *P. amoebophila* by interactions with OmcA and OmcB. Because of the lack of significant sequence similarities with other characterized proteins we propose the names PomS, PomT, PomU, and PomV (Pom for “*Protochlamydia* outer membrane protein”) for their designation.

In this study, we provide evidence that all members of the novel protein family found in *P. amoebophila* represent pore-forming proteins, and for two of them we confirmed their outer membrane location. The most abundant outer membrane protein of this family is expressed throughout the complete developmental cycle of *P. amoebophila*, and lipid bilayer measurements further confirmed its function as porin. Our study provides a first detailed analysis of outer membrane proteins of an environmental counterpart of pathogenic chlamydiae and shows that a novel porin family represents the functional equivalent of the *Chlamydiaceae* MOMP in *P. amoebophila*.

## Materials and Methods

### Cultivation of organisms and infection experiments

Uninfected *Acanthamoeba castellanii* Neff or *A. castellanii* Neff infected with *P. amoebophila* were grown axenically in 10 or 150 ml TSY medium (30 g/L trypticase soy broth, 10 g/L yeast extract, pH 7.3) at 20°C. Cultures were supplied with fresh medium every one to two weeks depending on amoebal growth. *Escherichia coli* strains were grown in standard LB medium at 37°C.

For infection experiments cultures of *A. castellanii* Neff were harvested and the number of amoebae was counted using a Neubauer counting chamber. Amoebae were seeded in the wells of a multiwell dish and were infected with purified *P. amoebophila* EBs at an MOI of 5 or 10. Multiwell dishes were centrifuged at 600 x g for 15 min at 20°C, and the end of centrifugation was regarded as time point 0

	PomS	PomT	PomU	PomV
<b>Locus tag</b>	pc1489	pc1077	pc0870	pc1860
<b>Molecular mass in kDa</b>	36.3	39.0	34.4	37.5
<b>Signal peptide</b>	yes	yes	yes	yes
<b>Prediction of alpha-helix formation</b>	no	no	no	no
<b>Localization to outer membrane</b>	yes	yes	unknown	yes
<b>Prediction of beta-barrel formation</b>	yes	yes	no	yes
<b>Predicted lipoprotein</b>	no	no	no	yes
<b>Probability to be an OMP</b>	97.72 %	100 %	97.68 %	97.22 %
<b>pCOMP prediction</b>	integral outer membrane protein (cluster 081)	integral outer membrane protein (cluster 081)	ambiguous prediction	lipoprotein (cluster 081)
<b>Best blastp hit except for members of porin family</b>	hypothetical protein of <i>Methylophaga</i> sp. JAM7 e-value 2e-07 19.9% identity	hypothetical protein of <i>Methylomicrobium alcaliphilum</i> e-value 3e-19 17.1 % identity	hypothetical protein of <i>Methylophaga</i> sp. JAM7 e-value 8e-04 19.1% identity	EGF-like domain-containing protein of <i>Dictyostelium discoideum</i> e-value 0.15 8.9 % identity
<b>Presence in outer membrane protein fractions [37]</b>	yes	yes	no	yes
<b>Experimental evidence for outer membrane location in this study</b>	yes	yes	no	no

**Table 1: Members of the putative porin family of *P. amoebophila* are predicted to be localized to the outer membrane by *in silico* analysis.** Signal peptides were predicted using SignalP4 [38], alpha-helix formation was predicted with TMHMM, localization to the outer membrane with Cpsortdb [39], beta-barrel formation with MCMBB, BOMP and Pred-TMBB [40,41], lipoprotein signal peptides with LipoP [42], the probability of the localization to the outer membrane using HHOMP [43] and chlamydial outer membrane proteins with pCOMP [44].

hours post infection (p.i.). After centrifugation, the medium was exchanged and infected cultures were grown at 20°C. At selected time points cells were fixed for immunofluorescence analysis.

### Purification of elementary bodies of *P. amoebophila* and isolation of Pc1489

*P. amoebophila* EBs for infection experiments were purified as previously described [37]. Highly enriched fractions of EBs were obtained using two additional centrifugation steps to further remove host cell debris [33]. Highly purified EBs were thawed and centrifuged at 10,621 x g for 15 min at 4°C. The resulting pellet was resuspended in 100 µl POP05-buffer (0.087 g/L EDTA, 5.84 g/L NaCl, 300 mM Na<sub>x</sub>PO<sub>4</sub>, 0.5% n-octyl-polyoxyethylen; pH 6.5) [45] with 100 mM freshly added dithiothreitol (DTT) per 3 mg EBs (wet weight) and incubated for 1 h at 37°C on a rocking platform. Cell debris was removed by centrifugation (10,621 x g, 10 min, 4°C), an equal volume of ice-cold acetone was added to the supernatant and proteins were precipitated for 1 h at -20°C. The suspension was centrifuged as before and the resulting pellet was resuspended in 400 µl Buffer A (2.9 g/L HEPES, pH 7.5, 0.292 g/L NaCl, 0.5% n-octyl-polyoxyethylen). Undissolved matter was removed by centrifugation at 10,621

x g for 10 min at 20°C. After equilibration of a Vivapure Q-Mini-spin column (Sartorius) with 400 µl Buffer A, the supernatant was applied onto the column and centrifuged at 2,000 x g for 5 min at 20°C. The column was washed twice with Buffer A. Elution of proteins was achieved by applying a gradient with increasing NaCl concentrations ranging from 0.1 to 1 M NaCl. The flow-through of all steps was collected. 4 x Laemmli buffer without DTT was added to the samples and samples were run on a 12.5% SDS-PAGE gel, followed by staining with colloidal Coomassie (100 g/L (NH<sub>4</sub>)<sub>2</sub>SO<sub>4</sub>, 20 g/L orthophosphoric acid, 25 % methanol, 0.625 g/L Coomassie Brilliant Blue G-250). Fractions that showed only a single band for Pc1489 at the correct size were collected and pooled. To concentrate samples, proteins were precipitated with ice-cold acetone and resuspended in Buffer A without n-octyl-polyoxyethylen (n-octyl-POE). Protein concentrations were determined using the BCA<sup>TM</sup> Protein Assay Kit (Pierce Biotechnology). The identity of the purified protein was confirmed by SDS-PAGE analysis in combination with mass spectrometry.

### **Mass spectrometry analysis**

Sample processing and high-performance liquid chromatography mass spectrometry (HPLC-MS) analysis were performed as described previously [37]. Briefly, bands were excised from the gel, reduced with DTT, alkylated with iodoacetamide and digested overnight with trypsin. Samples were separated on an Ultimate plus HPLC system (Dionex) coupled online to an LTQ mass spectrometer (Thermo Scientific). Raw files were searched with ProteomeDiscoverer 1.3.0.339 and Mascot 2.2 using the following settings: trypsin/P, maximum 2 missed cleavage sites, 1.5 Da precursor ion tolerance, 0.8 Da fragment ion tolerance, carbamidomethyl-cysteine as fixed modification, oxidation of methionine and deamidation of asparagine or glutamine as variable modifications. The fasta database comprised sequences from *P. amoebophila* as well as proteins of the amoeba host and contaminants. Proteins were quantified by calculating spectral counts and normalized spectral abundance factor (NSAF) for all *P. amoebophila* proteins identified with  $p < 0.05$  [46]. As the precision of spectral counting was shown to be optimal for proteins with five or more spectra, calculation of NSAF was restricted to proteins with a minimum of five spectra with a Mascot score of 20 or above [47]. NSAF values were converted to percentages as a measure of relative abundance.

### **Transcriptional analysis**

For the isolation of RNA, 3 ml of *A. castellanii* infected with *P. amoebophila* were harvested by centrifugation (7,323 x g, 10 min). The pellet was resuspended in 750 µl Trizol and cells were disrupted using a bead beater at an intensity of 4.5 for 30 sec. The cell suspension was then centrifuged at 12,000 x g for 5 min. The supernatant was incubated at room temperature for 5 min

followed by the addition of 200  $\mu$ l chloroform. The solution was shaken vigorously for 15 sec, further incubated for 5 min and finally centrifuged at 12,000 x g for 15 min at 4°C. The supernatant was taken off carefully, mixed with 500  $\mu$ l isopropyl alcohol per 750  $\mu$ l volume and incubated at room temperature for 10 min. After another centrifugation step (12,000 x g, 10 min, 4°C), the resulting RNA pellet was washed with 1 ml 75% ethanol and centrifuged for 5 min at 7,000 x g and 4°C. The pellet was air-dried for 10 min and dissolved in 30  $\mu$ l distilled water treated with diethylpyrocarbonate (DEPC). Isolated RNA was quantified using a NanoDrop® ND-1000 spectral photometer and either stored at -80°C or treated directly with DNaseI (Sigma-Aldrich). DNA was digested by adding 1 U DNaseI/2  $\mu$ g RNA and incubation at room temperature for 1 h. RNA was precipitated with pure ethanol at -20°C overnight and resolved in DEPC-treated distilled water. RNA quality was assessed by agarose gel electrophoresis. To test for DNA still present in the RNA preparations, PCR without reverse transcription was performed and no product was obtained (data not shown). Three independent biological replicates of RNA isolated at 0 h p.i., 24 h p.i., 48 h p.i. and 96h p.i were analyzed.

Reverse transcription was performed using the RevertAid™ First Strand cDNA Kit (Fermentas). 1  $\mu$ g RNA was applied per reaction and random hexamer primers were used for reverse transcription. A negative control without reverse transcriptase was performed in parallel. The RT conditions were 5 min at 25 °C, 60 min at 37 °C and 5 min at 70 °C. The obtained cDNA was stored at -20°C until further use. Primers targeting *pc1489* and the 16S rRNA gene of *P. amoebophila* were designed using the online tool Primer3plus [48] (Table S1). Primer concentrations and annealing temperatures were optimized using gradient PCR. Genes were cloned into the pCR-XL-TOPO vector (Invitrogen) and these constructs were used as standards for calibration of the PCR assay. The Platinum® SYBR® Green qPCR SuperMix-UDG Kit (Invitrogen) was used for amplification following the manufacturer's instructions by applying 1  $\mu$ l cDNA to the reaction mixture. All standards and samples were analyzed on one plate during a single run using an iCycler (Bio-Rad). Each plate included three different negative controls: a no template control (where all the reaction reagents except for cDNA were used), an RNA only control (to test for residual chlamydial DNA) and cDNA obtained from uninfected amoebae. The qPCR program was: denaturation at 95°C for 3 min, followed by 35 cycles of 40 sec at 95°C, 30 sec at 60°C and 30 sec at 72°C. Final elongation was allowed for 1 min at 72°C, followed by 30 sec at 95°C and a melting curve from 55-95°C. For interpretation and further analysis of the qPCR results the iCycler software was used. Copy numbers of *pc1489* were adjusted to the number of organisms present at the different stages of the developmental cycle by normalization with copy numbers of the 16S rRNA gene at the respective time point [49]. Analysis of the melting curves of the PCR products for *pc1489* and the 16S rRNA showed a single-peak for the amplicons, indicating that a

single PCR product was formed. This was confirmed by analysis of the products on a 2% agarose gel. The negative controls did not show any amplification product (data not shown).

### **Cloning and heterologous expression of proteins in *E. coli***

Genes encoding the predicted porins were cloned as full length copies or without the predicted signal peptide using two different cloning vectors. Full length *pc0870*, *pc1077*, and *pc1860* were cloned into the BamHI and NdeI restriction sites of the vector pet16b (Novagen). Full length *pc1489* was cloned into the XhoI site of pet16b. *Pc0870*, *pc1077* and *pc1489* were cloned into the KpnI and PstI sites of pQE-30 (Qiagen) excluding the first 21 bp encoding the predicted signal peptide. DnaK (*pc1499*), which served as control in immunofluorescence analysis, was cloned into the SmaI and PstI restriction sites of pQE-30. Genes were amplified using the High Fidelity PCR Enzyme Mix (Fermentas) or the Phusion High-Fidelity DNA Polymerase (New England BioLabs). Forward and reverse primers contained sequences to introduce recognition sites for the respective restriction enzymes. For cloning into the vector pet16b, an additional C-terminal 6x His-tag was introduced via the reverse primer to compensate for possible removal of the N-terminal His-tag by cleavage of the signal peptide. Amplified fragments were first cloned into the vector pCR-XL-TOPO (Invitrogen) and subsequently cloned into the expression vectors pet16b and pQE-30. All constructs were sequenced before transformation into *E. coli* BL21 (DE3) (Invitrogen) or *E. coli* M15 (Qiagen). Heterologous expression was induced by addition of 1 mM isopropyl  $\beta$ -D-1-thiogalactopyranoside (IPTG) to cultures at an OD<sub>600</sub> of 0.6. Heterologously expressed Pc1077 without leader sequence and Pc1499 were purified using HisTrap purification columns (GE Healthcare Biosciences) according to the instructions of the manufacturer. The identity of the purified proteins was verified by 1D gel electrophoresis combined with mass spectrometry (data not shown).

### **Toxicity assay**

To analyse the toxicity of the heterologously expressed proteins, LB medium was supplemented with 0.4% glucose to ensure repression of the T7 lac promoter of the vector pet16b. pet16b containing *pc0870*, *pc1077*, *pc1489* or *pc1860* was transformed into *E. coli* BL21 (DE3), and cells were grown on LB plates overnight at 37°C. Single colonies were inoculated in LB, and protein expression was induced by addition of 1 mM IPTG at an OD<sub>600</sub> of 0.6. As controls, the vector pet16b without insert and pet16b containing a gene fragment coding for the inclusion membrane protein IncA (*pc0399*) of *P. amoebophila* were used [33]. Samples were taken at 0, 10 and 60 min after induction, they were diluted in phosphate buffered saline (PBS, 130 mM NaCl, 10 mM Na<sub>x</sub>PO<sub>4</sub>; pH 7.2 – 7.4) and plated on LB plates. After incubation overnight, the number of colony forming units (cfu) was counted. All experiments were performed in three biological replicates.

### **Generation of polyclonal antibodies, immunofluorescence, and immunoelectron microscopy**

All antibodies used in this study were produced by Eurogentec (Belgium). To generate polyclonal antibodies against Pc1489, 400 µg of Pc1489 purified from *P. amoebophila* EBs in Buffer A without n-octyl-POE were used for immunization of one chicken. To generate antibodies against Pc1077, heterologously expressed protein without leader sequence purified from *E. coli* was used for immunization of two rabbits. To generate antibodies against DnaK, one chicken and two guinea pigs were immunized with heterologously expressed DnaK. IgY from pre-immune sera and egg yolk collections was purified using a HiTrap™ IgY Purification HP column (GE Healthcare) according to the manufacturer's instructions. Pre-immune sera were obtained for all immunizations and tested in Western Blot and immunofluorescence analyses. To remove antibodies targeting amoeba proteins, sera were adsorbed with amoeba lysate prior to experiments [37]. Pre-immune serum and antibodies targeting Pc1489 were affinity purified on a polyvinylidene fluoride (PVDF) membrane as previously described to further reduce unspecific background signals [50]. Immunofluorescence analysis of methanol and paraformaldehyde fixed cells and immunogold labelling of ultrathin cryosections was performed as described previously [33].

### **Western blot analysis**

Cells were harvested by centrifugation (18,000 x g for 2 min for *E. coli* or 7,323 x g for 5 min for amoebae). Pellets were resuspended in 4 x Laemmli buffer with 400 mM DTT and heated to 95°C for 5 min. Nucleic acids present in the samples were removed by digestion with the nuclease Benzonase (Novagen) for 1 h. Outer membrane fractions of *P. amoebophila* were obtained either by treatment with N-laurylsarcosine (sarkosyl) as described previously [37] or by incubation in POP05 buffer for 1 h as described above. Proteins were separated by 1D gel electrophoresis, transferred to a PVDF membrane (GE Healthcare) by semi dry blotting in transfer buffer (5.8 g/L Tris, 2.9 g/L glycine, 20% methanol) using a Trans-Blot® SD Semi-Dry Electrophoretic Transfer Cell (Bio-Rad) and proteins were detected using specific antibodies [37]. Detection of heterologously expressed Pc1077 in *E. coli* lysates by Western blot analysis proved to be difficult. The protein was not detectable in Western blot analysis after transfer with standard transfer buffer and staining of SDS-PAGE gels after blotting showed that Pc1077 did not elute from the gel (data not shown). Addition of 0.05 % SDS to the buffer improved transfer, but still a substantial amount of protein could be detected in the gel after blotting and blots showed high background (data not shown). The best results were obtained with a transfer buffer containing urea (12 mM Tris, 48 mM glycine, 5 mM NaH<sub>2</sub>PO<sub>4</sub>, 0.55% SDS, 3 M Urea) which was developed for the transfer of membrane proteins [51] and this buffer was used for the



detection of Pc1077 in subsequent experiments. To test for the presence of multimers of Pc1489 in the outer membrane, outer membrane protein fractions from highly enriched EBs were cross-linked as described previously using bis(sulfosuccinimidyl)suberate [31]. Cross-linked samples were analyzed by SDS-PAGE and Western blot analysis.

### **Infection inhibition assay**

*P. amoebophila* EBs were thawed at 37°C and 1 volume of PBS was added. Heat inactivation was achieved by incubation at 56°C for 30 min [52]. Anti-Pc1489 antibodies, targeting the putative porin, and anti-Pam antibodies, targeting the immunodominant components of the outer membrane of *P. amoebophila* [33], were diluted in FA Block solution (2% bovine serum albumin in PBS) to reach final dilutions of 1:15 and 1:150. EBs and heat-inactivated EBs were incubated with the antibody solutions for 30 min at 37°C with mild shaking. As controls, EBs and heat inactivated EBs were incubated with FA Block solution only. The pre-incubated EBs were used to infect amoebae at an MOI of 5 and samples were fixed at 0, 6, 12, 24, 48, 72 and 96 h p. i. and stored at 4°C for later analysis. Immunofluorescence analysis was performed as described above, and for the time point 48 h p.i. the ratio of infected amoebae to all amoebae was determined by counting at least 100 amoebae. All experiments were performed in three biological replicates.

### **Planar lipid bilayer assays**

The methods used for black lipid bilayer experiments have been described previously [53]. The black lipid bilayer instrumentation consisted of a Teflon chamber with two compartments of 5 ml volume, which were separated by a thin wall and connected by a small circular hole with an area of about 0.4 mm<sup>2</sup>. A 1 % (w/v) solution of diphytanoyl-phosphatidylcholine (PC) (Avanti Polar Lipids) in *n*-decane was used to form the membranes across the hole. The Pc1489 (PomS)-containing protein fractions were diluted 1:100 in 1 % Genapol (Roth) and added at a concentration of about 10 ng/ml to the aqueous phase after the membrane had turned black. The membrane current was measured with a pair of Ag/AgCl electrodes with salt bridges connected in series to a voltage source and a highly sensitive current amplifier (Keithley 427). The temperature was throughout kept at 20 °C. The amplified signal was recorded on a strip chart recorder. Zero-current membrane potential measurements were performed in the presence of a salt gradient as described earlier [54,55]. After the insertion of more than 100 channels into the PC membranes, the KCl concentration (300 mM KCl) was raised 2.5-fold by addition of 3 M KCl to one side of the membrane. The zero-current membrane potentials were measured with a high impedance electrometer (Keithley 617) and analyzed using the Goldman-Hodgkin-Katz equation [54,55].

## Results

### Toxicity of PomS, PomT, PomU, and PomV for *E. coli*

To characterize the putative novel outer membrane protein family of *P. amoebophila* [37,44], we initially tried to clone and express PomS (*pc1489*), PomT (*pc1077*), PomU (*pc0870*), and PomV (*pc1860*) in the heterologous host *E. coli*. Our first attempts to express the full length proteins using different expression vectors in *E. coli* failed. When protein expression was induced, the optical density (OD<sub>600</sub>) of the cultures decreased and no overexpression of the proteins was observed by SDS-PAGE, which indicates host cell lysis due to detrimental effects of the heterologous proteins.

The overexpression of *Chlamydiaceae* MOMP in *E. coli* resulted in a strong decrease in the number of colony forming units (cfus) after induction of protein expression [56]. To investigate whether the predicted porins of *P. amoebophila* show a similar effect, we performed a time-course experiment and compared induced and uninduced *E. coli* cultures with a control protein (IncA) and an empty vector. Consistent with our initial observations, expression of the proteins PomS, PomT, PomU, and PomV had an immediate lethal effect on *E. coli* as indicated by a strong decrease in the number of cfus already 10 min after induction of protein expression. No decrease was observed at this time point when the empty vector alone or the expression of a non-toxic *P. amoebophila* protein was induced (Fig. 1A and 1B). Sixty minutes after induction, the number of cfus decreased even further for cells expressing the putative porins. At this time point also induced cells containing the control vector without an insert or encoding the non-toxic protein showed a decrease in the number of viable cells (Fig. 1A). This decrease was not as strong as for the putative porins and could result from toxicity of the expression vector for the host cells [56,57] or from interference of the strong production of heterologous proteins with cellular processes because of the high transcription rate of the T7 RNA polymerase [58,59].

Previous studies have shown that removal of the signal peptide, which prevents secretion, can help in the overexpression of porins [30]. Indeed, when we tested PomS, PomT, and PomV without the predicted leader sequence overexpression was successful for all three proteins as indicated by bands at the correct size on SDS-PAGE gels. We chose to analyse PomS and PomT in more detail, which were most abundant in *P. amoebophila* outer membrane fractions [37]. Polyclonal anti-PomS and anti-PomT antibodies recognized PomS and PomT expressed in *E. coli* resulting in a strong band at the correct molecular mass (Fig. 2, upper panel).

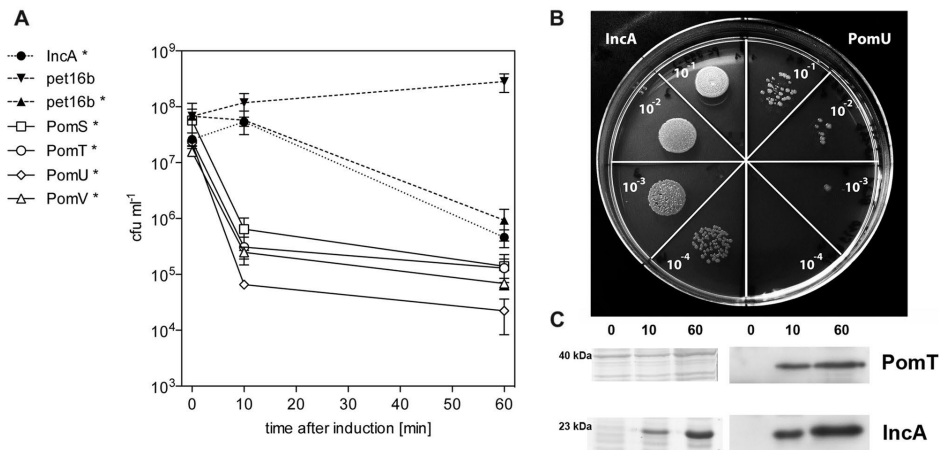


**Figure 1:** Toxic effect of the heterologous expression of PomS, PomT, PomU, and PomV in *E. coli*. (A) Survival of *E. coli* BL21 (DE3) carrying different pet16b plasmid constructs after induction of protein expression (labeled with \*) and without induction. As controls, the vector pet16b without insert and pet16b containing a gene fragment coding for the inclusion membrane protein IncA (*pc0399*) of *P. amoebophila* were used [33]. Induction of expression of proteins of the putative porin family lead to a rapid decrease in the number of colony forming units (cfus) compared to the non-toxic protein IncA. Ten minutes after induction, the numbers of cfus of *E. coli* expressing the putative porins were significantly lower than those of all controls ( $p < 0.05$ , one-way ANOVA test and Dunnett's post test); this difference was not significant anymore at sixty minutes after induction. The mean number of cfus for three independent replicates is shown +/- the standard error of the mean (SEM). (B) Visualization of the toxic effect of the putative porins on *E. coli* 10 min after induction of protein expression. Colonies formed by 10  $\mu$ l droplets of the same dilutions for the non-toxic IncA (left) and the putative porin PomU (right) are shown after incubation overnight at 37°C. Similar results were obtained for all four putative porins tested. Dilutions range from 1:10 to 1:10,000. (C) Detection of protein expression by SDS-PAGE (left) and Western blot analysis (right) for PomT and IncA. Time in min after induction of protein expression by addition of IPTG is indicated above the lanes. Expression of IncA can be detected by SDS-PAGE and Western blot analysis whereas expression of PomT can be detected only by the more sensitive Western blot analysis.

### Location of PomS and PomT in the outer membrane of *P. amoebophila*

The transport function of porins is inherently linked to their presence in the outer membrane. We therefore investigated the location of the putative porins PomS and PomT with Western blot, immunofluorescence analysis, and immuno-transmission electron microscopy (immuno-TEM). First, soluble and insoluble protein fractions of highly purified EBs after treatment with the detergent sarkosyl were analyzed by Western blot. In contrast to the cytoplasmic protein DnaK, which was absent in the sarkosyl-insoluble fraction containing proteins of the outer membrane complex, strong bands were observed for PomS and PomT (Fig. 2, lower panel). In addition, a band for PomS was also detected in the sarkosyl-soluble fraction at a higher molecular mass, possibly representing the full length protein before removal of the signal peptide. For PomT, the band detected in the sarkosyl-soluble fraction was much weaker than the band detected in the outer membrane fraction. For this protein, additional bands with lower molecular mass were observed. This is consistent with a

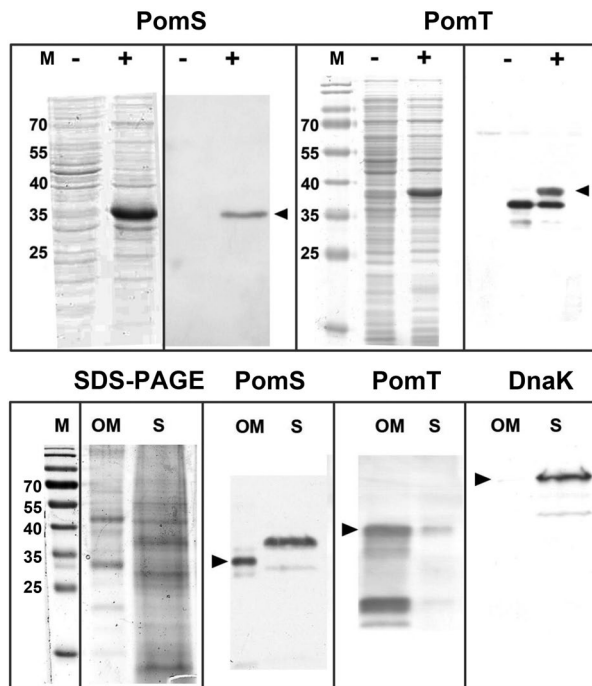


**Figure 2: Detection of PomS and PomT after overexpression in *E. coli* and in outer membrane fractions of *P. amoebophila*.** Upper panel: An additional band in SDS-PAGE gels (left) is present after induction of expression of leaderless PomS or PomT in *E. coli* (lanes labeled „+“) compared to uninduced samples (lanes labeled „-“). Western blot analysis (right) using polyclonal anti-PomS and anti-PomT antibodies demonstrates specificity for the heterologously expressed proteins. The anti-PomT antibodies additionally target one *E. coli* protein with a lower molecular mass. Bands at the correct molecular mass for the leaderless proteins (33.9 kDa for PomS and 36.9 kDa for PomT) are indicated by arrow heads. Molecular mass of marker bands (M) in kDa. Lower panel: Bands for leaderless PomS (33.9 kDa) and PomT (36.9 kDa) can be observed in the sarkosyl-insoluble outer membrane fraction (OM) and in the sarkosyl-soluble (S) fraction using specific polyclonal antibodies (bands at the correct molecular mass are indicated by arrow heads). The cytoplasmic heat-shock protein DnaK, which served as a control, is detected only in the sarkosyl-soluble fraction. For comparison, a SDS gel stained with colloidal coomassie is shown on the left. Molecular mass of marker bands (M) in kDa.

previous study, in which PomT was detected in lower molecular bands of outer membrane protein fractions of *P. amoebophila* by mass spectrometry [37]. Most known porins function as trimers [60], including MOMP of the *Chlamydiaceae* [61]. We therefore tested for the presence of multimers of PomS by crosslinking outer membrane preparations of EBs of *P. amoebophila*, but under the conditions used we could not observe any evidence for the presence of multimers (data not shown). Immunofluorescence analysis with antibodies targeting PomS and PomT resulted in a halo-shaped fluorescence signal surrounding single *P. amoebophila* cells, demonstrating the presence of these

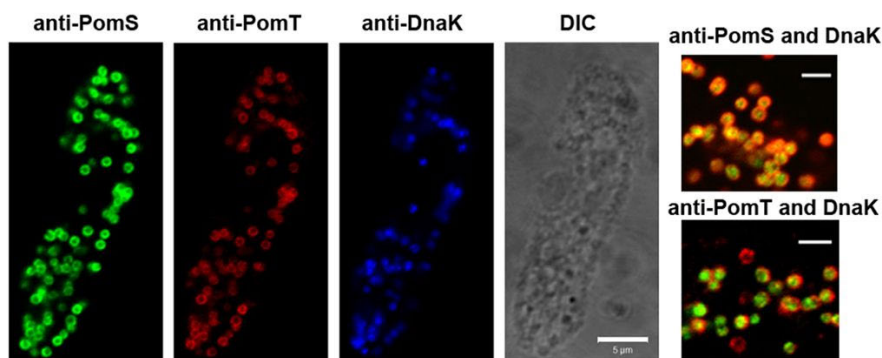


**Figure 3: Detection of PomS and PomT in *P. amoebophila* within its natural amoeba host.** Left panel: Localization of PomS and PomT by immunofluorescence in an asynchronous culture of *A. castellanii* containing *P. amoebophila*. Halo-shaped fluorescence signals were observed around intracellular *P. amoebophila*. In contrast, signals for the heat-shock protein DnaK were confined to the cytoplasm. No differences were observed for methanol- and PFA- fixed samples. Identical microscopic fields are shown. Bar, 5µm. Right panel: Magnification of intracellular *P. amoebophila*; overlay images of fluorescence signals for PomS and PomT (red), respectively, with DnaK (green) are shown. Bars, 2 µm.

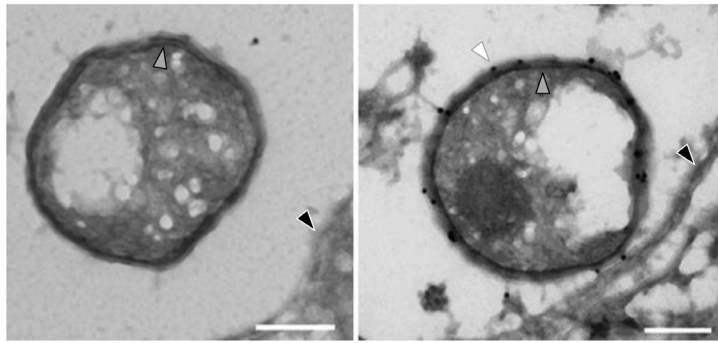


**Figure 4: Localization of PomS in the outer membrane of *P. amoebophila* by immunotransmission electron microscopy.** Immunogold labeling with pre-immune serum (left) and polyclonal anti-PomS antibodies (right). Gold particles indicating PomS were confined to the outer membrane of *P. amoebophila*. White arrow head, gold particle in the outer membrane; grey arrowhead, cytoplasmic membrane; black arrowhead, inclusion membrane. Bars, 200 nm.

proteins at the periphery of *P. amoebophila* cells (Fig. 3). As *P. amoebophila* is located in single-cell inclusions, it is difficult to distinguish between signals from the outer membrane, the inner membrane and the inclusion membrane by immunofluorescence. However, halo-shaped fluorescence signals were also observed when immunofluorescence analysis was performed with purified EBs. This is a strong evidence for a location of PomS and PomT in the bacterial outer membrane and excludes a location of these proteins in the host-derived inclusion membrane. To further demonstrate the location of the most abundant putative porin PomS in the outer membrane we exploited the higher resolution of immuno-TEM. With this technique, signals for PomS were observed only in the outer membrane of *P. amoebophila*, but not in the cytoplasmic membrane or the inclusion membrane (Fig. 4).

### **Transcription and expression of PomS throughout the developmental cycle**

To get first insights into the role of PomS during infection and intracellular replication of *P. amoebophila*, we analyzed expression of the gene coding for PomS by real-time quantitative reverse transcription PCR (RT-qPCR) throughout a complete developmental cycle. Expression of *pomS* was detected at all time points during the developmental cycle, with a significant increase from 0 to 48 h p.i. (Mann-Whitney U-test,  $p \leq 0.05$ ) and was highest at 96 h p.i. (Fig. 5).

In addition, the presence of PomS in *P. amoebophila* was monitored by immunofluorescence analysis during the developmental cycle. Consistent with our RT-qPCR data, PomS protein was detected at all investigated time points. Fluorescence signal intensities increased, and the halo-shaped signals were better defined at later time points, confirming an elevated expression of PomS at later time points and suggesting an increase of the amount of PomS during the developmental cycle (Fig. 5 and Fig. S1).

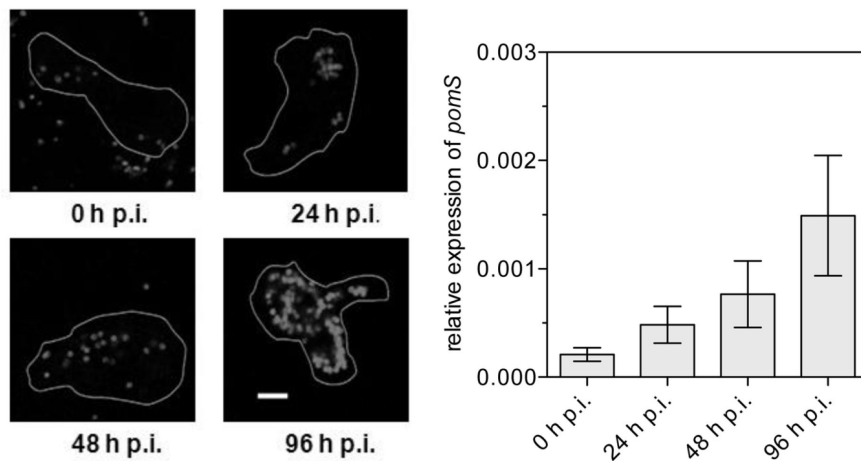


**Figure 5: Expression of PomS during the developmental cycle of *P. amoebophila* in its amoeba host.** Left panel: Expression of PomS at the indicated time points detected by anti-PomS antibody in methanol-fixed cells. Outlines of the amoebae are drawn in white. Bars 5  $\mu$ m. Right panel: Relative levels of *pomS* transcripts measured by real-time quantitative PCR. *pomS* transcripts were normalized to the 16S rRNA to account for an increase in copy numbers due to multiplication of *P. amoebophila*. Data are shown as the mean of five replicates  $\pm$  SEM from a total of three independent infection experiments.

### Preincubation with PomS antibodies does not alter infection of amoebae

Proteins in the bacterial outer membrane can be important for attachment to and uptake by host cells. As our and previous results identified PomS as a major component of the outer membrane of *P. amoebophila* [37], we tested whether this protein is required for attachment to amoeba host cells and whether infection can be blocked by preincubation of EBs with PomS-specific antibodies. To ensure that the antibodies used in this experiment bind to the outer membrane of unfixed cells, EBs were incubated with the specific antibodies prior to fixation, subsequently fixed and incubated with a secondary antibody. All antibodies were found to bind to the outer membrane of unfixed EBs (Fig. 6). Nevertheless, preincubation with the PomS antibody had no significant effect on bacterial uptake and entry, or on the progress of infection (Fig. 6). Interestingly, also no effect was observed when EBs were preincubated with polyclonal antibodies targeting the immunodominant components of *P. amoebophila* EBs (Fig. 6). High concentrations of this antibody lead to agglutination of EBs at the start of the infection experiment, but even this did not influence the outcome of the infection.

### Porin function of PomS

To investigate the putative porin function of PomS we purified this protein directly from *P. amoebophila* EBs. Outer membrane proteins were solubilized with the detergent n-octyl-POE, and DTT was added to reduce disulfide bridges, which are responsible for extensive crosslinking of proteins in the EB cell envelope. A single band at the expected size of PomS in fractions eluted with

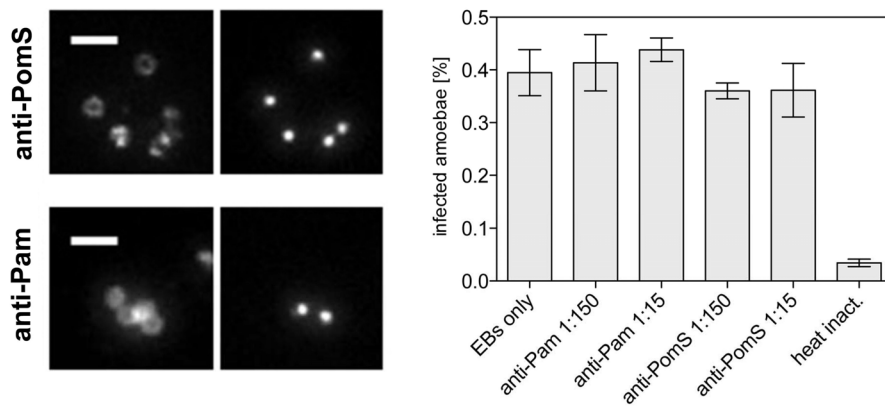


**Figure 6: Infection-inhibition assays using anti-Pam and anti-PomS antibodies.** Left panel: Incubation of host-free *P. amoebophila* EBs with anti-PomS and anti-Pam antibodies prior to fixation demonstrated that these antibodies can bind unfixed cells. Fluorescence signals derived from specific antibodies (left) and 4', 6-Diamidino-2-phenylindol (DAPI; right) are shown for identical microscopic fields. Bars, 2  $\mu$ m. The absence of DAPI signals for some cells indicates cells that lysed during the purification procedure. Right panel: Infection-inhibition assay using preincubations of EBs with anti-Pam and anti-PomS antibodies in different dilutions. The proportion of infected amoebae compared to all counted amoebae of three replicates at 48 h p.i. is shown +/- SEM. Heat-inactivated EBs, used as negative controls, were taken up by the amoebae but did not multiply.

250 mM NaCl from an anion exchange column was visible on protein gels, and no other bands were present in this fraction (Fig. 7). This indicates the absence of larger amounts of contaminating protein in this fraction and demonstrates the successful enrichment of PomS. To further analyze this protein fraction, quantitative mass spectrometry analysis was performed. This highly sensitive method identified several *P. amoebophila* proteins. In total, 767 peptide-spectrum matches were assigned to PomS, while only 121 peptide-spectrum matches were assigned to the other *P. amoebophila* proteins. This analysis confirmed that PomS was highly enriched and represented the by far most abundant protein in this fraction (86% based on NSAF quantification). Further proteins included other putative porins and outer membrane proteins with different molecular masses, and at least 18-fold lower abundance (5% and below, based on NSAF) (Table S2).

To perform planar lipid bilayer assays purified PomS was added to a lipid membrane consisting of phosphatidylcholine. Single-channel conductance increased in a stepwise fashion indicating that the protein formed defined channels (Fig. 8). The average single-channel conductance was about 3.25 nS

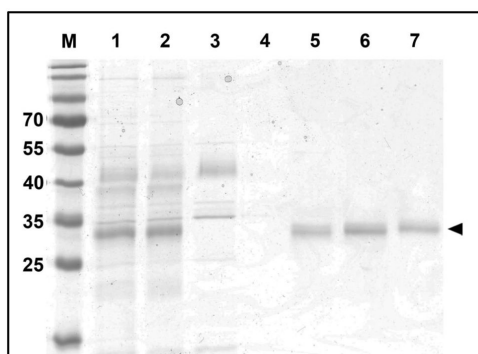


**Figure 7: Purification of PomS from *P. amoebophila* EBs.** A gel stained with colloidal coomassie is shown; 1, outer membrane fraction after incubation of EBs with n-octyl-POE; 2, outer membrane fraction after precipitation with acetone; 3, column flow through; 4-7, fractions after elution with 0.1, 0.25, 0.3, 0.35 and 0.4 M NaCl. Molecular mass of marker bands (M) in kDa; the expected size of PomS (33.9 kDa) is indicated by an arrow head.

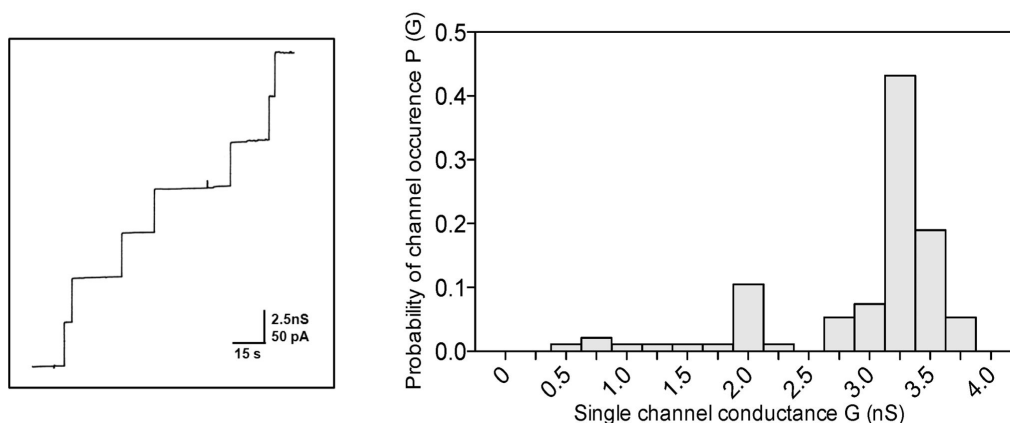


**Figure 8: Porin function of purified PomS.** Single channel experiments using a PC/*n*-decane membrane in the presence of purified PomS. The aqueous phase contained 1 M KCl and 10 ng ml<sup>-1</sup> PomS dissolved in 1% Genapol. The applied membrane potential was 20 mV; T = 20°C. Left panel: Single-channel recordings show a uniform stepwise increase as expected for a highly enriched purified porin. Right panel: Frequency of observed conductance increments. P(G) was calculated by dividing the number of fluctuations with a given conductance increment by the total number of conductance fluctuations. Data from both panels suggest that the purified protein fraction contains mainly PomS (about 82% of the total number of pores) and that there is only a very minor contribution of other pores in the histogram (about 18% of the total number of pores) caused either by contaminant porins or by degradation of PomS. The average single-channel conductance was 3.25 nS for 230 single-channel events.

in 1 M potassium chloride (KCl). Only a minor fraction of channels (about 18% of the total number of fluctuations) with other conductance was observed suggesting that the protein preparation was essentially free of pore-forming contaminants (Fig. 8). The channels formed by PomS had a long lifetime, similar to porins of other Gram-negative and Gram-positive bacteria [26,62-64]. Analysis of the average single-channel conductance at different KCl concentrations in the aqueous phase showed that the conductance was a nearly linear function of the KCl concentration (Table 2). This is characteristic of many porins of Gram-negative bacteria [26,27,55,64] and suggests that PomS forms a wide and water-filled channel, similar to MOMP of the *Chlamydiaceae*. Lipid bilayer assays were also performed with salts other than KCl to obtain information on the size and selectivity of the channels formed by PomS. Conductance was highest for KCl, followed by lithium chloride (LiCl), and lowest values were observed for potassium acetate (KCH<sub>3</sub>COO, Table 2). Replacement of the Cl<sup>-</sup> ion by the less mobile acetate-ion resulted in a stronger decrease in conductance than replacement of the K<sup>+</sup>-ion by the less mobile Li<sup>+</sup>-ion. This means that the influence of anions of different size and mobility on the conductance was more pronounced than that of cations, suggesting anion-selectivity of the PomS channel.

### Anion-selectivity and voltage-dependence of PomS

Additional information about the structure of the channel formed by PomS was obtained from zero-current membrane potential measurements in the presence of salt gradients. A 2.5-fold KCl gradient



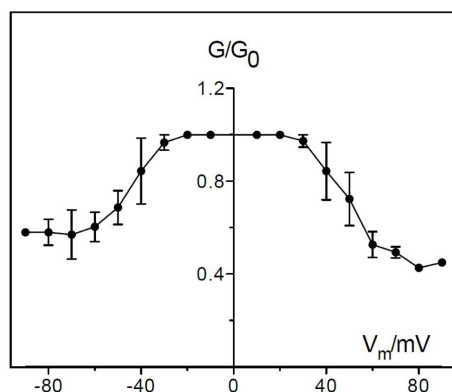


**Figure 9: Voltage dependence of PomS.** PomS was added in a concentration of  $500 \text{ ng ml}^{-1}$  to the trans-side side of a PC/n-decane membrane in multi-channel experiments. The aqueous phase contained 1 M KCl, pH 6.0. After 30 min the conductance had increased considerably. At this point different potentials were applied to the membrane. The ratio of the conductance  $G$  at a given membrane potential ( $V_m$ ) divided by the conductance  $G_0$  at 10 mV was calculated as a function of the membrane potential  $V_m$  [1]. The membrane potential refers to the cis-side of the membrane.  $T = 20^\circ\text{C}$ . Means ( $\pm$  SD) of three membranes are shown.

(300 mM versus 750 mM), across a lipid bilayer membrane in which about 100 to 1000 PomS channels were reconstituted, resulted in an asymmetry potential of  $-7.8 \text{ mV}$  at the more dilute side. This result indicated preferential movement of chloride over potassium ions through the pore at neutral pH. The ratio of the chloride permeability,  $P_{\text{Cl}}$ , divided by the potassium permeability,  $P_{\text{K}}$ , was around 2.0, indicating indeed low anion selectivity of the PomS channel. This was further confirmed by measurements with LiCl and potassium acetate; we observed under the same conditions as for KCl, diffusion potentials around  $-9.5$  and  $-2.6 \text{ mV}$  at the more dilute side, respectively (Table 3). The observed selectivity changes dependent on the mobility of the cations and anions indicated that PomS forms a general diffusion pore similar to OmpF and OmpC of *Escherichia coli* [26,55] and MOMP of *C. psittaci* [29].

Salt	Salt concentration (M)	Single-channel conductance $G$ (nS)
LiCl	0.3	1.0
	1.0	2.25
KCl	0.01	0.15
	0.03	0.25
	0.10	0.60
	0.30	1.20
	1.0	3.25
	3.0	11
KCH <sub>3</sub> COO (pH 7)	0.30	0.60
	1.0	1.5

**Table 2: Average single-channel conductance of PomS in different salt solutions.** The membranes were formed from diphtanoyl phosphatidylcholine (PC) dissolved to 1% in n-decane. The aqueous solutions were used unbuffered and had a pH of 6 unless otherwise indicated. The applied voltage was 20 mV, and the temperature was  $20^\circ\text{C}$ . The average single-channel conductance,  $G$ , was calculated from at least 80 single events.

Salt	$V_m$ /mV	$P_{\text{cation}}/P_{\text{anion}}$
KCl	-7.8	0.48
LiCl	-9.5	0.40
KCH <sub>3</sub> COO, pH 7	-2.6	0.79

**Table 3: Zero-current membrane potentials of PC/n-decane membranes in the presence of PomS measured for a 2.5-fold gradient of different salts (300 mM versus 750 mM).** The zero-current membrane potential  $V_m$  is defined as the difference between the potential at the dilute side and the potential at the concentrated side. The aqueous salt solutions were used unbuffered and had a pH of 6, if not indicated otherwise;  $T = 20^\circ\text{C}$ . The permeability ratio  $P_{\text{cation}}/P_{\text{anion}}$  was calculated using the Goldman-Hodgkin-Katz equation [54] from at least 3 individual experiments.

Some porins of Gram-negative bacteria show voltage-dependent closure in reconstitution bilayer experiments [65] although the physiological role of this channel gating is obscure [66]. This effect was also observed for PomS when voltages of positive and negative polarity higher than 30 mV or lower than -30 mV were applied (Fig. 9). The voltage dependence of PomS was essentially unchanged if the protein was added to either the trans- or to the cis-chamber of the membranes. These results indicated a symmetric response of the pore to the applied voltage.

## Discussion

In the *Chlamydiaceae*, the most abundant protein and a major structural component in the outer membrane is the porin MOMP [12,19]. While two copies of MOMP are encoded in the genome of *Simkania negevensis* [35], no homologue of this protein was found in the two sequenced genomes of members of the *Parachlamydiaceae* [34,35] – a major difference between this family and its pathogenic relatives from the *Chlamydiaceae*. In a previous study, the presence of a putative novel porin family in *P. amoebophila* has been proposed [37]. Here we show that two members of this porin family, PomS and PomT, are indeed localized in the outer membrane of *P. amoebophila* (Figures 2, 3, 4). PomS, the most abundant outer membrane protein [37], is expressed throughout the developmental cycle with an increase in expression in the later phase of the developmental cycle similar to the expression profile of MOMP in different serovars of *C. trachomatis* (Fig. 5) [67-69]. This is consistent with a key function of PomS in the outer membrane of both RBs and EBs.

MOMP is probably not the only factor with respect to attachment to host cells or tissue-specificity in *Chlamydiaceae* [70]. However, preincubations of EBs with antibodies targeting MOMP inhibited infection by either blocking attachment to host cells [71,72] or at steps after internalization [52,73]. Preincubation with antibodies targeting the outer membrane proteins OmcB, PorB and members of

the Pmp family also reduced infectivity [74-77]. In contrast, the infection of amoebae by *P. amoebophila* is not impaired by pre-incubation with anti-PomS or anti-Pam antibodies (Fig. 6). This suggests that neither PomS nor other immunodominant components of the outer membrane of *P. amoebophila* play an important role in attachment to and uptake into amoebae, a process which might be fundamentally different from the uptake into non-phagocytic mammalian cells.

Based on its abundance in the outer membrane it is likely that PomS is an important structural component of the *P. amoebophila* outer membrane. Similar to the *Chlamydiaceae* MOMP it is also a major porin, facilitating transport of small molecules across the outer membrane [25]. The pore formed by PomS is wide, water-filled and anion-selective, presumably because of an excess of positively charged amino acids in or near the pore. The single channel conductance was with 3.25 nS in 1 M KCl relatively high (Fig. 8, Table 3), about 3-times higher than that reported for MOMP which has a single channel conductance of 1 nS in *C. trachomatis* and 1.3 nS in *C. psittaci* [31,78]. The channels formed by PomS are voltage-dependent in a more or less symmetrical way starting at about  $\pm 30$  mV (Fig. 9). The voltage dependency of PomS is thus similar to that of the mitochondrial porin VDAC [79], and the channel conducts at high voltages about 50% of its open configuration. Different ion-selectivities have been reported for *Chlamydiaceae* MOMPs. Native MOMP of *C. psittaci* is weakly anion-selective [29], but cation-selective when expressed in *E. coli* [80]. Full length recombinant MOMP of *C. trachomatis* was reported to be either anion- [78] or cation-selective [30], suggesting that tags of the cloning-vector added during the cloning procedure may influence the functional characteristics of these proteins. In this study, ion selectivity was determined using native PomS. Therefore, modifications introduced by recombinant expression can be excluded.

MOMP is highly crosslinked and mostly present as a trimer in *Chlamydiaceae* EBs [31,61], whereas it is found mostly in its monomeric form in RBs [18]. For PomS we found no evidence for the formation of multimers, which might suggest that this protein is present in the outer membrane of EBs as monomer. Alternative explanations for our observation would be a highly instable PomS multimer that breaks down during purification, or an untypical migration behavior in SDS-PAGE. Trimers of MOMP are stabilized by disulfide-bridges between the monomeric subunits [30], and it has been suggested that opening of the pore is regulated by the reduction of these disulfide bonds [28]. PomS contains only two cysteine residues in contrast to 7-10 cysteine residues in MOMP [81] possibly hindering the formation of stable multimers by PomS and suggesting a different opening mechanism for this pore.

Whether the other members of the PomS protein family also function as porins has to be determined. The predicted beta-barrel structure of PomT and its location in the outer membrane strongly suggests a porin function. PomU is not predicted to form a beta-barrel, and PomV represents a lipoprotein according to *in silico* analysis [44]. However, all proteins of this family were predicted to encode a signal peptide and showed a pronounced toxic effect on *E. coli* when expression of the full length constructs was induced (Fig. 1). This is consistent with the notion that outer membrane proteins, and porins in particular, are generally difficult to overexpress in *E. coli*, because if properly folded, they might insert into the outer membrane, and their pore-forming activity can be toxic for the host [56,82].

The different members of the PomS protein family could play a role in the adaptation to different environmental conditions as they show an only low degree of amino acid sequence identity (22-28%) and hence likely differ in pore size, uptake rates or ion specificity. Well-studied examples of homologous yet differentially sized porins are OmpF and OmpC of *E. coli* whose levels of expression depends on the osmolarity of the extracellular milieu [83,84]. The smaller pore formed by OmpC is dominant under conditions of high osmolarity whereas OmpF is upregulated under iso- or hypoosmotic conditions (Benz et al., 1985). Expansions of genes encoding porins are apparent in several chlamydial genomes. In the *Chlamydiaceae*, the protein PorB was identified as putative porin based on its weak sequence similarity to MOMP by genome analysis; its pore-forming function was later confirmed [77]. The much larger genomes of *W. chondrophila* and *S. negevensis* encode 11 and 35 MOMP-like genes, respectively, which are more diverged from known *Chlamydiaceae* MOMPs [35,85]. Within the chlamydiae, the PomS protein family analyzed here seems to be restricted to *P. amoebophila* and *Parachlamydia acanthamoebae* and lacks close homologues in other bacteria. The *P. amoebophila* PomS corresponds to the MOMP of the *Chlamydiaceae* with respect to abundance in the outer membrane and its function as major porin, and it thus represents a specific adaptation of this amoeba symbiont.

### **Acknowledgement**

We thank Gustav Ammerer, Karl Mechtler and Sonja Kolar for access to and help with mass spectrometry analysis, Holger Daims for help with image analysis, and Barbara Sixt and Ilias Lagkouvardos for helpful discussions. Technical assistance by Christian Baranyi is greatly acknowledged.

## References

1. Ludwig O, De Pinto V, Palmieri F, Benz R (1986) Pore formation by the mitochondrial porin of rat brain in lipid bilayer membranes. *Biochim Biophys Acta* 860: 268-276.
2. Longbottom D, Coulter LJ (2003) Animal chlamydioses and zoonotic implications. *J Comp Pathol* 128: 217-244.
3. Horn M (2008) Chlamydiae as symbionts in eukaryotes. *Ann Rev Microbiol* 62: in press.
4. Blasi F, Tarsia P, Aliberti S (2009) *Chlamydomphila pneumoniae*. *Clinical Microbiology and Infection* 15: 29-35.
5. Bébéar C, De Barbeyrac B (2009) Genital *Chlamydia trachomatis* infections. *Clinical Microbiology and Infection* 15: 4-10.
6. Abdelrahman YM, Belland RJ (2005) The chlamydial developmental cycle. *FEMS Microbiol Rev* 29: 949-959.
7. Hackstadt T, Fischer ER, Scidmore MA, Rockey DD, Heinzen RA (1997) Origins and functions of the chlamydial inclusion. *Trends in Microbiology* 5: 288-293.
8. Hybiske K, Stephens RS (2007) Mechanisms of host cell exit by the intracellular bacterium *Chlamydia*. *Proc Natl Acad Sci U S A* 104: 11430-11435.
9. Pal S, Theodor I, Peterson EM, de la Maza LM (1997) Immunization with an acellular vaccine consisting of the outer membrane complex of *Chlamydia trachomatis* induces protection against a genital challenge. *Infect Immun* 65: 3361-3369.
10. Tan TW, Herring AJ, Anderson IE, Jones GE (1990) Protection of sheep against *Chlamydia psittaci* infection with a subcellular vaccine containing the major outer membrane protein. *Infect Immun* 58: 3101-3108.
11. Everett KD, Hatch TP (1995) Architecture of the cell envelope of *Chlamydia psittaci* 6BC. *J Bacteriol* 177: 877-882.
12. Hatch TP, Vance DW, Jr., Al-Hossainy E (1981) Identification of a major envelope protein in *Chlamydia* spp. *J Bacteriol* 146: 426-429.
13. Raulston JE (1995) Chlamydial envelope components and pathogen-host cell interactions. *Molecular Microbiology* 15: 607-616.
14. Hatch T (1996) Disulfide cross-linked envelope proteins: the functional equivalent of peptidoglycan in chlamydiae? *J Bacteriol* 178: 1-5.
15. Salari SH, Ward ME (1981) Polypeptide composition of *Chlamydia trachomatis*. *J Gen Microbiol* 123: 197-207.
16. Tanzer RJ, Hatch TP (2001) Characterization of outer membrane proteins in *Chlamydia trachomatis* LGV serovar L2. *J Bacteriol* 183: 2686-2690.
17. Liu X, Afrane M, Clemmer DE, Zhong G, Nelson DE (2010) Identification of *Chlamydia trachomatis* Outer Membrane Complex Proteins by Differential Proteomics. *Journal of Bacteriology* 192: 2852-2860.
18. Hatch TP, Allan I, Pearce JH (1984) Structural and polypeptide differences between envelopes of infective and reproductive life cycle forms of *Chlamydia* spp. *J Bacteriol* 157: 13-20.
19. Caldwell HD, Kromhout J, Schachter J (1981) Purification and partial characterization of the major outer membrane protein of *Chlamydia trachomatis*. *Infect Immun* 31: 1161-1176.

20. McCoy AJ, Maurelli AT (2006) Building the invisible wall: updating the chlamydial peptidoglycan anomaly. *Trends Microbiol* 14: 70-77.
21. Hatch TP, Miceli M, Sublett JE (1986) Synthesis of disulfide-bonded outer membrane proteins during the developmental cycle of *Chlamydia psittaci* and *Chlamydia trachomatis*. *J Bacteriol* 165: 379-385.
22. Hackstadt T, Todd WJ, Caldwell HD (1985) Disulfide-mediated interactions of the chlamydial major outer membrane protein: role in the differentiation of chlamydiae? *J Bacteriol* 161: 25-31.
23. Newhall WJt (1987) Biosynthesis and disulfide cross-linking of outer membrane components during the growth cycle of *Chlamydia trachomatis*. *Infect Immun* 55: 162-168.
24. Stephens RS, Tam MR, Kuo CC, Nowinski RC (1982) Monoclonal antibodies to *Chlamydia trachomatis*: antibody specificities and antigen characterization. *J Immunol* 128: 1083-1089.
25. Nikaido H (2003) Molecular basis of bacterial outer membrane permeability revisited. *Microbiol Mol Biol Rev* 67: 593-656.
26. Benz R (1994) Solute uptake through bacterial outer membrane. In *Bacterial cell wall.*; Ghuyssen JM, Hakenbeck, R, editor. Amsterdam: Elsevier Science B. V.
27. Benz R, and Bauer, K. (1988) Permeation of hydrophilic molecules through the outer membrane of gram-negative bacteria. *Eur J Biochem* 176 1-19.
28. Bavoil P, Ohlin A, Schachter J (1984) Role of disulfide bonding in outer membrane structure and permeability in *Chlamydia trachomatis*. *Infect Immun* 44: 479-485.
29. Wyllie S, Ashley RH, Longbottom D, Herring AJ (1998) The major outer membrane protein of *Chlamydia psittaci* functions as a porin-like ion channel. *Infect Immun* 66: 5202-5207.
30. Findlay H, McClafferty H, Ashley R (2005) Surface expression, single-channel analysis and membrane topology of recombinant *Chlamydia trachomatis* Major Outer Membrane Protein. *BMC Microbiology* 5: 5.
31. Sun G, Pal S, Sarcon AK, Kim S, Sugawara E, et al. (2007) Structural and Functional Analyses of the Major Outer Membrane Protein of *Chlamydia trachomatis*. *Journal of Bacteriology* 189: 6222-6235.
32. Newhall V, Wilbert JJ, Robert B (1983) Disulfide-linked oligomers of the Major Outer Membrane Protein of *Chlamydiae*. *J Bacteriol* 154: 998-1001.
33. Heinz E, Rockey DD, Montanaro J, Aistleitner K, Wagner M, et al. (2010) Inclusion Membrane Proteins of *Protochlamydia amoebophila* UWE25 Reveal a Conserved Mechanism for Host Cell Interaction among the *Chlamydiae*. *J Bacteriol* 192: 5093-5102.
34. Horn M, Collingro A, Schmitz-Esser S, Beier CL, Purkhold U, et al. (2004) Illuminating the evolutionary history of chlamydiae. *Science* 304: 728-730.
35. Collingro A, Tischler P, Weinmaier T, Penz T, Heinz E, et al. (2011) Unity in Variety—The Pan-Genome of the *Chlamydiae*. *Molecular Biology and Evolution* 28: 3253-3270.
36. Collingro A, Toenshoff ER, Taylor MW, Fritsche TR, Wagner M, et al. (2005) '*Candidatus* Protochlamydia amoebophila', an endosymbiont of *Acanthamoeba* spp. *Int J Syst Evol Microbiol* 55: 1863-1866.
37. Heinz E, Pichler P, Heinz C, op den Camp HJM, Toenshoff ER, et al. (2010) Proteomic analysis of the outer membrane of *Protochlamydia amoebophila* elementary bodies. *PROTEOMICS* 10: 4363-4376.

38. Petersen TN, Brunak S, von Heijne G, Nielsen H (2011) SignalP 4.0: discriminating signal peptides from transmembrane regions. *Nat Meth* 8: 785-786.
39. Rey S, Acab M, Gardy JL, Laird MR, deFays K, et al. (2005) PSORTdb: a protein subcellular localization database for bacteria. *Nucleic Acids Res* 33: D164-168.
40. Bagos PG, Hamodrakas SJ (2004) Finding beta-barrel outer membrane proteins with a markov chain model. *WSEAS Transactions on Biology and Biomedicine* 2: 186-189.
41. Bagos PG, Liakopoulos TD, Spyropoulos IC, Hamodrakas SJ (2004) PRED-TMBB: a web server for predicting the topology of beta-barrel outer membrane proteins. *Nucleic Acids Res* 32: W400-404.
42. Juncker AS, Willenbrock H, Von Heijne G, Brunak S, Nielsen H, et al. (2003) Prediction of lipoprotein signal peptides in Gram-negative bacteria. *Protein Sci* 12: 1652-1662.
43. Remmert M, Linke D, Lupas AN, Söding J (2009) HHomp—prediction and classification of outer membrane proteins. *Nucleic Acids Research* 37: W446-W451.
44. Heinz E, Tischler P, Rattei T, Myers G, Wagner M, et al. (2009) Comprehensive in silico prediction and analysis of chlamydial outer membrane proteins reflects evolution and life style of the *Chlamydiae*. *BMC Genomics* 10: 634.
45. Heinz C, Roth E, Niederweis M (2003) Purification of Porins from *Mycobacterium smegmatis*. pp. 139-150.
46. Zybailov B, Mosley AL, Sardi ME, Coleman MK, Florens L, et al. (2006) Statistical Analysis of Membrane Proteome Expression Changes in *Saccharomyces cerevisiae*. *Journal of Proteome Research* 5: 2339-2347.
47. Collier TS, Sarkar P, Franck WL, Rao BM, Dean RA, et al. (2010) Direct Comparison of Stable Isotope Labeling by Amino Acids in Cell Culture and Spectral Counting for Quantitative Proteomics. *Analytical Chemistry* 82: 8696-8702.
48. Untergasser A, Nijveen H, Rao X, Bisseling T, Geurts R, et al. (2007) Primer3Plus, an enhanced web interface to Primer3. *Nucl Acids Res* 35: W71-74.
49. Borges V, Ferreira R, Nunes A, Nogueira P, Borrego MJ, et al. (2010) Normalization strategies for real-time expression data in *Chlamydia trachomatis*. *Journal of Microbiological Methods* 82: 256-264.
50. Ritter K (1991) Affinity purification of antibodies from sera using polyvinylidenedifluoride (PVDF) membranes as coupling matrices for antigens presented by autoantibodies to triosephosphate isomerase. *Journal of Immunological Methods* 137: 209-215.
51. Abeyrathne PD, J.S. Lam (2007) Conditions that allow for effective transfer of membrane proteins onto nitrocellulose membrane in Western blots. *Can J Microbiol* 53: 526-532.
52. Caldwell HD, Perry LJ (1982) Neutralization of *Chlamydia trachomatis* infectivity with antibodies to the major outer membrane protein. *Infect Immun* 38: 745-754.
53. Benz R, Janko K, Boos W, Läger P (1978) Formation of large, ion-permeable membrane channels by the matrix protein (porin) of *Escherichia coli*. *Biochim Biophys Acta* 511: 305-319.
54. Benz R, Janko K, Läger P (1979) Ionic selectivity of pores formed by the matrix protein (porin) of *Escherichia coli*. *Biochim Biophys Acta* 551: 238-247.
55. Benz R, Schmid A, Hancock RE (1985) Ion selectivity of gram-negative bacterial porins. *Journal of Bacteriology* 162: 722-727.

56. Koehler JE, S. Birkelund, R.S. Stephens (1992) Overexpression and surface localization of the *Chlamydia trachomatis* major outer membrane protein in *Escherichia coli*. Mol Microbiol 6: 1087-1094.
57. Miroux B, Walker JE (1996) Over-production of Proteins in *Escherichia coli*: Mutant Hosts that Allow Synthesis of some Membrane Proteins and Globular Proteins at High Levels. Journal of Molecular Biology 260: 289-298.
58. Hoffmann F, Rinas U (2004) Stress Induced by Recombinant Protein Production in *Escherichia coli*. Physiological Stress Responses in Bioprocesses: Springer Berlin / Heidelberg. pp. 73-92.
59. Iost I, Guillerez J, Dreyfus M (1992) Bacteriophage T7 RNA polymerase travels far ahead of ribosomes in vivo. J Bacteriol 174: 619-622.
60. Welte W, Nestel, U., Wacker, T., Diederichs, K. (1995) Structure and function of the porin channel. Kidney Int 48: 930-940.
61. McCafferty MC, Herring AJ, Andersen AA, Jones GE (1995) Electrophoretic analysis of the major outer membrane protein of *Chlamydia psittaci* reveals multimers which are recognized by protective monoclonal antibodies. Infect Immun 63: 2387-2389.
62. Trias J, Benz R (1994) Permeability of the cell wall of *Mycobacterium smegmatis*. Molecular Microbiology 14: 283-290.
63. Trias J, Jarlier V, Benz R (1992) Porins in the cell wall of mycobacteria. Science 258: 1479-1481.
64. Benz R (2001) Porins - structure and function; Winkelmann G, editor. Weinheim: Wiley-VCH.
65. Schindler H, Rosenbusch JP (1978) Matrix protein from *Escherichia coli* outer membranes forms voltage-controlled channels in lipid bilayers. Proceedings of the National Academy of Sciences 75: 3751-3755.
66. Sen K, Hellman J, Nikaido H (1988) Porin channels in intact cells of *Escherichia coli* are not affected by Donnan potentials across the outer membrane. Journal of Biological Chemistry 263: 1182-1187.
67. Gomes JP, Hsia RC, Mead S, Borrego MJ, Dean D (2005) Immunoreactivity and differential developmental expression of known and putative *Chlamydia trachomatis* membrane proteins for biologically variant serovars representing distinct disease groups. Microbes Infect 7: 410-420.
68. Belland RJ, Zhong G, Crane DD, Hogan D, Sturdevant D, et al. (2003) Genomic transcriptional profiling of the developmental cycle of *Chlamydia trachomatis*. Proc Natl Acad Sci U S A 100: 8478-8483.
69. Albrecht M, Sharma CM, Reinhardt R, Vogel J, Rudel T (2010) Deep sequencing-based discovery of the *Chlamydia trachomatis* transcriptome. Nucleic Acids Research 38: 868-877.
70. Stothard DR, Boguslawski G, Jones RB (1998) Phylogenetic Analysis of the *Chlamydia trachomatis* Major Outer Membrane Protein and Examination of Potential Pathogenic Determinants. Infect Immun 66: 3618-3625.
71. Su H, Caldwell HD (1991) In vitro neutralization of *Chlamydia trachomatis* by monovalent Fab antibody specific to the major outer membrane protein. Infect Immun 59: 2843-2845.
72. Ward ME, Murray, A. (1984) Control mechanisms governing the infectivity of *Chlamydia trachomatis* for HeLa cells: mechanisms of endocytosis. J Gen Microbiol 130: 1765-1780.
73. Peeling R, Maclean IW, Brunham RC (1984) In vitro neutralization of *Chlamydia trachomatis* with monoclonal antibody to an epitope on the major outer membrane protein. Infect Immun 46: 484-488.



74. Moelleken K, Hegemann JH (2008) The *Chlamydia* outer membrane protein OmcB is required for adhesion and exhibits biovar-specific differences in glycosaminoglycan binding. *Mol Microbiol* 67: 403-419.
75. Wehrl W, Brinkmann V, Jungblut PR, Meyer TF, Szczepek AJ (2004) From the inside out--processing of the Chlamydial autotransporter PmpD and its role in bacterial adhesion and activation of human host cells. *Mol Microbiol* 51: 319-334.
76. Mölleken K, Schmidt E, Hegemann JH (2010) Members of the Pmp protein family of *Chlamydia pneumoniae* mediate adhesion to human cells via short repetitive peptide motifs. *Molecular Microbiology* 78: 1004-1017.
77. Kubo A, Stephens RS (2000) Characterization and functional analysis of PorB, a *Chlamydia* porin and neutralizing target. *Mol Microbiol* 38: 772-780.
78. Hughes ES, Shaw KM, Ashley RH (2001) Mutagenesis and functional reconstitution of chlamydial Major Outer Membrane Proteins: VS4 domains are not required for pore formation but modify channel function. *Infect Immun* 69: 1671-1678.
79. Benz R (1994) Permeation of hydrophilic solutes through mitochondrial outer membranes: review on mitochondrial porins. *Biochimica et Biophysica Acta (BBA) - Reviews on Biomembranes* 1197: 167-196.
80. Wyllie S, Longbottom D, Herring AJ, Ashley RH (1999) Single channel analysis of recombinant major outer membrane protein porins from *Chlamydia psittaci* and *Chlamydia pneumoniae*. *FEBS Lett* 445: 192-196.
81. Stephens RS (1999) *Chlamydia*. Washington DC: ASM Press.
82. Wagner S, Bader ML, Drew D, de Gier J-W (2006) Rationalizing membrane protein overexpression. *Trends in Biotechnology* 24: 364-371.
83. Alphen WV, Lugtenberg B (1977) Influence of osmolarity of the growth medium on the outer membrane protein pattern of *Escherichia coli*. *J Bacteriol* 131: 623-630.
84. Pratt LA, Hsing W, Gibson KE, Silhavy TJ (1996) From acids to osmZ: multiple factors influence synthesis of the OmpF and OmpC porins in *Escherichia coli*. *Molecular Microbiology* 20: 911-917.
85. Bertelli C, Collyn F, Croxatto A, Rückert C, Polkinghorne A, et al. (2010) The *Waddlia* Genome: A Window into Chlamydial Biology. *PLoS ONE* 5: e10890.
86. Daims H, Lückner S, Wagner M (2006) daime, a novel image analysis program for microbial ecology and biofilm research. *Environmental Microbiology* 8: 200-213.

## Supporting Information

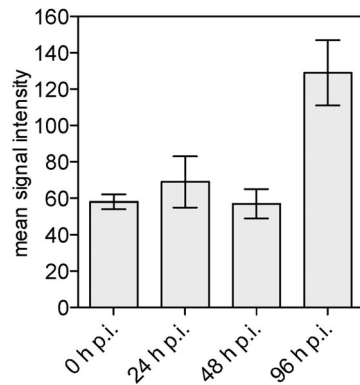


**Figure S1: Fluorescence intensity derived from anti-PomS antibodies increases during infection.** Quantification of fluorescence intensity was performed using the image analysis software daime [86]. The mean fluorescence intensity ( $\pm$  SD) is shown for each time point.

Primer	Target molecule	Primer sequence (5'-3')	Primer location	Size of amplicon
q16S_F	16S rRNA gene	GCA AGT CGA ACG AAA CCT C	30-47	88 bp
q16S_R	16S rRNA gene	TTC CAA CCG TTA TCC CAG AG	98-118	
q1489_F	pc1489 gene	TGG AAC CAA AAA GCT CCA TC	118-138	143 bp
q1489_R	pc1489 gene	CAG CCC CAA TTT ACA GAA GC	241-261	

**Table S1: Primers used for qPCR targeting genes of *P. amoebophila***

Locus tag	Protein description	Protein mass (kDa)	Protein length (aa)	Spectral counts	NSAF	% abundance	Fold lower than PomS
pc1489	PomS	36.3	317	767	2.42	85.7	1.0
pc1885	hyp. protein	24.5	217	29	0.13	4.7	18.1
pc1077	PomT	39.0	345	44	0.13	4.5	19.0
pc0675	hyp. protein	37.3	320	28	0.09	3.1	27.7
pc0575	hyp. protein	40.3	342	8	0.02	0.8	103.4
pc1860	PomV	37.5	325	7	0.02	0.8	112.3
pc0004	hyp. protein	53.8	470	5	0.01	0.4	227.4

**Table S2: Quantification by mass spectrometry shows that PomS is highly enriched in purified porin fractions.** The percent abundance of proteins with five or more assigned spectra was calculated based on the normalized spectral abundance factor (NSAF) [46,47].

# **Chapter VII**

## **Conclusions & Future Perspectives**

## Conclusions and future perspectives

Many of the early insights into chlamydial biology came from electron microscopy, and state-of-the-art cryo-electron microscopy played a major part in this thesis. The absence of chemical fixation and dehydration combined with the high resolution provided by this technique enabled again new insights into the biology of environmental chlamydiae.

The identification of a proposed developmental stage, the crescent body, as fixation artifact showed that the shape of chlamydiae is prone to deformation during chemical fixation and dehydration. Our findings are backed up by another study that recently showed that none of the fixative conditions tested for conventional electron microscopy ideally preserved the round shape of chlamydiae [1]. This strengthens the point that unusual shapes described solely based on electron microscopy images for environmental chlamydiae [2-8] should be validated under fixation-free conditions by cryo-electron microscopy. However, since this technique is not broadly available, a thorough testing of buffers with different osmolarity conditions and fixative concentrations could help in the differentiation between fixation artifacts and true shapes as this was shown to strongly influence the frequency of crescent bodies for *Parachlamydia acanthamoebae* in this thesis. Interestingly, the frequency of star- and crescent shapes varies between different environmental chlamydiae and members of the *Chlamydiaceae* [1], and variations in their cell envelope composition might play a role in this.

Cryo-electron tomography of chlamydiae inside their host cells showed for the first time that *Simkania negevensis* recruits the endoplasmic reticulum (ER) to the inclusion. In earlier studies based on conventional electron microscopy this association was not observed, probably due to the collapse of the ER membrane on the inclusion membrane during the dehydration step of sample processing. This is supported by an earlier description of ribosomes arranged like strings of pearls beneath the inclusion membrane of *S. negevensis* inside *Acanthamoeba castellanii* [9], which was however not linked to the presence of the ER. An association of *C. trachomatis* with the ER was also only recently reported based on high-pressure freezing and freeze-substitution of samples [10], a method that is well suited for the preservation of fragile structures, showing that alternative fixation techniques can still give new insights into well-studied systems. Interestingly, the recruitment of the ER by *S. negevensis* is conserved in the evolutionary distant human and amoeba hosts [11]. Mitochondria are additionally associated with *S. negevensis* containing inclusions during infection of mammalian cells [11], but not in amoebae, indicating that the recruitment of this organelle by *S. negevensis* is a host-dependent trait. Recruitment of mitochondria was also reported for *C. psittaci*, *C. caviae* and

*Waddlia chondrophila* [12-14], although different recruitment pathways seem to be used by *W. chondrophila* [13]. The conservation of the recruitment of these organelles in members of different families suggests a crucial role in the infection process, and it will be interesting to see whether also the underlying molecular mechanisms are conserved. As the ability to successfully infect mammalian cells overlaps with the ability to recruit organelles in chlamydiae, this might represent an adaptation and a requirement for the infection of mammalian host cells. Identification of the benefits chlamydiae gain by these interactions and of the effector proteins involved in the recruitment will not only help to better understand chlamydia-host interactions, but might provide new ways to inhibit infections by chlamydiae. However, the distribution of host cell organelles should first be compared in the same host under similar growth conditions followed by the same fixation protocol to exclude differences resulting from different treatment of samples or different host cells.

Another exciting finding obtained by cryo-electron tomography was the presence of a periplasmic layer in the cell envelope of *Protochlamydia amoebophila* followed by the detection of peptidoglycan in chlamydiae for the first time. Based on the functionality of the enzymes involved in the synthesis of peptidoglycan it had been hypothesized before that the peptidoglycan monomer assembled in Chlamydia is of the same biochemical structure as peptidoglycan monomers in other Gram-negative bacteria and contains D-amino acids [15]. We could prove the actual incorporation of D-alanine by the use of recently developed fluorescent probes in *P. amoebophila*, but not in *S. negevensis*. Shortly afterwards, Liechti *et al* showed that peptidoglycan is also present in members of the *Chlamydiaceae* [16]. However, *C. trachomatis* did only incorporate fluorescently labeled D-alanine dipeptides and not D-alanine [16]. It will be interesting to see whether *S. negevensis*, which shares a less complete peptidoglycan synthesis pathway with the *Chlamydiaceae* compared to *P. amoebophila*, is also able to incorporate these D-Ala-dipeptides. Differences in the enzymes of the pathways could lead to this need for different substrates, and might result in slightly different types or different amounts of peptidoglycan present in the organisms. A recent study showed that members of the *Chlamydiaceae* might indeed be able to synthesize D-alanine using the serine hydroxymethyltransferase GlyA despite the absence of typical alanine-racemases in their genomes [17]. Similarly, also the glycosyltransferase, which forms the beta 1,4 linkage of N-acetylglucosamine and N-acetylmuramic acid and which is missing in all chlamydial genomes, could be functionally replaced by a yet uncharacterized protein. Although difficult to achieve, the characterization of hypothetical proteins based on expression data could help in the identification of the substitute for this enzyme. The periplasmic layer observed by cryo-electron tomography in *P. amoebophila* was previously not observed in conventional electron microscopy images, suggesting that this layer might collapse during sample preparation. A recent cryo-electron tomography study on the cell envelope of *C. trachomatis* did not detect any additional layers in the periplasm [18], however the use of higher

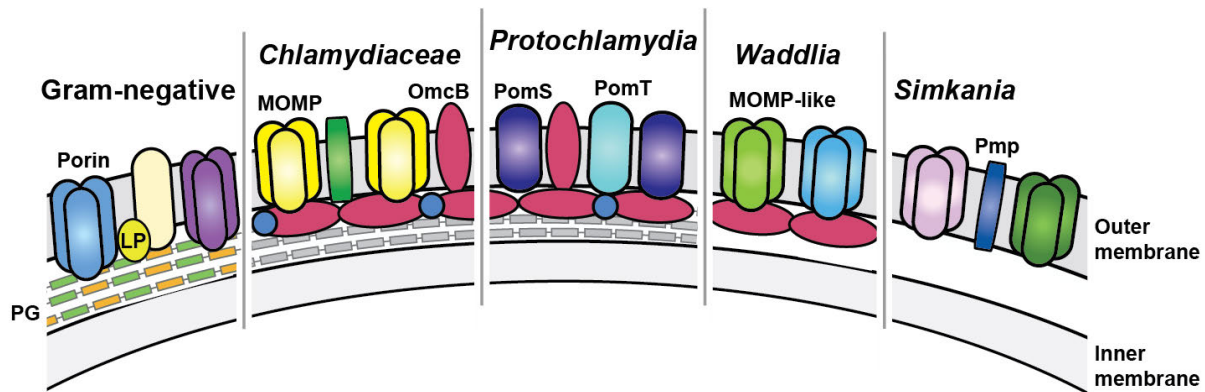


**Figure 1: Main components of the cell envelope of Gram-negative bacteria and chlamydiae – an update.** The outer membrane protein composition differs in main aspects between members of different chlamydial families: *P. amoebophila* and *P. acanthamoebae* (not shown) do not share MOMP as the main porin with other chlamydiae, while cysteine-rich proteins are absent from the cell envelope of *S. negevensis*. Evidence for the presence of peptidoglycan has been found for *C. trachomatis* [16] and *P. amoebophila*. LP, lipoprotein; PG, peptidoglycan;

electron energies and energy filtration might also give new insights into the envelope of *Chlamydiaceae*.

Chlamydiae were considered for a long time a small group of closely related bacteria. All members shared the main components of the outer membrane, which play a major role in the progression of the chlamydial developmental cycle. Two of the studies presented in this thesis highlight differences between environmental and pathogenic chlamydiae and show that not all chlamydiae share MOMP as the major porin and that not all chlamydiae are stabilized by disulfide-rich proteins. Both likely reflect the adaption to different environments and a different host spectrum compared to the *Chlamydiaceae*. The original host of *S. negevensis* is still not known, but the closest relative of this organism is found in marine environments in the worm-like *Xenoturbella* [19]. Marine environments might provide osmotically more stabilizing conditions for elementary bodies than terrestrial or freshwater environments, and cysteine-rich proteins might have become dispensable under these conditions. Genomic and proteomic comparisons of other marine chlamydiae could give insights into whether the absence of disulfide-rich proteins is a unique adaption of *S. negevensis* or a common theme associated with the marine habitat.

*S. negevensis* is not only missing the two stabilizing cysteine-rich proteins, but also other important components of the outer membrane, whose activity is regulated via disulfide-bridge formation in other chlamydiae, feature low cysteine contents. This leads to the question how *S. negevensis* regulates these processes. The permeability of the outer membrane could be regulated by differential expression of sets of the large family of MOMP-like proteins in the absence of disulfide-bridges in these proteins. Expression profiles of these proteins or the analysis of the outer membrane

proteome under different growth conditions and at different stages of the developmental cycle could help to analyze this regulation. This could be combined with a functional analysis of the proteins regarding differences in channel conductance and ion-selectivity to look for actual differences in pore-forming activity.

The activity of the type III secretion system is also suggested to be regulated by disulfide-bridge formation [20]. No homologue of the needle forming protein CdsF, which is involved in disulfide-bridge formation in *C. trachomatis* [20], is present in the genome of *S. negevensis*, and the structural proteins CdsC and CdsD have only one and two cysteine-residues compared to seven and four cysteines in *C. trachomatis*, respectively. However, type III-like secretion structures are present on EBs of *S. negevensis* as observed by cryo-electron tomography. Purification of these structures could not only help to identify the needle forming protein of *S. negevensis*, but might also help to understand how these proteins interact with each other and give first insights into the regulation of the type III secretion system in *S. negevensis*.

Amoeba symbionts of the *Parachlamydiaceae* not only differ in the major porin from other chlamydial families, but also from each other. Two members of the PomS-family dominate the outer membrane of *P. amoebophila* and were shown to functionally replace MOMP in this organism. Another member of the *Parachlamydiaceae*, *Neochlamydia* S13, was recently shown to encode only a homologue of PomS [21] but not the other members of the PomS family. Studies of the outer membrane proteome will show whether PomS is indeed the major porin in this organism or whether like in *P. acanthamoebae* a homologue of the PomS family is present, but other putative porins dominate the outer membrane. This higher diversity in regard to the major porin might be the result of adaptations to the more flexible environmental conditions amoeba symbionts face compared to the *Chlamydiaceae*. With the discovery of new chlamydial families and sequencing of their genomes, it will be interesting to see whether this variability is an exception within the *Chlamydiae* or whether other families show similar adaptations and variations.

Altogether, the study of environmental chlamydiae provides a new perspective on many aspects of chlamydial biology and will continue to contribute to a better understanding of this fascinating group of bacteria and the adaptations they acquired to become the successful intracellular symbionts and pathogens they are today.

## References

1. Rusconi B, Lienard J, Aeby S, Croxatto A, Bertelli C, et al. (2013) Crescent and star shapes of members of the *Chlamydiales* order: impact of fixative methods. *Antonie van Leeuwenhoek* 104: 521-532.

2. Kostanjsek R, Strus J, Drobne D, Avgustin G (2004) '*Candidatus* Rhabdochlamydia porcellionis', an intracellular bacterium from the hepatopancreas of the terrestrial isopod *Porcellio scaber* (Crustacea: Isopoda). *Int J Syst Evol Microbiol* 54: 543-549.
3. Karlsen M, Nylund A, Watanabe K, Helvik JV, Nylund S, et al. (2008) Characterization of '*Candidatus* Clavochlamydia salmonicola': an intracellular bacterium infecting salmonid fish. *Environ Microbiol* 10: 208-218.
4. Lienard J, Croxatto A, Prod'homme G, Greub G (2011) *Estrella lausannensis*, a new star in the Chlamydiales order. *Microbes and Infection* 13: 1232-1241.
5. Kahane S, Dvoskin B, Mathias M, Friedman MG (2001) Infection of *Acanthamoeba polyphaga* with *Simkania negevensis* and *S. negevensis* survival within amoebal cysts. *Appl Environ Microbiol* 67: 4789-4795.
6. Thomas V, Casson N, Greub G (2006) *Criblamydia sequanensis*, a new intracellular *Chlamydiales* isolated from Seine river water using amoebal co-culture. *Environ Microbiol* 8: 2125-2135.
7. Stride MC, Polkinghorne A, Miller TL, Groff JM, LaPatra SE, et al. (2013) Molecular Characterization of "*Candidatus* Parilichlamydia carangidicola," a Novel *Chlamydia*-Like Epitheliocystis Agent in Yellowtail Kingfish, *Seriola lalandi* (Valenciennes), and the Proposal of a New Family, "*Candidatus* Parilichlamydiaceae" fam. nov. (Order *Chlamydiales*). *Applied and Environmental Microbiology* 79: 1590-1597.
8. Draghi A, 2nd, Popov VL, Kahl MM, Stanton JB, Brown CC, et al. (2004) Characterization of "*Candidatus* Piscichlamydia salmonis" (order *Chlamydiales*), a chlamydia-like bacterium associated with epitheliocystis in farmed Atlantic salmon (*Salmo salar*). *J Clin Microbiol* 42: 5286-5297.
9. Michel R, Müller KD, Zöller L, Walochnik J, Hartmann M, et al. (2005) Free-living amoebae serve as a host for the *Chlamydia*-like bacterium *Simkania negevensis*. *Acta Protozoologica* 44: 113-121.
10. Dumoux M, Clare DK, Saibil HR, Hayward RD (2012) Chlamydiae Assemble a Pathogen Synapse to Hijack the Host Endoplasmic Reticulum. *Traffic* 13: 1612-1627.
11. Mehlitz A, Karunakaran K, Herweg J-A, Krohne G, van de Linde S, et al. (2014) The chlamydial organism *Simkania negevensis* forms ER vacuole contact sites and inhibits ER-stress. *Cellular Microbiology* in press.
12. Matsumoto A, Bessho H, Uehira K, Suda T (1991) Morphological studies of the association of mitochondria with chlamydial inclusions and the fusion of chlamydial inclusions. *J Electron Microsc (Tokyo)* 40: 356-363.
13. Croxatto A, Greub G (2010) Early intracellular trafficking of *Waddlia chondrophila* in human macrophages. *Microbiology* 156: 340-355.
14. Derré I, Pypaert M, Dautry-Varsat A, Agaisse H (2007) RNAi Screen in *Drosophila* Cells Reveals the Involvement of the Tom Complex in *Chlamydia* Infection. *PLoS Pathog* 3: e155.
15. McCoy AJ, Maurelli AT (2005) Characterization of *Chlamydia* MurC-Ddl, a fusion protein exhibiting D-alanyl-D-alanine ligase activity involved in peptidoglycan synthesis and D-cycloserine sensitivity. *Mol Microbiol* 57: 41-52.
16. Liechti GW, Kuru E, Hall E, Kalinda A, Brun YV, et al. (2014) A new metabolic cell-wall labelling method reveals peptidoglycan in *Chlamydia trachomatis*. *Nature* 506: 507-510.



17. de Benedetti S, Bühl H, Gaballah A, Klöckner A, Otten C, et al. (2014) Characterization of serine hydroxymethyltransferase GlyA as a potential source of D-alanine in *Chlamydia pneumoniae*. *Front Cell Infect Microbiol* 26.
18. Huang Z, Chen M, Li K, Dong X, Han J, et al. (2010) Cryo-electron tomography of *Chlamydia trachomatis* gives a clue to the mechanism of outer membrane changes. *Journal of Electron Microscopy* 59: 237-241.
19. Israelsson O (2007) Chlamydial symbionts in the enigmatic *Xenoturbella* (Deuterostomia). *Journal of Invertebrate Pathology* 96: 213-220.
20. Betts-Hampikian HJ, Fields KA (2011) Disulfide Bonding within Components of the *Chlamydia* Type III Secretion Apparatus Correlates with Development. *Journal of Bacteriology* 193: 6950-6959.
21. Ishida K, Sekizuka T, Hayashida K, Matsuo J, Takeuchi F, et al. (2014) Amoebal Endosymbiont *Neochlamydia* Genome Sequence Illuminates the Bacterial Role in the Defense of the Host Amoebae against *Legionella pneumophila*. *PLoS ONE* 9: e95166.



# **Chapter VIII**

## **Summary & Zusammenfassung**

## Summary

Chlamydiae are a group of highly successful obligate intracellular bacteria that have been associated with eukaryotes for more than 700 million years. In contrast to most other bacteria, chlamydiae seemed to lack the stabilizing peptidoglycan layer that helps bacterial cells to retain their shape. Instead, the cell envelope of the elementary body, the stable, extracellular and infectious developmental stage of chlamydiae, is stabilized by disulfide-bridges formed between cysteine-rich proteins. These disulfide-bridges are reduced after uptake by the host cell, which results in the more flexible, labile reticulate body that represents the metabolically highly active and dividing form. The cell envelope and the changes it undergoes during the chlamydial developmental cycle were investigated almost exclusively in members of the *Chlamydiaceae*, a family that includes important human and animal pathogens and has been studied for more than a century. The major outer membrane protein MOMP, a porin, and the two cysteine-rich proteins OmcA and OmcB were found to dominate the outer membrane of all investigated *Chlamydiaceae*.

In the last decade, the diversity of chlamydiae was discovered to be much larger than previously assumed and several families, collectively termed “environmental chlamydiae”, inhabiting amoebae, insects and fish were added to the phylum *Chlamydiae*. In this thesis I investigated selected aspects of the cell envelope of members of these environmental chlamydiae in order to identify conserved themes and variations. By the use of cryo-electron tomography, which allows the imaging of samples at macromolecular resolution without the need for chemical fixation or dehydration, we discovered a periplasmic layer reminiscent of peptidoglycan of Gram-negative bacteria in the cell envelope of the amoeba symbiont *Protochlamydia amoebophila*. *P. amoebophila* was shown to incorporate fluorescently labeled D-alanine, and peptidoglycan subunits were detected in purified sacculi by mass spectrometry. The detection of peptidoglycan in chlamydiae for the first time proves that at least some chlamydiae use the nearly complete peptidoglycan pathway, which is present in all chlamydial genomes. Interestingly, the cysteine-rich proteins suggested to stabilize chlamydiae in the absence of peptidoglycan are not present in all chlamydiae. No cysteine-rich proteins were detected in outer membrane protein fractions of *Simkania negevensis* by mass spectrometry, and in agreement with this the stability of this organism is not affected by reducing agents under low osmolarity conditions in contrast to other chlamydiae. The analysis of outer membrane protein fractions also showed differences in the most abundant porins in different chlamydial families. Large MOMP-like protein families dominate the outer membrane of *S. negevensis* and *Waddlia chondrophila*. In contrast, MOMP-homologues are either absent (*P. amoebophila*) or only present in low amounts (*Parachlamydia acanthamoebae*) in members of the *Parachlamydiaceae*. Instead, hypothetical proteins, for which beta barrel formation was predicted by *in silico* analysis, are the

most abundant proteins in these organisms. The characterization of the dominant protein family in *P. amoebophila* proved indeed the localization in the outer membrane and a porin function for one of the two most abundant proteins, PomS.

Finally, we visualized type III secretion structures of environmental chlamydiae for the first time by cryo-electron tomography. These secretion systems are encoded in the genomes of all chlamydiae and are used to secrete effector proteins into the host cell where they for example initiate the recruitment of host cell organelles to the chlamydia-containing vacuole. Similar to *C. trachomatis*, we observed recruitment of the endoplasmic reticulum by *Simkania negevensis*, showing that this host cell organelle manipulation is conserved between members of the pathogenic and environmental chlamydiae.

Differences in the outer membrane composition and the ability to recruit host cell organelles of some chlamydiae likely represent adaptations to different hosts and thereby contribute to the large host spectrum of chlamydiae, while conserved components like the type III secretion system are indispensable for the infection of all eukaryotic hosts and evolved early on, laying the foundation for the success of chlamydiae as obligate intracellular pathogens and symbionts.

## Zusammenfassung

Chlamydien sind eine Gruppe höchst erfolgreicher, obligat intrazellulärer Bakterien, die seit mehr als 700 Millionen Jahren mit eukaryotischen Wirtszellen assoziiert sind. Im Unterschied zu beinahe allen anderen Bakterien scheint der Zellhülle der Chlamydien eine stabilisierende und formgebende Peptidoglykanschicht zu fehlen. Stattdessen wird das Elementarkörperchen, das stabile, extrazelluläre und infektiöse Entwicklungsstadium der Chlamydien, durch eine starke Quervernetzung mittels Disulfidbrücken cysteinreicher Außenmembranproteine stabilisiert. Diese Disulfidbrücken werden nach Aufnahme der Elementarkörperchen in die Wirtszelle reduziert, wodurch das flexiblere und labilere Retikularkörperchen entsteht, die metabolisch hochaktive und sich teilende Form der Chlamydien. Dieser typische Aufbau der Zellhülle und die damit verbundenen Prozesse wurden an Mitgliedern der Familie *Chlamydiaceae* untersucht, die seit über einem Jahrhundert bekannt ist und wichtige human- und tierpathogene Arten umfasst. Da Proteine in der Außenmembran der *Chlamydiaceae* großes Potential als Impfstoffkandidaten haben, wurde die Proteinzusammensetzung der Außenmembran sowie die häufigsten Proteine der *Chlamydiaceae* ausführlich untersucht. Dabei zeigte sich, dass die Hauptkomponenten, das Porin MOMP und die beiden cysteinreichen Proteine OmcA und OmcB, in allen Arten der *Chlamydiaceae* konserviert sind.

In den vergangenen zwei Jahrzehnten hat sich die bekannte Diversität der Chlamydien stark erhöht und neue Familien, die auch als „Umweltchlamydien“ zusammengefasst werden, wurden als Symbionten von Amöben, Insekten und Fischen entdeckt. Im Rahmen dieser Doktorarbeit wurden unterschiedliche Aspekte der Zellhülle einiger Vertreter dieser Umweltchlamydien untersucht. Unter Verwendung von Cryo-Elektronentomographie, einer Technik die die Visualisierung von Organismen ohne chemische Fixierung mit makromolekularer Auflösung erlaubt, konnten wir im Periplasma des Amöbensymbionten *Protochlamydia amoebophila* eine zusätzliche Schicht detektieren, die Peptidoglykan anderer Gram-negativer Bakterien ähnelt. Der Einbau von fluoreszent markiertem D-Alanin, einem essentiellen Bestandteil von Peptidoglykan, zeigte, dass *P. amoebophila* Peptidoglykan synthetisiert, und mittels Massenspektrometrie konnten Bestandteile von Peptidoglykan in aufgereinigten Sacculi nachgewiesen werden. Dies war der erste Nachweis von Peptidoglykan in einem Vertreter der Chlamydien. Interessanterweise zeigten massenspektrometrische Untersuchungen von Außenmembranproteinpräparationen von Mitgliedern dreier unterschiedlicher Chlamydienfamilien, dass nicht alle Chlamydien cysteinreiche Proteine zur Stabilisierung der Zellhülle besitzen. In Abwesenheit dieser Proteine wird *Simkania negevensis* im Gegensatz zu anderen Chlamydien auch nicht durch das Reduktionsmittel Dithiothreitol destabilisiert. Auch hinsichtlich des häufigsten Porins in der Außenmembran gibt es Unterschiede zwischen den Chlamydienfamilien. Die Außenmembran von *S. negevensis* und *Waddlia chondrophila* wird von großen Familien MOMP-

ähnlicher Proteine dominiert. Im Gegensatz dazu sind MOMP-Homologe in Mitgliedern der *Parachlamydiaceae* entweder nicht (*P. amoebophila*) oder nur in sehr geringen Mengen (*Parachlamydia acanthamoebae*) in der Außenmembran vorhanden. Stattdessen dominieren hypothetische Proteine die Außenmembran dieser Organismen, für die *in silico* die Bildung von Beta-Barrel-Strukturen, ein Merkmal von Porinen, vorhergesagt wurde. Durch die Charakterisierung der zwei häufigsten Vertreter dieser Proteine in *P. amoebophila* konnten wir zeigen, dass diese tatsächlich in der Außenmembran lokalisiert sind. Darüberhinaus konnte für eines der Proteine auch die Funktion als Porin nachgewiesen werden.

Um über die Barriere der Zellhülle und die Membran der Vakuole, in der sich Chlamydien in der Wirtszelle befinden, Effektorproteine in die Wirtszelle zu sekretieren verwenden Chlamydien Typ-III-Sekretionssysteme, wodurch beispielsweise Organellen der Wirtszelle zur Vakuole rekrutiert werden. Unter Verwendung von Cryo-Elektronentomographie konnten wir erstmals Typ-III-Sekretionssysteme von Umweltchlamydien visualisieren und zudem zeigen, dass *S. negevensis* ähnlich wie *Chlamydia trachomatis* das endoplasmatische Retikulum der Wirtszelle zur Vakuole rekrutiert.

All dies zeigt, dass einige Komponenten, wie das Typ-III-Sekretionssystem, in Mitgliedern verschiedener Chlamydienfamilien konserviert sind und somit für die erfolgreiche Infektion eukaryotischer Zellen durch Chlamydien notwendig sind. Die Diversität in der Proteinzusammensetzung der Außenmembran sowie die Fähigkeit einiger Chlamydien Wirtzellorganellen zu rekrutieren stellt hingegen eine Anpassung an unterschiedliche Wirte dar und trägt damit zu dem immensen Wirtsspektrum dieser Bakterien bei.





# Appendix

---

## Acknowledgments

I am fully aware that none of the work presented here would have been possible without the contributions of others. Therefore, I want to start this (assumedly most frequently read) part of my thesis by generally thanking everyone who helped me in whatever way through the past five years.

Special thanks go to my supervisor Matthias Horn, for his support and for the wonderful opportunities he gave me in the course of my thesis. You not only taught me a lot about science and scientific writing (including the necessity to be careful with “volunteering chickens”), but also about the importance of knowing how to prepare a good party and some Erdbeerbowle.

For the different parts of my thesis I had several great collaboration partners and I immensely enjoyed working with and learning from them.

In the course of my stay at the Caltech and in the projects resulting from this stay I had the great pleasure to work with Martin Pilhofer – thank you for all your enthusiasm, for getting me hooked on cryo-electron tomography (coolest thing ever!) and for being an absolutely awesome collaboration partner! Many thanks also to Grant Jensen, for the chance to work in his lab twice and for all the support for our projects! I also want to thank my collaboration partners Waldemar Vollmer and Jacob Biboy for the nice stay in Newcastle and the good English beer, Dorothea Anrather for her patience with me and my samples, Julia, Ingrid and Monika for the beautiful TEM-pictures and Roland Benz for analyzing the most interesting of all porins.

For parts of the lab work presented in this thesis I had the help of my two great diploma students Alex and Tomi and my practical students Simone and Frederik – thank you for your help, and especially to Alex for your never-ceasing motivation on the porin work!

During my time at dome I had lots of great colleagues and many of them became my friends. I really enjoyed my time with you – thank you for all the help in the lab, for your patience with me and for making my PhD much, much more fun (sometimes with the help of some after work beers and gin tonics)! Special thanks to my nearly-identical twin Hanna, my chief concert motivator Albert, Mr. pseudo-Grumpy Alex S., my dome-long lunch partner Chrissy, my main cookie supply Faaaaaris and

to Bergbauer-in-spe Thomas P.: for tea-times, working dates and your special sense of humor, for cheering me up if necessary (even if you needed to punch me), for our personalized Gruppenkaffees, hair cutting sessions, your supply of good music and for the fun at and outside of work - I'm glad I had you GEBUCHT! Many thanks also to Nina for the food supply that frequently saved me from starvation!

Ilias, for many years the second shareholder of my office table, is greatly acknowledged for feeding me (and my dog) with Kringel, as is my office neighbor Roland for his ambitions to tell me all the important things in the world (preferably within one day) and for watching the Simpsons with me.

I'm also deeply indebted to my "outside" friends, for taking me to the real world from time to time and for uncomplainingly listening to me babbling about PhD-related stuff. However, I hope you will at some point stop again to associate me with chlamydiae. Special thanks to Claudsch, still the best best-friend ever, I would be lost without you! And I hereby officially state that Linz is not that bad. Thanks to my "therapy dog" Pazuzu, for the long walks in any weather that cleared my head, for making me laugh and for teaching me (at least some) patience and to Matteo for the good times.

Finally, I want to thank my parents and my family for their never-ending support.

---

## Curriculum vitae

### Personal details

---

Karin Aistleitner  
born 17. 12. 1984 in Steyr



### Education

---

since 05/2009 PhD at the Department of Microbial Ecology and Ecosystem Science;  
Advisor: Matthias Horn  
Dissertation title: "The cell envelope of environmental chlamydiae"

01/2008 – 03/2009 Diploma thesis at the Department of Microbial Ecology;  
„Characterization of a novel porin from *Protochlamydia amoebophila*"

10/2003 – 03/2009 Master in Biology (Diplomstudium Biologie) at the University of  
Vienna; Major subject: Microbiology

09/1994 – 06/2003 A-levels (Matura), Bundesgymnasium Werndlpark, Steyr

### Research stays

---

07/2013 Research stay at Newcastle University (Prof. Waldemar Vollmer)

08/2011 and 03/2012 Research stay at the California Institute of Technology (Prof. Grant Jensen)

### Teaching activities

---

2009-2012 Supervision of two diploma students and two practical students

04/2008 – 06/2011 Tutor at the Vienna Open Lab

2010, 2011 and 2012 Tutor of the student course “Fluorescence *in situ* hybridization - identification of non-cultivable microorganisms”

## **Publications in peer-reviewed journals**

---

### **Inclusion membrane proteins of *Protochlamydia amoebophila* UWE25 reveal a conserved mechanism for host cell interaction among the *Chlamydiae***

Heinz E., Rockey D.D., Montanaro J., Aistleitner K., Wagner M., Horn M.  
*J Bacteriol.* 2010, 192(19):5093-102

### **Identification and characterization of a novel porin family highlights a major difference in the outer membrane of chlamydial symbionts and pathogens**

Aistleitner K., Heinz C., Hörmann A., Heinz E., Montanaro J., Schulz F., Maier E., Pichler P., Benz R., Horn M.  
*PLoS One.* 2013, 8(1):e55010.

### **Chlamydial peptidoglycan: bacteria with a murein sacculus but without FtsZ**

Pilhofer M.\*, Aistleitner K.\*, Biboy J., Gray J., Kuru E., Hall E., Brun Y. V., Van Nieuwenhze M.S., Vollmer W., Horn M., Jensen G.J.  
\* contributed equally  
*Nat. Commun.* 2013, 4:2856

### **Architecture and host interface of environmental chlamydiae revealed by electron cryotomography**

Pilhofer M.\*, Aistleitner K.\*, Ladinsky M. S., König L., Horn M., Jensen G.J.  
\* contributed equally  
*Environ Microbiol.* 2014, 16:2

### **Life in an unusual intracellular niche – a bacterial symbiont infecting the nucleus of amoebae**

Schulz F., Lagkouvardos I., Wascher F., Aistleitner K., Kostanjšek R., Horn M.  
*ISME journal*, in press

---

**Conserved features and major differences in the outer membrane protein composition of chlamydiae**

**Aistleitner K.**, Anrather D., Schott T., Kloze J., Bright M., Ammerer G., Horn M.

*submitted to Environ Microbiol.*

**Oral presentations at scientific conferences**

---

**03/2009 Deutscher Chlamydienworkshop, Lübeck, Germany**

**Aistleitner K.**, Heinz C., Heinz E., Benz R., Montanaro J., Kolar J., Pichler P., Ammerer G., Mechtler K., Wagner M., Horn M.

Characterization of pc1489, a member of a novel porin family discovered in the amoeba symbiont *Protochlamydia amoebophila*

**03/2010 Tagung der Deutschen Gesellschaft für Hygiene und Mikrobiologie (DGHM) e.V. und der Vereinigung für Allgemeine und Angewandte Mikrobiologie (VAAM), Hannover, Deutschland**

**Aistleitner K.**, Hörmann A., Heinz C., Heinz E., Benz R., Montanaro J., Kolar J., Pichler P., Ammerer G., Mechtler K., Wagner M., Horn M.

Characterization of two members of a novel porin family discovered in the amoeba symbiont *Protochlamydia amoebophila*

**10/2011 18<sup>th</sup> International meeting on Novel Techniques in Microbial Ecology (INTIME), Slettestrand, Denmark**

**Aistleitner K.**, Schott T., Anrather D., Ammerer G., Horn M.

The role of cysteine-rich proteins for the stability of chlamydial endosymbionts of amoebae

**06/2012 Seventh meeting of the European Society for Chlamydia Research, Amsterdam, Netherlands**

**Aistleitner K.**, Schott T., Anrather D., Pilhofer M, Jensen G., Pichler P., Ammerer G., Horn M.

Variation in outer membrane protein composition among *Simkania negevensis*, *Waddlia chondrophila*, and *Parachlamydia acanthamoebae*

**03/2013 Science Day of the Faculty Center of Ecology, Vienna**

**Aistleitner K.**, Pilhofer M., Ladinsky M., König L., Jensen G., Horn M.

Architecture and host interactions of environmental chlamydiae revealed by electron cryotomography

**Public presentations**

---

**11/2012 Pecha Kucha contest “Biology on stage – 400 seconds of life”, Vienna**

Training in the gym pays off: Amoebae as training ground for bacterial pathogens

**Poster presentations at scientific conferences**

---

**03/2011 CBRS 2011: 5th Biennial Meeting of the Chlamydia Basic Research Society, Redondo Beach, USA**

**Aistleitner K.**, Hörmann A., Heinz C., Heinz E., Benz R., Montanaro J., Schulz F., Kolar J., Pichler P., Ammerer G., Mechtler K., Wagner M., Horn M.

Functional replacement of the major outer membrane protein MOMP by proteins constituting a novel porin family in *Protochlamydia amoebophila*

---

**03/2013 CBRS 2013: 6th Biennial Meeting of the Chlamydia Basic Research Society, San Antonio, USA**

**Aistleitner K., Pilhofer M., Ladinsky M., König L., Jensen G., Horn M.**

Architecture and host interactions of environmental chlamydiae revealed by electron cryotomography

## **Awards & grants**

---

- |           |   |
|-----------|---|
| 12/2013   | PhD completion grant of the Faculty of Life Sciences (University of Vienna)   |
| 03/2013   | Award for the best oral presentation given by a PhD student at the Science Day of the Faculty Center of Ecology (University of Vienna)                        |
| 11/2012   | Award for the best Pecha Kucha presentation given at "Biology on Stage - 400 Seconds of Life"   |
| 09/2012   | Short-term grant abroad (University of Vienna)  |
| 03/2011   | Jane E. Raulston Award at the 5 <sup>th</sup> Biennial Meeting of the Chlamydia Basic Research Society for the best poster presentation by a graduate student |
| 2006-2008 | Merit scholarships (University of Vienna)   |